

**IMPROVING HISTONE DEACETYLASE INHIBITION THERAPY
THROUGH ISOFORM SELECTIVITY AND TARGETED
DELIVERY**

A Dissertation
Presented to
The Academic Faculty

by

Quaovi Sodji

In Partial Fulfillment
of the Requirements for the Degree
Doctor of Philosophy in the
School of Chemistry and Biochemistry

Georgia Institute of Technology
May 2014

COPYRIGHT 2014 BY QUAOVI SODJI

**IMPROVING HISTONE DEACETYLASE INHIBITION THERAPY
THROUGH ISOFORM SELECTIVITY AND TARGETED
DELIVERY**

Approved by:

Dr. Adegboyega Oyelere, Advisor
School of Chemistry and Biochemistry
Georgia Institute of Technology

Dr. Charles Liotta
School of Chemistry and Biochemistry
Georgia Institute of Technology

Dr. Yuhong Fan
School of Biology
Georgia Institute of Technology

Dr. Stefan France
School of Chemistry and Biochemistry
Georgia Institute of Technology

Dr. John McDonald
School of Biology
Georgia Institute of Technology

Dr. Jennifer Pollock
School of Medicine
University of Alabama at Birmingham

Date Approved: March 24th, 2014

To my parents Ahlinvi Sodji and Kapou Adjoavi

ACKNOWLEDGEMENTS

I would first like to thank God for all He has done for me thus far and will continue to do for me. I am especially thankful for Him for putting me at the right places at the right time and for putting on my path people who have molded me into the person I am today. Acknowledging all these individuals by name is nearly impossible.

I am deeply indebted to my advisor Dr. Adegboyega Oyelere, for taking me into his lab since my undergraduate years and orienting me towards the path that I am currently on. His guidance and support have always been there when I needed it and I would not have chosen a better advisor to learn from. He is a mentor that I can always come back to for advice.

I would like to thank my thesis committee members, Dr. Charles Liotta, Dr. John McDonald, Dr. Jennifer Pollock, Dr. Stefan France and Dr. Yuhong Fan for the invaluable discussions throughout my thesis research and for their commitment to helping me through my graduate school journey.

I would also like to acknowledge our collaborators for their expertise, James Kornacki and Dr. Milan Mrksich at Northwestern University, Dr. Babu Tekwani at the University of Mississippi and Dr. John McDonald.

None of this work would have been possible without the training and support that I received from the Oyelere research group members. I would like to thank Daniel Yao, Dr. Celinah Mwakwari and Dr. Vishal Patil for their training in organic synthesis. I am greatly indebted to Dr. Patil for the scientific discussions and for being a great support throughout his time in the lab. I also want to extend my gratitude to former and current

group members whose support and camaraderie have made this journey enjoyable: Dr. Josh Canzoneri, Dr. William Guerrant, Dr. Subhashish Tapadar, Dr. Berkley Gryder, Arren Washington, Michelle Akbashev, Idris Raji, Shaghayegh Fathi, Brian Moskowitz, Imani Jones, Eric Raftery and Leslie Dionne White .

I also want to thank the University System of Georgia MD/PhD Program whose past and current leadership have been very supportive of my scientific endeavors. I would like to especially thank Dr. Edward Inscho (former program director) and Laura Hutcheson for taking a chance on me by accepting me into the program, Dr. Jennifer Pollock (former program director) for all she has done for the MD/PhD program and for being such a great mentor, Dr. Nevin Lambert (current program co-director) for all his support and Christina Ostrowski (program manager) for being a great support for all MD/PhD students.

I would like to thank my parents Ahlinvi Etin Sodji and Adjoavi Kapou for their unconditional love and support, I can never repay them for all the sacrifices that they made so that I can be here today but to the best of my ability I will always try to make them proud. I also would like to thank Mr. Kashta Williams and Ms. Carmen Caines for taking me in during my time of need and treating me as one of their own, I thank God everyday for having met them. I want to also extend my gratitude to my aunt Ms. Pauline Elavagnon Agbodji for her support. I am also grateful for my brother Joseph Sodji and my sister Christelle Sodji.

I am indebted to those who believed in me, said a prayer for me, fed me when I was hungry, consoled me when I was down. Last but not least, I would also like to thank

those who did not support me, as their skepticism pushed me to work even harder than I thought I could.

TABLE OF CONTENTS

	Page
ACKNOWLEDGEMENTS	iv
LIST OF TABLES	xiii
LIST OF FIGURES	xv
LIST OF ABBREVIATIONS	xvii
SUMMARY	xxv
 <u>CHAPTER</u>	
1 INTRODUCTION	1
1.1. Background	1
1.2. Histone acetylation	2
1.3. Histone deacetylation	2
1.4. Histone deacetylase (HDAC)	3
1.5. Role of HDACs in healthy cells	6
1.6. Regulation of HDAC activity	7
1.7. HDAC in cancer	8
1.8. HDAC inhibitor (HDACi) for cancer therapy	9
1.8.1. HDACi pharmacophoric model	10
1.8.2. Mechanisms of action of HDACi	12
1.9. HDACi clinical trials	14
1.9.1. Monotherapy trials	15
1.9.1.1. Hydroxamic acids	15
SAHA (Vorinostat)	15
PCI-24871	15

1.9.1.2. Cyclic peptides	17
FK228 (Romidepsin)	17
1.9.1.3. Benzamides	17
MS275 (Entinostat)	17
1.9.1.4. Short fatty acid	18
1.9.2. Combination therapy of HDACi with other chemotherapy agents	18
1.10. Problems associated with HDACi therapy	19
1.10.1. Gastrointestinal	19
1.10.2. Constitutional	19
1.10.3. Hematologic	19
1.10.4. Cardiac	20
1.11. Mechanisms of QT prolongation	21
1.12. Improving HDACi therapy	22
1.12.1. Drug discovery	23
1.12.1.1. Incorporation of cardiac safety assessment in early stages of drug development	23
1.12.1.2. Isoform selective HDACi	24
1.12.1.3. Targeted delivery of HDACi	25
1.12.2. Clinical improvement to HDACi therapy	28
1.12.2.1. Patients stratification	28
1.12.2.2. Identification and use of predictive biomarkers	29
1.12.2.3. Understanding the mechanisms of HDACi-induced side effects	29
1.12.2.4. Understanding of mechanisms of resistance to HDACi	30

1.13. Conclusion	30
1.14. References	32
2 ISOFORM SELECTIVE HDAC INHIBITORS	41
2.1. Introduction	41
2.2. 3-Hydroxypyridin-2-thione as novel ZBG for HDAC inhibition	44
2.3. Anticancer activity of the 1 st generation of 3-HPT based inhibitors	47
2.4. Anticancer activity of the 2 nd generation 3-HPT inhibitors	51
2.5. Intracellular target validation of 3-HPT based inhibitors	56
2.6. Conclusion	57
2.7. General procedures and experimental	58
2.7.1. Histone deacetylase inhibition	58
2.7.2. Cell viability assay	60
2.7.3. Solubility measurement	60
2.7.4. Western blot analysis for tubulin acetylation	61
2.7.5. MMP assay	61
2.7.6. Statistical analysis	62
2.8. References	63
3 TARGETED DELIVERY OF HDAC INHIBITORS USING FOLATE AND PTEROIC ACID	67
3.1. Introduction	67
3.2. Design of Folate receptor ligand-HDACi conjugates	69
3.3. Folate γ -hydroxamic and pteronic hydroxamic acids as HDAC inhibitors	69

3.3.1. Synthesis of folate γ -hydroxamic and pteronic hydroxamic acids	70
3.3.2. HDAC inhibition profile of folate γ -hydroxamic and pteronic hydroxamic acids	72
3.3.3. Molecular docking studies	73
3.4. SAR on pteronic based hydroxamate HDAC inhibitors	74
3.4.1. Synthesis of pteronic based hydroxamates	75
3.4.2. HDAC inhibition profile of pteronic based hydroxamates	76
3.4.3. Molecular docking studies of pteronic based hydroxamates	78
3.5. Folic acid based hydroxamate HDACi	80
3.5.1. Synthesis of folate based hydroxamic acids	80
3.5.2. HDAC inhibition profile of folate based hydroxamic acids	81
3.5.3. Molecular docking studies of the folate based hydroxamate compound 15c	82
3.6. Targeted delivery of isoform selective HDACi	84
3.6.1. Synthesis of folate based biaryl benzamide compounds	84
3.6.2. HDAC inhibition profile of folate based biaryl benzamide HDACi	86
3.7. Anticancer activity of pteronate and folate-derived HDACi	87
3.8. Intracellular targets validation	89
3.9. Conclusion	95
3.10. Experimental section	97
3.10.1. Materials and methods	97
3.10.2. Histone deacetylase inhibition	98
3.10.3. Molecular docking analysis	99

3.10.4. Cell viability assay	100
3.10.5. Western blot analysis of tubulin and histone H4 acetylation	100
3.10.6. Statistical analysis	101
3.11. References	136
4 MECHANISM OF HDAC INHIBITOR RESISTANCE IN JURKAT J- γ	142
4.1. Introduction	142
4.2. Mechanisms of resistance to HDACi	142
4.2.1. Efflux pumps	142
4.2.2. Changes in HDAC expression level	143
4.2.3. Expression of apoptosis related proteins	143
4.2.4. Increased antioxidant production	143
4.3. Novel mechanism of resistance to HDACi	144
4.3.1. Anticancer activity of selected compounds against wild type Jurkat and the Jurkat subline J γ	146
4.3.2. Phospholipase C- γ 2 may be responsible for apoptosis potentiation in Jurkat J γ subline	148
4.3.3. Mutations in PLC- γ 1 activation pathways as potentially novel mechanisms of HDACi resistance	148
4.4. Conclusion	149
4.5. General procedures and experimental	150
4.6. References	151

5	COMPARISON OF HDAC INHIBITION PROFILE USING THE STANDARD FLUOROGENIC ASSAY FLUOR DE LYS AND SELF-ASSEMBLED MONOLAYERS FOR MATRIX-ASSISTED LASER DESORPTION MASS SPECTROMETRY (SAMDI-MS)	155
5.1.	Introduction	155
5.2.	History of HDAC assays	156
5.2.1.	Sirtuins assays	156
5.2.2.	Zinc dependent HDAC assays	160
5.3.	Fluorogenic HDAC assay	161
5.4.	Pitfalls of the fluorogenic assay	163
5.5.	HDAC assay using the self-assembled mono-layers for matrix assisted laser desorption ionization time-of-flight mass spectrometry (SAMDI-MS)	164
5.6.	Comparison of the fluorogenic and SAMDI-MS for monitoring HDAC activity: HDAC inhibition profile of pterotic hydroxamate based compounds	166
5.7.	Conclusion	170
5.8.	References	172
6	CONCLUSION AND FUTURE PERSPECTIVES	176
APPENDIX :	Synthesis scheme of pteroyl azide and ^1H and ^{13}C NMR characterization of folate and pterotic based HDACi (Chapter 3)	181
VITA		254

LIST OF TABLES

	Page
Table 1.1: Characteristics of Zinc dependent HDACs	5
Table 1.2: HDACs overexpression in cancer	9
Table 1.3: Percentage of common non cardiac side effects seen during HDACi therapy (SAHA and Romidepsin)	21
Table 2.1: Phenotypic defects in mice following HDAC isoforms knockout experiments	42
Table 2.2: Inhibition of HDAC1, 6 and 8 by 1 st generation 3-HPT based inhibitors	45
Table 2.3: Inhibition of HDAC1, 6 and 8 by 2 nd generation 3-HPT based inhibitors	46
Table 2.4: MTS Cell Viability Assay. IC ₅₀ of selected 1 st generation of 3-HPT based inhibitors against various cancer cell lines	48
Table 2.5: Aqueous solubility of selected 1 st generation 3-HPT inhibitors	50
Table 2.6: MTS Cell Viability Assay. IC ₅₀ of selected 2 nd generation of 3-HPT based inhibitors against various cancer cell lines	52
Table 2.7: Aqueous solubility of selected 2 nd generation 3-HPT inhibitors	53
Table 3.1: Inhibition profile of folate γ -hydroxamic and pteronic hydroxamic acids (IC ₅₀ in nM)	73
Table 3.2: HDAC inhibition of Pteronic based hydroxamates (IC ₅₀ in nM)	77
Table 3.3: HDAC inhibition of folate based hydroxamates (IC ₅₀ in nM)	82
Table 3.4: Inhibition of various HDAC isoforms by folate based biaryl benzamides (IC ₅₀ in nM)	86

Table 3.5: Folate receptor-dependent anti-proliferative activity of folate- and pteroate- derived hydroxamates (IC ₅₀ in μM)	88
Table 4.1: Structures and HDAC inhibition profile of selected HDAC inhibitors	145
Table 4.2: Anticancer activity of selected compounds (IC ₅₀ in μM)	147
Table 5.1: Specific substrate of selected deacetylase enzymes	166
Table 5.2: HDAC inhibition profile of pteronic acid based HDAC inhibitors: Fluorogenic assay vs SAMDI-MS	167

LIST OF FIGURES

	Page
Figure 1.1: Proposed mechanism of acetyl-Lys deacetylation by HDAC8.	4
Figure 1.2: Cross section of the homology model of HDAC1 built from HDAC2 (PDB code: 3MAX)	6
Figure 1.3: Examples of cellular processes regulated by HDAC/HAT	7
Figure 1.4: HDACi pharmacophoric model	10
Figure 1.5: Example of HDACi	11
Figure 1.6: Phenotypical outcome of HDACi on healthy and cancer cells	12
Figure 1.7: Mechanisms of action of HDACi	13
Figure 1.8: Clinical trials of HDACi as monotherapy or in combination with other chemotherapeutic agents	14
Figure 1.9: Structures of other hydroxamates based HDACi in clinical trials	16
Figure 1.10: Key strategies for improving HDACi therapy	23
Figure 1.11: Active targeting of HDACi	27
Figure 2.1: Processes potentially targeted by HDAC pan-inhibitors	42
Figure 2.2: Structures of selected HDACi	43
Figure 2.3: MMP activity in presence of various inhibitors	55
Figure 2.4: Western blot analysis of tubulin acetylation (HDAC6 inhibition) in LNCaP cell line (1 st generation 3-HPT based inhibitors)	56
Figure 2.5: Western blot analysis of tubulin acetylation (HDAC6 inhibition) in LNCaP cell line (2 nd generation 3-HPT based inhibitors)	57
Figure 3.1: HDACi pharmacophoric model and structures of folic acid, pteronic acid folate γ -hydroxamic acid and pteronic hydroxamic acid	70

Figure 3.2: Molecular docking studies of folate γ -hydroxamate 6 with homology models of HDAC1 and 6	74
Figure 3.3: Structure of pterotic based hydroxamates 11a-g	75
Figure 3.4: Molecular docking poses explaining the inhibitory profile of selected pterotic based hydroxamates against HDAC1 and HDAC6	79
Figure 3.5: Structure of folate based hydroxamates 15a-g	80
Figure 3.6: Molecular basis for isoform selectivity of 15c	83
Figure 3.7: Structure of folate based biaryl benzamide HDACi	84
Figure 3.8: Folic acid (FA) competition assay	89
Figure 3.9: Molecular docking of FR (PDB code: 4LRH) with folic acid pterotic hydroxamate 7, 11d, 11e	91
Figure 3.10: Western blot analysis of tubulin acetylation in KB cell	92
Figure 3.11: Structures and HDAC inhibition profile of Tubastatin A and SHI-1:2	93
Figure 3.12: Western blot analysis of Histone H4 acetylation in KB cell	94
Figure 3.13: Molecular docking of FR (PDB code: 4LRH) with folic acid 24b and 24c	95
Figure 4.1: HDACs inhibition profile of FK228 and reduced FK228 (Red-FK228)	147
Figure 5.1: Schematic of sirtuins mediated deacetylation	158
Figure 5.2: Schematic of selected sirtuins assays	159
Figure 5.3: Schematic of the non-radioactive HDAC assay	162
Figure 5.4: HDAC activity assay using SAMDI-MS	165

LIST OF ABBREVIATIONS

°C	Degree Celsius
3D	Three-dimensional
3-HPT	3-Hydroxypyridin-2-thione
Å	Angstrom
A549	Non-small cell lung cancer cell line
Ac	Acetyl
AMC	7-Amino-4-methylcoumarin
APL	Acute promyelocitic leukemia
ARG	R, Arginine
ASN	N, Asparagine
ASP	D, Aspartic acid
Au	Gold
Bak	Bcl-2 antagonist killer (pro-apoptotic)
Bax	Bcl-2 associated X protein (pro-apoptotic)
Bcl-2	B-cell lymphoma 2 (anti-apoptotic)
Bcl _{xl}	B-cell lymphoma-extra large (anti-apoptotic)
Boc	<i>tert</i> -Butoxycarbonyl
C	Carbon
Ca ²⁺	Calcium ion
CD ₃ OD	Deuterated methanol
CDCl ₃	Deuterated chloroform

CO ₂	Carbon dioxide
COPD	Chronic obstructive pulmonary disease
CTCL	Cutaneous T-cell lymphoma
CuSO ₄ .5H ₂ O	Copper (II) sulfate pentahydrate
CYS	C, Cysteine
d	Doublet
DCM	Dichloromethane
DMEM	Dulbecco's modified eagle medium
DMSO	Dimethyl sulfoxide
DNA	Deoxyribonucleic acid
DU-145	Androgen independent prostate cancer cell line
ECG	Electrocardiogram
EDCI	1-Ethyl-3-(3-dimethylaminopropyl)carbodiimide
EMEM	Eagle's minimum essential medium
ER	Estrogen receptor
ESI	Electrospray ionization
Et ₂ O	Diethyl ether
EtOAc	Ethyl acetate
EtOH	Ethanol
FA	Folic acid
FBS	Fetal bovine serum
FDA	Food and Drug Administration
FK228	Romidepsin (HDAC inhibitor)

fmoc	Fluorenylmethyloxycarbonyl
FR	Folate receptor
FR (+)	Folate receptor positive
FR (-)	Folate receptor negative
GLU	E, Glutamic acid
H ₂ O	Water
H4	Histone H4
HAT	Histone acetyl transferase
hCE1	Human carboxylesterase 1
HDAC	Histone deacetylase
HDACi	Histone deacetylase inhibitor
HeLa	Cervical carcinoma cell line
hERG	Human-ether-à-go-go
HIV	Human immunodeficiency virus
HOBt	Hydroxybenzotriazole
HPLC	High-performance liquid chromatography
HRMS	High resolution mass spectrometry
HSP90	Heat shock protein 90
HTS	High throughput screening
Hz	Hertz
IBCF	Isobutyl chloroformate
IC ₅₀	Half maximal inhibitory concentration
IP ₃ R	Inositol 1,4,5-triphosphate receptor

J	Coupling constant
Jurkat	T-cell leukemia cell line
Jurkat J- γ	Subline of Jurkat with no phospholipase C- γ 1 activity
K ⁺	Potassium ion
K ₂ CO ₃	Potassium carbonate
KB	Oral carcinoma cell line
K _m	Binding constant
LNCaP	Androgen dependent prostate cancer cell line
LYS	K, Lysine
m	Multiplet
m/z	Mass to charge ratio
MCF-7	Breast cancer cell line
MDR-1	Multidrug resistance protein 1
MeOH	Methanol
MHC	Major histocompatibility complex
MHz	Mega Hertz
mL	Milliliter
MMP	Matrix metalloproteinase
MS	Mass spectrometry
MTS	3-(4,5-dimethylthiazol-2-yl)-5-(3-carboxymethoxyphenyl)-2-(4-sulfophenyl)-2H-tetrazolium
Na ⁺	Sodium ion

Na ₂ SO ₄	Sodium sulfate
NAD ⁺	Nicotinamide adenine dinucleotide
NaHCO ₃	Sodium Bicarbonate
NaN ₃	Sodium azide
NH ₄ Cl	Ammonium chloride
NH ₄ OH	Ammonium hydroxide
NI	No inhibition
nM	Nanomolar
NMM	<i>N</i> -Methylmorpholine
NMR	Nuclear magnetic resonance
NT	Not tested
O-trityl	<i>O</i> -Triphenylmethyl
p21	Cyclin dependent kinase inhibitor
p53	Tumor suppressor protein
PBS	Phosphate buffered saline
PCFT	Proton coupled folate transporter
PDB	Protein databank
pen/strep	Penicillin/streptomycin
P-gp	Permeability glycoprotein
Phe	Phenyl
PHE	F, phenylalanine
PLC-γ1	Phospholipase C-γ1
PLC-γ2	Phospholipase C-γ2

PML	Promyelocytic leukemia protein
PPh ₃	Triphenylphosphine
ppm	Parts per million
PPV	Positive predictive value
prep TLC	Preparatory thin layer chromatography
q	Quartet
	Time between the beginning of the Q wave
QT interval	and the end of T wave in the cardiac electrical cycle
RAR	Retinoic acid receptor
RFC	Reduced folate carrier
RNA	Ribonucleic acid
ROS	Reactive oxygen species
RPMI	Roswell Park Memorial Institute medium
rt	Room temperature
s	Singlet
SAHA	Suberoylanilide hydroxamic acid
	Self-assembled monolayers for matrix-assited laser desorption
SAMDI	ionization
SAR	Structure activity relationship
SDS	Sodium dodecyl sulfate
SER	S, Serine
SHI-1:2	Selective HDAC inhibitor for isoform 1 and 2

siRNA	Small interfering RNA
SIRT	Sirtuin
t	Triplet
$t_{1/2}$	Half life
TBP-2	Thioredoxin-binding protein
TCP	Thrombocytopenia
<i>tert</i>	Tertiary
TFA	Trifluoroacetic acid
TfN ₃	Trifluoromethanesulfonyl azide
THF	Tetrahydrofuran
TIPS	Triisopropylsilane
TLC	Thin layer chromatography
TMG	Tetramethylguanidine
TPO	Thrombopoietin
t_{ret}	Retention time
TSA	Trichostatin A
TYR	Y, Tyrosine
UV	Ultra violet
VEGF	Vascular endothelial growth factor
Vero	Monkey kidney epithelial cell line
XIAP	X-Linked inhibitor of apoptosis protein (anti-apoptotic)
ZBG	Zinc binding group
Zn ²⁺	Zinc ion

λ_{em}	Emission wavelength
λ_{ex}	Excitation wavelength
μg	Microgram
μM	Micromolar

SUMMARY

Epigenetic mechanisms have recently emerged as key regulators of many cellular processes. Among such mechanisms, covalent post-translational modifications to histone are the most studied. Such covalent modifications include methylation, ubiquitination, sumoylation and acetylation which impact the chromatin structure. Histone acetylation by histone acetyl transferase (HAT) results in the unwinding of the chromatin leading to the accessibility of the cellular transcription machinery to the genome. HAT's function is counterbalanced by that of histone deacetylase (HDAC) leading to a highly coiled chromatin thus silencing genes. To date, there are 11 zinc dependent HDAC isoforms, which will be the focus of my discussion, and 8 nicotinamide adenine dinucleotide (NAD⁺) dependent isoforms. Despite being referred to as HDACs, substrates of these enzymes include non-histone proteins. Due to their involvement in gene regulation, HDACs are upregulated in various malignancies leading to the development of HDAC inhibitors (HDACi) as potential cancer therapeutics. Most inhibitors of HDACs follow a pharmacophoric model which includes a surface recognition group connected by a linker to a zinc binding group (ZBG). HDAC as a target for cancer chemotherapy was validated by the approvals of SAHA and FK228 (Romidepsin) by the FDA in 2006 and 2009 respectively for the treatment of cutaneous T cell lymphoma. Despite the successes of these inhibitors against leukemias and lymphomas as demonstrated through various clinical trials, there are many problems associated with the clinical use of HDACi including the lack of efficacy against solid tumors. SAHA which constitutes the gold standard of HDACi, is a pan-inhibitor thus inhibits isoforms not involved in

tumorigenesis such as HDAC4, 5, 7 and 9 resulting in adverse side effects. Furthermore, both clinically approved agents have been associated with a severe cardiotoxicity.

My thesis work aimed at addressing some of the aforementioned issues through the development of isoform-selective HDACi, and the targeted delivery of isoform-selective HDACi and HDAC pan-inhibitors. Previous work in our lab by Dr. Vishal Patil identified the 3-hydroxy-pyridin-2-thione (3-HPT) as a novel ZBG for HDAC inhibition. Incorporation of this novel ZBG into the pharmacophoric model conferred a selectivity towards HDAC6 or 8 as the small molecules obtained were devoid of HDAC1 inhibition. I established that the 3-HPT containing HDACi possess anticancer activity against various cancer cell lines including the androgen independent prostate cancer line DU-145, the androgen dependent prostate cancer LNCaP, the T cell leukemia Jurkat and its mutant subline Jurkat J γ which was resistant to SAHA-induced apoptosis. Furthermore, these selective HDACi were not cytotoxic to the healthy cell Vero at the highest tested concentration of 20 μ M.

Based on the previously described overexpression of the folate receptors (FR) in cancer cells, I also selectively delivered various HDACi to FR positive (+) tumors such the oral carcinoma KB and the cervical cancer cell line HeLa. Pan-inhibition of HDACs in cancer cell constitutes an important methodology for cancer therapy as the damages inflicted can be compounded. However, the risk of having off target effects due to toxicity to healthy cells is also increased. As such, using the folic and pteronic acids which have been shown to deliver cytotoxic cargo to cancer cells, I designed and synthesized folate- and pteronic- based HDAC inhibitors bearing the hydroxamate ZBG. These folate and pteronic based inhibitors may not only be less cytotoxic to healthy cells which lack the

FR but will also lead to high intratumoral drugs concentration thus addressing the described lack of efficacy of HDACi against solid tumors. These constructs were achieved by incorporating the folate or the pterioic acid in the pharmacophoric model as surface recognition groups. From the structure activity relationship (SAR) conducted, the pterioic based hydroxamates were pan-inhibitors, whereas the folate based were selective for HDAC6. I also selectively delivered isoform selective HDACi using the folic acid as homing tool. This represented the first time that both methodologies were combined yielding folate based biaryl benzamide HDACi selective for HDAC1. It followed from cell viability assays that only the pterioic based hydroxamates HDACi possess anticancer activity against the KB and HeLa cells. I confirmed the intracellular targets of the pterioic based hydroxamates (HDAC1 and 6) through immunoblotting. Furthermore, I established that in KB cells HDAC1 inhibition led to cell death whereas HDAC6 inhibition has no impact on cell viability. To my knowledge, this represents the first literature report of such impact of HDAC isoform inhibition in KB cells.

Understanding the mechanisms of resistance to HDACi constitutes another avenue by which their clinical use can be improved. Such knowledge can result in the selection of appropriate drugs to be used alongside HDACi as part of combination therapy thus potentiating their therapeutic effects. Balasubramanian et al. reported that the lack of phospholipase C- γ 1 (PLC- γ 1) conferred to Jurkat J γ cells resistance to apoptosis induced by a HDAC8 selective inhibitor. Through my thesis work, I was able to demonstrate that Jurkat J γ cells were also resistant to apoptosis induced by HDAC1 or HDAC6 selective inhibitors, pan-inhibitors including SAHA and the clinically approved

FK228 (Romidepsin) suggesting that a loss-of-function mutation of PLC- γ 1 can constitute a novel mechanism of resistance to HDACi-induced apoptosis.

Although my thesis work aimed at improving HDACi therapy from the drug discovery perspective, improvements still need to be made from the clinical standpoint such as the identification of patients who can truly benefit from HDACi therapy and the use of better biomarkers to monitor the outcome of the treatment.

CHAPTER 1

INTRODUCTION

1.1. Background

Since its initial use by Conrad Waddington in 1939, the term "epigenetics" has evolved from the interactions between genes and their products leading to a phenotype to be understood as the study of mechanisms controlling gene expression.^{1,2} The study of epigenetic mechanisms is not only crucial in fields such as developmental biology but has become prominent for biomedical research as many of pathological conditions can be linked to the cellular epigenetic machinery going awry.^{1,3} Such diseases include cancer whose hallmarks are all controlled by epigenetic mechanisms.^{4,5,6} Among the epigenetic mechanisms which include DNA methylation, histone modifications and nucleosome positioning, certain covalent changes to histone have been suggested to affect the chromatin structure through modulation of electrostatic interactions between DNA and histones and provide interfaces for proteins-proteins interactions.^{2,7}

Post-translational modifications to histones encompass methylation, phosphorylation, ubiquitination, sumoylation and acetylation.⁸ Although all these modifications are crucial for epigenetic regulation of cellular activity, acetylation and deacetylation have now emerged as key regulatory mechanisms not only for histones activities but for more than 2000 proteins.⁹

1.2. Histone acetylation

Despite being called histone acetyl transferases (HATs), these enzymes catalyze the addition of an acetyl group to lysine residue of various targets including non-histone proteins.¹⁰ Histone acetylation results in the unwinding of the chromatin allowing the cellular transcription machinery to access the genome. Aberrant HAT activity has been linked to diseases such as asthma, COPD, cancer and viral infections such as HIV.¹¹ In cancer, the altered HAT activity is a result of mutation as opposed to change in expression levels in asthma or COPD.^{12,13} Even though HATs inhibition seem to be a way forward in the treatment of selected illnesses, current inhibitors suffer from low cellular permeability resulting in a decreased interest in their clinical development and use.^{11,14} Moreover, the activity of HAT is modulated by the multiproteins complexes they are part of, rendering the *in vivo* activity of HAT inhibitors highly unpredictable.¹⁴

1.3. Histone deacetylation

Just as acetylation is crucial for the regulation of a multitude of proteins, deacetylation is also key in their activity. Substrates targeted by deacetylation include HSP90, tubulin, androgen receptors, p53, histones, etc.^{12, 15} For instance, the deacetylation of HSP90 results in its dissociation from its clients proteins leading to their degradation, whereas histones deacetylation leads to chromatin structure remodeling. The deacetylation of proteins including histones is mediated by histone deacetylases (HDACs), which catalytically hydrolyze the acetyl moiety from lysine (Figure 1.1).¹⁶

1.4. Histone deacetylase (HDAC)

Equally important to histones acetylation is their deacetylation suggesting that the overall activity of histone is dictated by the equilibrium between acetylated and deacetylated lysine residues. The removal of acetyl groups from histone tails yields positive charges on the lysine residues leading to favorable electrostatic interactions with the negatively charged phosphate backbone of the DNA. This results in a tightly coiled chromatin leading to gene silencing. Based on their sequences, there are 18 HDAC isoforms grouped into four classes comprised of the zinc dependent classes I, II and IV and the NAD^+ dependent class III (Table 1.1). Members of Class I HDAC are HDAC1, 2, 3, and 8 which are localized in the nucleus. HDAC4, 5, 7 and 9 form the class IIa which shuttle between the nucleus and the cytoplasm. The cytoplasmic HDAC6 and 10 constitute the class IIb. The final zinc dependent, HDAC11, is the sole member of class IV.¹⁶ The class III HDAC is comprised of the NAD^+ dependent sirtuins which will not be the focus of my discussion. Any further mention of HDAC will be referring to the zinc dependent isozymes. The active site of these enzymes is located inside a hydrophobic pocket and has a Zn^{2+} (Fig. 1.2). During the hydrolysis of the acetylated lysine residue, it penetrates the enzymatic pocket enabling the coordination of its acetate moiety by the Zn^{2+} followed by the nucleophilic attack of water yielding a tetrahedral intermediate which collapses to release the deacetylated lysine and an acetate ion (Fig.1.1).¹⁷

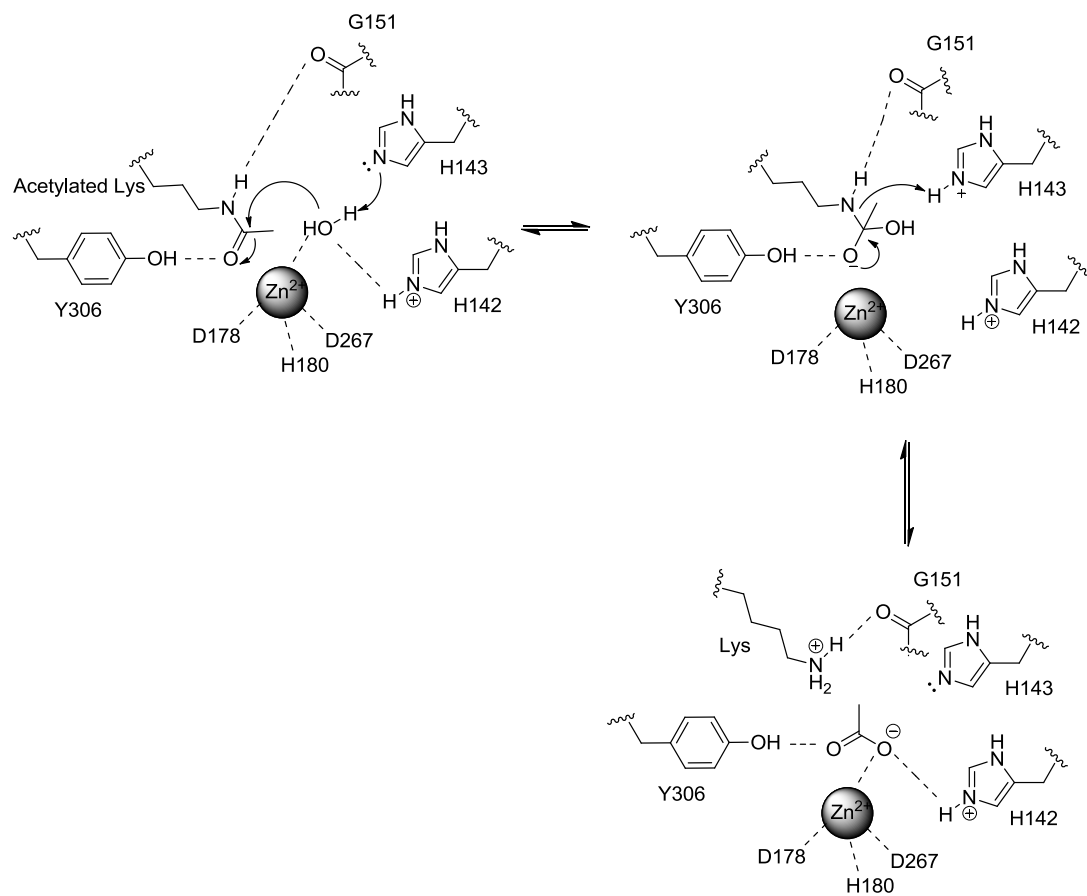


Figure 1.1: Proposed mechanism of acetyl-Lys deacetylation by HDAC8. G151 refers to the backbone C=O of glycine 151.¹⁷

Table 1.1: Characteristics of Zinc dependent HDACs.^{12,16}

Class	Isoform	Cellular localization	Substrate
I	HDAC1	Nucleus	p53
	HDAC2		Bcl-6
	HDAC3		RelA
	HDAC8		-
IIA	HDAC4	Nucleus/Cytoplasm	GATA-1
	HDAC5		Smad7
	HDAC7		PLAG1
	HDAC9		-
IIB	HDAC6	Cytoplasm	Tubulin, HSP90
	HDAC10		-
IV	HDAC11	Nucleus/Cytoplasm	-

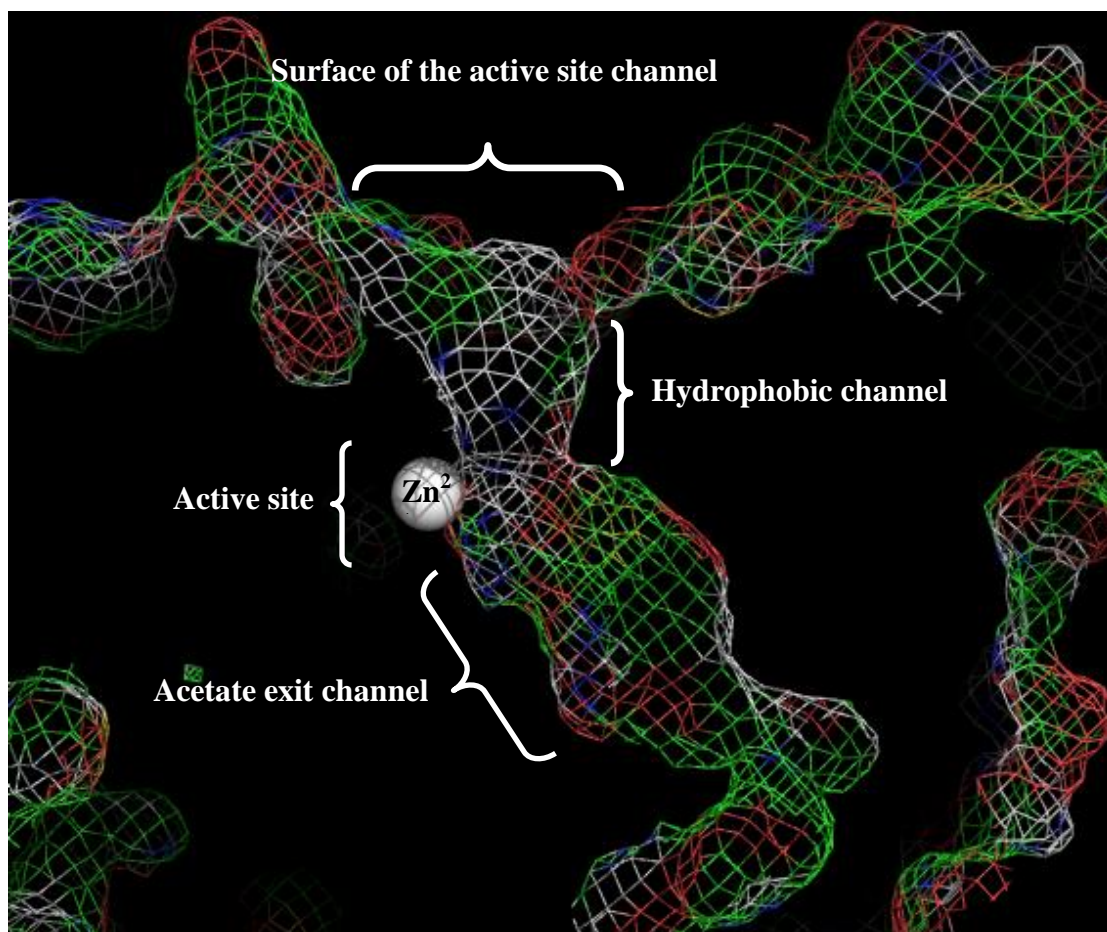


Figure 1.2: Cross section of the homology model of HDAC1 built from HDAC2 (PDB code: 3MAX). Key regions of the enzyme are highlighted. Interactions of a potential inhibitor with the vicinity of the surface of the HDAC channel, the hydrophobic channel and Zn^{2+} are crucial for optimal anti-HDAC activity.

1.5. Role of HDACs in healthy cells

Knockout experiments of HDAC in mice revealed the importance of class I enzymes for cellular proliferation. The lack of HDAC1 is lethal during the embryonic stage and that of HDAC2 results in severe proliferation defect of cardiomyocytes.^{15,18} HDAC6 knockout is not detrimental to the overall health of mice, whereas the lack of any class IIa isoforms lead to various degree of cardiovascular anomalies.^{12, 15} Other studies designate HDAC6 as the primary deacetylase of non-histone proteins such as tubulin and

many other cytosolic proteins.¹⁹ Although these knockout experiments in mice demonstrated the crucial role of HDACs in embryonic development and survival, HDACs activities are important for many other cellular processes such as metabolism, endocytosis, etc (Fig.1.3).^{9,20}

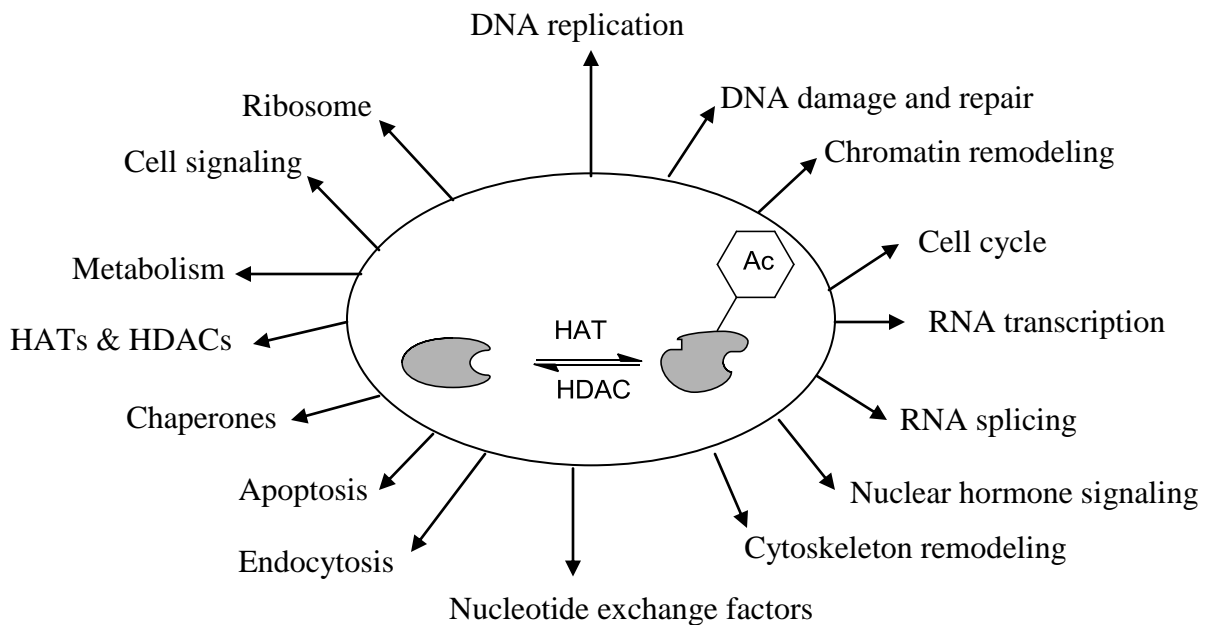


Figure 1.3: Examples of cellular processes regulated by HDAC/HAT.^{9,20}

1.6. Regulation of HDAC activity

The function of HDACs is modulated through complex protein-protein interactions and covalent modifications, such as sumoylation and phosphorylation, whose impact is determinant for the cellular localization of class IIa isoforms. Specifically, phosphorylation of HDAC4 and 5 results in their association with 14-3-3 proteins preventing their translocation to the nucleus where they function as transcription repressor.²¹ Phosphorylation although not involved in the cellular localization of class I HDACs is still crucial for the modulation of HDAC1 activity as HDAC1 mutant lacking

specific sites of phosphorylation (Ser⁴²¹ and Ser⁴²³) has a reduced activity including transcription repression. Other regulation mechanisms of HDAC activity include the modulation of their genes' expression and their proteolytic degradation.²²

1.7. HDAC in cancer

Due to their involvement in gene regulation, HDACs are implicated in various biological phenomena such as embryogenesis, metabolic homeostasis and diseases such as neurodegenerative, parasitic infections and cancer.²³⁻³¹ The correlation between the latter and HDAC activity has been best described in leukemias where fusion proteins resulting from chromosomal translocations recruit HDAC enzymes as part of gene silencing complexes non-responsive to cellular control.¹³ In acute promyelocytic leukemia (APL), chromosomal translocations result in an aberrant fusion protein containing the retinoic acid receptor (RAR) α and promyelocytic-leukemia protein (PML), which upon dimerization binds to the DNA, recruits HDACs and represses the RAR controlled genes. The ensuing gene silencing cannot be overcome in the presence of retinoic acid as it is the case in healthy cells.³² Despite the scarcity of cancer resulting from direct mutations of HDACs, a multitude of malignancies have been reported to possess altered HDAC expression levels (Table 1.2). In prostate cancer, class I HDACs such 1, 2, and 3 are overexpressed relative to healthy prostate cells.³³ A similar HDAC pattern was also detected in selected subtypes of ovarian and endometrial cancers,³⁴ whereas in cutaneous T-cell lymphoma (CTCL), the overexpressed trio is comprised of HDAC1, 2 and 6.³⁵ Furthermore, selective silencing of HDAC1 through siRNA

knockdown resulted in the growth inhibition of human cancer cells such as MCF7, emphasizing the involvement of this HDAC isozyme in tumorigenesis.³⁶

Table 1.2: HDACs overexpression in cancer.³⁵

Malignancy	HDAC isoforms
Cutaneous T-cell lymphoma	1, 2, 6
Gastric carcinoma	1, 2, 3
Colorectal carcinoma	1, 2, 3
Hepatocellular carcinoma	1
Prostate carcinoma	1, 2, 3
Ovarian serous carcinoma	1, 2, 3
Ovarian endometrioid carcinoma	1, 2, 3
Endometrial endometrioid carcinoma	1, 2, 3
Estrogen positive breast carcinoma	6
Breast carcinoma	6

1.8. HDAC inhibitor (HDACi) for cancer therapy

Based on the involvement of HDAC in the tumorigenesis of selected malignancies, HDAC inhibition has become an attractive target for cancer therapy. Starting from DMSO in 1971 which induced differentiation of leukemia cells, many HDAC inhibitors (HDACi) have been designed resulting today in a myriad of small molecules such as SAHA as novel therapeutics for cancer therapy.³⁷

1.8.1. HDACi pharmacophoric model

Most HDACi are competitive inhibitors of the acetylated lysine substrate. Hence, HDACi need to bind to the enzyme's active site to elicit anti-deacetylase activity. For optimum interaction with HDAC active sites, all HDACi have a pharmacophoric model consisting of: a surface recognition group which interacts with the amino acid side chains at the enzyme outer rim in the vicinity of the active site; a linker traversing the hydrophobic channel leading to the active site; and a zinc binding group (ZBG) which chelates the zinc ion at the base of the active site (Figures 1.4 and 1.5). Although many ZBGs such as benzamide, carboxylic acid, thiols, etc. have been used to achieve zinc chelation, hydroxamic acid remains by far the most employed due to the strength of its bidentate chelation of the catalytic Zn^{2+} .¹⁶

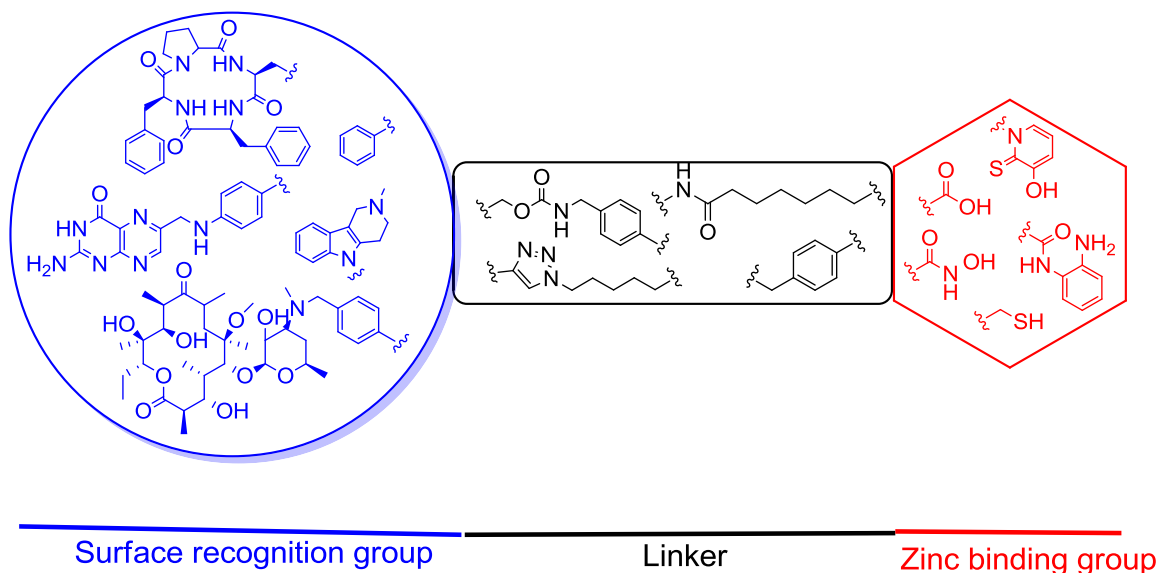


Figure 1.4: HDACi pharmacophoric model. The various structures displayed under each segment represent examples of chemical moieties used in the literature to model the said segment. Note the color code, Blue: surface recognition group; Black: linker; Red: Zinc binding group.

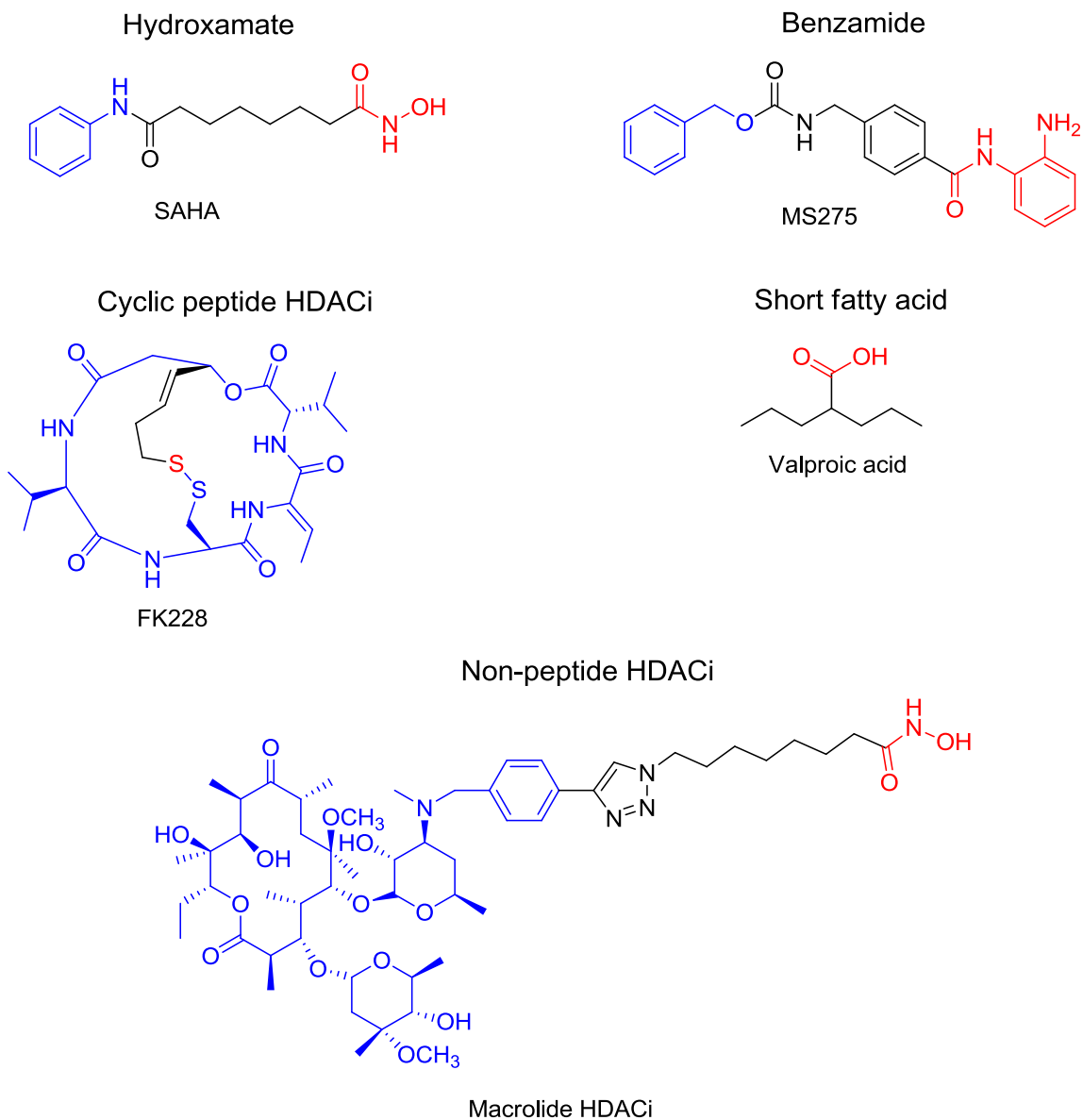


Figure 1.5: Example of HDACi. Note the color code, Blue: surface recognition group; Black: linker; Red: Zinc binding group.

1.8.2. Mechanisms of action of HDACi

Exposure of malignant cells to HDACi can result in phenotypical outcomes such as differentiation, immunogenicity, and apoptosis (Figure 1.6).¹³ The induction of apoptosis has been linked to an increased reactive oxygen species (ROS) production, expression of p21, activation of both extrinsic (death toll receptors) and intrinsic (mitochondrial) apoptotic pathways and acetylation of the chaperone HSP90 resulting in the degradation of its clients proteins (Figure 1.7).³⁸ Furthermore, HDACi downregulate proangiogenic factors such as VEGF and genes contributing to metastasis resulting in a decrease in tumor size and invasiveness.³⁹

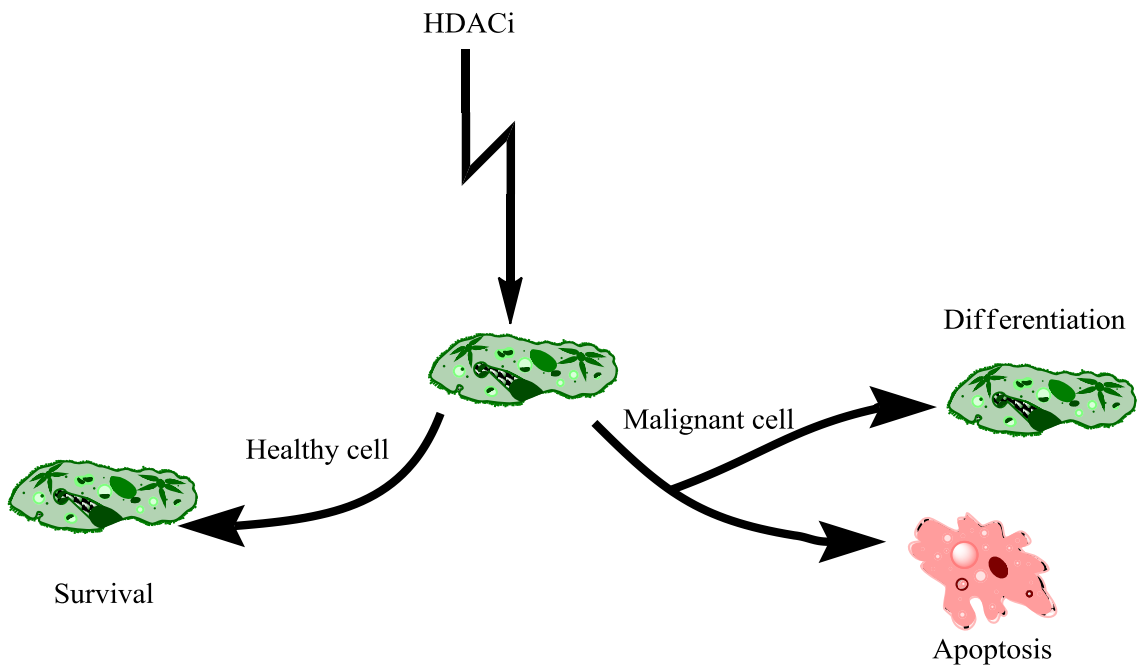


Figure 1.6: Phenotypical outcome of HDACi on healthy and cancer cells. Exposure of malignant cells to HDACi results in two phenotypes: cell cycle arrest leading to differentiation or apoptosis, whereas similar cell cycle arrest has no impact on healthy cells rendering cancer cells more sensitive to HDACi.¹³

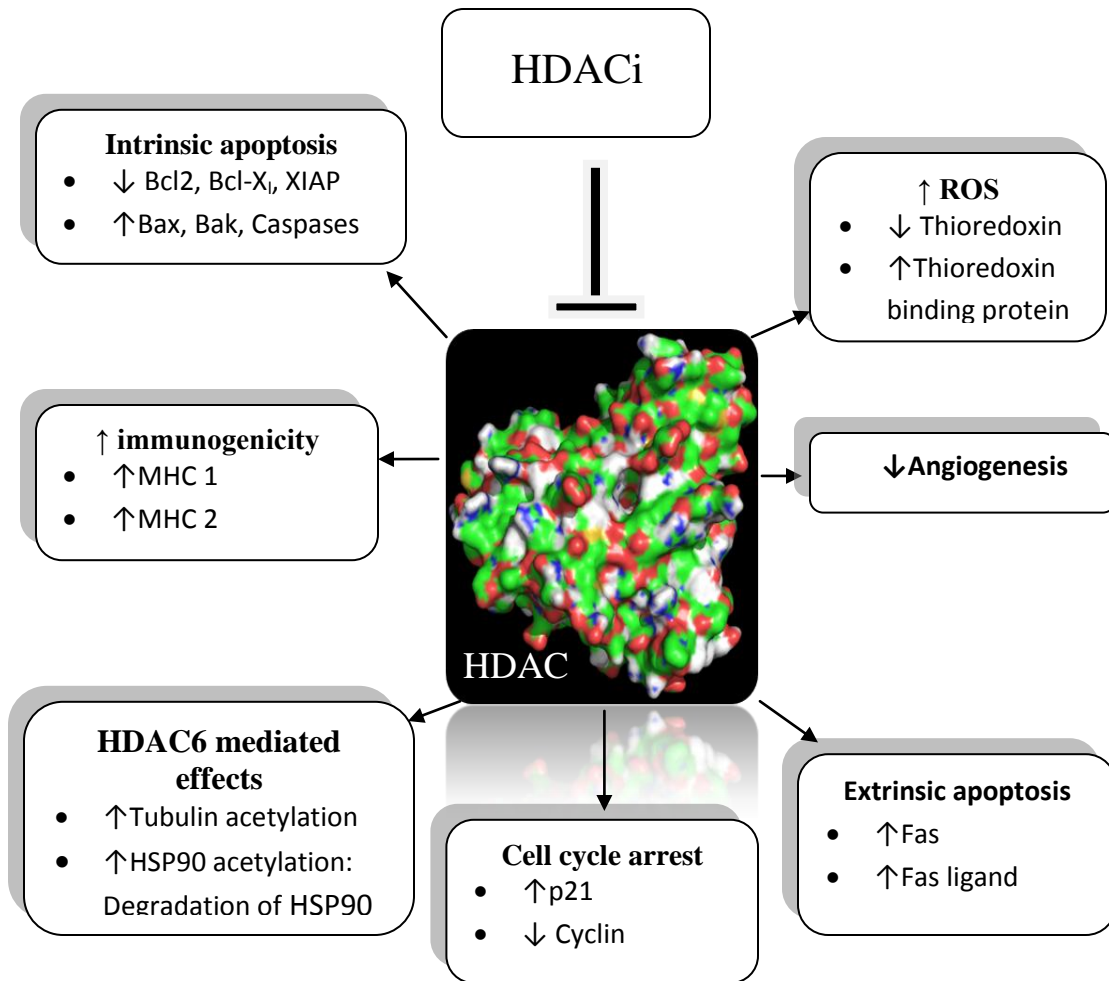


Figure 1.7: Mechanisms of action of HDACi.^{13,20}

1.9. HDACi clinical trials

Since the first clinical trial of the HDACi phenyl butyrate in patients with refractory malignancies in the 1990's, there has been a tremendous increase in clinical trials exploring the anticancer potential of HDACi (Figure 1.8).⁴⁰ Up-to-date, there have been 354 clinical trials reported to clinicaltrials.gov that looked or are looking at HDACi as monotherapy or in combination with other chemotherapeutic agents, but the exact number may potentially be higher as a time delay can exist between a trial beginning and its report date to the database.

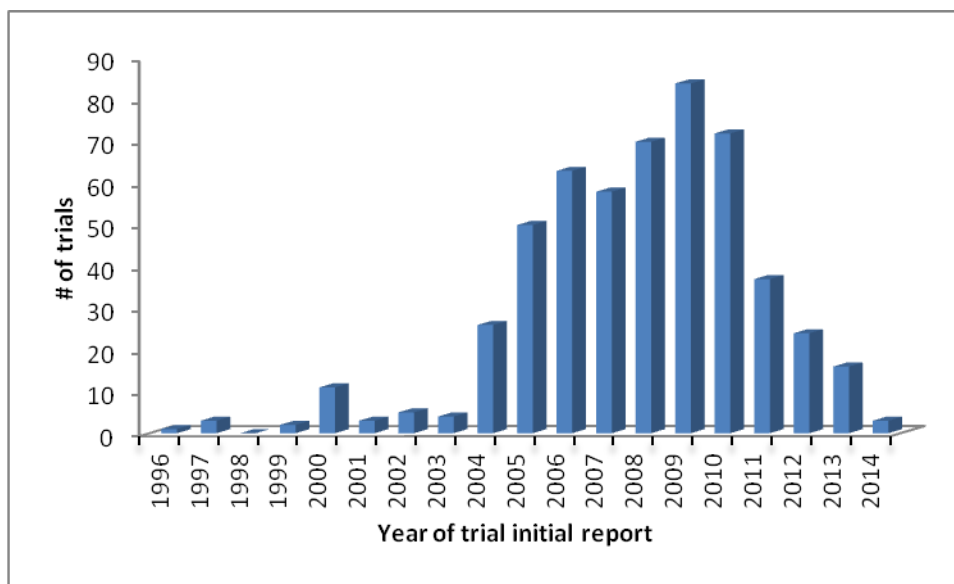
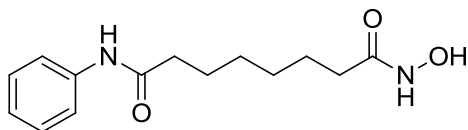


Figure 1.8: Clinical trials of HDACi as monotherapy or in combination with other chemotherapeutic agents. Data compiled from clinicaltrials.gov (last access 02/06/2014)

1.9.1. Monotherapy trials

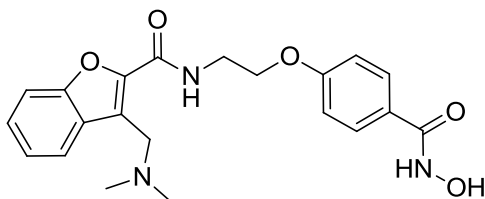
1.9.1.1. Hydroxamic acids

SAHA (Vorinostat)



SAHA, a hydroxamate-based HDAC pan-inhibitor, was the first clinically approved HDACi by the FDA in 2006 for patients with CTCL.⁴¹ During one of its clinical trials in patients with refractory CTCL, almost 30% of patients showed an objective response lasting more than 185 days. Moreover, 21% of participants had been relieved of their pruritis, a debilitating symptom often associated with the disease.^{42,43} In another trial, up to 45% of pruritic patients saw a reduction of their symptoms.⁴⁴ Although well tolerated by participants of the trials, administration of SAHA was associated with side effects seen with other chemotherapy agents such as nausea, vomiting, fatigue, diarrhea, thrombocytopenia, anemia and serious adverse events such as sepsis and pulmonary embolism.^{43,44}

PCI-24871



Following the approval of SAHA, other hydroxamate-based HDACi including PCI-24871 have been designed and are currently in clinical trials. Despite the observation of side effects such as nausea, vomiting, fatigue and diarrhea, PCI-24871 was

well tolerated and disease stabilization was observed in 5 out of 13 patients with refractory advanced solid tumors.⁴⁵ Although the majority of novel hydroxamate based HDACi (Figure 1.9) are relative well tolerated by clinical trials participants, early indications suggest that they are more efficacious in hematological malignancies compared to solid tumors.⁴⁶

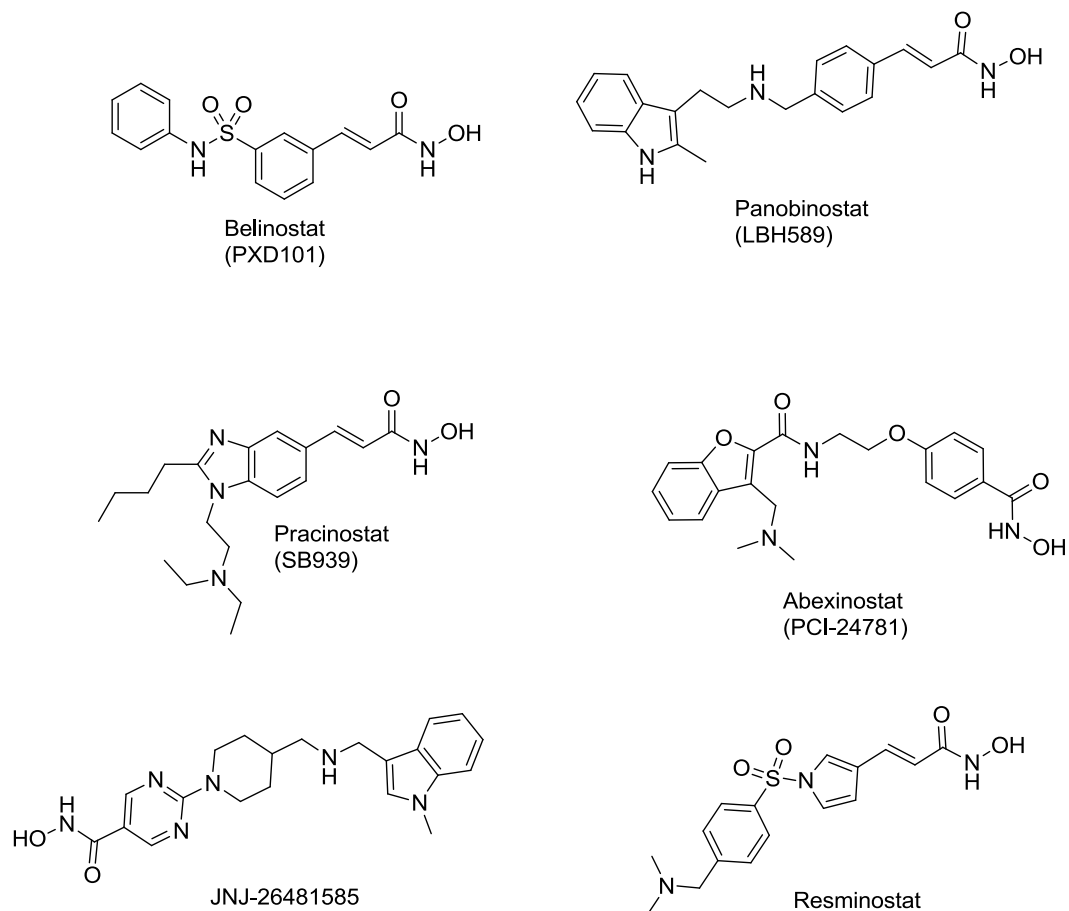
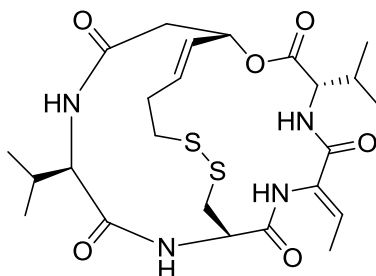


Figure 1.9: Structures of other hydroxamate based HDACi in clinical trials.⁴⁶

1.9.1.2. Cyclic peptides

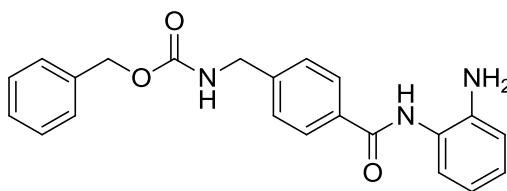
FK228 (Romidepsin)



This antibiotic agent isolated from *Chromobacterium Violaceum* is the second HDACi approved for clinical use in patients with CTCL by the FDA in 2009.^{47,48} During a phase II trial, it demonstrated a similar response rate as SAHA in patients with CTCL, however, the median duration response was significantly higher (13.7 months). Furthermore, three patients with Sézary syndrome, the most severe form of the disease, had complete remission. Side effects, such as fatigue, nausea and vomiting and hematologic abnormalities such as pancytopenia, were observed. In 71% of subjects, an asymptomatic electrocardiogram (ECG) was also seen.⁴⁹

1.9.1.3. Benzamides

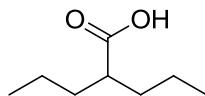
MS275 (Entinostat)



Although this class I selective HDACi has been shown to possess anti-proliferative effect in preclinical studies^{50,51} and its oral administration is well tolerated during clinical trials⁵², it has shown little to no efficacy in patients with refractory

leukemia and metastatic melanoma.^{53,54} This lack of efficacy during the oral administration may not be linked to its stability in the plasma as its half life ($T_{1/2}$) was greater than 50 hours.⁵²

1.9.1.4. Short fatty acid



Valproic acid (VPA)

This class of HDACi is not as potent as their hydroxamate or benzamide congeners but is well tolerated. Valproic acid, a prototypical carboxylic acid based HDACi, has shown activity in patients with myelodysplastic syndromes.⁵⁵

1.9.2. Combination therapy of HDACi with other chemotherapy agents

Except SAHA and FK228 (Romidepsin), no other HDACi has been approved for the treatment of cancer. Clinical indication of these drugs is solely for CTCL, a lymphoma, highlighting their lack of efficacy as monotherapy against solid tumors.^{56,57,58} The only silver lining is the disease stabilization observed during their clinical trials as standalone therapeutic agents, suggesting that their combination with other chemotherapy may yield more efficacious treatments against solid tumors. Indeed, SAHA, FK228, valproic acid and other HDACi inhibitors are currently being evaluated in combination with tamoxifen, Isotretinoin, gemcitabine paclitaxel, bortezomib and many other drugs.^{59,60,39,55} A potential setback for such combination therapies may be a premature development of resistance by the cancer to the other chemotherapeutic used in the combination. HDACi, through gene expression modulation, upregulate the P-

glycoprotein (P-gp) multidrug resistance protein 1 (MDR-1) which efflux chemotherapy drugs from cancer cells.^{61,62} As such, the efficacy of the combination chemotherapy agents may be undermined by the efflux pumps upregulated upon exposure to HDACi.

1.10. Problems associated with HDACi therapy

Besides the lack of clinical efficacy of HDACi against solid tumors, other issues have been associated with their clinical trials and use. Like other chemotherapy drugs, HDACi are associated with multiple side effects (Table 1.3). I limit my discussion to the side effects induced by the FDA approved HDACi as they are the most studied.

1.10.1. Gastrointestinal

Nausea and vomiting were commonly observed leading to the prophylactic recommendation of anti-emetic. Dehydration was also present in several patients. Other gastrointestinal related issues included anorexia, constipation, and dry mouth.⁶³

1.10.2. Constitutional

Fatigue was the most common side effect related to HDACi although fever was also noted. These effects are believed to be cytokine (Interleukin-6) mediated as they did not correlate with anemia or abnormal bloodworks.⁶³

1.10.3. Hematologic

A transient pancytopenia is associated with HDACi therapy, however, the blood counts returned to baseline within 10 days after the removal of the offending agents

suggesting a lack of true myelosuppression. Furthermore, *in vitro* studies revealed that the IC₅₀ of FK228 (Romidepsin) during a granulocyte-macrophage colony forming assay was greater than 3 μM, whereas its peak plasma concentration was 700 nM in CTCL patients, implying the existence of a cytotoxicity mechanism other than a direct impact on the bone marrow.⁶³

1.10.4. Cardiac

Based on the side effect profile of HDACi discussed thus far, they appear to be well tolerated compared to other chemotherapy agents. However, ECG changes have been observed in individuals treated with HDACi leading to an extensive monitoring of their cardiac functions. ECG changes described in patients receiving SAHA or FK228 (Romidepsin) include ST depression and QT prolongation which can lead to the potentially fatal ventricular arrhythmia *torsades de pointes*.⁶⁴ Although the QT prolongation due to HDACi may be clinically insignificant, it becomes a greater concern in patients with predisposing factors such as diabetes mellitus, obesity, hypothyroidism, and long QT syndrome.⁶⁵ Prior cerebrovascular and heart diseases can also exacerbate minor QT prolongation.^{65,66} A baseline ECG study in cancer patients prior to therapy revealed the existence of cardiac abnormalities such as atrial fibrillation in 36% of participants, putting this population group at an increased risk of HDACi induced adverse cardiac event.⁶⁷ Predisposition to QT prolongation can be iatrogenic as well. Antiemetics, antibiotics, antifungal, and antidepressants which are concomitantly administered with chemotherapy drugs to alleviate side effects can increase QT interval.^{66,65,68} Furthermore, there are several drugs currently available on the market that may induce QT

prolongation.⁶⁸ Metabolic disturbances such as electrolyte imbalance ensuing from chemotherapy related anorexia or vomiting constitute other non negligible risk factors of QT prolongation.^{65,69}

Table 1.3: Percentage of common non cardiac side effects seen during HDACi therapy (SAHA and Romidepsin).⁶³

Side effects	SAHA	Romidepsin
Fatigue	59	53
Nausea	49	57
Vomiting	20	38
Anorexia	38	38
Weight loss	29	3
Diarrhea	53	12
Anemia	23	29
Thrombocytopenia	39	33
Neutropenia	4	24

1.11. Mechanisms of QT prolongation

To date, QT prolongation has been linked to improper cellular trafficking or functioning of the human ether-à-go-go (hERG) K⁺ channel.⁷⁰ Opening of the hERG channel during the cardiac cycle is required for proper ventricular repolarization, hence any interference with its activity can result in a prolongation of the QT interval.^{70,71} Most

drugs known to block this membrane protein, thus impeding on K^+ transport, bind to the inner cavity where key aromatic amino acids mitigate hydrophobic interactions with various lipophilic molecules.⁷² Although the hERG channel binding is the most accepted mechanism of drug-induced QT prolongation, increased degradation rate of the said channel can have the same outcome on QT interval as proven by Guo and coworkers with probucol, a cholesterol lowering drug known to induce QT prolongation.⁷³ Impact of HDACi on any key regulators of hERG channel activity such as MinK can also increase the QT interval in the absence of direct binding of the HDACi to the channel.^{72,74,75} Moreover, HDACi, as modulators of gene expression, can affect the expression of the hERG channel and that of its coregulators. Finally, the hERG channel has been the sole ion channel studied for HDACi-induced QT prolongation, however, enhancement of the Na^+ channel can have similar impact on QT interval as demonstrated with Alfuzosin a QT prolonging drug with no effect on hERG channel.⁷⁶

1.12. Improving HDACi therapy

Despite the involvement of HDAC in tumorigenesis, HDAC inhibition as a monotherapeutic agent for cancer is only effective and approved in CTCL, highlighting the need to develop novel HDACi. Extension of HDACi clinical use to other malignancies including solid tumors will require collaboration between researchers in the drug discovery and clinicians (Figure 1.10).

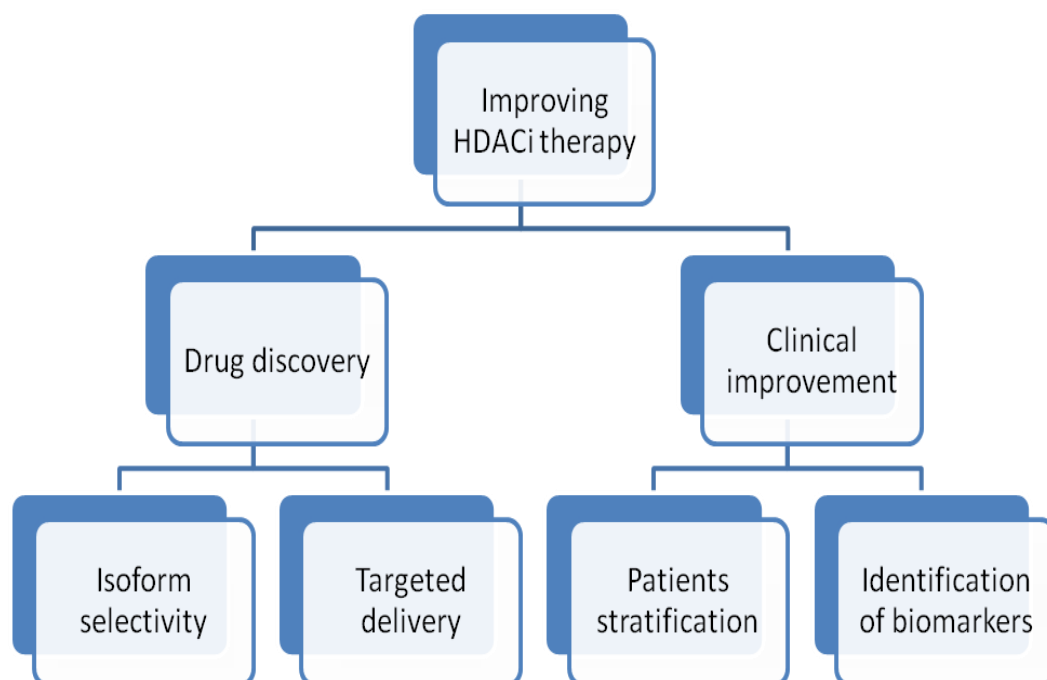


Figure 1.10: Key strategies for improving HDACi therapy.

1.12.1. Drug discovery

1.12.1.1. Incorporation of cardiac safety assessment in early stages of drug development

Currently, measuring the cardiac safety of a drug requires data from early clinical studies, where significant financial resources have already been used. To minimize the financial loss caused by failed clinical trials, incorporating a cardiac safety assay during the early (pre-clinical) stages of the drug development is an attractive avenue. Doing so will not only be beneficial for HDACi but also for other drugs as well. Shultz and his coworkers have used this method to develop HDACi with no hERG channel binding and potentially safe for the endocardium, however, clinical data is still needed to ensure that their HDACi are truly devoid of cardiotoxicity.⁷⁷

1.12.1.2. Isoform selective HDACi

Most HDACi shown to increase the QT interval clinically are pan-inhibitors.⁷⁸ Although hERG channel blocking has been the most accepted mechanism of cardiotoxicity of these drugs, it is conceivable that inhibition of class IIa isoforms may generate cardiotoxicity as HDAC5 and 9 have been shown to be cardioprotective by preventing the stress-induced cardiac remodeling.⁷⁹ Furthermore, these class IIa isoforms are not overexpressed in cancer as their class I congeners rendering their inhibition unnecessary. These facts suggest that isoform selective inhibitors devoid of class IIa inhibition may have fewer side effects and be well tolerated than the pan-inhibitors. Indeed earlier clinical trials results seem to support this observation as MS275 and CI-994, class I selective HDACi, are well tolerated and lack any QT effects.⁷⁸ The safety of isoform selective HDACi extend beyond that of class I selective compounds as ACY-1215, a selective HDAC6 (class IIb) inhibitor, is also safe with no dose-limiting toxicity.⁸⁰ If selective HDACi are well tolerated during clinical trials, the jury is still out when it comes to their efficacy as a monotherapy, although clinical trials with MS275 point to a lack of therapeutic efficacy.^{53,54} From a safety standpoint, isoform selective inhibitors are an attractive way for boosting clinical development and use of HDACi, however, their lack of efficacy highlighted during preliminary clinical trials suggest that their combination with other chemotherapy agents that are not substrates of the efflux pumps (P-gp) may be the only way forward.

1.12.1.3. Targeted delivery of HDACi

The clinically approved SAHA, a pan-inhibitor, is efficacious as a single agent against CTCL whereas most isoform selective inhibitors are not. These observations point to pan-inhibitors as the sole HDACi with potential use as monotherapy agents against cancer. In such a case, addressing the side effects (cardiotoxicity) ensuing from HDAC pan-inhibition becomes primordial. Targeting these small molecules has the potential of increasing their intratumoral concentration while minimizing delivery to healthy cells. This may not only address HDACi off target cytotoxic profile but also solve their lack of efficacy against solid tumors. The basic methodology for this targeted delivery which is localized administration is currently being evaluated in clinical trial through the use of the topical formulation of FK228 (Romidepsin) for CTCL patients with limited disease.⁸¹ Minimal systemic exposure of FK228 (Romidepsin) in this formulation may lessen its side effects. A prodrug strategy has also been utilized to selectively accumulate the HDACi CHR-2845 in monocytes/macrophages and monocytic malignancies expressing the intracellular esterase human carboxylesterase-1 (hCE1).⁸² Subsequent hydrolysis of the cell permeable CHR-2845 results in a charged molecule whose intracellular accumulation leads to a 20- to 100-fold increase in potency against tumors from monocytic lineage while being well tolerated by patients.⁸³ Another active targeting approach which has yet to go into clinical trials has been developed in our laboratory. This involves the modification of the HDACi pharmacophoric model to include ligands such as folic acid, antiestrogens and antiandrogen, whose receptors' expression is upregulated in cancer cells, leading to a selective accumulation in malignant cells (Figure 1.11) (Unpublished data).^{84,85} An alternate choice of ligand such as

macrolides can result in selective HDACi accumulation in the lung enabling the targeting of various cancers involving this organ.⁸⁶ The attractiveness of our active targeting strategies lies in their potential to minimize side effects while boosting anticancer activity against tumors. Recent studies have described the *de novo* expression of hERG channel in various malignancies enabling them to bypass mitotic signals such as Ca²⁺ influx⁸⁷ suggesting a potentially novel mechanism of action for the HDACi with affinity for the hERG channel. The targeted delivery of these inhibitors will ensure the selective accumulation of dual acting drugs (HDACi and hERG channel blocker) only in cancer cells.

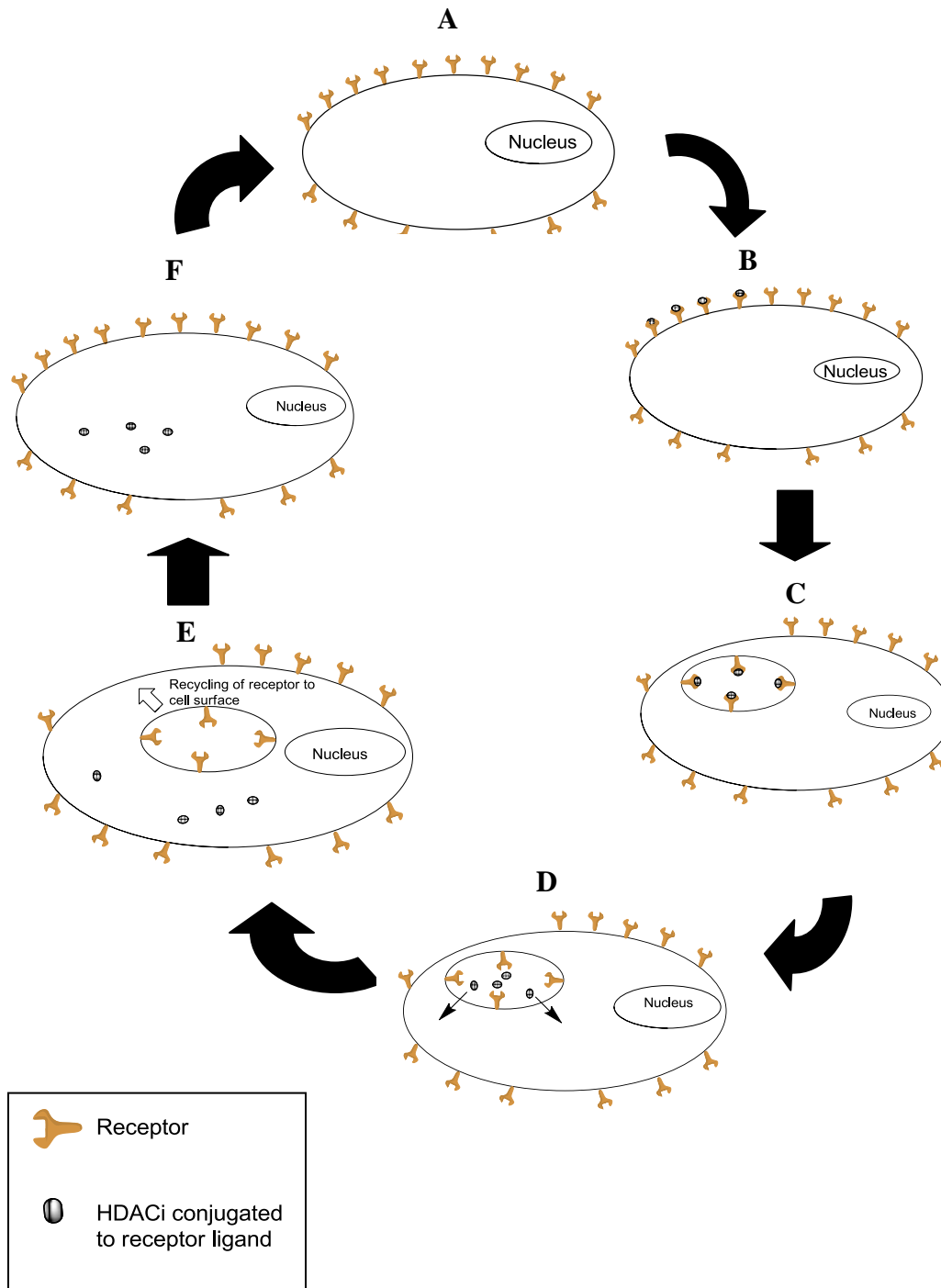


Figure 1.11: Active targeting of HDACi. **A)** The malignant cell overexpresses on its plasma membrane the receptors of a ligand required for its metabolism such as folate; **B)** The HDACi is conjugated to the ligand and exposed to the cell leading to binding of the ligand/HDACi complex to the receptors; **C)** Endocytosis of the HDACi/ligand conjugates; **D)** Release of the HDACi/ligand conjugates from the receptors and escape from the endosome into cytoplasm; **E)** Recycling of the receptors to cell surface; **F)** The HDACi is in the cytoplasm where it can hit its target (cytoplasmic HDAC isoforms) or diffuse to the nucleus for inhibition of class I isoforms.

1.12.2. Clinical improvement to HDACi therapy

Designing isoform-selective HDACi or targeting their delivery to malignant cells are only the initial steps in the endeavor aiming at making HDACi part of our medicine cabinets. The steps needed to be taken from the clinical standpoint are equally as important as those asked from the drug discovery field.

1.12.2.1. Patients stratification

Patient care has been moving towards personalized medicine since the advent of the human genome sequencing. This novel approach to medicine aims at developing diagnostic and therapeutic tools based on individual or patient specific biomarkers.⁸⁸ The use of HDACi for cancer treatment fits well with this main objective of personalized medicine as the HDAC overexpression pattern may vary from one patient to another. It becomes crucial to identify the patient population that may benefit from a specific HDACi as to not only maximize positive outcome from clinical trials but also the therapeutic benefits for patients. The implementation of personalized medicine in HDACi therapy should lead to a systematic profiling of intratumoral HDAC isoforms in patients and the modification of the HDACi clinical trial inclusion criteria to include the overexpression of HDAC isozymes shown to be inhibited by the said HDACi during preclinical studies. The HDACs overexpression status is a specific example that can determine the choice of HDACi, but other inclusion factors can also be used.

1.12.2.2. Identification and use of predictive biomarkers

HDAC enzymes as biomarkers for HDACi therapy are attractive options, however, certain tumors may be sensitive to HDACi despite lacking HDACs overexpression. As such, the use of predictive biomarkers can be beneficial. A marker which has recently garnered attention is HR23B, a protein which transports ubiquitinated substrates to the proteasome for degradation.⁸⁹ In various CTCL cell lines, depletion of HR23B through siRNA resulted in resistance to SAHA-induced apoptosis suggesting a positive correlation between HR23B level and the responsiveness to HDACi.⁹⁰ Furthermore, an analysis of biopsies from CTCL patients who received SAHA during a phase II clinical trial corroborates the aforementioned positive correlation. Individuals whose biopsies showed marked expression of HR23B prior to the treatment had an objective response rate of 68.8%, giving HR23B a positive predictive value (PPV) of nearly 70%.⁹⁰ Similar PPVs were also observed in CTCL patients receiving other HDACi such as FK228 (Romidepsin), LBH589.⁹⁰ To highlight the importance of the HR23B as a positive predictor of response to HDACi therapy, a clinical trial evaluating the novel HDACi CXD101 has established a high HR23B expression as an inclusion criterion in patients with solid tumors, lymphoma and myeloma.⁹¹

1.12.2.3. Understanding the mechanisms of HDACi-induced side effects

The side effects of HDACi can be minimized but never completely eliminated. As such, management of these adverse reactions is important, but one ought to first understand the mechanism of these side effects. Unlike most anticancer agents, whose thrombocytopenia (TCP) is due to a decrease in megakaryocytes,⁹² HDACi-induced

thrombocytopenia is not due to a reduction in platelets half-life but to a decreased shedding of platelets from megakaryocytes.^{93,94} Moreover, a megakaryocyte hyperplasia was observed due to an increase in thrombopoietin (TPO). Despite the supraphysiological level of TPO, the transient TCP was overcome by the counterintuitive use of the TPO mimetic AMP-4. The example of HDACi-induced TCP represents a vivid example where the understanding of the mechanism of side effects can yield a clinical management protocol for patients receiving HDACi.

1.12.2.4. Understanding of mechanisms of resistance to HDACi

Though certain mechanisms of resistance to HDACi have been described, there are still many which remained to be elucidated. The understanding of such mechanisms may not only help in the patients stratification by selecting individuals whose malignancies are sensitive to HDACi but also in the design of combination therapy with other agents which can interfere with the HDACi resistance pathways.

1.13. Conclusion

Epigenetic mechanisms such DNA methylation, histones positioning and post-translational histone modifications are involved in various cellular processes including pathological conditions. Among the covalent histone modifications, acetylation and deacetylation have been shown to be indispensable for the regulation of more than 2000 proteins and implicated in various diseases including cancer, making HATs and HDACs important targets in cancer therapy. HDACi have been investigated in several clinical trials culminating with the approvals of SAHA and FK228 (Romidepsin) for CTCL.

Despite the successes of these drugs, the full therapeutic potential of HDACi in cancer remains untapped due to severe cardiotoxicity or lack of efficacy in solid tumors. Expanding the clinical indications of HDACi in our pharmacopeia may require designing isoform-selective HDACi, thus sparing the cardioprotective effects of class IIa isoforms, targeting pan-inhibitors to cancer cells, using predictive biomarkers such as HR23B to identify the patients population who can benefit from HDACi and understanding the mechanisms of side effects in order to provide a better clinical management of HDACi-induced adverse reactions.

1.14. References

1. Esteller, M., Epigenetics in evolution and disease. *The Lancet* **2008**, 372, *Supplement 1* (0), S90-S96.
2. Portela, A.; Esteller, M., Epigenetic modifications and human disease. *Nat Biotech* **2010**, 28 (10), 1057-1068.
3. Feinberg, A. P., Phenotypic plasticity and the epigenetics of human disease. *Nature* **2007**, 447 (7143), 433-440.
4. Esteller, M., Epigenetics in Cancer. *The New England Journal of Medicine* **2008**, 358 (11), 1148-1159.
5. Hanahan, D.; Weinberg, R. A., The Hallmarks of Cancer. *Cell* **2000**, 100 (1), 57-70.
6. Azad, N.; Zahnow, C. A.; Rudin, C. M.; Baylin, S. B., The future of epigenetic therapy in solid tumours-lessons from the past. *Nature Review Clinical Oncology* **2013**, 10 (5), 256-266.
7. Strahl, B. D.; Allis, C. D., The language of covalent histone modifications. *Nature* **2000**, 403 (6765), 41-45.
8. Cruickshank, M.; Besant, P.; Ulgiati, D., The impact of histone post-translational modifications on developmental gene regulation. *Amino Acids* **2010**, 39 (5), 1087-1105.
9. Choudhary, C.; Kumar, C.; Gnäd, F.; Nielsen, M. L.; Rehman, M.; Walther, T. C.; Olsen, J.V.; Mann, M., Lysine Acetylation Targets Protein Complexes and Co-Regulates Major Cellular Functions. *Science* **2009**, 325 (5942), 834-840.
10. Marmorstein, R., Structure and function of histone acetyltransferases. *CMLS, Cellular and Molecular Life Sciences* **2001**, 58 (5-6), 693-703.
11. Dekker, F. J.; Haisma, H. J., Histone acetyl transferases as emerging drug targets. *Drug Discovery Today* **2009**, 14 (19-20), 942-948.
12. Dokmanovic, M.; Clarke, C.; Marks, P. A., Histone Deacetylase Inhibitors: Overview and Perspectives. *Molecular Cancer Research* **2007**, 5 (10), 981-989.
13. Johnstone, R. W., Histone-deacetylase inhibitors: novel drugs for the treatment of cancer. *Nature Review Drug Discovery* **2002**, 1 (4), 287-299.
14. Bojang Jr, P.; Ramos, K. S., The promise and failures of epigenetic therapies for cancer treatment. *Cancer Treatment Reviews* **2014**, 40 (1), 153-169.

15. Kim, H. J.; Bae, S. C., Histone deacetylase inhibitors: molecular mechanisms of action and clinical trials as anti-cancer drugs. *American Journal of Translational Research* **2011**, *3* (2), 166-179.
16. Gryder, B. E.; Sodji, Q. H.; Oyelere, A. K., Targeted cancer therapy: giving histone deacetylase inhibitors all they need to succeed. *Future Medicinal Chemistry* **2012**, *4* (4), 505-524.
17. Lombardi, P. M.; Cole, K. E.; Dowling, D. P.; Christianson, D. W., Structure, mechanism, and inhibition of histone deacetylases and related metalloenzymes. *Current Opinion in Structural Biology* **2011**, *21* (6), 735-743.
18. Lagger, G.; O'Carroll, D.; Rembold, M.; Khier, H.; Tischler, J.; Weitzer, G.; Schuettengruber, B.; Hauser, C.; Brunmeir, R.; Jenuwein, T.; Seiser, C., Essential function of histone deacetylase 1 in proliferation control and CDK inhibitor repression. *EMBO Journal* **2002**, *21* (11), 2672-2681.
19. Kalin, J. H.; Bergman, J. A., Development and Therapeutic Implications of Selective Histone Deacetylase 6 Inhibitors. *Journal of Medicinal Chemistry* **2013**.
20. Yang, X. J.; Seto, E., HATs and HDACs: from structure, function and regulation to novel strategies for therapy and prevention. *Oncogene* **2007**, *26* (37), 5310-5318.
21. Grozinger, C. M.; Schreiber, S. L., Regulation of histone deacetylase 4 and 5 and transcriptional activity by 14-3-3-dependent cellular localization. *Proceedings of the National Academy of Sciences* **2000**, *97* (14), 7835-7840.
22. Sengupta, N.; Seto, E., Regulation of histone deacetylase activities. *Journal of Cellular Biochemistry* **2004**, *93* (1), 57-67.
23. Lee, J.-H.; Hart, S. R. L.; Skalnik, D. G., Histone deacetylase activity is required for embryonic stem cell differentiation. *Genesis* **2004**, *38* (1), 32-38.
24. Brunmeir, R.; Lagger, S.; Seiser, C., Histone deacetylase 1 and 2-controlled embryonic development and cell differentiation. *International Journal of Developmental Biology* **2009**, *53* (2-3), 275-289.
25. Rodriguez-Paredes, M.; Esteller, M., Cancer epigenetics reaches mainstream oncology. *Nature Medicine* **2011**, 330-339.
26. Kazantsev, A. G.; Thompson, L. M., Therapeutic application of histone deacetylase inhibitors for central nervous system disorders. *Nature Reviews Drug Discovery* **2008**, *7* (10), 854-868.

27. Georgopoulos, K., From immunity to tolerance through HDAC. *Nature Immunology* **2009**, *10* (1), 13-14.
28. Karpac, J.; Jasper, H., Metabolic Homeostasis: HDACs Take Center Stage. *Cell* **2011**, *145* (4), 497-499.
29. Patil, V.; Guerrant, W.; Chen, P. C.; Gryder, B.; Benicewicz, D. B.; Khan, S. I.; Tekwani, B. L.; Oyelere, A. K., Antimalarial and antileishmanial activities of histone deacetylase inhibitors with triazole-linked cap group. *Bioorganic & Medicinal Chemistry* **2010**, *18* (1), 415-425.
30. Cardinale, J. P.; Sriramula, S.; Pariaut, R.; Guggilam, A.; Mariappan, N.; Elks, C. M.; Francis, J., HDAC Inhibition Attenuates Inflammatory, Hypertrophic, and Hypertensive Responses in Spontaneously Hypertensive Rats. *Hypertension* **2010**, *56* (3), 437-444.
31. Rotili, D.; Simonetti, G.; Savarino, A.; Palamara, A. T.; Migliaccio, A. R.; Mai, A., Non-cancer uses of histone deacetylase inhibitors: effects on infectious diseases and beta-hemoglobinopathies. *Current Topics In Medicinal Chemistry* **2009**, *9* (3), 272-291.
32. Zelent, A.; Guidez, F.; Melnick, A.; Waxman, S.; Licht, J. D., Translocations of the RAR alpha gene in acute promyelocytic leukemia. *Oncogene* **2001**, *20* (49), 7186-7203.
33. Weichert, W.; Roske, A.; Gekeler, V.; Beckers, T.; Stephan, C.; Jung, K.; Fritzsche, F. R.; Niesporek, S.; Denkert, C.; Dietel, M.; Kristiansen, G., Histone deacetylases 1, 2 and 3 are highly expressed in prostate cancer and HDAC2 expression is associated with shorter PSA relapse time after radical prostatectomy. *British Journal of Cancer* **2008**, *98* (3), 604-610.
34. Weichert, W.; Denkert, C.; Noske, A.; Darb-Esfahani, S.; Dietel, M.; Kalloger, S. E.; Huntsman, D. G.; Kobel, M., Expression of class I histone deacetylases indicates poor prognosis in endometrioid subtypes of ovarian and endometrial carcinomas. *Neoplasia* **2008**, *10* (9), 1021-1027.
35. Weichert, W., HDAC expression and clinical prognosis in human malignancies. *Cancer Letters* **2009**, *280* (2), 168-176.
36. Senese, S.; Zaragoza, K.; Minardi, S.; Muradore, I.; Ronzoni, S.; Passafaro, A.; Bernard, L.; Draetta, G. F.; Alcalay, M.; Seiser, C.; Chiocca, S., Role for Histone Deacetylase 1 in Human Tumor Cell Proliferation. *Molecular and Cellular Biology* **2007**, *27* (13), 4784- 4795.

37. Marks, P. A.; Breslow, R., Dimethyl sulfoxide to vorinostat: development of this histone deacetylase inhibitor as an anticancer drug. *Nature Biotechnology* **2007**, *25* (1), 84-90.
38. Robey, R. W.; Chakraborty, A. R.; Basseville, A.; Luchenko, V.; Bahr, J.; Zhan, Z. R.; Bates, S. E., Histone Deacetylase Inhibitors: Emerging Mechanisms of Resistance. *Molecular Pharmaceutics* **2011**, *8* (6), 2021-2031.
39. Wagner, J.; Hackanson, B.; Lübbert, M.; Jung, M., Histone deacetylase (HDAC) inhibitors in recent clinical trials for cancer therapy. *Clinical Epigenetics* **2010**, *1* (3-4), 117-136.
40. Marks, P. A.; Rifkind, R. A.; Richon, V. M.; Breslow, R.; Miller, T.; Kelly, W. K., Histone deacetylases and cancer: causes and therapies. *Nature Review Cancer* **2001**, *1* (3), 194-202.
41. Mann, B. S.; Johnson, J. R.; Cohen, M. H.; Justice, R.; Pazdur, R., FDA Approval Summary: Vorinostat for Treatment of Advanced Primary Cutaneous T-Cell Lymphoma. *The Oncologist* **2007**, *12* (10), 1247-1252.
42. Meyer, N.; Paul, C.; Misery, L., Pruritus in Cutaneous T-cell Lymphomas: Frequent, Often Severe and Difficult to Treat. *Acta Dermato-Venereologica* **2010**, *90* (1), 12-17.
43. Olsen, E. A.; Kim, Y. H.; Kuzel, T. M.; Pacheco, T. R.; Foss, F. M.; Parker, S.; Frankel, S. R.; Chen, C.; Ricker, J. L.; Arduino, J. M.; Duvic, M., Phase IIB multicenter trial of vorinostat in patients with persistent, progressive, or treatment refractory cutaneous T-cell lymphoma. *Journal of Clinical Oncology* **2007**, *25* (21), 3109-3115.
44. Duvic, M.; Talpur, R.; Ni, X.; Zhang, C.; Hazarika, P.; Kelly, C.; Chiao, J. H.; Reilly, J. F.; Ricker, J. L.; Richon, V. M.; Frankel, S. R., Phase 2 trial of oral vorinostat (suberoylanilide hydroxamic acid, SAHA) for refractory cutaneous T-cell lymphoma (CTCL). *Blood* **2007**, *109* (1), 31-39.
45. Undevia, S. D.; Janisch, L.; Schilsky, R. L.; Louny, D.; Balasubramanian, S.; Mani, C.; Sirisawad, M.; Buggy, J. J.; Miller, R. A.; Ratain, M. J., Phase I study of the safety, pharmacokinetics (PK) and pharmacodynamics (PD) of the histone deacetylase inhibitor (HDACi) PCI-24781. *Journal of Clinical Oncology* **2008**, *26* (15).
46. Grassadonia, A.; Cioffi, P.; Simiele, F.; Iezzi, L.; Zilli, M.; Natoli, C., Role of Hydroxamate- Based Histone Deacetylase Inhibitors (Hb-HDACi) in the Treatment of Solid Malignancies. *Cancers* **2013**, *5* (3), 919-942.

47. Tan, J. H.; Cang, S. D.; Ma, Y. H.; Petrillo, R. L.; Liu, D. L., Novel histone deacetylase inhibitors in clinical trials as anti-cancer agents. *Journal of Hematology & Oncology* **2010**, *3*, 5-18.
48. Porcu, P.; Wong, H. K., We Should Have a Dream: Unlocking the Workings of the Genome in Cutaneous T-Cell Lymphomas. *Clinical Lymphoma and Myeloma* **2009**, *9* (6), 409-411.
49. Piekarz, R. L.; Frye, R.; Turner, M.; Wright, J. J.; Allen, S. L.; Kirschbaum, M. H.; Zain, J.; Prince, H. M.; Leonard, J. P.; Geskin, L. J.; Reeder, C.; Joske, D.; Figg, W. D.; Gardner, E. R.; Steinberg, S. M.; Jaffe, E. S.; Stetler-Stevenson, M.; Lade, S.; Fojo, A. T.; Bates, S. E., Phase II Multi-Institutional Trial of the Histone Deacetylase Inhibitor Romidepsin As Monotherapy for Patients With Cutaneous T-Cell Lymphoma. *Journal of Clinical Oncology* **2009**, *27* (32), 5410-5417.
50. Hess-Stumpp, H.; Bracker, T. U.; Henderson, D.; Politz, O., MS-275, a potent orally available inhibitor of histone deacetylases—The development of an anticancer agent. *The International Journal of Biochemistry & Cell Biology* **2007**, *39* (7–8), 1388-1405.
51. Lucas, D. M.; Davis, M. E.; Parthun, M. R.; Mone, A. P.; Kitada, S.; Cunningham, K. D.; Flax, E. L.; Wickham, J.; Reed, J. C.; Byrd, J. C.; Grever, M. R., The histone deacetylase inhibitor MS-275 induces caspase-dependent apoptosis in B-cell chronic lymphocytic leukemia cells. *Leukemia* **2004**, *18* (7), 1207-1214.
52. Ryan, Q. C.; Headlee, D.; Acharya, M.; Sparreboom, A.; Trepel, J. B.; Ye, J.; Figg, W. D.; Hwang, K.; Chung, E. J.; Murgo, A.; Melillo, G.; Elsayed, Y.; Monga, M.; Kalnitskiy, M.; Zwiebel, J.; Sausville, E. A., Phase I and Pharmacokinetic Study of MS-275, a Histone Deacetylase Inhibitor, in Patients With Advanced and Refractory Solid Tumors or Lymphoma. *Journal of Clinical Oncology* **2005**, *23* (17), 3912-3922.
53. Gojo, I.; Jiemjit, A.; Trepel, J. B.; Sparreboom, A.; Figg, W. D.; Rollins, S.; Tidwell, M. L.; Greer, J.; Chung, E. J.; Lee, M.-J.; Gore, S. D.; Sausville, E. A.; Zwiebel, J.; Karp, J. E., Phase 1 and pharmacologic study of MS-275, a histone deacetylase inhibitor, in adults with refractory and relapsed acute leukemias. *Blood* **2007**, *109* (7), 2781-2790.
54. Hauschild, A.; Trefzer, U.; Garbe, C.; Kaehler, K. C.; Ugurel, S.; Kiecker, F.; Eigentler, T.; Krissel, H.; Schott, A.; Schadendorf, D., Multicenter phase II trial of the historic deacetylase inhibitor pyridylmethyl-N-{4-(2-aminophenyl)-carbamoyl-benzyl}- carbamate in pretreated metastatic melanoma. *Melanoma Research* **2008**, *18* (4), 274- 278.

55. Kuendgen, A.; Strupp, C.; Aivado, M.; Bernhardt, A.; Hildebrandt, B.; Haas, R.; Germing, U.; Gattermann, N., Treatment of myelodysplastic syndromes with valproic acid alone or in combination with all-trans retinoic acid. *Blood* **2004**, *104* (5), 1266-1269.
56. Vansteenkiste, J.; Van Cutsem, E.; Dumez, H.; Chen, C.; Ricker, J.; Randolph, S.; Schöffski, P., Early phase II trial of oral vorinostat in relapsed or refractory breast, colorectal, or non-small cell lung cancer. *Investigational New Drugs* **2008**, *26* (5), 483-488.
57. Woyach, J. A.; Kloos, R. T.; Ringel, M. D.; Arbogast, D.; Collamore, M.; Zwiebel, J. A.; Grever, M.; Villalona-Calero, M.; Shah, M. H., Lack of Therapeutic Effect of the Histone Deacetylase Inhibitor Vorinostat in Patients with Metastatic Radioiodine-Refractory Thyroid Carcinoma. *The Journal of Clinical Endocrinology & Metabolism* **2009**, *94* (1), 164-170.
58. Whitehead, R.; Rankin, C.; Hoff, P. G.; Gold, P.; Billingsley, K.; Chapman, R.; Wong, L.; Ward, J.; Abbruzzese, J.; Blanke, C., Phase II trial of romidepsin (NSC-630176) in previously treated colorectal cancer patients with advanced disease: a Southwest Oncology Group study (S0336). *Investigational New Drugs* **2009**, *27* (5), 469-475.
59. Nebbioso, A.; Carafa, V.; Benedetti, R.; Altucci, L., Trials with 'epigenetic' drugs: An update. *Molecular Oncology* **2012**, *6* (6), 657-682.
60. Cang, S.; Ma, Y.; Liu, D., New clinical developments in histone deacetylase inhibitors for epigenetic therapy of cancer. *Journal of Hematology & Oncology* **2009**, *2* (1), 22.
61. Jin, S.; Scotto, K. W., Transcriptional Regulation of the MDR1 Gene by Histone Acetyltransferase and Deacetylase Is Mediated by NF-Y. *Molecular and Cellular Biology* **1998**, *18* (7), 4377-4384.
62. Morrow, C. S.; Nakagawa, M.; Goldsmith, M. E.; Madden, M. J.; Cowan, K. H., Reversible transcriptional activation of mdrl by sodium butyrate treatment of human colon cancer cells. *Journal of Biological Chemistry* **1994**, *269* (14), 10739-46.
63. Subramanian, S.; Bates, S. E.; Wright, J. J.; Espinoza-Delgado, I.; Piekarz, R. L., Clinical Toxicities of Histone Deacetylase Inhibitors. *Pharmaceuticals* **2010**, *3* (9), 2751-2767.
64. Antzelevitch, C., Ionic, molecular, and cellular bases of QT-interval prolongation and torsade de pointes. *Europace* **2007**, *9* (suppl 4), iv4-iv15.

65. Brana, I.; Taberner, J., Cardiotoxicity. *Annals of Oncology* **2010**, *21* (suppl 7), vii173-vii179.
66. Wood, A. ; Roden, D., DRUG THERAPY: Drug-Induced Prolongation of the QT Interval. *The New England Journal of Medicine* **2004**, *350* (10), 1013-22.
67. Barbey, J. T.; Pezzullo, J. C.; Soignet, S. L., Effect of Arsenic Trioxide on QT Interval in Patients With Advanced Malignancies. *Journal of Clinical Oncology* **2003**, *21* (19), 3609- 3615.
68. De Ponti, F.; Poluzzi, E.; Montanaro, N., Organising evidence on QT prolongation and occurrence of Torsades de Pointes with non-antiarrhythmic drugs: a call for consensus. *European Journal of Clinical Pharmacology* **2001**, *57* (3), 185-209.
69. Khan, I. A., Clinical and therapeutic aspects of congenital and acquired long QT syndrome. *The American Journal of Medicine* **2002**, *112* (1), 58-66.
70. Ponte ML, K. G., Girolamo GD, Mechanisms of Drug Induced QT Interval Prolongation. *Current Drug Safety* **2010**, *5* (1), 9.
71. Gupta, A.; Lawrence, A. T.; Krishnan, K.; Kavinsky, C. J.; Trohman, R. G., Current concepts in the mechanisms and management of drug-induced QT prolongation and torsade de pointes. *American Heart Journal* **2007**, *153* (6), 891-899.
72. Hoffmann, P.; Warner, B., Are hERG channel inhibition and QT interval prolongation all there is in drug-induced torsadogenesis? A review of emerging trends. *Journal of Pharmacological and Toxicological Methods* **2006**, *53* (2), 87-105.
73. Guo, J.; Li, X.; Shallow, H.; Xu, J.; Yang, T.; Massaeli, H.; Li, W.; Sun, T.; Pierce, G. N.; Zhang, S., Involvement of Caveolin in Probucol-Induced Reduction in hERG Plasma-Membrane Expression. *Molecular Pharmacology* **2011**, *79* (5), 806-813.
74. Abbott, G. W.; Sesti, F.; Splawski, I.; Buck, M. E.; Lehmann, M. H.; Timothy, K. W.; Keating, M. T.; Goldstein, S. A. N., MiRP1 Forms IKr Potassium Channels with HERG and Is Associated with Cardiac Arrhythmia. *Cell* **1999**, *97* (2), 175-187.
75. Splawski, I.; Tristani-Firouzi, M.; Lehmann, M. H.; Sanguinetti, M. C.; Keating, M. T., Mutations in the hminK gene cause long QT syndrome and suppress IKs function. *Nature Genetics* **1997**, *17* (3), 338-340.

76. Lacerda, A. E.; Kuryshev, Y. A.; Chen, Y.; Renganathan, M.; Eng, H.; Danthi, S. J.; Kramer, J. W.; Yang, T.; Brown, A. M., Alfuzosin Delays Cardiac Repolarization by a Novel Mechanism. *Journal of Pharmacology and Experimental Therapeutics* **2008**, *324* (2), 427-433.
77. Shultz, M. D.; Cao, X. Y.; Chen, C. H.; Cho, Y. S.; Davis, N. R.; Eckman, J.; Fan, J. M.; Fekete, A.; Firestone, B.; Flynn, J.; Green, J.; Growney, J. D.; Holmqvist, M.; Hsu, M.; Jansson, D.; Jiang, L.; Kwon, P.; Liu, G.; Lombardo, F.; Lu, Q.; Majumdar, D.; Meta, C.; Perez, L.; Pu, M. Y.; Ramsey, T.; Remiszewski, S.; Skolnik, S.; Traebert, M.; Urban, L.; Uttamsingh, V.; Wang, P.; Whitebread, S.; Whitehead, L.; Yan-Neale, Y.; Yao, Y. M.; Zhou, L.P.;Atadja, P., Optimization of the in Vitro Cardiac Safety of Hydroxamate-Based Histone Deacetylase Inhibitors. *Journal of Medicinal Chemistry* **2011**, *54* (13), 4752-4772.
78. Strevel, E. L.; Ing, D. J.; Siu, L. L., Molecularly Targeted Oncology Therapeutics and Prolongation of the QT Interval. *Journal of Clinical Oncology* **2007**, *25* (22), 3362-3371.
79. Backs, J.; Olson, E. N., Control of Cardiac Growth by Histone Acetylation/Deacetylation. *Circulation Research* **2006**, *98* (1), 15-24.
80. Raje, N.; Hari, P. N.; Vogl, D. T.; Jagannath, S.; Orłowski, R. Z.; Supko, J. G.; Stephenson, P.; Jones, S. S.; Wheeler, C.; Lonial, S., Rocilinostat (ACY-1215), a Selective HDAC6 Inhibitor, Alone and in Combination with Bortezomib in Multiple Myeloma: Preliminary Results From the First-in-Humans Phase I/II Study. *Blood* **2012**, *120* (21).
81. Jain, S.; Zain, J.; O'Connor, O., Novel therapeutic agents for cutaneous T-Cell lymphoma. *Journal of Hematology & Oncology* **2012**, *5* (1), 24.
82. Needham, L. A.; Davidson, A. H.; Bawden, L. J.; Belfield, A.; Bone, E. A.; Brotherton, D. H.; Bryant, S.; Charlton, M. H.; Clark, V. L.; Davies, S. J.; Donald, A.; Day, F. A.; Krige, D.; Legris, V.; McDermott, J.; McGovern, Y.; Owen, J.; Patel, S. R.; Pintat, S.; Testar, R. J.; Wells, G. M. A.; Moffat, D.; Drummond, A. H., Drug Targeting to Monocytes and Macrophages Using Esterase-Sensitive Chemical Motifs. *Journal of Pharmacology and Experimental Therapeutics* **2011**, *339* (1), 132-142.
83. Ossenkoppele, G. J.; Lowenberg, B.; Zachee, P.; Vey, N.; Breems, D.; Van de Loosdrecht, A. A.; Davidson, A. H.; Wells, G.; Needham, L.; Bawden, L.; Toal, M.; Hooftman, L.; Debnam, P. M., A phase I first-in-human study with tefinostat – a monocyte/macrophage targeted histone deacetylase inhibitor – in patients with advanced haematological malignancies. *British Journal of Haematology* **2013**, *162* (2), 191-201.

84. Gryder, B. E.; Akbashev, M. J.; Rood, M. K.; Raftery, E. D.; Meyers, W. M.; Dillard, P.; Khan, S.; Oyelere, A. K., Selectively Targeting Prostate Cancer with Antiandrogen Equipped Histone Deacetylase Inhibitors. *ACS Chemical Biology* **2013**, *8* (11), 2550-2560.
85. Gryder, B. E.; Rood, M. K.; Johnson, K. A.; Patil, V.; Raftery, E. D.; Yao, L. P. D.; Rice, M.; Azizi, B.; Doyle, D. F.; Oyelere, A. K., Histone Deacetylase Inhibitors Equipped with Estrogen Receptor Modulation Activity. *Journal of Medicinal Chemistry* **2013**, *56* (14), 5782-5796.
86. Mwakwari, S. C.; Guerrant, W.; Patil, V.; Khan, S. I.; Tekwani, B. L.; Gurard-Levin, Z. A.; Mrksich, M.; Oyelere, A. K., Non-Peptide Macrocyclic Histone Deacetylase Inhibitors Derived from Tricyclic Ketolide Skeleton. *Journal of Medicinal Chemistry* **2010**, *53* (16), 6100-6111.
87. Jehle, J.; Schweizer, P. A.; Katus, H. A.; Thomas, D., Novel roles for hERG K⁺ channels in cell proliferation and apoptosis. *Cell Death and Disease* **2011**, *2*, e193.
88. Ginsburg, G. S.; McCarthy, J. J., Personalized medicine: revolutionizing drug discovery and patient care. *Trends in Biotechnology* **2001**, *19* (12), 491-496.
89. Chen, L.; Madura, K., Rad23 Promotes the Targeting of Proteolytic Substrates to the Proteasome. *Molecular and Cellular Biology* **2002**, *22* (13), 4902-4913.
90. Khan, O.; Fotheringham, S.; Wood, V.; Stimson, L.; Zhang, C. L.; Pezzella, F.; Duvic, M.; Kerr, D. J.; La Thangue, N. B., HR23B is a biomarker for tumor sensitivity to HDAC inhibitor-based therapy. *Proceedings of the National Academy of Sciences of the United States of America* **2010**, *107* (14), 6532-6537.
91. Clinicaltrials.gov, Phase 1 Trial of CXD101 in Patients With Advanced Cancer. 2013.
92. Kenney, B.; Stack, G., Drug-Induced Thrombocytopenia. *Archives of Pathology & Laboratory Medicine* **2009**, *133* (2), 309-314.
93. Giver, C. R.; Jaye, D. L.; Waller, E. K.; Kaufman, J. L.; Lonial, S., Rapid recovery from panobinostat (LBH589)-induced thrombocytopenia in mice involves a rebound effect of bone marrow megakaryocytes. Nature Publishing Group: 2011; Vol. 25, pp 362-365.
94. Bishton, M. J.; Harrison, S. J.; Martin, B. P.; McLaughlin, N.; James, C.; Josefsson, E. C.; Henley, K. J.; Kile, B. T.; Prince, H. M.; Johnstone, R. W., Deciphering the molecular and biologic processes that mediate histone deacetylase inhibitor-induced thrombocytopenia. *Blood* **2011**, *117* (13), 3658-3668.

CHAPTER 2

ISOFORM SELECTIVE HDAC INHIBITORS

This work has been published in two articles:

Journal of Medicinal Chemistry **2013**, 56 (9), 3492-3506

Journal of Medicinal Chemistry **2013**, 56 (24), 9969-9981

2.1. Introduction

Due to their role as transcription repressors, HDACs are overexpressed in various malignancies establishing them as valid targets for cancer therapy.¹ Among the 11 zinc dependent HDAC isoforms identified to date, isoforms 1, 2 and 3 are overexpressed in gastric, colorectal and ovarian carcinomas whereas hepatocellular carcinoma and estrogen receptor positive (ER+) breast cancer overexpress HDAC1 and 6, respectively.² The observed correlation between these malignancies and HDAC isoforms overexpression suggests that isoform selective inhibitors may be equally as effective as HDAC pan-inhibitor such as SAHA for cancer chemotherapy. For example, an HDAC1 selective inhibitor can be effective against hepatocellular carcinoma and class I selective HDACi against gastric and colorectal cancers.

Each HDAC isoform possesses a specific role in proper cellular homeostasis as demonstrated through a series of knockout experiments in mice (Table 2.1). Such studies established the requirement of HDAC1 in cellular proliferation, whereas HDAC3 and 5 were indispensable for cardiomyocytes development and function respectively.³ Furthermore, there are many cellular processes (metabolic enzymes, chaperones, etc) requiring the involvement of an HDAC or HAT (Figure 2.1).⁴ A pan-inhibitor of HDAC can interfere with all the pathways aforementioned in healthy cells and result in severe side effects. In such instances, cancer patients stand to benefit from isoform selective

HDAC inhibitors as the specific isoform overexpressed can be targeted while minimizing inhibition of other isoforms not involved in the tumorigenesis.

Table 2.1: Phenotypic defects in mice following HDAC isoforms knockout experiments.³

Class	Isoforms	Phenotype	Related disease
I	1	Lethal. Severe proliferation defects	-
	2	Death 24 hrs after birth. Severe cardiac defect	Cardiac diseases
	3	Lethal. Defect in cardiomyocytes	Cardiac diseases
IIa	4	Lethal	Skeletal diseases
	5	Viable but cardiac defects	Cardiac diseases
	7	Embryonic lethality. Vascular instability	Vascular diseases
	9	Viable but cardiac defects	Cardiac diseases
IIb	6	Viable with no obvious phenotype	-

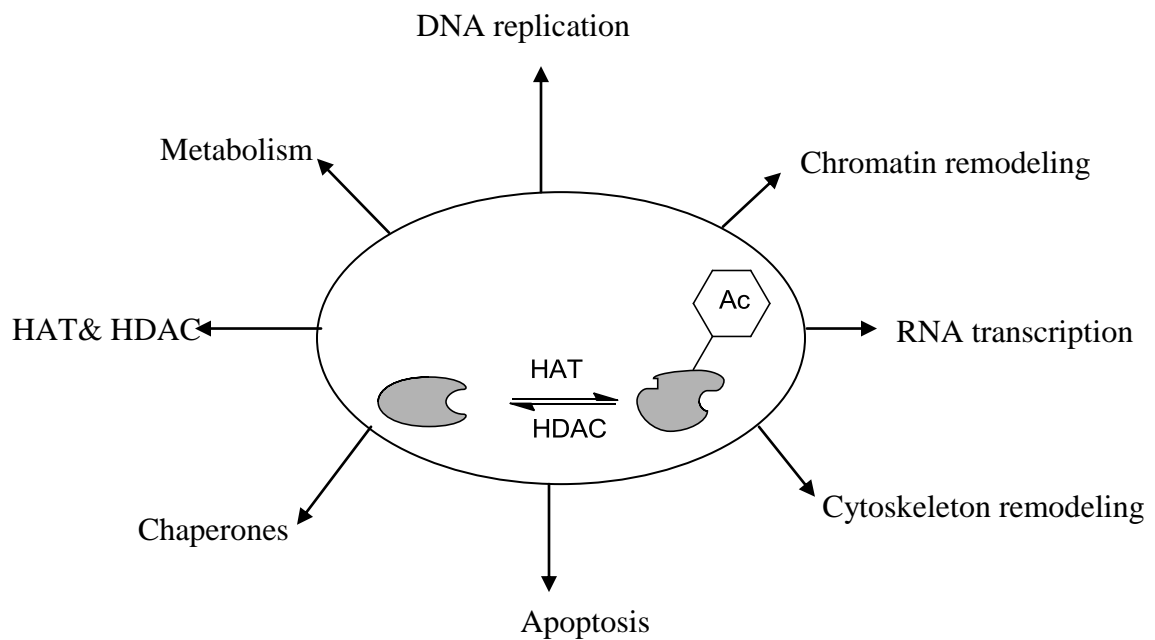


Figure 2.1: Processes potentially targeted by HDAC pan-inhibitors.⁴

Most HDACi, including the clinically useful SAHA, fit a pharmacophoric model comprised of a surface recognition group connected by a linker to a zinc binding group (ZBG) required for the chelation of active Zn^{2+} (Figure 2.2).⁵ Approaches to designing isoform selective inhibitors include modifications of the surface recognition group or the ZBG as to exploit the differences in amino acids sequences in each isoform.^{6,7}

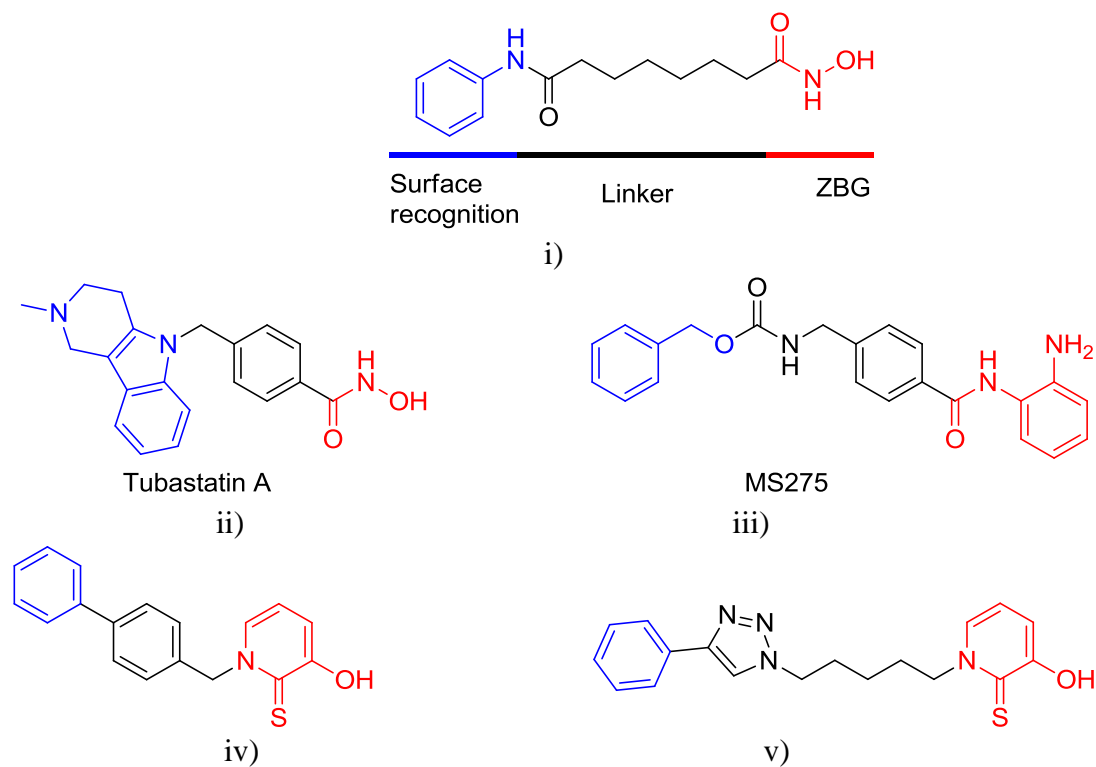
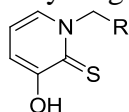


Figure 2.2: Structures of selected HDACi: **i)** HDACi pharmacophoric model with SAHA as prototypical HDACi (Note color code: Blue, surface recognition group; Black, linker; Red, ZBG); **ii)** Tubastatin A as an HDAC6 selective inhibitor⁶ (Example of surface recognition group modification); **iii)** MS275 as an HDAC1 selective inhibitor⁷ (Example of ZBG modification); **iv)** 1st generation of 3-Hydroxypyridin-2-thione (3-HPT) based HDACi;⁸ **v)** 2nd generation of 3HPT based HDACi.⁹

2.2. 3-hydroxypyridin-2-thione as novel ZBG for HDAC inhibition

A vast majority of HDACi have incorporated the hydroxamic acid as the preferred ZBG due to its strong Zn^{2+} chelation. However, due to pharmacokinetic challenges (short half-life) ensuing from enzymatic hydrolysis and poor bioavailability^{10,11,12}, extensive efforts have been deployed to develop novel ZBG for HDAC inhibition.^{13,14} A fragment-based approach used in our laboratory by Dr. Vishal Patil has identified previously used zinc chelating moieties for matrix metalloproteases (MMP) inhibition as potential candidates for HDAC inhibition. He identified the 3-hydroxypyridin-2-thione (3-HPT) as a valid replacement for the metabolically liable hydroxamate resulting in the synthesis of the first generation of 3-HPT based inhibitors with phenyl or biphenyl linkers and second generation of inhibitors with alkyl linkers.^{8,9} Furthermore, the 3-HPT conferred isoform selectivity as the 3-HPT based inhibitors were devoid of HDAC1 inhibition but were active against HDAC6 and/or HDAC8 (Tables 2.2 and 2.3).

Table 2.2: Inhibition of HDAC1, 6 and 8 by 1st generation 3-HPT based inhibitors.

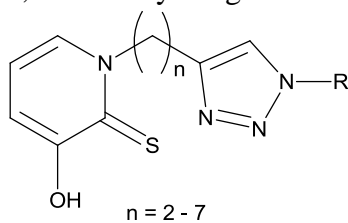


Compound	R	HDAC1 IC ₅₀ (nM)	HDAC6 IC ₅₀ (nM)	HDAC8 IC ₅₀ (nM)
1		NI	457 ± 27	1272±200
2		NI	847 ± 188	4283±1548
3		NI	957±159	2075±459
4		NI	44%	1701±717
5		NI	372 ± 35	1907±771
6		NI	454 ± 42	800±304
7		NI	812 ± 286	2496±1180
8		NI	306 ± 69	3105±1649
9		NI	NI	2858±944
10		NI	2390 ± 458	34%
11		NI	2204 ± 355	2780±323
12		NI	41%	1570±1067
13		NI	1023 ± 99	1868±723
SAHA	-	38 ± 2	144 ± 23	232 ± 19

NI: No Inhibition (below 20% Inhibition at 10 μM concentration)

% inhibition of the compounds at 10 μM are given if the IC₅₀ was above 10 μM

Table 2.3: Inhibition of HDAC1, 6 and 8 by 2nd generation 3-HPT inhibitors.



Compound	R	n	HDAC1 IC ₅₀ (nM)	HDAC6 IC ₅₀ (nM)	HDAC8 IC ₅₀ (nM)
14		2	NI	14%	56%
15		3	NI	3628±1363	63%
16		4	NI	1085±333	3303±260
17		5	NI	911± 173	917±139
18		6	NI	22%	6751±910
19		7	NI	955 ±150	1377±205
20			5	NI	807 ± 207
21		NI		1100 443	1660 ± 416
22		NI		637 ± 160	2402 ± 263
23		NI		905 ± 249	1465±217
24		NI		356 ± 72	2831 ± 520
25		NI		1006 ± 425	1482 ± 389
26		NI		661 ± 121	2258 ± 1005
SAHA	-	-		38±2	144±23

NI: No Inhibition (below 20% Inhibition at 10 μM concentration)
 % inhibition of the compounds at 10 μM are given if the IC₅₀ was above 10 μM

2.3. Anticancer activity of the 1st generation of 3-HPT based inhibitors

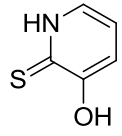
Using the MTS assay, I evaluated the anticancer activity of several of these 1st generation compounds in cell lines such as DU145 (androgen independent prostate cancer), LNCaP (androgen dependent prostate cancer) and the T-cell leukemia cell line Jurkat. The tested compounds included a selective HDAC8 inhibitor **9**, dual inhibitors of HDAC6 and 8, **5** and **8**, and a triazole-based inhibitor **12** that was selective for HDAC8.

Although 3-HPT is active against HDAC6 ($IC_{50} = 681 \pm 110$ nM) and to some extent against HDAC8 ($IC_{50} = 3675 \pm 1201$ nM), it is inactive against the three cancer cell lines tested (Table 2.4). The discrepancy between the HDAC inhibition profile and the anti-proliferative activity of 3-HPT may be due to solubility problems that limit its diffusion across the cell membrane.¹⁵ Against DU145, a prostate cancer line known to be responsive to HDACi such as SAHA or TSA, only **8** exhibited a weak activity; all other compounds were inactive at the highest tested concentration of 20 μ M (Table 2.4). SAHA, which was used as a positive control, had an IC_{50} value comparable to that reported in the literature.¹⁶

The compounds were more active on the LNCaP cell line (Table 2.4). Compound **8** is the most potent of the biphenyls, followed by **5** and **9**. Interestingly, the cell growth inhibition activity of the triazolyl compound **12** is comparable to that of **5** although **12** is a weak HDAC6 inhibitor (only 41% inhibition at 10 μ M). With the exception of **12**, the observed trend of the cell growth inhibition activity mirrored that of the HDAC6 inhibition seen in Table 2. This may be due to the fact that LNCaP cells are sensitive to the acetylation state of HSP90. Hyperacetylation of HSP90, induced by the tested 3-HPT

derived HDACi, attenuates its interactions with proteins such as androgen receptors, which are key to the survival of LNCaP cells.^{17, 18}

Table 2.4: MTS Cell Viability Assay. IC₅₀ of selected 1st generation of 3-HPT based inhibitors against various cancer cell lines.

Compound	Cellular IC ₅₀ (μ M)			
	DU-145	LNCaP	Jurkat	Jurkat J. γ
	NI	NI	NI	NT
5	>20	14.7 \pm 0.8	9.0 \pm 0.7	NT
8	13.6 \pm 2.9	7.8 \pm 0.7	3.2 \pm 0.3	NI
9	>20	16.2 \pm 1.1	10.6 \pm 0.7	NI
12	>20	13.1 \pm 1.5	4.7 \pm 0.3	NI
SAHA	2.5 \pm 0.2	2.3 \pm 0.7	1.5 \pm 0.1	NI

NT = Not Tested; NI = No inhibition

Because T-cell-derived leukemia cell line Jurkat has been previously shown to be sensitive to selective HDAC8 inhibitor,¹⁹ we investigated the effects of our compounds on the viability of Jurkat cells. Overall, all the compounds, excluding 3-HPT, potently induce Jurkat cell death with low IC₅₀ values (Table 2.4). Compound **8**, which inhibited both HDAC6 and HDAC8, is the most potent against the Jurkat cells (IC₅₀ = 3.19 μ M) in a similar manner to its activity against LNCaP cells. The HDAC8 selective compounds **9** and **12** are cytotoxic to the Jurkat cells with **12**, the more potent HDAC8 inhibitor of the

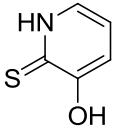
two, being twice as potent. The enhanced cytotoxicity of **12** relative to **9** could suggest a causal relationship between HDAC8 inhibition and the apoptotic effect against Jurkat cells.

The apoptotic pathway, which is mediated by the activity of phospholipase C- γ 1 (PLC- γ 1) in Jurkat cells, is believed to be initiated by an HDAC8 specific enzyme.¹⁹ Balasubramanian and coworkers reported that an HDAC8 specific inhibitor, PCI-34051, lost its ability to induce apoptosis in Jurkat J. γ , a mutant Jurkat cell line which has no detectable PLC- γ 1 activity.¹⁹ To further delineate the contribution of HDAC8 to apoptosis induction, we probed the effect of compounds **8**, **9**, **12** and SAHA on the viability of Jurkat J. γ cells. As anticipated for HDAC8 selective inhibitors, compounds **9** and **12** are devoid of anti-proliferative activity against Jurkat J. γ (Table 2.4). Quite unexpectedly, **8** (which inhibited HDACs 6 and 8) and SAHA (a much broader HDACi) are non-cytotoxic to this mutant Jurkat cell line. The inactivity of **9** and **12** against Jurkat J. γ confirmed HDAC8 contribution to their bioactivity. In the Jurkat cell line, Ca²⁺ released through PLC- γ 1 triggers cascade of events resulting in mitochondrial cytochrome c release and caspase-dependent apoptosis. The defect in intracellular Ca²⁺ mobilization in the Jurkat J. γ mutant may also explain the inactivity of **8** and SAHA as this prevents the increase in cytochrome c release observed in the wild type Jurkat.¹⁹ Alternatively, the observed dependence of the cytotoxicity activity of **8** and SAHA on PLC- γ 1 activity may be due to the attenuation of caspase-dependent apoptosis which is crucial for the cytotoxicity of HDACi.

There is a discrepancy between HDAC inhibition and the whole cell activities of some of the tested compounds. This is to be expected as it is not unusual to observe such

a lack of correlation between the two experiments. It is however possible that compound solubility could play a significant role in cell penetration which may perturb the whole cell activities. Therefore, we estimated the solubility of all compounds tested in cell growth inhibition assay to probe for the effect of solubility on anti-proliferative activity (Table 2. 5).

Table 2.5: Aqueous solubility of selected 1st generation 3-HPT inhibitors.

Compound	Estimated solubility (µg/mL)
	46
9	34
12	142*
8	148*
5	172*

* 40 mM DMSO stock solution was made in order to achieve final concentrations above 500 µM

Among these compounds, 3-HPT and **9** had solubility less than 65µg/mL which is the solubility threshold that can limit a drug's cellular activity. For these two compounds, poor solubility may explain the lack of cellular activity.^{20, 21} However, the solubility of the other compounds tested are beyond the suggested solubility threshold.^{20, 21} Hence, the reduced efficacy of many of these compounds may be attributable to factors other than solubility issues.

2.4. Anticancer activity of 2nd generation 3-HPT inhibitors

We also tested selected 2nd generation 3-HPT based compounds **17** and **24** and comparable compounds **19** and **22** on the survival of DU145, LNCaP, T-cell leukemia cell line Jurkat and Jurkat J.γ, a mutant Jurkat cell line resistant to HDAC inhibition using the MTS assay.^{8,19}

Table 2.6 shows the IC₅₀ values of each compound against the cancer cell lines studied. The lead *meta*-cyano compound **24** is about 2-fold more potent, relative to the unsubstituted congener **19**, against DU145 and LNCaP prostate cancer cell lines. Such improved sensitivity with **24** toward prostate cancer lines, particularly LNCaP, may be rationalized by its HDAC6 selectivity.²² Inhibition of HSP90 has been shown to compromise the viability of DU145 offering a similar rationale for the enhanced cytotoxicity of **17** against this cell line.^{23,17} Compounds **17** and **24** are equipotent against the wild type Jurkat cell line, despite the enhanced HDAC8 inhibition activity of the former (Table 2.3) which is expected to favor cytotoxicity to the Jurkat cell line.^{19,24} It is reasonable that the compensation of the weaker HDAC8 inhibition activity of **24** by the 3-fold increase in its anti-HDAC6, relative to that of **17**, may contribute to its cytotoxicity in the Jurkat cell. The cytotoxicity of **19**, analog containing a seven-methylene linker, and the *ortho*-methyl substituted five-methylene compound **22** do not completely trend with the pattern of their HDAC inhibition activities. Against both prostate cancer lines investigated, **19** is 2- and 3-fold less cytotoxic compared with lead compounds **17** and **24** respectively, while it is 3-fold less cytotoxic relative to both lead compounds against the wild type Jurkat cell line. The *ortho*-substituted compound **22** is 2-fold less cytotoxic

against DU145 while it is only marginally less cytotoxic against LNCaP and wild type Jurkat cell line compared with **24**.

Although **17** and **19** have similar IC₅₀ against HDAC6, the latter has a significantly higher cellular IC₅₀ against LNCaP cells. Against Jurkat cell line, **22** and **24** also display similar incongruity, which we first attributed to solubility differences. To partially account for such pharmacokinetic liabilities, we estimated the solubility of each tested compound^{20,21} but found that the four compounds had solubilities greater than the threshold of 65 µg/mL proposed to adversely affect cell activity (Table 2.7). This suggests that the observed discrepancies may be attributed to factors other than solubility.

Table 2.6. MTS Cell Viability Assay. IC₅₀ of selected 2nd generation of 3-HPT based inhibitors against various cancer cell lines.

Compound	Cellular IC ₅₀ (µM)				
	DU-145	LNCaP	Jurkat	Jurkat J.γ	Vero
17	9.3 ± 1.0	5.4 ± 0.5	3.3 ± 0.60	1.9 ± 0.2	>20
19	17.7 ± 3.3	11.0 ± 1.9	9.0 ± 1.3	>20	NT
22	11.1 ± 2.4	5.0 ± 0.4	5.2 ± 1.2	NT	NT
24	5.0 ± 1.1	3.5 ± 0.3	3.4 ± 0.6	0.90 ± 0.1	>20
SAHA	2.5 ± 0.2	2.3 ± 0.7	1.5 ± 0.1	NI	5.2 ± 1.0*
Tubastatin A	NT	10.9 ± 1.5	3.4 ± 0.3	NI	>20

NT: Not Tested

NI: No inhibition at 20µM; * :reference²⁵

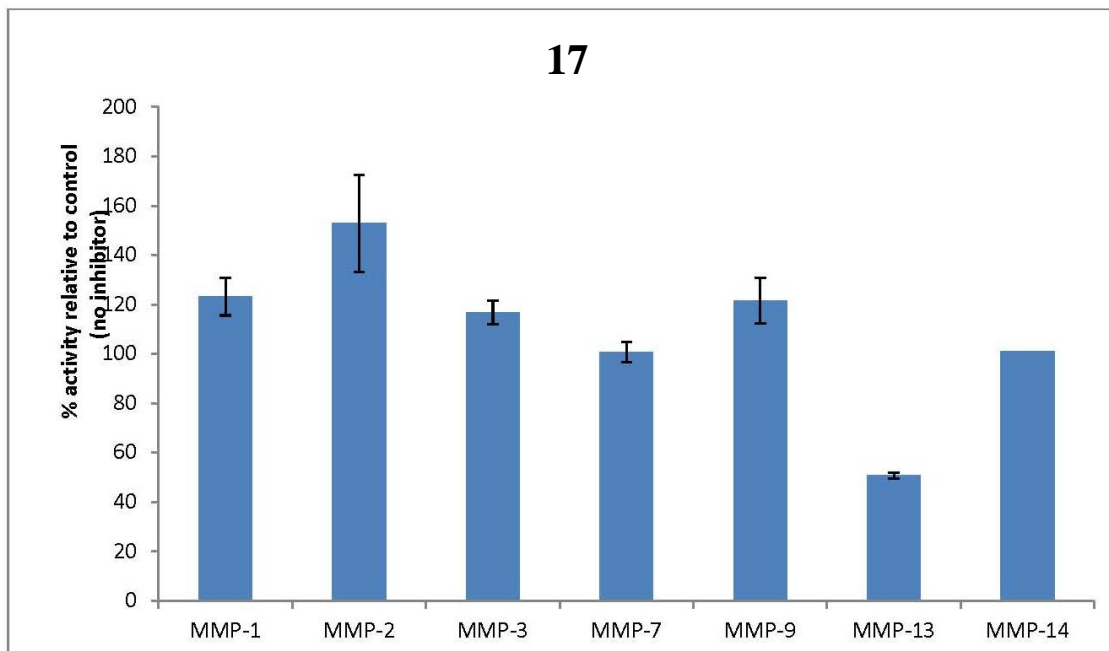
Table 2.7: Aqueous solubility of selected 2nd generation 3-HPT based inhibitors.

Compound	Estimated solubility (µg/mL)
17	74
19	110
22	71
24	73

We have shown previously that the Jurkat J γ cell line, a mutant Jurkat cell line lacking phospholipase C activity, is resistant to SAHA.⁸ To check if the 2nd generation 3-HPT compounds would be similarly innocuous, we investigated the effect of the lead compounds **17**, **19** and **24** on Jurkat J γ cell growth. We observed that compound **19** is significantly less cytotoxic to Jurkat J γ cells versus their wild type counterpart. Surprisingly, both **17** and **24** are potently cytotoxic to Jurkat J γ cells with IC₅₀ values of 1 and 2 µM respectively. Comparatively, the IC₅₀s of **17** and **24** against the healthy mammalian cell line Vero were estimated to be greater than 20µM, the highest tested concentration (Table 2.6). In order to indirectly evaluate the contribution of HDAC6 inhibition to the anticancer activity of the compounds, the anti-proliferative activity of the HDAC6 selective inhibitor tubastatin A was evaluated against these cell lines as well. Although tubastatin A was as potent as **17** and **24** in Jurkat cells, it was 2 to 3 fold less potent against LNCaP and inactive against Jurkat J γ (Table 2.6). Given that the pan-inhibitor SAHA and the HDAC6 selective tubastatin A are inactive against Jurkat J γ , the cytotoxic activity of lead compounds **17** and **24** against Jurkat J γ could be through inhibition of other yet to be identified cellular target(s).

Toward identifying other possible targets of the lead compounds **17** and **24**, we screened for their effect on the activity of a collection matrix metalloproteases (MMPs) which have been suggested to be involved in apoptosis.²⁶ The rationale for screening against MMPs is based on the fact that 3HPT has been previously used as ZBG for MMP inhibition.²⁷ At the tested concentration of 10 μ M, **17** and **24** were inactive against MMP1, 2, 3, 7, 9 and 14, while the activity of MMP13 was halved at this very high concentration (Figure 2.3). Despite the inhibition of MMP13, MMP inhibition is less likely to have contributed to the observed cellular activity as the HDAC enzymatic IC₅₀s were in the nanomolar range. We also tested these lead compounds against HDAC2 which has been shown to be upregulated in certain malignancies and whose inhibition could result in apoptosis.^{28,29} However, the IC₅₀ of **17** and **24** were 5840 \pm 740 nM and 3680 \pm 800 nM respectively suggesting that HDAC2 may not be a target responsible for cellular activity.

A



B

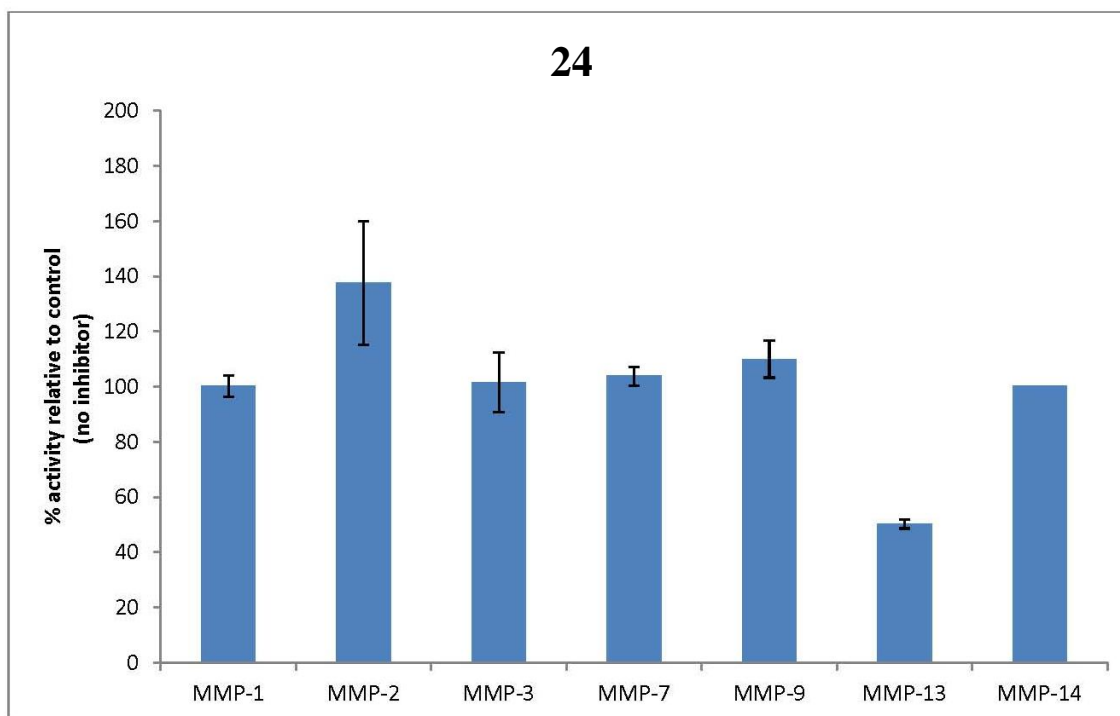


Figure 2.3: MMP activity in presence of various inhibitors A) **17** at 10 μ M; B) **24** at 10 μ M.

2.5. Intracellular target validation of 3-HPT based inhibitors

Among the 1st generation compounds tested for anti-cancer activity, **8** is approximately 10-fold more selective toward HDAC6 compared to HDAC8. To probe the contribution of HDAC6 inhibition to the cytotoxic activity of **8**, we determined the level of tubulin acetylation, a common marker for intracellular HDAC6 inhibition, in LNCaP cells through Western blot. We observed that **8** led to an increase in tubulin acetylation in LNCaP cells at IC₅₀ concentration and at 20 μ M (Figure 2.4). While SAHA, used as a positive control, showed concentration dependent tubulin hyperacetylation as observed before.³⁰ This data provides evidence for the involvement of intracellular HDAC6 inhibition as part of the mechanisms of anti-proliferative activity of **8**.

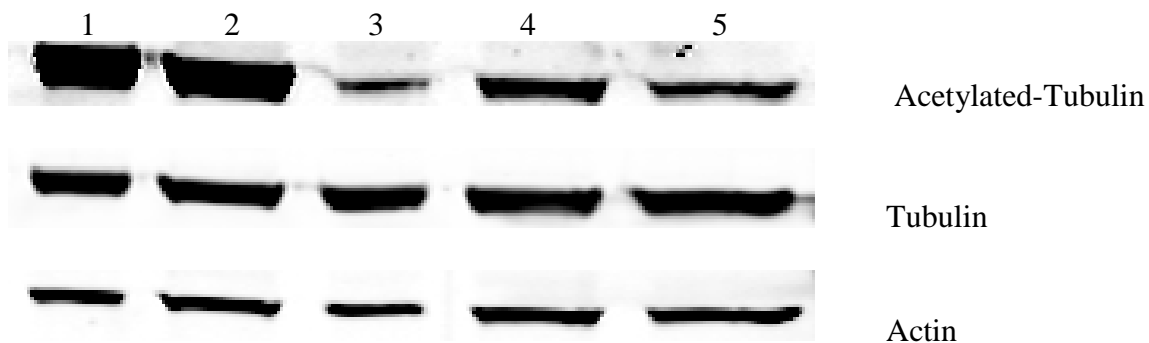


Figure 2.4: Western blot analysis of tubulin acetylation (HDAC6 inhibition) in LNCaP cell line (1st generation 3-HPT based inhibitors). Lanes - 1. SAHA (20 μ M); 2. SAHA IC₅₀ (2.31 μ M); 3. Control; 4. **8** (20 μ M); 5. **8** IC₅₀ (7.75 μ M).

The data presented above showed that some of these 2nd generation 3-HPT based compounds were HDAC6 inhibitors (Table 2.3); we nevertheless sought to confirm the involvement of HDAC6 inhibition in the mechanism of action of compounds **17** and **24**. We examined the level of tubulin acetylation in LNCaP cells following exposure to **17**, **24**³¹ and the positive control SAHA. We observed that **17** and **24** increased tubulin

acetylation but to a lesser extent than SAHA (Figure 2.5). These data propose that compounds **17** and **24** may derive their anti-proliferative effects in LNCaP cell line from an HDAC6-dependent pathway.

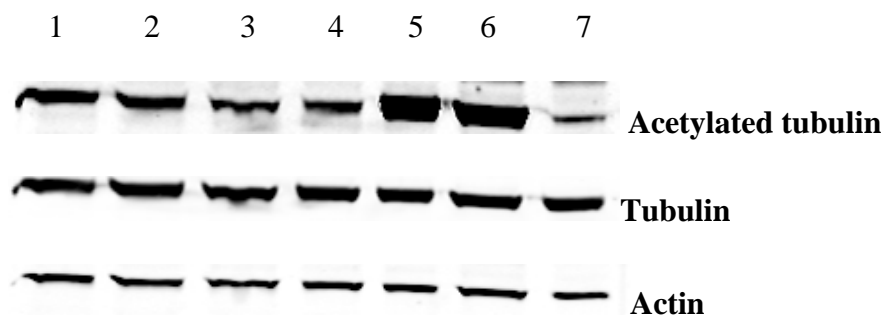


Figure 2.5. Western blot analysis of tubulin acetylation (HDAC6 inhibition) in LNCaP cell line (2nd generation 3-HPT based inhibitors). Lanes - 1. **17** (20 μM); 2. **17** (5.43 μM – IC_{50}); 3. **24** (20 μM); 4. **24** (3.49 μM – IC_{50}); 5. SAHA (20 μM); 6. SAHA (2.31 μM – IC_{50}); 7. Control.

2.6. Conclusion

In an attempt to address the metabolic liabilities and the pan-inhibition of the prototypical HDACi SAHA, a fragment-based approach was used in our laboratory to identify 3HPT as a novel ZBG for HDAC inhibition. This discovery led to the syntheses of 1st and 2nd generations of HDACi with 3HPT as ZBG. All the 3HPT derived compounds reported herein are inactive against HDAC1 but many possessed varying degrees of activity against HDAC6 and HDAC8. Additionally, a subset of these compounds is cytotoxic to various cancer cell lines including Jurkat J- γ 1 against which SAHA and Tubastatin A are inactive. The increase in acetylated tubulin level induced by representative compounds confirmed the contribution of HDAC6 inhibition to their bioactivity. Due to their anticipated immunity to many of the metabolic and pharmacokinetic that has beleaguered the hydroxamate, these 3HPT derived HDACi may display improved *in vivo* activity.

2.7. General procedures and experimental

DU145, LNCaP, Jurkat J. γ were obtained from ATCC (Manassas, VA, USA), Jurkat E6-1 cell line was kindly donated by Dr. John McDonald and grown on recommended medium supplemented with 10% fetal bovine serum (Global Cell Solutions, Charlottesville, VA, USA) and 1% pen/strep (Cellgro, Manassas, VA) at 37°C in an incubator with 5% CO₂. Mouse anti-acetylated α -Tubulin antibody was obtained from Invitrogen (Life Technologies, Grand Island, NY, USA), rabbit anti-actin, rabbit anti-tubulin α antibodies and Tubastatin A were purchased from Sigma-Aldrich (St. Louis, MO, USA). Secondary antibodies, goat anti-rabbit conjugated to IRDye680 and goat anti-mouse conjugated to IRDye800 were purchased from LI-COR Biosciences (Lincoln, NE, USA). The CellTiter 96 AQueous One Solution Cell Proliferation assay (MTS) kit was purchased from Promega (Madison, WI, USA).

2.7.1. Histone deacetylase inhibition (Performed by James Kornacki at Northwestern University)

The HDAC activity in presence of various compounds was assessed by SAMDI mass spectrometry. As a label-free technique, SAMDI is compatible with a broad range of native peptide substrates without requiring potentially disruptive fluorophores. To obtain IC₅₀ values, we incubated isoform-optimized substrates (50 μ M, detailed below) with enzyme (250nM, detailed below) and inhibitor (at concentrations ranging from 10nM to 1.0mM), in HDAC buffer (25.0 mM Tris-HCl pH 8.0, 140 mM NaCl, 3.0 mM KCl, 1.0 mM MgCl₂, 0.1 mg/mL BSA) in 96-well microtiter plates (60 min, 37°C). Solution-phase deacetylation reactions were quenched with trichostatin A (TSA) and

transferred to SAMDI plates to immobilize the substrate components. SAMDI plates were composed of an array of self-assembled monolayers (SAMs) presenting maleimide in standard 384-well format for high-throughput handling capability. Following immobilization, plates were washed to remove buffer constituents, enzyme, inhibitor, and any unbound substrate and analyzed by MALDI mass spectrometry using automated protocols.³² Deacetylation yields in each triplicate sample were determined from the integrated peak intensities of the molecular ions for the substrate and the deacetylated product ion by taking the ratio of the former over the sum of both. Yields were plotted with respect to inhibitor concentration and fitted to obtain IC₅₀ values for each isoform-inhibitor pair.

Isoform-optimized substrates were prepared by traditional Fmoc solid phase peptide synthesis (reagents supplied by Anaspec) and purified by semi preparative HPLC on a reverse phase C18 column (Waters). The peptide of sequence GRK^{ac}FGC was prepared for HDAC1 and HDAC8 experiments, while the peptide of sequence GRK^{ac}YGC was prepared for HDAC6 and HDAC2 experiments. Isoform preference for the indicated substrates was determined by earlier studies on peptide arrays.³³

HDAC1, HDAC6, and HDAC2 were purchased from BPS Biosciences. The catalytic domain of HDAC8 was expressed as previously reported.³³ Briefly, an amplicon was prepared by PCR with the following primers: forward 5'-3' TATTCTCGAGGACCACATGCTTCA and reverse 5'-3' ATAAGCTAGCATGGAGGAGCCGGA. A pET21a construct bearing the genetic insert between NheI and XhoI restriction sites was transformed into *E. coli* BL21(DE3) (Lucigen) and expressed by standard protocols. Following purification by affinity

chromatography, the His-tagged enzyme-containing fractions were purified by FPLC (AKTA) on a superdex size exclusion column (GE), spin concentrated, and stored at -80°C in HDAC buffer with 10% glycerol.

2.7.2. Cell viability assay

DU145 and Vero cells were maintained in EMEM and DMEM respectively supplemented with 10 % FBS and 1% pen/strep while all other cell lines were maintained in RPMI 1640 supplemented with 10 % FBS and 1% pen/strep. DU145, Vero and LNCaP cells were incubated on a 96-wells plate (4500 cells/well) for 24 hours prior to a 72 hours drug treatment while Jurkat and Jurkat J.γ cells (25,000 cells/well) were incubated in media containing the various compounds for 72 hours. Cell viability was measured using the MTS assay according to manufacturer protocol (Promega, CellTiter 96® AQueous One Solution Cell Proliferation Assay, Catalog# G3580). The DMSO concentration in the cell media during the cell viability experiment was maintained at 0.1%.

2.7.3. Solubility Measurement

This experiment was performed according to reported protocol using a 10 mM stock solution of the test compound in DMSO.²⁰ The DMSO was kept at 5% of the final volume. Following incubation at room temperature and centrifugation to remove precipitate, the absorbance was measured using a UV-vis spectrophotometer (Varian, Palo Alto, CA).

2.7.4. Western blot analysis for tubulin acetylation

LNCaP cells were plated for 24 hours and treated with various concentrations of compounds for 4 hours. The cells were washed with PBS buffer and resuspended in CellLytic™M buffer containing a cocktail of protease inhibitor (Sigma-Aldrich, St. Louis, MO, USA). Following quantification through a Bradford protein assay, equal amount of protein was loaded onto an SDS-page gel (Bio-Rad, Hercules, CA, USA) and resolved by electrophoresis at a constant voltage of 100V for 2 hours. The gel was transfer onto a nitrocellulose membrane and probed for selected proteins using primary antibodies against: for acetylated tubulin (LifeTechnologies, catalog# 32-2700), tubulin (Sigma-Aldrich, catalog# SAB4500087) and actin (Sigma-Aldrich, catalog# A2066).

2.7.5. MMP assay

MMP inhibitor profiling kit was purchased from Enzo Life Sciences (Farmingdale, NY). The selection of the MMP tested was guided by the reported anti-proliferative of AG3340, a MMP inhibitor selective for isoforms 1, 2, 3, 7, 9, 13, 14.²⁶ Each MMP was incubated with the inhibitor (10µM) for 30 minutes at 37°C in the assay buffer. The OmniMMP™ fluorogenic substrate peptide was added and the reaction was allowed to proceed at 37°C for 30 minutes. The fluorescence was measured using a fluorescence plate reader with excitation at 328 nm and emission at 420nm.³⁴

2.7.6. Statistical analysis

The values reported as mean \pm standard deviation from at least 2 independent triplicate experiments. A student's t-test was performed in Excel, and results with p value less than 5% were considered statistically different.

2.8. References

1. Gryder, B. E.; Sodji, Q. H.; Oyelere, A. K., Targeted cancer therapy: giving histone deacetylase inhibitors all they need to succeed. *Future Medicinal Chemistry* **2012**, *4* (4), 505-524.
2. Weichert, W., HDAC expression and clinical prognosis in human malignancies. *Cancer Letters* **2009**, *280* (2), 168-176.
3. Kim, H. J.; Bae, S. C., Histone deacetylase inhibitors: molecular mechanisms of action and clinical trials as anti-cancer drugs. *American Journal of Translational Research* **2011**, *3* (2), 166-179.
4. Yang, X. J.; Seto, E., HATs and HDACs: from structure, function and regulation to novel strategies for therapy and prevention. *Oncogene* **2007**, *26* (37), 5310-5318.
5. Marks, P. A.; Breslow, R., Dimethyl sulfoxide to vorinostat: development of this histone deacetylase inhibitor as an anticancer drug. *Nature Biotechnology* **2007**, *25* (1), 84-90.
6. Butler, K. V.; Kalin, J.; Brochier, C.; Vistoli, G.; Langley, B.; Kozikowski, A. P., Rational Design and Simple Chemistry Yield a Superior, Neuroprotective HDAC6 Inhibitor, Tubastatin A. *Journal of the American Chemical Society* **2010**, *132* (31), 10842-10846.
7. Saito, A.; Yamashita, T.; Mariko, Y.; Nosaka, Y.; Tsuchiya, K.; Ando, T.; Suzuki, T.; Tsuruo, T.; Nakanishi, O., A synthetic inhibitor of histone deacetylase, MS-27-275, with marked in vivo antitumor activity against human tumors. *Proceedings of the National Academy of Sciences* **1999**, *96* (8), 4592-4597.
8. Patil, V.; Sodji, Q. H.; Kornacki, J. R.; Mrksich, M.; Oyelere, A. K., 3-Hydroxypyridin-2-thione as Novel Zinc Binding Group for Selective Histone Deacetylase Inhibition. *Journal of Medicinal Chemistry* **2013**, *56* (9), 3492-3506.
9. Sodji, Q. H.; Patil, V.; Kornacki, J. R.; Mrksich, M.; Oyelere, A. K., Synthesis and Structure–Activity Relationship of 3-Hydroxypyridine-2-thione-Based Histone Deacetylase Inhibitors. *Journal of Medicinal Chemistry* **2013**, *56* (24), 9969-9981.

10. Reiter, L. A.; Robinson, R. P.; McClure, K. F.; Jones, C. S.; Reese, M. R.; Mitchell, P. G.; Otterness, I. G.; Bliven, M. L.; Liras, J.; Cortina, S. R.; Donahue, K. M.; Eskra, J. D.; Griffiths, R. J.; Lame, M. E.; Lopez-Anaya, A.; Martinelli, G. J.; McGahee, S. M.; Yocum, S. A.; Lopresti-Morrow, L. L.; Tobiassen, L. M.; Vaughn-Bowser, M. L., Pyran-containing sulfonamide hydroxamic acids: potent MMP inhibitors that spare MMP-1. *Bioorganic & Medicinal Chemistry Letters* **2004**, *14* (13), 3389-3395.
11. Frey, R. R.; Wada, C. K.; Garland, R. B.; Curtin, M. L.; Michaelides, M. R.; Li, J.; Pease, L. J.; Glaser, K. B.; Marcotte, P. A.; Bouska, J. J.; Murphy, S. S.; Davidsen, S. K., Trifluoromethyl ketones as inhibitors of histone deacetylase. *Bioorganic & Medicinal Chemistry Letters* **2002**, *12* (23), 3443-3447.
12. Coussens, L. M.; Fingleton, B.; Matrisian, L. M., Matrix Metalloproteinase Inhibitors and Cancer—Trials and Tribulations. *Science* **2002**, *295* (5564), 2387-2392.
13. Miller, T. A.; Witter, D. J.; Belvedere, S., Histone Deacetylase Inhibitors. *Journal of Medicinal Chemistry* **2003**, *46* (24), 5097-5116.
14. Monneret, C., Histone deacetylase inhibitors. *European Journal of Medicinal Chemistry* **2005**, *40* (1), 1-13.
15. Egan, W. J.; Lauri, G., Prediction of intestinal permeability. *Advanced Drug Delivery Reviews* **2002**, *54* (3), 273-289.
16. Guerrant, W.; Patil, V.; Canzoneri, J. C.; Oyelere, A. K., Dual Targeting of Histone Deacetylase and Topoisomerase II with Novel Bifunctional Inhibitors. *Journal of Medicinal Chemistry* **2012**, *55* (4), 1465-1477.
17. Namdar, M.; Perez, G.; Ngo, L.; Marks, P. A., Selective inhibition of histone deacetylase 6 (HDAC6) induces DNA damage and sensitizes transformed cells to anticancer agents. *Proceedings of the National Academy of Sciences* **2010**, *107* (46), 20003-20008.
18. Yamaki, H.; Nakajima, M.; Shimotohno, K. W.; Tanaka, N., Molecular basis for the actions of Hsp90 inhibitors and cancer therapy. *Journal of Antibiotics* **2011**, *64* (9), 635-644.
19. Balasubramanian, S.; Ramos, J.; Luo, W.; Sirisawad, M.; Verner, E.; Buggy, J. J., A novel histone deacetylase 8 (HDAC8)-specific inhibitor PCI-34051 induces apoptosis in T-cell lymphomas. *Leukemia* **2008**, *22* (5), 1026-1034.

20. Lipinski, C. A.; Lombardo, F.; Dominy, B. W.; Feeney, P. J., Experimental and computational approaches to estimate solubility and permeability in drug discovery and development settings. *Advanced Drug Delivery Reviews* **1997**, *23* (1–3), 3-25.
21. Kerns, E. H.; Di, L.; Carter, G. T., In Vitro Solubility Assays in Drug Discovery. *Current Drug Metabolism* **2008**, *9* (9), 879-885.
22. Aldana-Masangkay, G. I.; Sakamoto, K. M., The Role of HDAC6 in Cancer. *Journal of Biomedicine and Biotechnology* **2011**, *2011* Article number: 875824.
23. Williams, C. R.; Tabios, R.; Linehan, W. M.; Neckers, L., Intratumor Injection of the Hsp90 Inhibitor 17AAG Decreases Tumor Growth and Induces Apoptosis in a Prostate Cancer Xenograft Model. *The Journal of Urology* **2007**, *178* (4), 1528-1532.
24. Hackanson, B.; Rimmel, L.; Benkiser, M.; Abdelkarim, M.; Fliegau, M.; Jung, M.; Lubbert, M., HDAC6 as a target for antileukemic drugs in acute myeloid leukemia. *Leukemia Research* **2012**, *36* (8), 1055-1062.
25. Mwakwari, S. C.; Guerrant, W.; Patil, V.; Khan, S. I.; Tekwani, B. L.; Gurard-Levin, Z. A.; Mrksich, M.; Oyelere, A. K., Non-Peptide Macrocyclic Histone Deacetylase Inhibitors Derived from Tricyclic Ketolide Skeleton. *Journal of Medicinal Chemistry* **2010**, *53* (16), 6100-6111.
26. Shalinsky, D. R.; Brekken, J.; Zou, H.; McDermott, C. D.; Forsyth, P.; Edwards, D.; Margosiak, S.; Bender, S.; Truitt, G.; Wood, A.; Varki, N. M.; Appelt, K., Broad Antitumor and Antiangiogenic Activities of AG3340, a Potent and Selective MMP Inhibitor Undergoing Advanced Oncology Clinical Trials. *Annals of the New York Academy of Sciences* **1999**, *878* (1), 236-270.
27. Jacobsen, J. A.; Fullagar, J. L.; Miller, M. T.; Cohen, S. M., Identifying Chelators for Metalloprotein Inhibitors Using a Fragment-Based Approach. *Journal of Medicinal Chemistry* **2010**, *54* (2), 591-602.
28. Ropero, S.; Esteller, M., The role of histone deacetylases (HDACs) in human cancer. *Molecular Oncology* **2007**, *1* (1), 19-25.
29. Huang, B. H.; Laban, M.; Leung, C. H. W.; Lee, L.; Lee, C. K.; Salto-Tellez, M.; Raju, G. C.; Hooi, S. C., Inhibition of histone deacetylase 2 increases apoptosis and p21Cip1/WAF1 expression, independent of histone deacetylase 1. *Cell Death & Differentiation* **2005**, *12* (4), 395-404.

30. Kulp, S. K.; Chen, C.-S.; Wang, D.-S.; Chen, C.-Y.; Chen, C.-S., Antitumor Effects of a Novel Phenylbutyrate-Based Histone Deacetylase Inhibitor, (S)-HDAC-42, in Prostate Cancer. *Clinical Cancer Research* **2006**, *12* (17), 5199-5206.
31. Haggarty, S. J.; Koeller, K. M.; Wong, J. C.; Grozinger, C. M.; Schreiber, S. L., Domain-selective small-molecule inhibitor of histone deacetylase 6 (HDAC6)-mediated tubulin deacetylation. *Proceedings of the National Academy of Sciences* **2003**, *100* (8), 4389-4394.
32. Gurard-Levin, Z. A.; Scholle, M. D.; Eisenberg, A. H.; Mrksich, M., High-Throughput Screening of Small Molecule Libraries using SAMDI Mass Spectrometry. *ACS Combinatorial Science* **2011**, *13* (4), 347-350.
33. Gurard-Levin, Z. A.; Kilian, K. A.; Kim, J.; Bähr, K.; Mrksich, M., Peptide Arrays Identify Isoform-Selective Substrates for Profiling Endogenous Lysine Deacetylase Activity. *ACS Chemical Biology* **2010**, *5* (9), 863-873.
34. Day, J. A.; Cohen, S. M., Investigating the Selectivity of Metalloenzyme Inhibitors. *Journal of Medicinal Chemistry* **2013**, *56* (20), 7997-8007.

CHAPTER 3

TARGETED DELIVERY OF HDAC INHIBITORS USING FOLATE AND PTEROIC ACID

3.1. Introduction

Recent advances in cancer biology have led to the identification of novel targets for cancer therapy.^{1,2} Such, targets include histone deacetylases (HDACs) which are components of the cellular epigenetic machinery.^{3,4,5} There are 11 zinc dependent HDAC isoforms grouped into 3 classes (Classes I, II and IV) and 7 NAD⁺ dependent which form the class III. The class I include HDAC1, 2, 3 and 8 located in the nucleus. Isoforms 4, 5, 7 and 9 constitute the class IIa which shuttle between the nucleus and the cytoplasm. The cytoplasmic HDAC6 and 10 are members of the class IIb and HDAC11 represents the sole member of class IV. HDACs catalyze the removal of acetyl group from lysine residues of histones tail resulting in favorable electrostatic interactions between the phosphate backbone of DNA and the positively charged lysine residues. Such interactions lead to chromatin condensation which concomitantly impedes the access of transcription factors to promoter segments within the condensed chromatin.³ HDACs substrates are not limited to histone proteins. Other non-histone proteins whose activities are directly regulated by HDACs include HSP90, tubulin, androgen receptors, p53 etc.^{6,7} The activity of the HDACs is counterbalanced by histone acetyl transferases (HATs) which add acetyl groups to lysine residues.³

Due to their involvement in gene expression regulation, HDACs are recruited into various complexes by many cancers to purposely silence key pro-apoptotic genes. Consequently, specific HDAC isoforms are overexpressed in various cancer-types.^{8,9}

Inhibition of HDACs activity is now recognized as a novel approach for cancer treatment. Efforts by several pharmaceutical and academic laboratories have led to various histone deacetylase inhibitors (HDACi), many of which have been evaluated in clinical trials against hematological and solid tumors. These efforts have so far resulted in the FDA approvals of Vorinostat and Romidepsin for the treatment of cutaneous T-cell lymphoma (CTCL) in 2006 and 2009 respectively.^{10,11} Similar to many anticancer drugs, HDACi have been associated with various side effects including neutropenia, thrombocytopenia and potentially fatal cardiac arrhythmias.¹² In light of these shortcomings, HDACi therapy could benefit from a targeted therapeutic approach as it is the case for some currently available drugs.¹³ Furthermore, this approach may address other deficiencies of HDACi, primarily their lack of efficacy towards solid tumors attributable to low therapeutic concentration within the malignant cells.^{14,15}

To meet their high metabolic demands, cancer cells overexpress various ligands receptors including those of vitamins.^{16,17} Such receptors include the folate receptor (FR) whose expression is limited to certain epithelial cells including the choroid plexus, lung, thyroid, kidneys and various malignancies.¹⁸⁻²⁰ This selective overexpression in cancer cells has made the FR an ideal candidate for targeted cancer therapy. FR mediated endocytic uptake of folate conjugates into malignant cells has been exploited for the delivery of diagnostic and therapeutic agents²¹⁻²⁴ while minimizing delivery to healthy cells since folate delivery to healthy cells is mediated by the ubiquitously expressed reduced folate carrier (RFC) which does not uptake folate conjugates.^{25,26} Herein we describe the development of tumor-homing HDACi which derive their tumor selective accumulation from targeting FR. Although both folate- and pteronic acid- based

hydroxamates were potent inhibitors of HDAC1 and 6, only the pterioic conjugated HDACi displayed anticancer activities against the folate receptor positive (FR+) tumors KB and HeLa. Moreover, HDAC1 inhibition is sufficient to induce apoptosis in KB cells whereas HDAC6 inhibition has no impact on KB cells' survival.

3.2. Design of Folate receptor ligand-HDACi conjugates

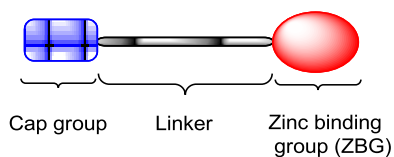
Folic acid, which is comprised of pterioic acid and a glutamate residue (Figure 3.1), has been commonly used to target the FR. Recent reports have however suggested that pterioic acid is also capable of mediating selective delivery of ligands to FR overexpressing tumors despite having minimal affinity for the FR.^{27,28,29} Our main objective in this study is to investigate the prospect of folic and pterioic acids as mediators of selective delivery of HDACi to FR overexpressing cancer cells. To this end, I designed a set of folate- and pteroate-HDACi conjugates in which the folate or pteroate moiety is integrated into the surface recognition group of a prototypical HDACi.³ This design approach furnished minimally-perturbed folate and pteroate analogs (Figure 3.1C) and morphed folate- and pteroate-HDACi hybrids (Figures 3.3, 3.5 and 3. 7).

3.3. folate γ -hydroxamic and pterioic hydroxamic acids as HDAC inhibitors

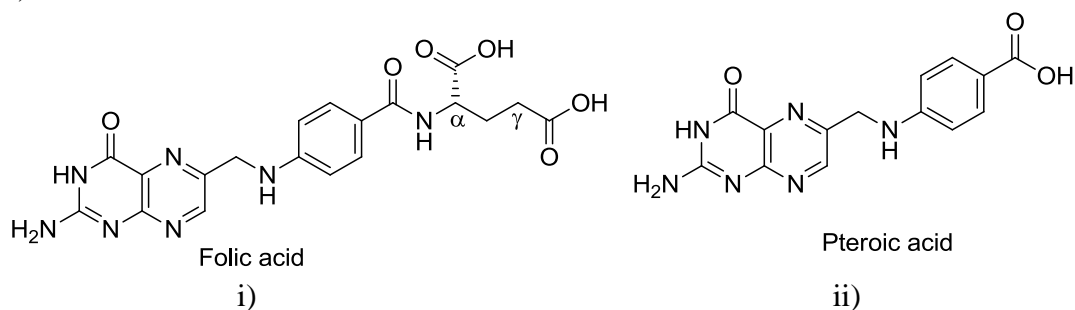
Due to the structural similarity of the pteroate group with HDACi surface recognition groups, we envisioned that the substitution of the carboxylic acid group of folic and pterioic acids with a zinc binding group (ZBG), essential for HDAC inhibition, will furnish the corresponding tumor-homing HDACi. Hence, the γ -carboxyl of folate and the carboxylate moiety of pterioic acid were converted to hydroxamic acid, the most

commonly used ZBG for HDAC inhibition, to furnish compounds **6** and **7** respectively (Figure 3.1C).

A)



B)



C)

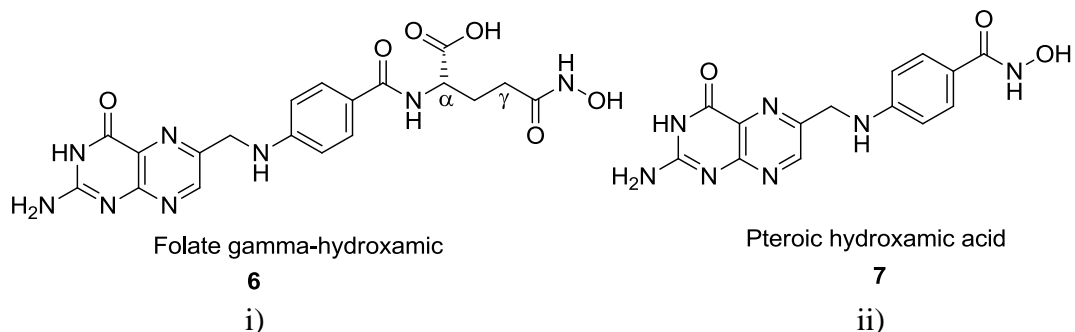


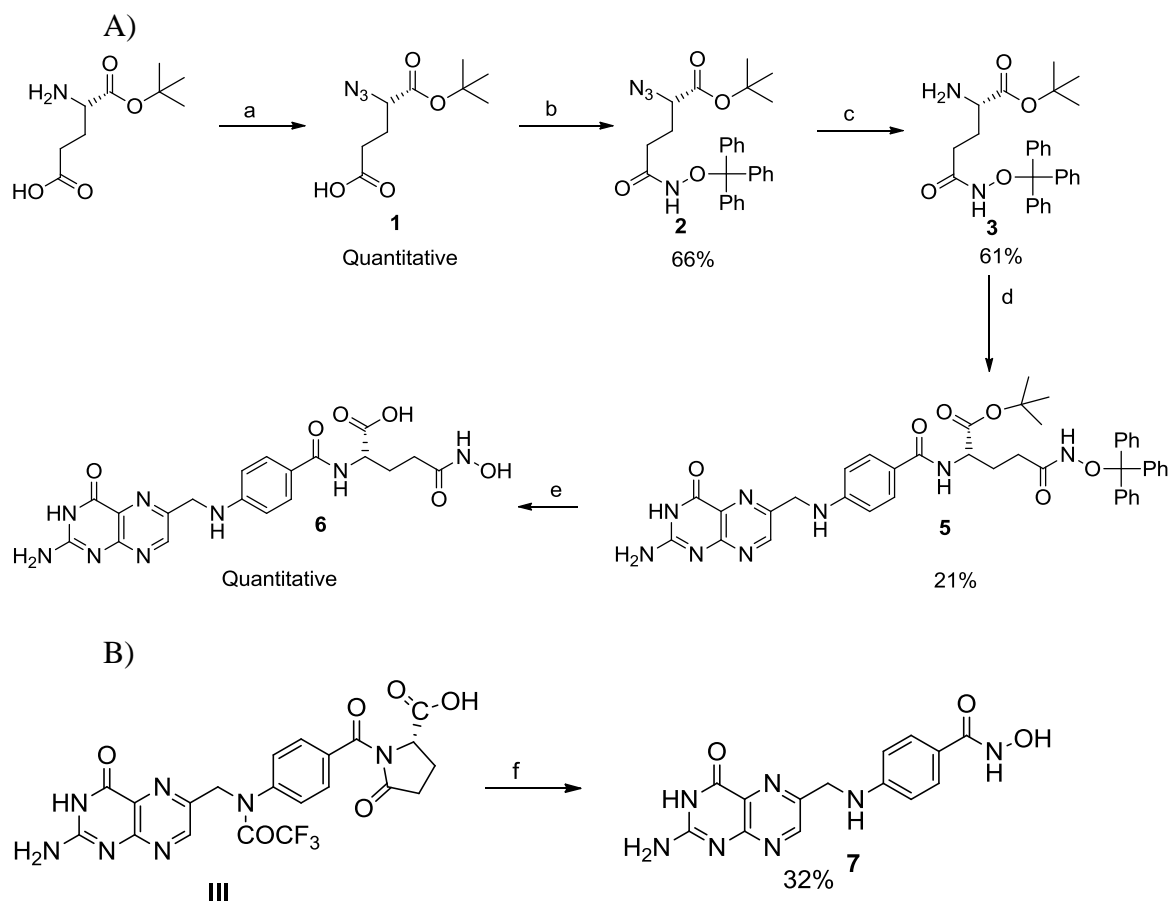
Figure 3.1: HDACi pharmacophoric model A) and structures of folic acid (Bi), pteric acid (Bii), folate γ -hydroxamic acid (Ci) and pteric hydroxamic acid (Cii).

3.3.1. Synthesis of folate γ -hydroxamic and pteric hydroxamic acids

The reaction route for the synthesis of the folate γ -hydroxamate **6** and pteric hydroxamate **7** is shown in Scheme 3.1. L-Glutamic acid α -tert-butyl ester was subjected to diazo-transfer resulting quantitatively in the α -azido L-glutamic acid α -tert-butyl ester **1**.³⁰ The α -azido glutamic acid **1** was coupled with *O*-tritylhydroxylamine in the presence of isobutylchloroformate (IBCF) and *N*-methyl-morpholine (NMM) resulting in

compound **2**.³¹ The azide moiety was then reduced to an amine with Zn and NH₄Cl yielding compound **3**.³² The coupling of **3** with pteroyl azide **4** (see Appendix, scheme S1 for the synthesis of **4**) in the presence of tetramethylguanidine (TMG)³³ resulted in the penultimate intermediate **5**. Exposure of this intermediate to trifluoroacetic acid (TFA) in the presence of triisopropylsilane (TIPS) yielded the desired folate γ -hydroxamate **6** (Scheme 3.1A).³⁴

To obtain the pterotic hydroxamate **7**, N₁₀-(Trifluoroacetyl)pyrofolic acid (See Appendix scheme S1), an intermediate in the synthesis of pteroyl azide **4**,³³ was reacted with a 50% aqueous hydroxylamine in DMSO (Scheme 3.1B).



Scheme 3.1: Syntheses of folate γ -hydroxamate **6** (A) and pterotic hydroxamate **7** (B). a) TfN_3 , K_2CO_3 , $\text{CuSO}_4 \cdot 5\text{H}_2\text{O}$, DCM, H_2O , MeOH, rt; b) IBCF, NMM, NH_2 -O-trityl; c) NH_4Cl , Zn, EtOH/ H_2O (3:1), reflux; d) Pteroyl azide (**4**), TMG, DMSO, rt; e) TFA, TIPS; f) 50% aqueous NH_2OH , DMSO, rt.

3.3.2. HDAC inhibition profile of folate γ -hydroxamic and pterotic hydroxamic acids

We then investigated the HDAC inhibition potential of the folate γ -hydroxamate **6** and pterotic hydroxamate **7** against HDAC1, 6 and 8 using SAMDI mass spectrometry HDAC activity assay as previously described.^{35,36} We observed that the folate γ -hydroxamate **6** was inactive against all three isoforms while the pterotic hydroxamate **7** inhibited all three HDACs. Compound **7** is particularly more effective against HDAC6 with an IC_{50} of 17.6 nM, and HDAC6 selectivity of 130- and 32-fold relative to HDAC1 and HDAC8 respectively (Table 3.1).

Table 3.1: Inhibition profile of folate γ -hydroxamic and pteronic hydroxamic acids (IC₅₀ in nM)

	HDAC1	HDAC6	HDAC8
Folate γ-hydroxamate (6)	NI	NI	NI
Pteronic hydroxamate (7)	2390±470	17.6 ± 2.2	581±198

NI: No inhibition (inhibition below 20% at 10 μ M)

3.3.3. Molecular docking studies.

To rationalize the lack of HDAC inhibition by the folate γ -hydroxamate **6**, it was docked against the homology models of HDAC1 and 6 built respectively from human HDAC2 (PDB code: 3MAX) and HDAC8 (PDB code: 3F0R) using Autodock 4.2 as previously described.^{35,36} Although with both isoforms the folate γ -hydroxamate **6** adopts poses resulting in Zn²⁺ chelation, it does so by positioning the α -carboxylate moiety in locations that are entropically unfavorable. With HDAC6, the α -carboxylate is inserted deep into the hydrophobic pocket where aromatic amino acids are located (Figure 3.2i). The ensuing interactions are so unfavorable potentially preventing entrance of the channel. Docking with HDAC1 provide a different picture. Due to the shallow enzyme channel, the α -carboxylate is precluded from entering the channel resulting in its being in close proximity (<3 Å) to the carboxylate of ASP99 near the channel's entrance (Figure

3.2ii). The repulsion due to this close proximity may prevent the insertion of the ZBG into the active site potentially explaining the lack of activity against HDAC1.

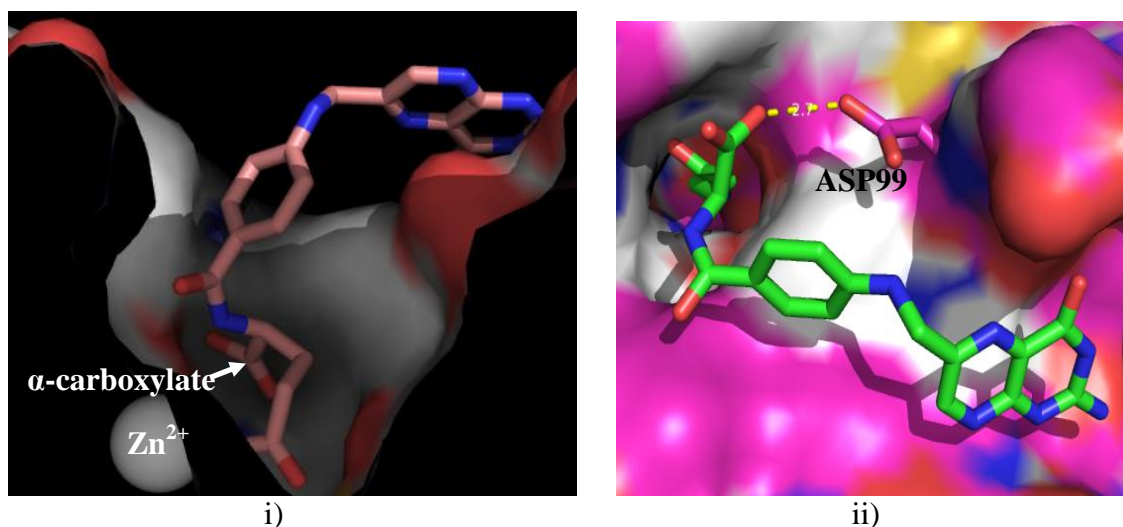


Figure 3.2: Molecular docking studies of folate γ -hydroxamate **6** with homology models of HDAC1 and 6. For Zn^{2+} chelation to occur, the α -carboxylate must be involved in unfavorable interactions; **i)** In HDAC6: The α -carboxylate is inserted in the hydrophobic pocket; **ii)** HDAC1: The α -carboxylate of **6** is unable to enter the hydrophobic channel but is placed in close proximity of the carboxylate of ASP99.

3.4. SAR on pterotic based hydroxamate HDAC inhibitors

In light of the lack of HDAC inhibition by the folate γ -hydroxamate **6**, we focused on the pterotic acid construct in order to optimize the observed HDAC inhibition profile of the pterotic hydroxamate **7**. Toward this end, we designed various pterotic acid based HDACi which incorporated the pterotate moiety into HDACi surface recognition group, maintained the hydroxamic acid as the ZBG but vary the length of the methylene linker separating the ZBG and the surface recognition group (Figure 3.3).

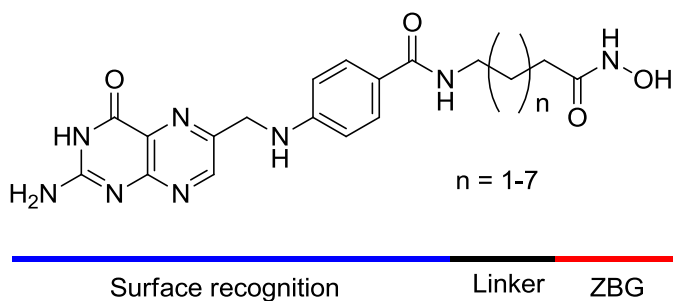
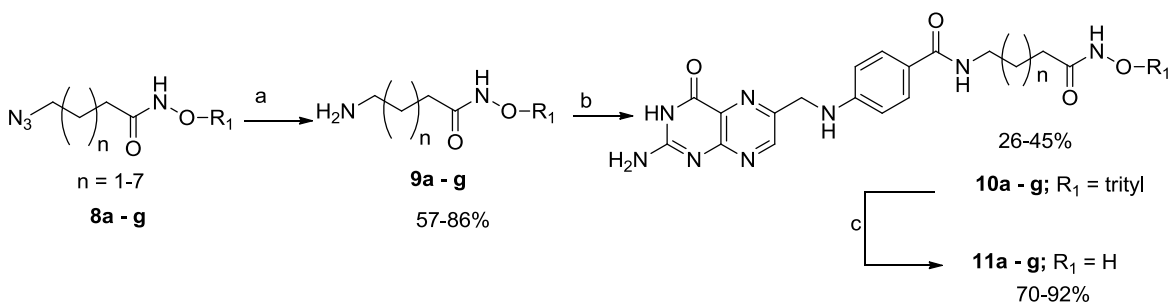


Figure 3.3: Structure of Pterioic based hydroxamates **11a-g**.

3.4.1. Synthesis of pterioic based hydroxamates

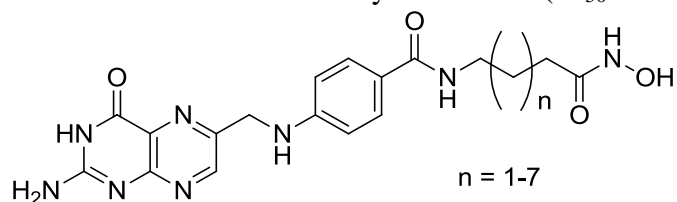
The synthesis of the pterioate hydroxamates **11a-g** is depicted in Scheme 3.2. Reduction of the previously described trityl azido hydroxamates **8a-g** with PPh_3 furnished the corresponding amines **9a-g** which were subsequently reacted with pteroyl azide **4** to yield the *O*-trityl protected hydroxamates **10a-g**.^{37,38} The trityl protecting group was removed with TFA in presence of TIPS to give the requisite hydroxamates **11a-g** (Scheme 3.2).³⁴



Scheme 3.2: Synthesis of Pterioic based hydroxamates **11a-g**. a) i) PPh_3 , THF, rt ii) H_2O ; b) Pteroyl azide **4**, TMG, DMSO, rt; c) TFA, TIPS.

3.4.2. HDAC inhibition profile of pterotic based hydroxamates

To evaluate the impact of the linker on their potency and isoform selectivity, we profiled the HDAC inhibition activity of hydroxamates **11a-g** against HDACs 1, 6 and 8 (Table 3.2). Relative to the linkerless compound **7**, the 3-methylene linker compound **11a** is a significantly weaker HDACi. Despite the loss of potency, **11a** is also selective for HDAC6. Subsequent increase in the methylene linker length, up to 8-methylene groups largely resulted in improved HDAC1 and HDAC6 inhibition activities. We observed that a further increase in linker length is detrimental to HDAC inhibition activity (Table 3.2, compare **11f** and **11g**). Among these pterotic hydroxamates, **11e** is the most potent HDAC1 inhibitor whereas **11f** is the most potent HDAC6 inhibitor. Interestingly, we did not notice any direct correlation between changes in the linker length and the HDAC8 inhibition activity of these pterotic hydroxamates.

Table 3.2: HDAC inhibition of Pteoric based hydroxamates (IC₅₀ in nM)

	n	HDAC1	HDAC6	HDAC8
11a	(1)	22.1 ± 1.7%	1460 ± 310	25 ± 18%
11b	(2)	6150 ± 1320	212 ± 15	39 ± 6%
11c	(3)	79.6 ± 12.6	43.6 ± 8.4	41 ± 17%
11d	(4)	23.4 ± 4.2	12.2 ± 0.2	1060 ± 320
11e	(5)	16.1 ± 2.8	55.4 ± 2.2	9380 ± 1720
11f	(6)	524 ± 36	10.2 ± 1.0	7590 ± 2120
11g	(7)	53 ± 7%	476 ± 48	40 ± 10%
SAHA	-	38 ± 2	144 ± 23	232 ± 19

% inhibition at 10 μM are given if the IC₅₀ was above 10 μM

3.4.3. Molecular docking studies of pteric based hydroxamates

To understand the basis of HDAC1 inhibition by the pteric based hydroxamates, **11a**, **11c** and **11e** were docked against the homology model of HDAC1 built from HDAC2 (PDB code: 3MAX). To provide similar insights into the HDAC6 inhibition, **11a**, **11c** and **11f** were docked against the homology model of HDAC6 built HDAC8 (PDB code: 3F0R).

With HDAC1, Zn^{2+} chelation seems to be the major determinant of HDAC inhibition. The 3-carbon methylene linker of **11a** was not long enough to achieve optimal Zn^{2+} chelation (Figure 3.4Ai). An increase to 5 carbon-methylene linker as in **11c** brought the ZBG closer to Zn^{2+} to achieve chelation. Besides the zinc chelation, **11e** is further stabilized by a T-shape interaction between its pterin ring and the aromatic ring of TYR204 (Figure 3.4Aii). Analysis of the docking poses of the compounds aforementioned with HDAC6 suggest the involvement of Zn^{2+} chelation along with additional stabilizing interactions in the HDAC6 inhibition trend. All three compounds display optimal Zn^{2+} chelation (Figure 3.4Bi), however, **11a** is not further stabilized by any other observable interaction. On the other hand, the pterin moiety of **11c** and **11f** is involved in π -stacking interaction with the aromatic ring of PHE680. The geometry of the π -stacking may explain the increased potency of **11f** compared to **11c** as the pterin ring in **11f** is perfectly parallel to the ring of PHE680 (Figure 3.4Bii).

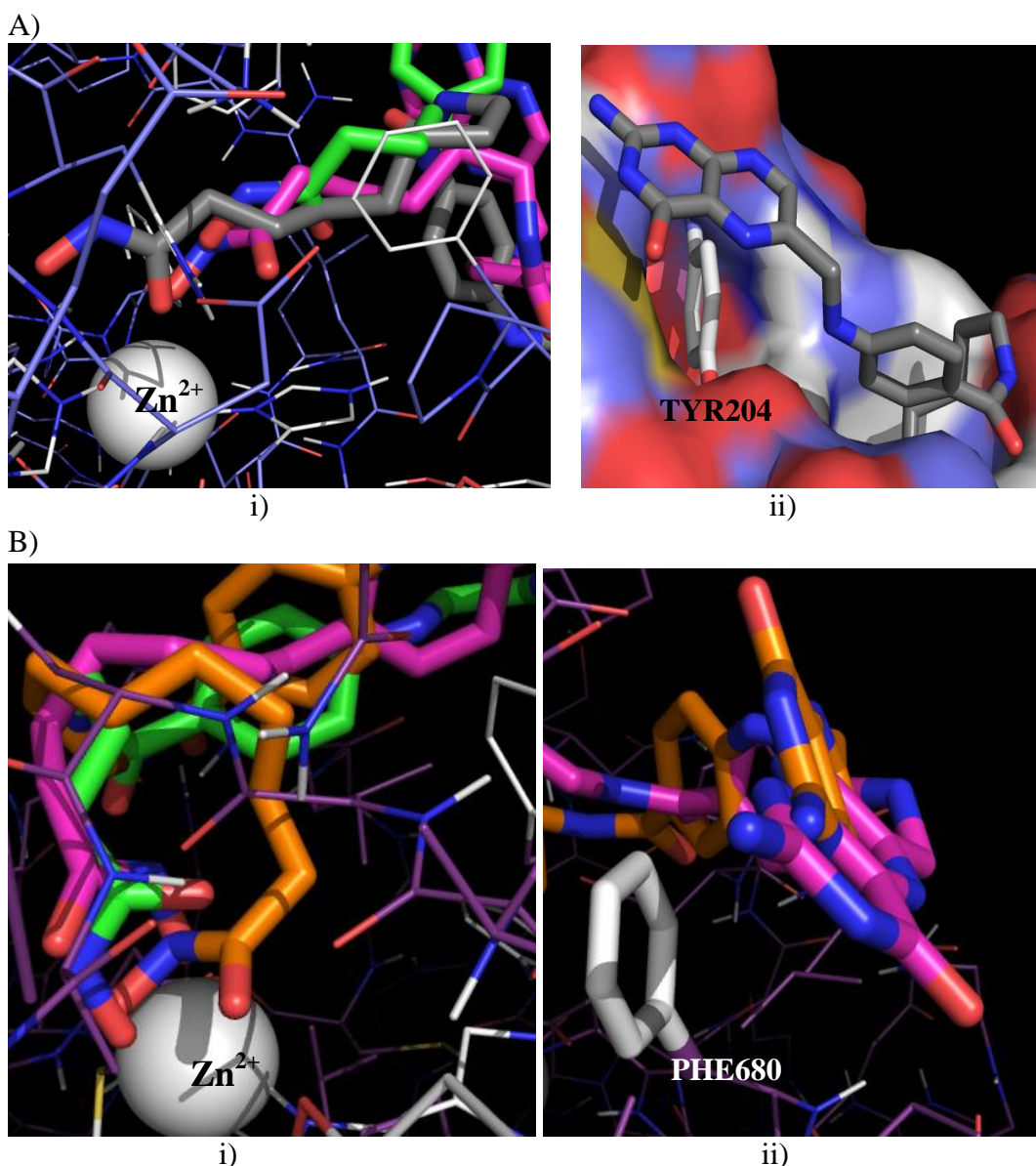


Figure 3.4 : Molecular docking poses explaining the inhibitory profile of selected pteric based hydroxamates against HDAC1 and HDAC6; **A) HDAC1**: i) Both **11c** (purple) and **11e** (grey) chelate the active site Zn^{2+} but **11a** (green) does not due to a short linker; ii) Besides the Zn^{2+} chelation, **11e** (grey) is further stabilized by a T-shape interaction between its pterin and the aromatic ring of TYR204. **B) HDAC6**: i) All three inhibitors, **11a** (green), **11c** (purple) and **11f** (orange) chelate the Zn^{2+} ; ii) Both **11c** and **11f** are further stabilized by a π -stacking between their respective pterin ring and PHE680, furthermore the pterin ring of **11f** is perfectly parallel to the aromatic ring of PHE680 unlike in **11c**.

3.5. Folic acid based hydroxamate HDACi

Encouraged by the results from the aforementioned SAR study on the pteroate hydroxamates, we performed similar structural alterations to the folate template (Figure 3.5) as folate-derived compounds may possess greater affinity for the FR compare to their pteronic acid congeners. The synthesis of the folate-derived hydroxamates **15a-g** is depicted in Scheme 3.3.

3.5.1. Synthesis of folate based hydroxamic acids

The α -azido L-glutamic acid α -tert-butyl ester **1** was coupled to the trityl amino hydroxamates **9a**, **9d**, **9e**, **9f** in the presence of IBCF and NMM yielding the azido trityl protected hydroxamate compounds **12a-d**.^{31,39} Subsequent azide reduction with NH_4Cl and Zn followed by coupling to the pteroyl azide **4** as previously mentioned gave the protected folate based hydroxamate HDACi **14a-d**.^{32,33} Removal of the trityl and *t*-Butyl protecting groups was accomplished in TFA with TIPS furnishing the folate based hydroxamate compounds **15a-d**.³⁴

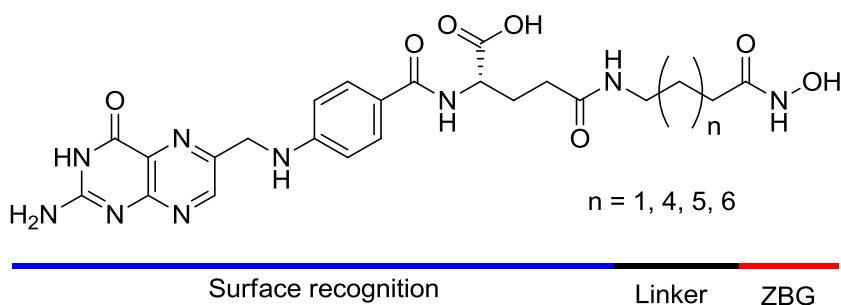
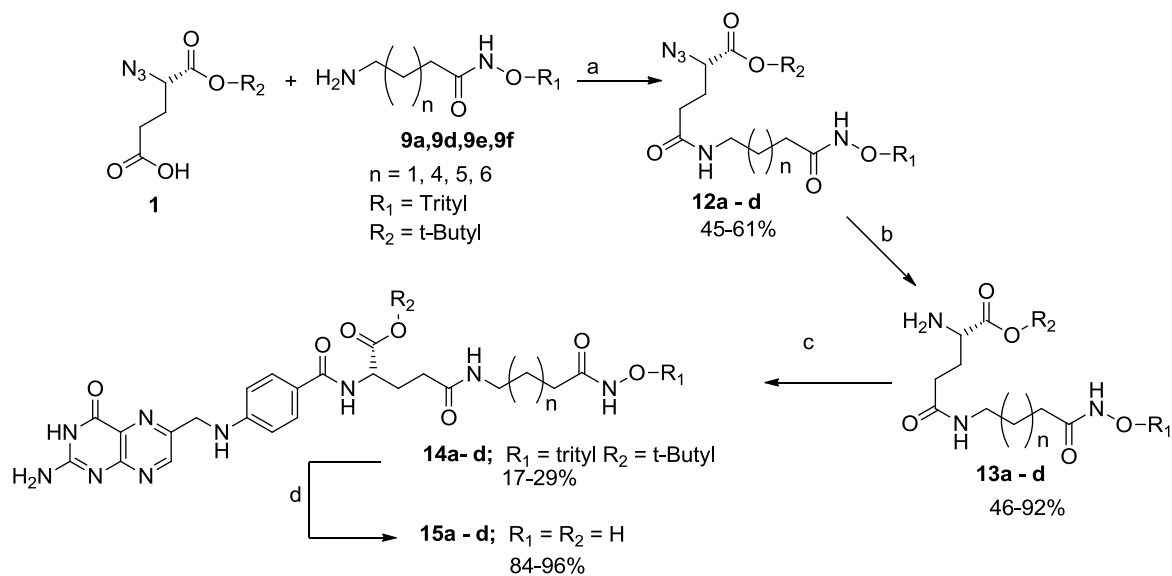


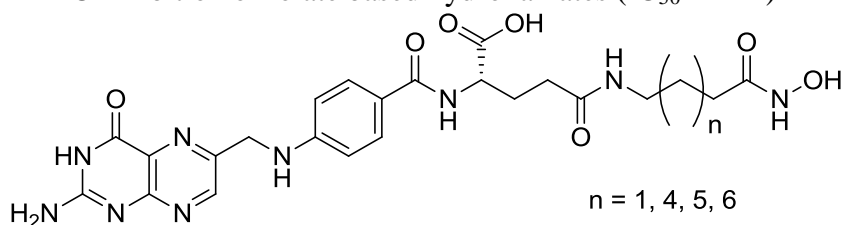
Figure 3.5: Structure of folate based hydroxamates **15a-g**.



Scheme 3.3: Synthesis of folate based hydroxamates. a) IBCF, NMM; b) Zn, NH_4Cl , EtOH/ H_2O (3:1), reflux; c) Pteroyl azide **4**, TMG, DMSO, rt; d) TFA, TIPS

3.5.2. HDAC inhibition profile of folate based hydroxamic acids

Unlike the folate γ -hydroxamate **6**, compounds **15a-d** displayed linker length-dependent anti-HDAC activity with a clear preference for HDAC6 (Table 3.3). Against the three HDAC isoforms investigated, **15b** is the most potent among this series of HDACi. Relative to pteroate hydroxamates **11a-g**, compounds **15a-d** are generally less potent. However, selected members of this series – **15c** and **15d** – are more active against HDAC8 relative to their pteroate hydroxamate congeners **11e** and **11f**.

Table 3.3: HDAC inhibition of folate based hydroxamates (IC₅₀ in nM)

	n	HDAC1	HDAC6	HDAC8
15a	(1)	NI	8050 ± 330	40 ± 5%
15b	(4)	1770 ± 100	132 ± 23	2390 ± 640
15c	(5)	1800 ± 180	193 ± 41	2370 ± 430
15d	(6)	2760 ± 550	179 ± 19	1560 ± 340
SAHA	-	38 ± 2	144 ± 23	232 ± 19

% inhibition at 10 μM are given if the IC₅₀ was above 10 μM.
 NI: No Inhibition (below 20% Inhibition at 10 μM concentration)

3.5.3. Molecular docking studies of the folate based hydroxamate compound **15c**

To understand the basis of the HDAC6 selectivity by the folate based hydroxamates, **15c** was docked against the homology models of HDAC1 and 6 built respectively from human HDAC2 (PDB code: 3MAX) and HDAC8 (PDB code: 3F0R) using Autodock 4.2 as previously described.^{35,36} Against HDAC6, the hydroxamate ZBG of **15c** chelates to the zinc (Figure 3.6Ai) and is stabilized by hydrogen bonds with the side chain of ASP567 and the C=O backbone of PHE566. Further stabilizing interactions may also be provided by the π -stacking interaction between the pterin ring and the phenyl ring of PHE680 (Figure 3.6Aii). With HDAC1, the zinc chelation is not optimal due to other interactions obliging the hydroxamate ZBG to adopt the observed binding mode (Figure 3.6Bi). These interactions include hydrogen bonds between **15c** and side chains

of GLU146, ASN95, ASP99, backbone C=O of GLU203, NH of PHE205 whose phenyl ring also participate in a T-shape interaction with the pterin ring of **15c** (Figure 3.6Bii).

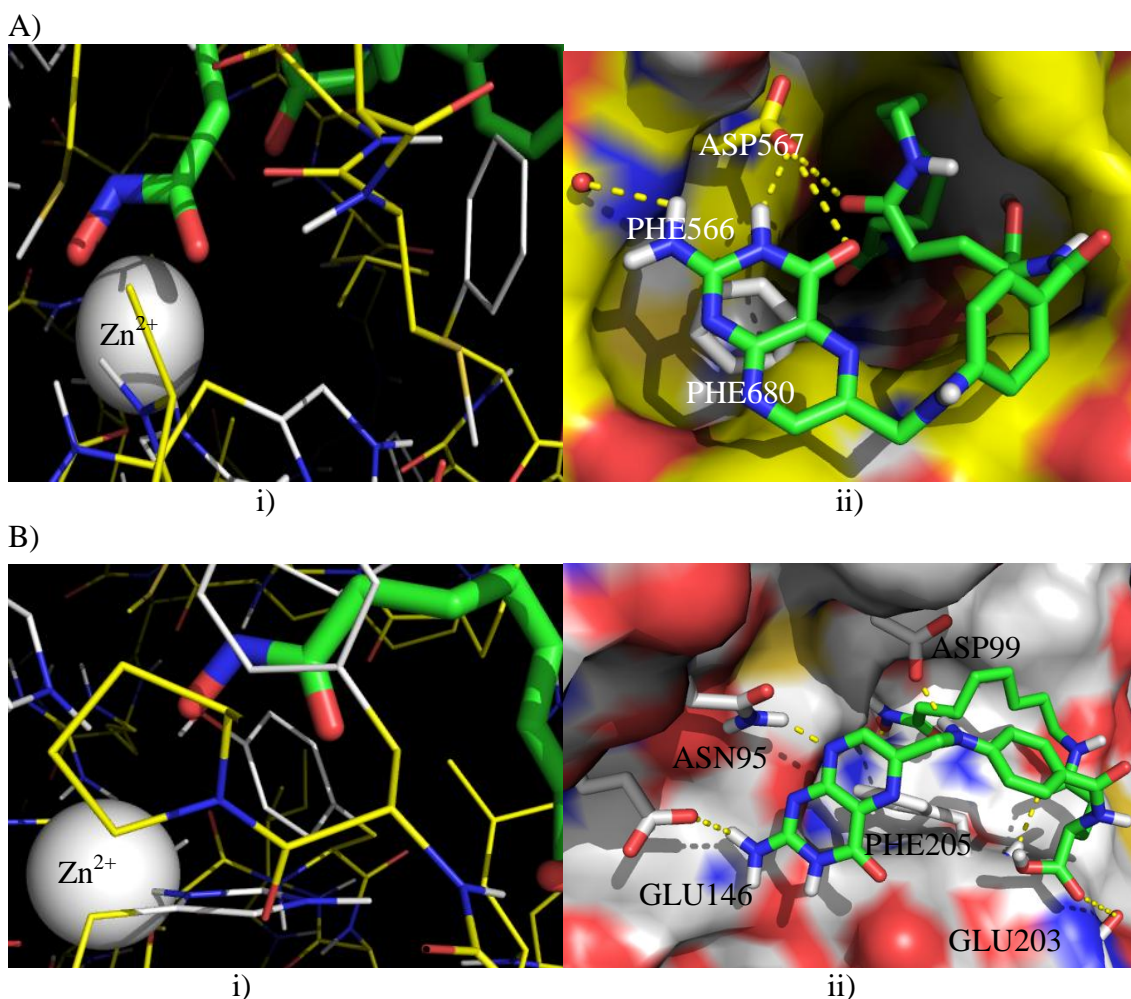


Figure 3.6 : Molecular basis for isoform selectivity of **15c**. **A**) Molecular docking of **15c** with HDAC6 homology model built from HDAC8 (PDB code: 3F0R); i) Zinc chelation by **15c**; ii) Polar interactions between **15c** and HDAC6 homology model and π -stacking of phenyl of PHE680 with **15c**; **B**) Molecular docking of **15c** with HDAC1 homology model built from HDAC2 (PDB code: 3MAX); i) Orientation of the hydroxamate ZBG at the active site; ii) Stabilizing interactions between **15c** and HDAC1 homology model include H-bonds and T-shape interaction of PHE205 with pterin ring of **15c**.

3.6. Targeted delivery of isoform selective HDACi

From the observation that the class I selective inhibitor MS275 and HDAC6 selective inhibitor ACY-1215 are well tolerated in clinical trials, isoform selectivity of HDACi has been suggested as a mean of enhancing the safety of HDACi therapy.^{3,40} I decided to combine this approach to the targeted delivery by designing folate based benzamide HDACi. Such compounds will embody the targeted delivery of HDAC1 selective inhibitors which may be well tolerated as MS275 while having a significantly high intratumoral concentration (Figure 3.7).

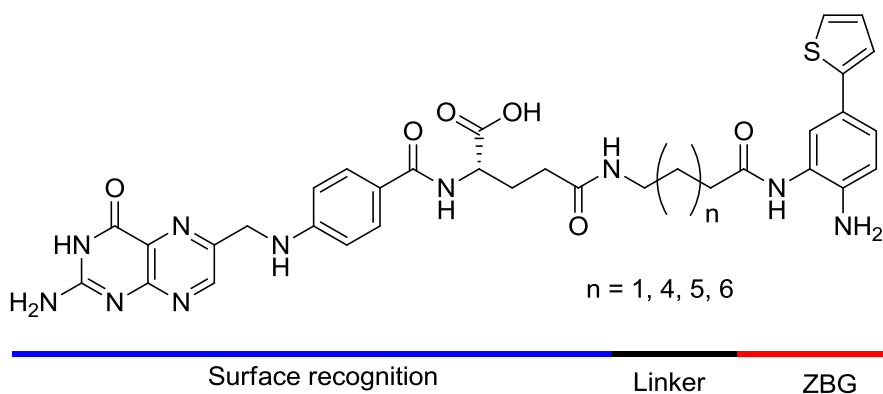
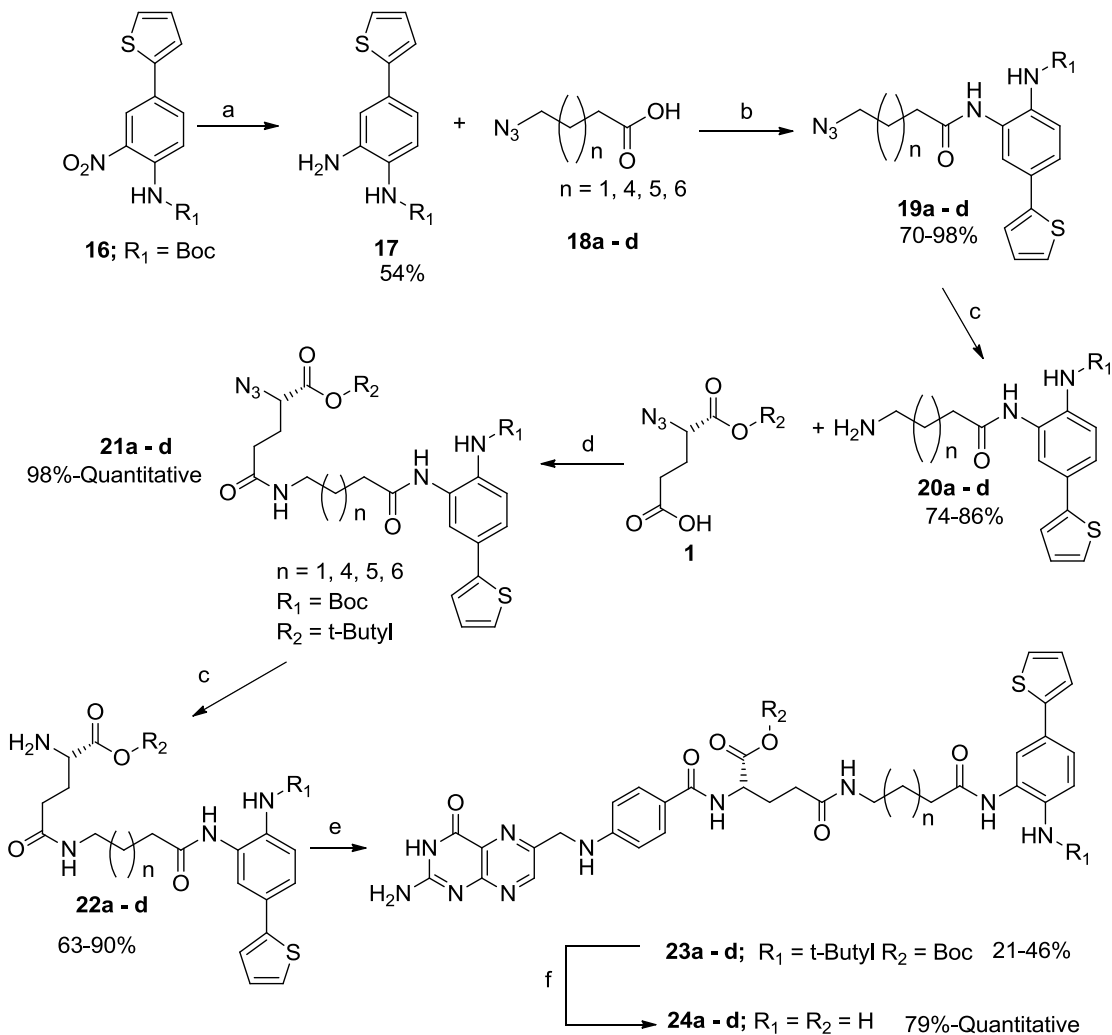


Figure 3.7: Structure of folate based biaryl benzamide HDACi.

3.6.1. Synthesis of folate based biaryl benzamide compounds

Precursor of the biaryl benzamide ZBG **16** was synthesized as previously reported (See Appendix scheme S2).⁴¹ The biaryl benzamide ZBG **17** was obtained following the reduction of the nitro group in presence of Zn in dioxane/H₂O (4:1) (Scheme 3.4).⁴² In presence of EDCI and HOBT, the ZBG **17** was coupled to various azido carboxylic acids (**18a-d**) yielding compounds **19a-d**.^{37,31} Following the reduction of the azide with zinc and NH₄Cl, compounds **20a-d** were coupled to α -azido glutamic acid **1** resulting in the intermediates **21a-d**, which were reduced prior to their coupling with pteroyl azide **4**.

Final removal of protecting groups was conducted in TFA containing TIPS to afford the folate-based biaryl benzamide HDACi **24a-d** (Scheme 3.4).³⁴

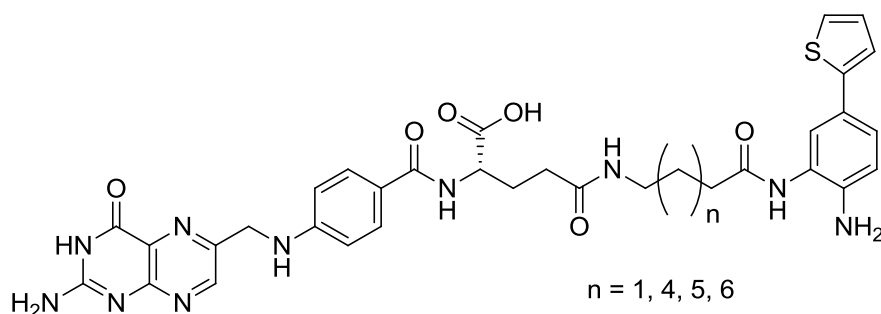


Scheme 3.4: Synthesis of folate based biaryl benzamide HDACi. a) Zn, Dioxane/H₂O (4:1), 70°C; b) EDCI, HOBT, DMF, 70°C; c) Zn, NH₄Cl, EtOH/H₂O (3:1), reflux; d) EDCI, HOBT, DMF, rt; e) Pteroyl azide **4**, TMG, DMSO; f) TFA, TIPS

3.6.2. HDAC inhibition profile of folate based biaryl benzamide HDACi

As opposed to their hydroxamate congeners, the biaryl benzamides are devoid of HDAC6 and 8 inhibition (Table 3.4). This selectivity for HDAC1 was expected as the biaryl benzamide ZBG is selective for HDAC1.⁴¹ A trend in the potency against HDAC1 is observable starting from the 3-methylene linker **24a** (least potent) to the 7-methylene spacer **24c** which is the optimal inhibitor in the series.

Table 3.4: Inhibition of various HDAC isoforms by folate based biaryl benzamides (IC₅₀ in nM).



	n	HDAC1	HDAC6	HDAC8
24a (C4)	(1)	2940 ± 330	22.8 ± 0.3%	23 ± 6%
24b (C7)	(4)	435 ± 35	NI	NI
24c (C8)	(5)	287 ± 53	NI	67 ± 1%
24d (C9)	(6)	309 ± 74	NI	NI
SAHA	-	38 ± 2	144 ± 23	232 ± 19

% Inhibition at 10 μM are given if the IC₅₀ was above 10 μM.

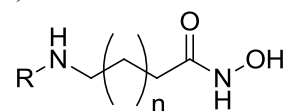
NI: No Inhibition (below 20% Inhibition at 10 μM concentration)

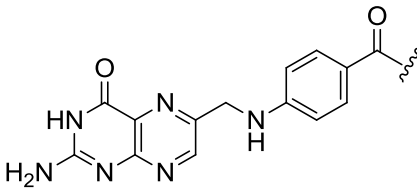
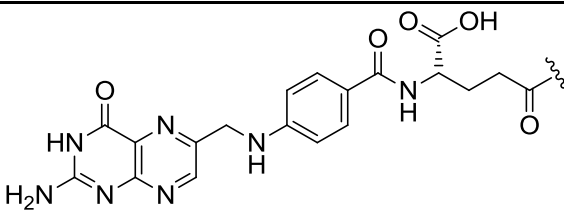
3.7. Anticancer activity of pteroate and folate-derived HDACi

Most HDACi are unselective for tumor cells, consequently they have off-target toxic effects.³ Tumor cell-selective uptake of HDACi could potentially ameliorate many of their shortcomings. To evaluate the influence of the FR on the cytotoxic activity of the folate- and pteroate-derived HDACi identified above, we investigated the effects of their exposure on the viability of two FR (+) transformed cell lines, KB (oral carcinoma) and HeLa (cervical carcinoma) cells.⁴³ We observed that none of the folate-based hydroxamates and biaryl benzamides was active against both cell lines. Among the pteroate hydroxamates, only the 6- and 7-methylene linkers **11d** and **11e**, respectively, were active with micromolar IC₅₀ (Table 3.5). KB cells were more responsive to these compounds as reflected by the lower IC₅₀ compared to those in HeLa cells. This observed difference in sensitivity is in agreement with previous observations since HeLa cells have a lower FR density than the KB cells.⁴⁴

To confirm the FR as the route of entry of the pteric based hydroxamates into the KB cells, we measured the cell viability in the presence and absence of folic acid as previously described.⁴⁵ The presence of 250 μM of folic acid reduced the cytotoxicity effects of 25 μM of **11e** in KB cells (Figure 3.8). Furthermore, we observed that both **11d** and **11e** are inactive against the FR (-) lung cancer cell line A549. The inactivity against the A549 along with the reduced cytotoxicity of **11e** during the folate competition assay suggest the involvement of the FR in cellular uptake of the pteric hydroxamate compounds.⁴⁶

Table 3.5: Folate receptor-dependent anti-proliferative activity of folate- and pteroate - derived hydroxamates (IC₅₀ in μM).



R		n	KB	HeLa	A549
	11a	1	NI	NI	NT
	11b	2	NI	NI	NT
	11c	3	25 ± 2%	NI	NT
	11d	4	53.7 ± 2.4	34 ± 3%	NI
	11e	5	30.3 ± 2.1	56.6 ± 1.1	NI
	11f	6	33 ± 3%	35 ± 3%	NT
	11g	7	47 ± 3%	36 ± 8%	NT
	15a	1	NT	NT	NT
	15b	4	NI	NI	NT
	15c	5	NI	NI	NT
	15d	6			NT
SAHA	-		1.8 ± 0.3	3.7 ± 0.2	NT

NI: No inhibition (below 20% inhibition at 100 μM); % inhibition at 100μM ; NT: Not tested.

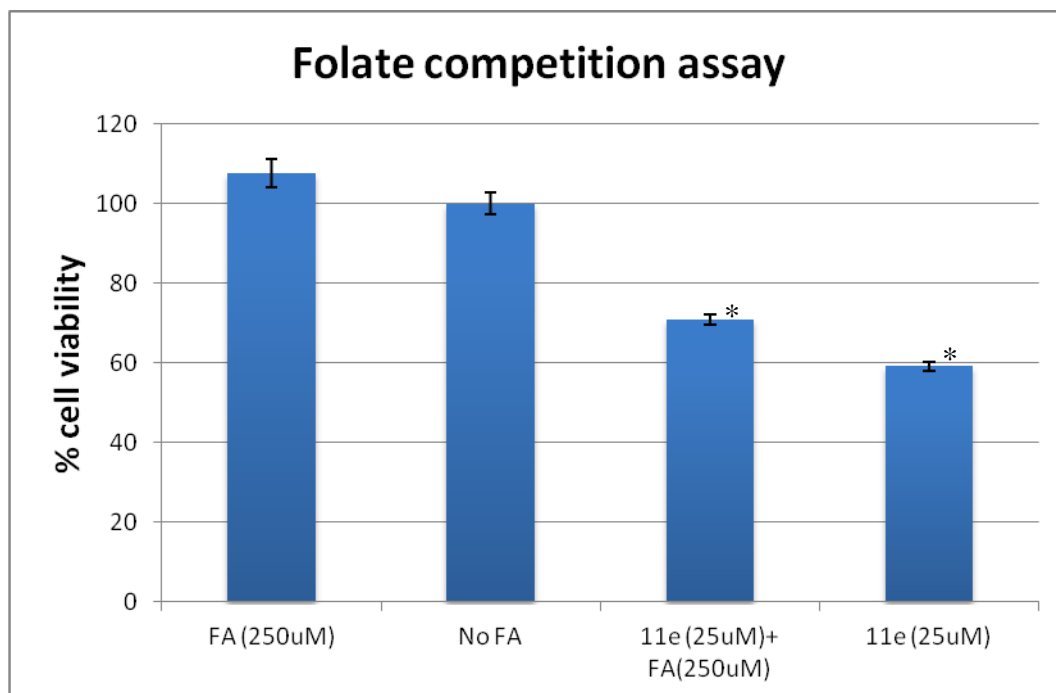


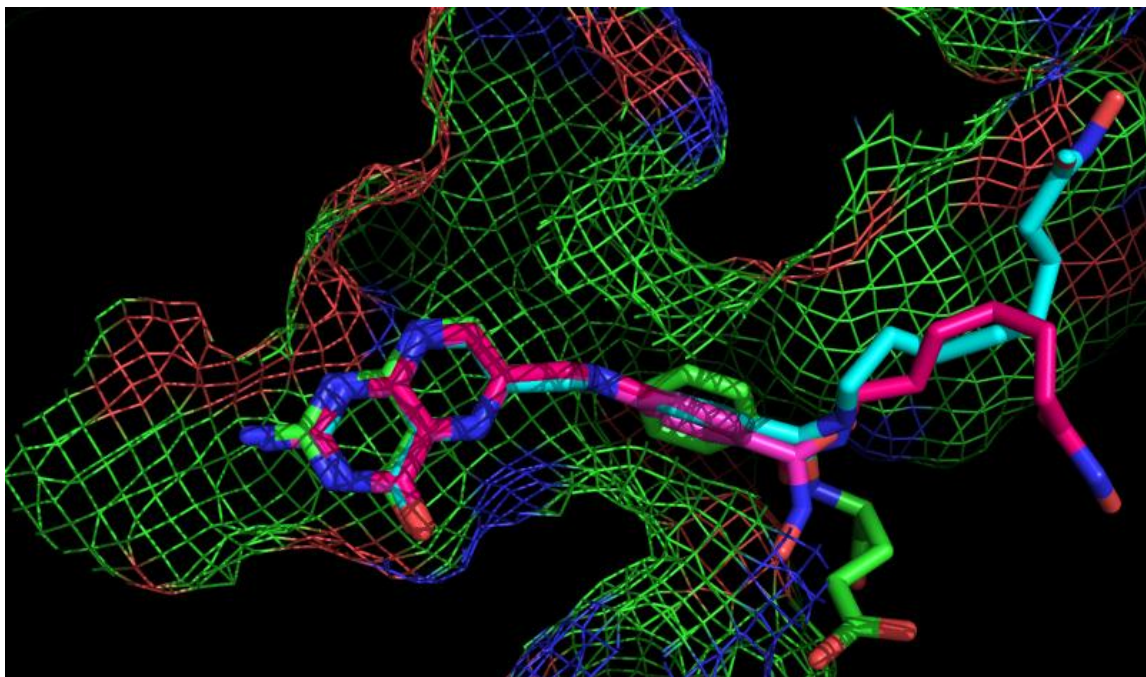
Figure 3.8: Folic acid (FA) competition assay. Viability of KB cells treated with 25 μM of **11e** in the absence and presence of FA. * $p < 0.01$ (Student's *t*-test).

3.8. Intracellular targets validation

I decided to parse out the contribution of each isoform inhibition in the cellular activity of **11d** and **11e** as selective inhibition of HDAC1 or 6 have been associated with cancer cell death.^{47,41,48} The most potent HDAC6 selective inhibitor synthesized thus far, pterotic hydroxamate **7** (Table 3.1) was tested against KB and HeLa cell lines. However, no cytotoxicity effect was observed up to 100 μM . The lack of activity of the pterotic hydroxamate **7** may suggest that HDAC6 inhibition does not lead to KB cell death or **7** is unable to penetrate the cell. However, when docked against the FR crystal structure (PDB code: 4LRH) using Autodock 4.2, the pterotic hydroxamate **7** binds to the FR and its pterin moiety is involved in stabilizing interactions similar to those between the active lead-compounds **11d** and **11e** and the FR. Furthermore, these interactions between the

pterin ring of the pterotic hydroxamate **7**, **11d**, **11e** and the FR are analogous to those previously reported between folic acid and its receptor (Figure 3.9) suggesting the capacity of the pterotic hydroxamate **7** to be delivered through the FR.⁴⁹

A)



B)

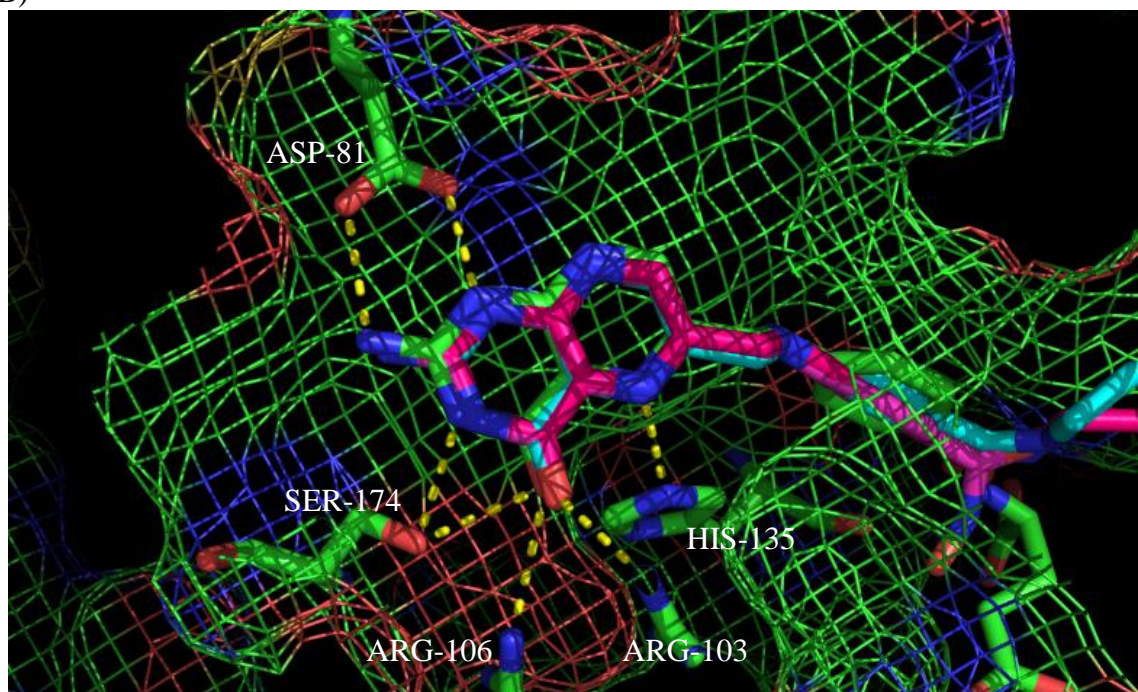


Figure 3.9: Molecular docking of the FR (PDB code: 4LRH) with folic acid (green), Pteric hydroxamate **7** (purple), **11d** (pink) and **11e** (blue). **A)** The pterin ring of pteric hydroxamate **7**, **11d** and **11e** have a similar binding mode to the ligand binding pocket as folic acid. **B)** Stabilizing interactions between the FR and the pterin ring of Pteric hydroxamate **7**, **11d** and **11e** are analogous to those reported for between the FR and folic acid.⁴⁹

In light of the suggestions derived from the *in silico* studies, we measured the cellular response to HDAC6 inhibition, tubulin acetylation, following exposure to pterioic hydroxamate **7**, **11d**, **11e** and SAHA.⁵⁰ As expected, SAHA and the lead-compounds **11d** and **11e**, induced an increase in acetylated tubulin level at IC₅₀ and at higher doses confirming HDAC6 as a target of these inhibitors (Figure 3.10). Similar increase was also seen upon exposure to 100 μM of pterioic hydroxamate **7** (Figure 3.10). This finding suggested that the pterioic hydroxamate **7**, a selective HDAC6 inhibitor, is absorbed through the FR leading to an increase in acetylated tubulin level, however, such isoform inhibition does not result in cytotoxicity to KB cells.

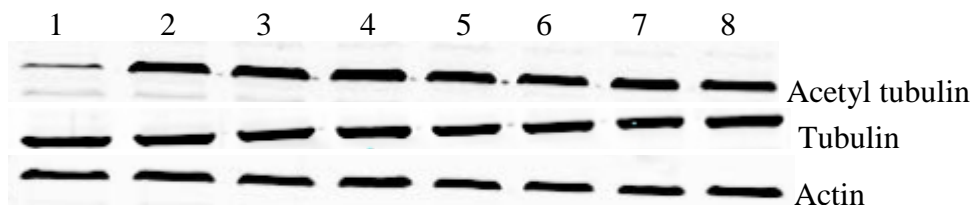


Figure 3.10: Western blot analysis of tubulin acetylation in KB cell. 1) Control; 2) SAHA (2μM); 3) SAHA (20μM); 4) **11d** (50μM); 5) **11d** (100μM); 6) **11e** (30μM); 7) **11e** (100μM); 8) **7** (100μM).

To confirm the HDAC1 inhibition as the mechanism of cytotoxicity of the pterioic based hydroxamates **11d** and **11e** to KB cells, the selective HDAC6 inhibitor Tubastatin A and a biaryl benzamide selective for HDAC1 were employed (Figure 3.11).

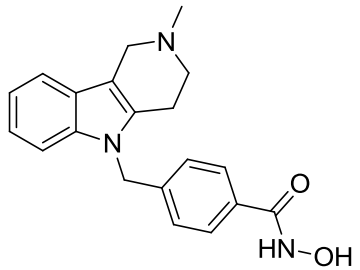
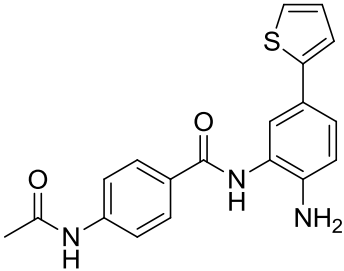
	
Tubastatin A	SHI-1:2
HDAC1 (μM)	0.007 [†]
HDAC6 (μM)	> 10 [†]

Figure 3.11: Structures and HDAC inhibition profile of Tubastatin A and SHI-1:2.
*⁵¹, †⁴¹

In KB cells, Tubastatin A had an IC_{50} of $14.81 \pm 2.74 \mu\text{M}$ suggesting that selective HDAC6 inhibition may result in cellular death. However, the cellular IC_{50} of Tubastatin A was similar to its reported IC_{50} against HDAC1 ($16.4 \pm 2.6 \mu\text{M}$), as such, the observed cytotoxicity may still be a consequence of HDAC1 inhibition.⁵¹ To determine the plausibility of this scenario, the cellular response to HDAC1 inhibition (histones acetylation) was measured in KB cells in response to SAHA, pterioic hydroxamate **7**, **11d**, **11e** and Tubastatin A.⁵⁰ As expected, SAHA, **11d** and **11e**, led to a dose-dependent increase in histone H4 acetylation establishing the intracellular HDAC1 inhibition of these compounds (Figure 3.12). At $14 \mu\text{M}$, Tubastatin A also show a significant increase in H4 acetylation, confirming indeed that its cellular activity against KB cells can be attributed to HDAC1 inhibition. To our surprise, pterioic hydroxamate **7** at $100 \mu\text{M}$ led to only a minimal increase in H4 acetylation compared to the control implying that it is devoid of HDAC1 activity (Figure 3.12). Furthermore, the HDAC1 selective SHI-1:2 was more potent ($\text{IC}_{50} = 5.27 \pm 0.84 \mu\text{M}$) than Tubastatin A.

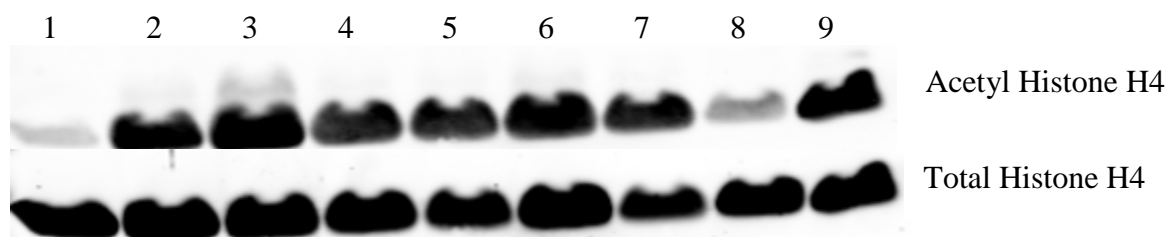


Figure 3.12: Western blot analysis of Histone H4 acetylation in KB cell. 1) Control; 2) SAHA (2 μ M); 3) SAHA (20 μ M); 4) **11d** (50 μ M); 5) **11d** (100 μ M); 6) **11e** (30 μ M); 7) **11e** (100 μ M); 8) **7** (100 μ M); 9) Tubastatin A (14 μ M).

The correlation between HDAC1 inhibition and KB cell viability may explained the lack of anticancer activity of the folate based hydroxamates compounds, but seems to be in contradiction with the inactivity of the folate based biaryl benzamides. In an attempt to understand this apparent contradiction, I speculated that the biaryl benzamide ZBG may be perturbing the FR binding. However, molecular docking studies of **24b** and **24c** reveal that the binding interactions with the FR that are similar to the ones between the receptor and folic acid (Figure 3.13) suggesting that the ZBG is not perturbing the stabilizing interactions between these compounds and the FR and as such they are being delivered to the cell. Recent studies have described the proton-coupled folate transporter (PCFT) as responsible for the export of folates from endosomes following endocytosis.⁵² The folate based biaryl benzamides may not be efficiently transported by the PCFT leading to their retention in the endosomes upon endocytosis. Although the folate receptor has been successfully targeted for the delivery of therapeutic agents, observations made by Philip Low revealed that only 15 to 25% of the bound FR release their substrates following endocytosis, the rest of the bound receptors are returned to the cell surface.²² With such a low delivery efficiency, it is possible that compounds which

are very potent against their primary target (in our case HDAC1) may be the ones to possess cellular activity through FR targeting.²¹

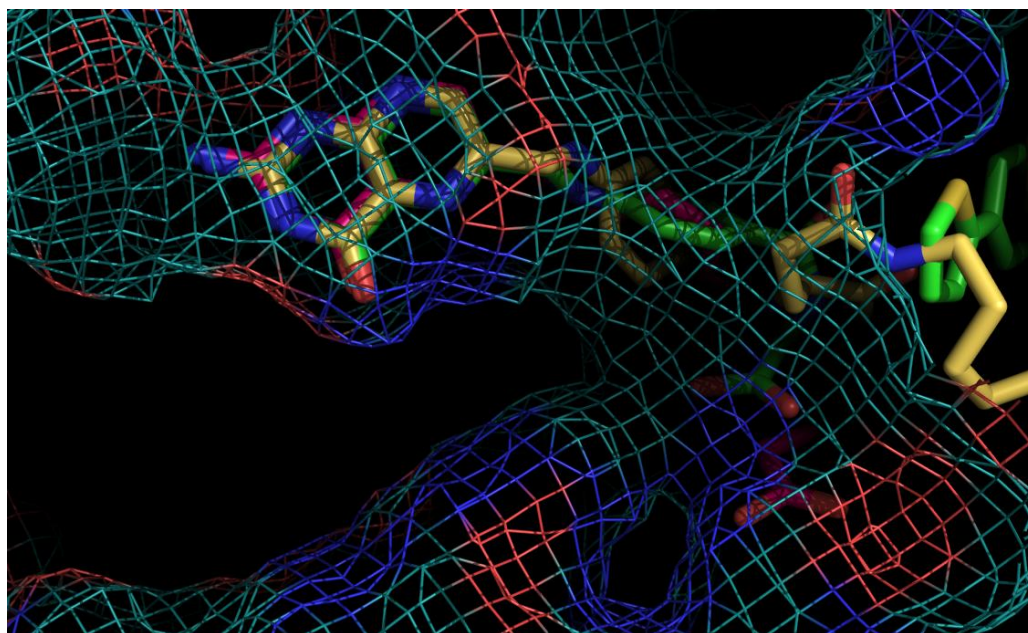


Figure 3.13: Molecular docking of the FR (PDB code: 4LRH) with folic acid (pink), **24b** (gold) and **24c** (green) showing similar binding mode between the pterin moiety and its binding pocket on the FR.

3.9. Conclusion

Despite having great success against hematological malignancies, HDACi have not been efficacious against solid tumors. In an attempt to address this concern and improve their cytotoxicity profile, I targeted HDACi to FR (+) cancers by modifying their pharmacophoric model to encompass folic and pteric acids. The pteric based hydroxamates were potent inhibitors of HDAC1 and 6, whereas the presence of the α -carboxylate conferred a HDAC6 selectivity to the folate based hydroxamates. Furthermore, only the pteric hydroxamates displayed anticancer activity against KB and HeLa cells. I also established that inhibition of HDAC1 correlates with KB cells viability,

justifying the lack of anticancer activity of the folate based hydroxamate compounds which were weaker HDAC1 inhibitors with IC_{50} s in the micromolar. The combination of targeted delivery with isoform selectivity, the other strategy suggested to improve HDACi therapy, led to the design of folate based biaryl benzamide HDACi. To my knowledge, this represents the first attempt to selectively deliver isoform selective HDACi. These inhibitors, though selective for HDAC1, failed to show any anticancer activity against KB cells. This suggests that for a drug to be successfully targeted using the FR, it must be very potent against its primary target as the FR has a low delivery efficiency (15-25%).

3.10. Experimental section

3.10.1. Materials and methods

Folic acid and other reagents used were purchased from Sigma-Aldrich (St. Louis, MO, USA) and Alfa Aesar (WardHill, MA, USA). Analtech silica gel plates (60 F₂₅₄) were used for analytical TLC, and Analtech preparative TLC plates (UV 254, 2000 μm) were used for purification. UV light was used to examine the spots. Silica gel (200–400 Mesh) was used in column chromatography. NMR spectra were recorded on a Varian-Gemini 400 magnetic resonance spectrometer. ¹H NMR spectra were recorded in parts per million (ppm) relative to the peak of CDCl₃, (7.24 ppm), CD₃OD (3.31 ppm), or DMSO-*d*₆ (2.49 ppm). ¹³C spectra were recorded relative to the central peak of the CDCl₃ triplet (77.0 ppm), CD₃OD (49.0 ppm), or the DMSO-*d*₆ septet (39.7 ppm), and were recorded with complete heterodecoupling. Multiplicities are described using the abbreviation s, singlet; d, doublet, t, triplet; q, quartet; m, multiplet; and app, apparent. High-resolution mass spectra were recorded at the Georgia Institute of Technology mass spectrometry facility in Atlanta. KB and A549 cells were obtained from ATCC (Manassas, VA, USA), HeLa cell line was kindly donated by Dr. Christoph Farhni and grown on folate free RPMI medium supplemented with 10% fetal bovine serum (Global Cell Solutions, Charlottesville, VA, USA) and 1% pen/Strep (Cellgro, Manassas, VA) at 37°C in an incubator with 5% CO₂. Mouse anti-acetylated α-Tubulin antibody was obtained from Invitrogen (Life Technologies, Grand Island, NY, USA), rabbit anti-actin, rabbit anti-tubulin α, rabbit anti-histone H4 antibodies and Tubastatin A were purchased from Sigma-Aldrich (St. Louis, MO, USA). Secondary antibodies, goat anti-rabbit conjugated to IRDye680 and goat anti-mouse conjugated to IRDye800 were purchased

from LI-COR Biosciences (Lincoln, NE, USA). The CellTiter 96 AQueous One Solution Cell Proliferation assay (MTS) kit was purchased from Promega (Madison, WI, USA).

3.10.2. Histone deacetylase inhibition (Performed by James Kornacki at Northwestern University)

The HDAC activity in presence of various compounds was assessed by SAMDI mass spectrometry. As a label-free technique, SAMDI is compatible with a broad range of native peptide substrates without requiring potentially disruptive fluorophores. To obtain IC₅₀ values, we incubated isoform-optimized substrates (50µM, detailed below) with enzyme (250nM, detailed below) and inhibitor (at concentrations ranging from 10nM to 1.0mM), in HDAC buffer (25.0 mM Tris-HCl pH 8.0, 140 mM NaCl, 3.0 mM KCl, 1.0 mM MgCl₂, 0.1 mg/mL BSA) in 96-well microtiter plates (60 min, 37°C). Solution-phase deacetylation reactions were quenched with trichostatin A (TSA) and transferred to SAMDI plates to immobilize the substrate components. SAMDI plates were composed of an array of self-assembled monolayers (SAMs) presenting maleimide in standard 384-well format for high-throughput handling capability. Following immobilization, plates were washed to remove buffer constituents, enzyme, inhibitor, and any unbound substrate and analyzed by MALDI mass spectrometry using automated protocols.⁵³ Deacetylation yields in each triplicate sample were determined from the integrated peak intensities of the molecular ions for the substrate and the deacetylated product ion by taking the ratio of the former over the sum of both. Yields were plotted with respect to inhibitor concentration and fitted to obtain IC₅₀ values for each isoform-inhibitor pair.

Isoform-optimized substrates were prepared by traditional Fmoc solid phase peptide synthesis (reagents supplied by Anaspec) and purified by semi preparative HPLC on a reverse phase C18 column (Waters). The peptide of sequence GRK^{ac}FGC was prepared for HDAC1 and HDAC8 experiments, while the peptide of sequence GRK^{ac}YGC was prepared for HDAC6 and HDAC2 experiments. Isoform preference for the indicated substrates was determined by earlier studies on peptide arrays.⁵⁴

HDAC1, HDAC6, and HDAC2 were purchased from BPS Biosciences. The catalytic domain of HDAC8 was expressed as previously reported.⁵⁴ Briefly, an amplicon was prepared by PCR with the following primers: forward 5'-3' TATTCTCGAGGACCACATGCTTCA and reverse 5'-3' ATAAGCTAGCATGGAGGAGCCGGA. A pET21a construct bearing the genetic insert between NheI and XhoI restriction sites was transformed into *E. coli* BL21(DE3) (Lucigen) and expressed by standard protocols. Following purification by affinity chromatography, the His-tagged enzyme-containing fractions were purified by FPLC (AKTA) on a superdex size exclusion column (GE), spin concentrated, and stored at -80°C in HDAC buffer with 10% glycerol.

3.10.3. Molecular docking analysis

The docking studies were performed as previously reported with Autodock Vina through PyRx.^{55,56} Following the 3D energy minimization of the ligand by ChemBioDraw 3D, the docking was run in a 25 Å cubic space encompassing the active site, the binding pocket and its surrounding.

3.10.4. Cell viability assay

KB and HeLa cells were maintained in folate free-RPMI supplemented with 10 % FBS and 1% pen/strep while A549 cells were maintained in DMEM supplemented with 10 % FBS and 1% pen/strep. All cells were incubated on a 96-wells plate (4500 cells/well) in folate free-RPMI for 24 hours prior to a 72 hours drug treatment. Cell viability was measured using the MTS assay according to manufacturer protocol (Promega, CellTiter 96® AQueous One Solution Cell Proliferation Assay, Catalog# G3580). The DMSO concentration in the cell media during the cell viability experiment was maintained at 0.1%.

3.10.5. Western blot analysis for tubulin and histone H4 acetylation

KB cells were plated for 24 hours and treated with various concentrations of compounds for 4 (tubulin acetylation) or 24 hours (histone H4 acetylation). The cells were washed with PBS buffer and resuspended in CellLytic™ buffer containing a cocktail of protease inhibitor (Sigma-Aldrich, St. Louis, MO, USA). Following quantification through a Bradford protein assay, equal amount of protein was loaded onto an SDS-page gel (Bio-Rad, Hercules, CA, USA) and resolved by electrophoresis at a constant voltage of 100V for 2 hours. The gel was transfer onto a nitrocellulose membrane and probed for selected proteins using primary antibodies against: acetylated tubulin (LifeTechnologies, catalog# 32-2700); tubulin (Sigma-Aldrich, catalog# SAB4500087); acetylated histone H4 (Sigma-Aldrich, catalog# SAB4500307); histone H4 (abcam, catalog# ab31830) and actin (Sigma-Aldrich, catalog# A2066). Following the detection of acetylated H4 level, the membrane was stripped using a stripping buffer

(LI-COR, NewBlot Nitro Stripping Buffer, part # 928-40030) and probed for total histone H4.

3.10.6. Statistical analysis

The values reported as mean \pm standard deviation from at least 2 independent triplicate experiments. A student's t-test was performed in Excel, and results with p value less than 5% were considered statistically different.

Trifluoromethanesulfonyl Azide. NaN₃ (1.36 g, 20.86 mmol) was dissolved in DCM (7.5 mL) and H₂O (4.5 mL) and cooled in an ice bath. Upon addition of triflyl anhydride (0.71 mL, 4.17 mmol) dropwise, the reaction was stirred at room temperature for 2 hours. The DCM layer was removed using a separatory funnel and the aqueous layer was extracted with DCM (2 x 4 mL). The organic layers were combined and washed with Na₂CO₃ and dried with Na₂SO₄. No further purification was done.

(S)-4-Azido-5-(tert-butoxy)-5-oxopentanoic acid (1).

L-Glutamic acid α -*tert*-butyl ester (0.5 g, 2.09 mmol), K₂CO₃ (0.43 g, 3.13 mmol), and CuSO₄·5H₂O (0.0050 g, 0.021 mmol) were dissolved in MeOH (18 mL) and H₂O (9 mL). The previously synthesized TfN₃ in DCM was added and the mixture was stirred overnight at room temperature. The organic solvents were evaporated off and the aqueous layer was acidified to pH 2 with a 2M HCl solution and extracted with DCM (4 x 20mL). The DCM extracts were combined, washed with brine and dried with Na₂SO₄. Evaporation of the DCM resulted in **1** (0.52 g, quantitative yield). ¹H NMR (400 MHz,

CDCl₃) δ 3.85 (dd, $J = 8.7, 5.2$ Hz, 1H), 2.47 (t, $J = 6.8$ Hz, 2H), 2.17 – 2.04 (m, 1H), 2.01 – 1.88 (m, 1H), 1.47 (d, $J = 1.5$ Hz, 9H). ¹³C NMR (101 MHz, CDCl₃) δ 178.6, 169.0, 83.4, 61.4, 29.9, 27.9, 26.1.

(S)-tert-Butyl 2-azido-5-oxo-5-((trityloxy)amino)pentanoate (2): Representative procedure for amide bond formation through a mixed anhydride intermediate.

A THF solution of **1** (0.49 g, 2.15 mmol) and *N*-methylmorpholine (0.22 g, 2.15 mmol) was cooled to -15°C and stirred for 5 min. Isobutylchloroformate (0.29 g, 2.15 mmol) was added and the mixture stirred at -15°C for 10 min. *O*-Tritylhydroxylamine (1.19 g, 4.30 mmol) and *N*-methylmorpholine (0.44 g, 4.30 mmol) were added and the reaction was stirred at -15°C for 15 min and at room temperature for 2 h. Upon reaction completion, DCM was added and the mixture was washed with H₂O, NaHCO₃ (1X), 1M HCl (1X), brine (1X) and dried with Na₂SO₄. Following the evaporation of the organic layer, the crude product was dissolved in EtOAc and addition of Hexanes resulted in the precipitation of the product **2** as a white solid (0.69 g, 66% yield). ¹H NMR (400 MHz, CDCl₃) δ 7.61 – 7.28 (m, 15H), 3.66 – 3.49 (m, 1H), 2.06 – 1.91 (m, 1H), 1.80 – 1.66 (m, 2H), 1.62 – 1.55 (m, 1H), 1.46 (s, 9H). ¹³C NMR (101 MHz, cdcl₃) δ 175.8, 169.2, 141.8, 141.0, 129.1, 128.2, 93.6, 82.8, 61.6, 28.0, 27.4, 25.3.

(S)-tert-Butyl 2-amino-5-oxo-5-((trityloxy)amino)pentanoate (3): Representative procedure for azide reduction to amine using Zn and NH₄Cl.

To a solution of **2** (0.25 g, 0.51 mmol) in EtOH (3 mL) and H₂O (1 mL), NH₄Cl (0.066 g, 1.23 mmol) and zinc powder (0.047 g) were added and the resulting mixture was stirred

at room temperature. After completion of the reaction, the mixture was filtered through a celite pad. Following the removal of the solvent, the crude product was purified by preparative TLC with DCM:MeOH (20:1) yielding **3** (0.15 g, 61% yield). ^1H NMR (400 MHz, CDCl_3) δ 7.55 – 7.18 (m, 15H), 3.12 – 3.01 (m, 1H), 2.17 – 1.98 (m, 1H), 1.96 – 1.83 (m, 1H), 1.81 – 1.56 (m, 2H), 1.41 (s, 9H). ^{13}C NMR (101 MHz, CDCl_3) δ 177.8, 171.1, 142.2, 141.0, 129.0, 127.8, 82.3, 81.4, 56.0, 29.3, 28.0, 24.9.

***tert*-Butyl-2-(4-(((2-amino-4-oxo-3,4-dihydropteridin-6-yl)methyl)amino)benzamido)-5-oxo-5-((trityloxy)amino)pentanoate (5):**

Representative procedure for amide bond formation from acyl azide and amine.

Pteroyl azide (0.13 g, 0.40 mmol) and **3** (0.14g, 0.30 mmol) were dissolved in DMSO. Upon addition of tetramethylguanidine (0.07 g, 0.61 mmol), the reaction was stirred overnight at room temperature. Dropwise addition of acetonitrile resulted in a yellow precipitate which was collected by centrifugation and washed by Et_2O . The crude product was purified by preparative TLC with $\text{Et}_2\text{O}:\text{NH}_4\text{OH}:\text{Isopropanol}:\text{EtOH}$ (2:1:1:1) to yield a yellow powder **5** (0.048 g, 21%). ^1H NMR (400 MHz, $\text{DMSO}-d_6$) δ 8.62 (s, 1H), 7.59 (d, $J = 8.4$ Hz, 2H), 7.29 (s, 15H), 6.60 (d, $J = 7.5$ Hz, 2H), 4.47 (s, 2H), 4.20 – 3.87 (m, 1H), 1.98 – 1.77 (m, 2H), 1.74 – 1.49 (m, 2H), 1.34 (s, 9H). ^{13}C NMR (101 MHz, $\text{DMSO}-d_6$) δ 171.8, 166.8, 154.3, 151.2, 149.0, 142.8, 129.4, 128.4, 128.0, 121.7, 111.6, 92.3, 80.7, 56.3, 53.2, 46.3, 28.1.

2-(4-(((2-Amino-4-oxo-3,4-dihydropteridin-6-yl)methyl)amino)benzamido)-5-

(hydroxyamino)-5-oxopentanoic acid (6): Representative procedure for protecting groups removal.

Compound **5** (0.046 g, 0.061 mmol) was dissolved in neat TFA (2 mL) containing TIPS (0.5 mL) and stirred at room temperature for 2 h. The slurry residue obtained upon the TFA evaporation was added to acetonitrile dropwise resulting in a precipitate which was collected by centrifugation. The precipitate was washed with Et₂O (4 x 40 mL) and dried yielding a yellow powder **6** (0.028 g, quantitative yield). ¹H NMR (400 MHz, DMSO-*d*₆) δ 8.67 (s, 1H), 7.60 (d, *J* = 8.6 Hz, 2H), 6.61 (d, *J* = 8.5 Hz, 2H), 4.51 (s, 2H), 4.27 – 4.17 (m, 1H), 2.12 – 1.96 (m, 3H), 1.95 – 1.83 (m, 1H). ¹³C NMR (126 MHz, DMSO-*d*₆) δ 174.2, 174.0, 168.9, 166.7, 151.1, 148.9, 129.3, 128.2, 121.6, 111.5, 52.4, 30.7, 29.3. HRMS (ESI) calcd for C₁₉H₂₁N₈O₆ [M+H]⁺ 457.1579 found 457.1567.

4-(((2-Amino-4-oxo-3,4-dihydropteridin-6-yl)methyl)amino)-*N*-hydroxybenzamide

(7):

An intermediate in the synthesis of pteroyl azide, N₁₀-(trifluoroacetyl)pyrofolinic acid (0.25 g), was dissolved in DMSO (6 mL) followed by the addition of a 50% aqueous hydroxylamine solution (0.15 mL). After stirring at room temperature for 5 h, the reaction was added dropwise to acetonitrile. The yellow precipitate thus obtained was collected by centrifugation and washed with Et₂O (4X), MeOH (2 x 30 mL) and dried. Multiple rounds of DMSO dissolution and precipitation were conducted to obtain the desired purity of **7**, a dark yellow precipitate (0.050 g, 32% yield). ¹H NMR (400 MHz, DMSO-*d*₆) δ 8.62 (s, 1H), 7.49 (d, *J* = 8.7 Hz, 2H), 6.59 (d, *J* = 8.8 Hz, 2H), 4.44 (d, *J* =

6.2 Hz, 2H). ^{13}C NMR (126 MHz, $\text{DMSO-}d_6$) δ 167.7, 165.1, 154.1, 152.2, 150.9, 148.9, 131.4, 128.6, 128.2, 120.3, 118.4, 111.6, 46.2. HRMS (ESI) calcd for $\text{C}_{14}\text{H}_{14}\text{N}_7\text{O}_3$ $[\text{M}+\text{H}]^+$ 328.1153 found 328.1160.

4-Amino-*N*-(trityloxy)butanamide (9a): Representative procedure of azide reduction with PPh_3 .

Trityl protected hydroxamate azide **8a** (1.5 g, 3.88 mmol) and PPh_3 (2.44 g, 9.32 mmol) were dissolved in anhydrous THF (6 mL) and stirred at room temperature under inert atmosphere overnight. H_2O was then added and the reaction allowed to proceed at room temperature for 2 h. DCM was added to the reaction and washed with H_2O (3 x 50 mL), brine (50 mL) and dried with Na_2SO_4 . The crude product was purified by column chromatography eluted with $\text{DCM}:\text{MeOH}:\text{NH}_4\text{OH}$ (10:1:0.1) to yield **9a** (0.91 g, 65% yield). ^1H NMR (400 MHz, $\text{DMSO-}d_6$) δ 7.29 (dd, $J = 13.7, 4.6$ Hz, 15H), 2.29 (t, $J = 6.4$ Hz, 2H), 1.81 (t, $J = 7.0$ Hz, 2H), 1.36 – 1.22 (m, 2H). ^{13}C NMR (101 MHz, CDCl_3) δ 174.7, 146.0, 144.9, 133.0, 132.0, 131.6, 131.5, 96.9, 44.2, 34.0, 31.4.

5-Amino-*N*-(trityloxy)pentanamide (9b):

Compound **8b** (1.5 g, 3.75 mmol) was reacted with PPh_3 (2.36 g, 8.99 mmol) in THF as described for the synthesis of **9a** to give **9b** (0.8 g, 57% yield). ^1H NMR (400 MHz, $\text{DMSO-}d_6$) δ 7.28 (dd, $J = 10.3, 3.6$ Hz, 15H), 2.35 (t, $J = 7.0$ Hz, 2H), 1.74 (t, $J = 7.3$ Hz, 2H), 1.26 – 1.15 (m, 2H), 1.09 – 1.00 (m, 2H). ^{13}C NMR (101 MHz, CDCl_3) δ 141.8, 140.8, 129.0, 128.2, 127.8, 93.2, 38.9, 31.5, 30.2, 26.3.

6-Amino-*N*-(trityloxy)hexanamide (9c):

Compound **8c** (0.5 g, 1.21 mmol) was reacted with PPh₃ (0.76 g, 1.9 mmol) in THF as described for the synthesis of **9a** to give **9c** (0.34 g, 72 % yield). ¹H NMR (500 MHz, CDCl₃) δ 7.64 – 7.21 (m, 15H), 2.61 (t, *J* = 6.2 Hz, 2H), 1.95 – 1.82 (m, 1H), 1.69 – 1.53 (m, 1H), 1.49 – 0.96 (m, 6H). ¹³C NMR (126 MHz, CDCl₃) δ 177.0, 141.9, 140.9, 128.9, 128.0, 127.8, 127.5, 93.2, 50.1, 41.5, 32.7, 31, 26.1, 24.6, 23.

7-Amino-*N*-(trityloxy)heptanamide (9d):

Compound **8d** (1.5 g, 3.5 mmol) was reacted with PPh₃ (2.2 g, 8.4 mmol) in THF as described for the synthesis of **9a** to give **9d** (1.25 g, 89% yield). ¹H NMR (400 MHz, DMSO-*d*₆) δ 7.30 (s, 15H), 2.43 (t, *J* = 6.8 Hz, 2H), 1.75 (t, *J* = 7.0 Hz, 2H), 1.27 – 1.02 (m, 6H), 0.98 – 0.87 (m, 2H). ¹³C NMR (101 MHz, DMSO-*d*₆) δ 170.7, 142.9, 129.4, 127.9, 127.8, 92.1, 41.9, 33.3, 32.4, 28.7, 26.5, 25.3.

8-Amino-*N*-(trityloxy)octanamide (9e):

Compound **8e** (1.5 g, 3.39 mmol) was reacted with PPh₃ (2.13 g, 8.13 mmol) in THF as described for the synthesis of **9a** to give **9e** (1.16 g, 82 % yield). ¹H NMR (400 MHz, DMSO-*d*₆) δ 7.38 – 7.15 (m, 15H), 2.46 (t, *J* = 5.3 Hz, 2H), 1.75 (t, *J* = 7.2 Hz, 2H), 1.32 – 1.21 (m, 2H), 1.20 – 1.01 (m, 6H), 0.99 – 0.88 (m, 2H). ¹³C NMR (101 MHz, DMSO-*d*₆) δ 170.6, 143.0, 129.4, 128, 127.8, 92.1, 55.4, 42.0, 33.6, 29.1, 28.8, 26.7, 25.2.

9-Amino-*N*-(trityloxy)nonanamide (9f):

Compound **8f** (0.98 g, 2.15 mmol) was reacted with PPh₃ (1.35 g, 5.15 mmol) in THF as described for the synthesis of **9a** to give **9f** (0.8 g, 86 % yield). ¹H NMR (400 MHz,

CDCl₃) δ 7.56 – 7.21 (m, 15H), 2.65 (t, J = 7.0 Hz, 2H), 1.65 – 1.50 (m, 2H), 1.48 – 1.36 (m, 2H), 1.31 – 0.98 (m, 10H). ¹³C NMR (101 MHz, CDCl₃) δ 177.4, 141.1, 129.0, 128.1, 128.1, 105.0, 93.3, 53.4, 42.0, 33.5, 29.2, 29.0, 26.8, 23.5.

10-Amino-*N*-(trityloxy)decanamide (9g):

Compound **8g** (1.5 g, 3.19 mmol) was reacted with PPh₃ (2.0 g, 7.65 mmol) in THF as described for the synthesis of **9a** to give **9g** (1.22 g, 86 % yield). ¹H NMR (400 MHz, CDCl₃) δ 7.63 – 7.13 (m, 15H), 2.71 (t, J = 6.8 Hz, 2H), 2.01 – 1.70 (m, 2H), 1.57 – 1.47 (m, 2H), 1.33 – 0.93 (m, 12H). ¹³C NMR (101 MHz, CDCl₃) δ 177.4, 141.1, 129.0, 128.8, 128.1, 127.8, 105.0, 93.3, 41.2, 31.2, 30.9, 29.2, 29.1, 26.7, 23.4.

4-(((2-Amino-4-oxo-3,4-dihydropteridin-6-yl)methyl)amino)-*N*-(4-oxo-4-((trityloxy)amino)butyl)benzamide (10a):

Compound **9a** (0.2 g, 0.55 mmol) was coupled to pteroyl azide (0.24 g, 0.72 mmol) in the presence of TMG (0.13 g, 1.11 mmol) in DMSO as described for the synthesis of **5** to yield **10a** (0.11 g, 31% yield). ¹H NMR (400 MHz, DMSO-*d*₆) δ 8.62 (s, 1H), 7.54 (d, J = 8.5 Hz, 2H), 7.29 (s, 15H), 6.59 (d, J = 8.6 Hz, 2H), 4.45 (d, J = 5.8 Hz, 2H), 2.98 (dd, J = 12.5, 7.1 Hz, 2H), 1.77 (t, J = 7.5 Hz, 2H), 1.39 (t, J = 8.1 Hz, 2H). ¹³C NMR (101 MHz, DMSO-*d*₆) δ 166.6, 161.8, 154.4, 150.9, 149.0, 142.8, 129.3, 129.1, 128.0, 127.9, 111.7, 92.2, 65.4, 56.5, 46.3, 18.9, 15.6.

4-(((2-Amino-4-oxo-3,4-dihydropteridin-6-yl)methyl)amino)-N-(4-(hydroxyamino)-4-oxobutyl)benzamide (10b):

Compound **9b** (0.2 g, 0.53 mmol) was coupled to pteroyl azide (0.23 g, 0.69 mmol) in the presence of TMG (0.12 g, 1.07 mmol) in DMSO as described for the synthesis of **5** to yield **10b** (0.12 g, 33% yield). ¹H NMR (400 MHz, DMSO-*d*₆) δ 8.62 (s, 1H), 7.57 (d, *J* = 8.0 Hz, 2H), 7.29 (s, 14H), 6.60 (d, *J* = 8.0 Hz, 2H), 4.45 (d, *J* = 5.9 Hz, 2H), 3.09 – 2.93 (m, 2H), 1.90 – 1.69 (m, 2H), 1.30 – 1.02 (m, 4H). ¹³C NMR (101 MHz, DMSO-*d*₆) δ 166.4, 154.3, 150.9, 149.0, 142.9, 129.4, 129.0, 128.4, 127.9, 127.8, 122.6, 111.6, 92.1, 46.4, 29.1, 22.8.

4-(((2-Amino-4-oxo-3,4-dihydropteridin-6-yl)methyl)amino)-N-(6-oxo-6-((trityloxy)amino)hexyl)benzamide (10c):

Compound **9c** (0.2 g, 0.52 mmol) was coupled to pteroyl azide (0.26 g, 0.77 mmol) in the presence of TMG (0.12 g, 1.03 mmol) in DMSO as described for the synthesis of **5** to yield **10c** (0.10 g, 29% yield). ¹H NMR (400 MHz, DMSO-*d*₆) δ 8.62 (s, 1H), 7.57 (d, *J* = 8.3 Hz, 2H), 7.30 (s, 14H), 6.59 (d, *J* = 8.1 Hz, 2H), 4.45 (d, *J* = 5.7 Hz, 2H), 3.07 (dd, *J* = 11.6, 6.0 Hz, 2H), 1.74 (t, *J* = 11.6 Hz, 2H), 1.38 – 1.11 (m, 4H), 1.04 – 0.88 (m, 2H). ¹³C NMR (101 MHz, DMSO-*d*₆) δ 166.4, 154.3, 150.9, 149.0, 142.9, 129.4, 129.0, 127.9, 122.6, 111.6, 105.0, 92.2, 46.4, 32.4, 29.5, 26.4, 25.0.

4-(((2-Amino-4-oxo-3,4-dihydropteridin-6-yl)methyl)amino)-N-(7-oxo-7-

((trityloxy)amino)heptyl)benzamide (10d):

Compound **9d** (0.2 g, 0.5 mmol) was coupled to pteroyl azide (0.22 g, 0.65 mmol) in the presence of TMG (0.11 g, 0.99 mmol) in DMSO as described for the synthesis of **5** to yield **10d** (0.14 g, 41% yield). ¹H NMR (400 MHz, DMSO-*d*₆) δ 8.61 (s, 1H), 7.56 (d, *J* = 8.1 Hz, 2H), 7.29 (s, 16H), 6.58 (d, *J* = 8.8 Hz, 2H), 4.44 (d, *J* = 5.2 Hz, 2H), 3.13 – 3.03 (m, 2H), 1.80 – 1.68 (m, 2H), 1.41 – 1.28 (m, 2H), 1.20 – 1.04 (m, 4H), 1.00 – 0.87 (m, 2H). ¹³C NMR (101 MHz, DMSO-*d*₆) δ 172.7, 166.4, 154.3, 150.9, 149.9, 149.0, 129.4, 129.0, 127.9, 127.8, 122.6, 111.6, 92.1, 55.4, 29.6, 26.6.

4-(((2-Amino-4-oxo-3,4-dihydropteridin-6-yl)methyl)amino)-N-(8-oxo-8-

((trityloxy)amino)octyl)benzamide (10e):

Compound **9e** (0.2 g, 0.48 mmol) was coupled to pteroyl azide (0.21 g, 0.62 mmol) in the presence of TMG (0.11 g, 0.96 mmol) in DMSO as described for the synthesis of **5** to yield **10e** (0.15 g, 45% yield). ¹H NMR (400 MHz, DMSO-*d*₆) δ 8.61 (s, 1H), 7.57 (d, *J* = 8.5 Hz, 2H), 7.29 (s, 15H), 6.59 (d, *J* = 8.5 Hz, 2H), 4.44 (d, *J* = 5.9 Hz, 2H), 3.13 (d, *J* = 6.0 Hz, 2H), 1.73 (t, *J* = 7.5 Hz, 2H), 1.44 – 1.32 (m, 2H), 1.24 – 1.08 (m, 6H), 0.97 – 0.87 (m, 2H). ¹³C NMR (101 MHz, DMSO-*d*₆) δ 166.4, 154.3, 150.9, 149.0, 142.9, 129.4, 129.0, 127.9, 122.6, 111.6, 92.1, 65.4, 46.4, 29.8, 28.9, 26.8, 25.2, 15.6.

4-(((2-Amino-4-oxo-3,4-dihydropteridin-6-yl)methyl)amino)-N-(9-oxo-9-((trityloxy)amino)nonyl)benzamide (10f):

Compound **9f** (0.2 g, 0.46 mmol) was coupled to pteroyl azide (0.20 g, 0.60 mmol) in the presence of TMG (0.11 g, 0.93 mmol) in DMSO as described for the synthesis of **5** to yield **10f** (0.088 g, 26% yield). ¹H NMR (400 MHz, DMSO-*d*₆) δ 8.62 (s, 1H), 7.58 (d, *J* = 8.6 Hz, 2H), 7.30 (s, 15H), 6.60 (d, *J* = 8.7 Hz, 2H), 4.45 (d, *J* = 5.8 Hz, 2H), 3.19 – 3.10 (m, 2H), 1.74 (t, *J* = 7.8 Hz, 2H), 1.42 (t, *J* = 8.5 Hz, 2H), 1.22 – 1.00 (m, 8H), 0.99 – 0.88 (m, 2H). ¹³C NMR (101 MHz, DMSO-*d*₆) δ 166.4, 154.3, 150.9, 149.0, 142.9, 129.4, 129.0, 128.4, 127.9, 127.8, 122.6, 111.6, 106.0, 96.3, 46.4, 29.8, 29.1, 26.9.

4-(((2-Amino-4-oxo-3,4-dihydropteridin-6-yl)methyl)amino)-N-(10-oxo-10-((trityloxy)amino)decyl)benzamide (10g):

Compound **9g** (0.2 g, 0.45 mmol) was coupled to pteroyl azide (0.2 g, 0.59 mmol) in the presence of TMG (0.10 g, 0.89 mmol) in DMSO as described for the synthesis of **5** to yield **10a** (0.15 g, 45% yield). ¹H NMR (400 MHz, DMSO-*d*₆) δ 8.62 (s, 1H), 7.57 (d, *J* = 8.8 Hz, 2H), 7.30 (s, 15H), 6.59 (d, *J* = 8.8 Hz, 2H), 4.44 (d, *J* = 5.9 Hz, 2H), 3.14 (dd, *J* = 12.8, 6.4 Hz, 2H), 1.74 (t, *J* = 7.9 Hz, 2H), 1.48 – 1.35 (m, 2H), 1.26 – 1.04 (m, 10H), 0.98 – 0.87 (m, 2H). ¹³C NMR (101 MHz, DMSO-*d*₆) δ 166.4, 154.3, 150.9, 149.0, 142.9, 129.4, 129.0, 127.9, 127.8, 122.7, 122.0, 111.6, 85.9, 46.4, 29.8, 29.3, 29.2, 29.1, 28.8, 28.7, 27.0.

4-(((2-Amino-4-oxo-3,4-dihydropteridin-6-yl)methyl)amino)-N-(4-(hydroxyamino)-4-oxobutyl)benzamide (11a):

Compound **10a** (0.099 g, 0.15 mmol) was dissolved in neat TFA (2 mL) and TIPS (0.5 mL) and stirred at room temperature for 2 h. The desired product **11a** (0.05 g, 81% yield) was obtained as described for the synthesis of **6**. ¹H NMR (500 MHz, DMSO-*d*₆) δ 8.65 (s, 1H), 7.61 (d, *J* = 8.0 Hz, 2H), 6.63 (d, *J* = 8.0 Hz, 2H), 4.48 (d, *J* = 5.3 Hz, 2H), 3.24 – 3.13 (m, 2H), 1.98 (t, *J* = 7.2 Hz, 2H), 1.81 – 1.59 (m, 2H). ¹³C NMR (126 MHz, DMSO-*d*₆) δ 174.42, 169.2, 166.4, 161.1, 156.9, 154.0, 150.8, 149.0, 128.9, 128.2, 122.3, 111.5, 46.2, 33.0, 30.3, 25.8, 25.6. HRMS (ESI) calcd for C₁₈H₂₁N₈O₄ [M+H]⁺ 413.1680 found 413.1692.

4-(((2-Amino-4-oxo-3,4-dihydropteridin-6-yl)methyl)amino)-N-(5-(hydroxyamino)-5-oxopentyl)benzamide (11b):

Compound **10b** (0.054 g, 0.081 mmol) was dissolved in neat TFA (2 mL) and TIPS (0.5 mL) and stirred at room temperature for 2 h. The desired product **11b** (0.025 g, 72% yield) was obtained as described for the synthesis of **6**. ¹H NMR (400 MHz, DMSO-*d*₆) δ 8.61 (s, 1H), 7.57 (d, *J* = 7.4 Hz, 2H), 6.59 (d, *J* = 7.4 Hz, 2H), 4.43 (s, 2H), 3.20 – 3.04 (m, 2H), 1.92 (t, *J* = 6.3 Hz, 2H), 1.56 – 1.30 (m, 4H). ¹³C NMR (126 MHz, DMSO-*d*₆) δ 169.3, 166.3, 154.0, 150.7, 148.9, 128.9, 128.2, 122.4, 111.5, 46.2, 32.3, 29.3, 23.0. HRMS (ESI) calcd for C₁₉H₂₃N₈O₄ [M+H]⁺ 427.1837 found 427.1845.

4-(((2-Amino-4-oxo-3,4-dihydropteridin-6-yl)methyl)amino)-N-(6-(hydroxyamino)-6-oxohexyl)benzamide (11c):

Compound **10c** (0.081 g, 0.12 mmol) was dissolved in neat TFA (2 mL) and TIPS (0.5 mL) and stirred at room temperature for 2 h. The desired product **11c** (0.048 g, 92% yield) was obtained as described for the synthesis of **6**. ¹H NMR (400 MHz, DMSO-*d*₆) δ 8.62 (s, 1H), 7.57 (d, *J* = 7.0 Hz, 2H), 6.59 (d, *J* = 7.2 Hz, 2H), 4.44 (s, 2H), 3.15 – 3.05 (m, 2H), 1.90 (t, *J* = 7.2 Hz, 2H), 1.54 – 1.33 (m, 4H), 1.33 – 1.12 (m, 2H). ¹³C NMR (126 MHz, DMSO-*d*₆) δ 169.4, 166.2, 161.2, 154.0, 150.7, 148.9, 128.9, 128.2, 122.5, 111.5, 46.2, 32.5, 29.4, 26.4, 25.2. HRMS (ESI) calcd for C₂₀H₂₅N₈O₄ [M+H]⁺ 441.1993 found 441.1977.

4-(((2-Amino-4-oxo-3,4-dihydropteridin-6-yl)methyl)amino)-N-(7-(hydroxyamino)-7-oxoheptyl)benzamide (11d):

Compound **10d** (0.12 g, 0.17 mmol) was dissolved in neat TFA (2 mL) and TIPS (0.5 mL) and stirred at room temperature for 2 h. The desired product **11d** (0.066 g, 85% yield) was obtained as described for the synthesis of **6**. ¹H NMR (500 MHz, DMSO-*d*₆) δ 8.65 (s, 1H), 7.60 (d, *J* = 8.5 Hz, 2H), 6.62 (d, *J* = 8.6 Hz, 2H), 4.48 (d, *J* = 5.8 Hz, 2H), 3.17 (dd, *J* = 12.7, 6.4 Hz, 2H), 1.93 (t, *J* = 7.3 Hz, 2H), 1.53 – 1.40 (m, 4H), 1.26 (d, *J* = 2.8 Hz, 4H). ¹³C NMR (126 MHz, DMSO-*d*₆) δ 169.4, 166.3, 154.0, 150.7, 149.0, 128.9, 128.2, 122.5, 111.5, 46.2, 32.5, 29.5, 28.7, 26.5, 25.4. HRMS (ESI) calcd for C₂₁H₂₇N₈O₄ [M+H]⁺ 455.2150 found 455.2137.

4-(((2-Amino-4-oxo-3,4-dihydropteridin-6-yl)methyl)amino)-N-(8-(hydroxyamino)-8-oxooctyl)benzamide (11e):

Compound **10e** (0.13 g, 0.18 mmol) was dissolved in neat TFA (2 mL) and TIPS (0.5 mL) and stirred at room temperature for 2 h. The desired product **11e** (0.082 g, 97% yield) was obtained as described for the synthesis of **6**. ¹H NMR (500 MHz, DMSO-*d*₆) δ 8.65 (s, 1H), 7.60 (d, *J* = 8.0 Hz, 2H), 6.62 (d, *J* = 8.0 Hz, 2H), 4.48 (d, *J* = 4.4 Hz, 2H), 3.21 – 3.12 (m, 2H), 1.92 (t, *J* = 14.3 Hz, 2H), 1.55 – 1.39 (m, 4H), 1.33 – 1.16 (m, 6H). ¹³C NMR (126 MHz, DMSO-*d*₆) δ 169.4, 166.3, 154.0, 150.7, 149.0, 128.9, 128.2, 122.5, 112.8, 111.5, 55.2, 46.2, 32.5, 29.6, 28.8, 28.8, 26.7, 25.4. HRMS (ESI) calcd for C₂₂H₂₉N₈O₄ [M+H]⁺ 469.2306 found 469.2290.

4-(((2-Amino-4-oxo-3,4-dihydropteridin-6-yl)methyl)amino)-N-(9-(hydroxyamino)-9-oxononyl)benzamide (11f):

Compound **10f** (0.053 g, 0.073 mmol) was dissolved in neat TFA (2 mL) and TIPS (0.5 mL) and stirred at room temperature for 2 h. The desired product **11f** (0.024 g, 70% yield) was obtained as described for the synthesis of **6**. ¹H NMR (400 MHz, DMSO-*d*₆) δ 8.71 (s, 1H), 7.57 (d, *J* = 6.4 Hz, 2H), 6.60 (d, *J* = 8.0 Hz, 2H), 4.53 (s, 2H), 3.14 (t, *J* = 11.7 Hz, 2H), 1.89 (t, *J* = 8.4 Hz, 2H), 1.52 – 1.34 (m, 4H), 1.29 – 1.06 (m, 10H). HRMS (ESI) calcd for C₂₃H₃₁N₈O₄ [M+H]⁺ 483.2463 found 483.2452.

4-(((2-Amino-4-oxo-3,4-dihydropteridin-6-yl)methyl)amino)-N-(10-(hydroxyamino)-10-oxodecyl)benzamide (11g):

Compound **10g** (0.13 g, 0.17 mmol) was dissolved in neat TFA (2 mL) and TIPS (0.5 mL) and stirred at room temperature for 2 h. The desired product **11g** (0.075 g, 89% yield) was obtained as described for the synthesis of **6**. ¹H NMR (400 MHz, DMSO-*d*₆) δ 8.66 (s, 1H), 7.56 (d, *J* = 8.5 Hz, 2H), 6.58 (d, *J* = 7.8 Hz, 2H), 4.48 (s, 2H), 3.21 – 3.05 (m, 2H), 1.89 (t, *J* = 6.5 Hz, 2H), 1.54 – 1.37 (m, 4H), 1.21 (dd, *J* = 14.9, 5.8 Hz, 10H). ¹³C NMR (126 MHz, DMSO-*d*₆) δ 175.5, 167.2, 160.1, 152.8, 130.3, 128.8, 114.0, 66.5, 39.8, 33.8, 29.2, 28.9, 28.8, 28.7, 28.6, 26.5, 25.2, 24.6. HRMS (ESI) calcd for C₂₆H₂₅N₈O₃ [M+H]⁺ 497.2044 found 497.2060.

(S)-tert-Butyl 2-azido-5-oxo-5-((4-oxo-4-((trityloxy)amino)butyl)amino)pentanoate (12a): Representative protocol for amide synthesis with EDCI.

The α-azido L-glutamic acid α-tert-butyl ester **1** (0.27 g, 1.17 mmol), EDCI (0.22 g, 1.17 mmol) and HOBT (0.16 g, 1.17 mmol) were dissolved in DMF and stirred at room temperature for 30 min. The *O*-trityl protected hydroxamate **9a** (0.3 g, 0.83 mmol) was added and the mixture allowed to stir overnight at room temperature. DCM was added to the reaction and then washed with H₂O (3 x 50 mL), NaHCO₃ (1 x 50 mL), brine (1x 50 mL) and dried with Na₂SO₄. The crude product was purified by preparative TLC using EtOAc:Hexanes (1:1) to yield **12a** (0.23g, 45% yield). ¹H NMR (400 MHz, CDCl₃) δ 7.54 – 7.20 (m, 15H), 3.87 – 3.70 (m, 1H), 3.12 – 2.99 (m, 1H), 2.96 – 2.85 (m, 1H), 2.28 – 2.05 (m, 3H), 2.00 – 1.81 (m, 2H), 1.70 – 1.54 (m, 2H), 1.53 – 1.35 (m, 10H). ¹³C NMR

(101 MHz, CDCl₃) δ 169.2, 141.9, 140.9, 129.0, 128.2, 127.8, 93.6, 83.0, 61.8, 39.3, 32.1, 29.2, 28.0, 27.0, 22.5.

(S)-tert-Butyl 2-azido-5-oxo-5-((7-oxo-7-((trityloxy)amino)heptyl)amino)pentanoate (12b):

The α -azido L-glutamic acid α -tert-butyl ester **1** (0.2 g, 0.87 mmol) was coupled to **9d** (0.35 g, 0.87 mmol) in the presence of IBCF (0.12 g, 0.87 mmol) and NMM (0.27 g, 2.62 mmol) as described for the synthesis of **2**. Purification of the crude product was done by prep TLC in EtOAc:Hexanes (1:1) resulting in **12b** (0.33g, 61 % yield). ¹H NMR (400 MHz, CDCl₃) δ 7.53 – 7.12 (m, 15H), 3.78 (dd, *J* = 9.0, 4.8 Hz, 1H), 3.20 – 3.04 (m, 2H), 2.28 – 2.19 (m, 2H), 2.19 – 2.08 (m, 1H), 1.93 (dt, *J* = 13.8, 10.5 Hz, 1H), 1.85 – 1.76 (m, 1H), 1.62 – 1.51 (m, 1H), 1.46 (s, 9H), 1.42 – 1.29 (m, 3H), 1.28 – 0.92 (m, 5H). ¹³C NMR (101 MHz, CDCl₃) δ 177.3, 171.4, 169.2, 141.9, 141.1, 129.0, 128.1, 127.8, 93.4, 83.0, 61.8, 39.4, 32.1, 31.1, 29.2, 28.6, 28.0, 27.1, 26.5, 23.2.

(S)-tert-Butyl 2-azido-5-oxo-5-((8-oxo-8-((trityloxy)amino)octyl)amino)pentanoate (12c):

The α -azido L-glutamic acid α -tert-butyl ester **1** (0.19 g, 0.83 mmol) was coupled to **9e** (0.45 g, 1.08 mmol) in the presence of IBCF (0.11 g, 0.83 mmol) and NMM (0.25 g, 2.49 mmol) as described for the synthesis of **2**. Purification of the crude product was done by prep TLC in EtOAc:Hexanes (1:1) resulting in **12c** (0.28g, 54% yield). ¹H NMR (500 MHz, CDCl₃) δ 7.43 (d, *J* = 65.5 Hz, 15H), 3.85 (dd, *J* = 8.9, 4.9 Hz, 1H), 3.28 – 3.16 (m, 2H), 2.30 (t, *J* = 7.2 Hz, 2H), 2.21 (dt, *J* = 13.5, 7.0 Hz, 1H), 1.99 (dq, *J* = 14.2, 7.0

Hz, 1H), 1.92 – 1.82 (m, 1H), 1.66 – 1.56 (m, 1H), 1.52 (s, 9H), 1.49 – 1.42 (m, 2H), 1.31 – 0.99 (m, 8H). ¹³C NMR (126 MHz, CDCl₃) δ 171.1, 169.1, 128.9, 128.0, 82.9, 61.6, 39.4, 32.0, 29.2, 28.6, 27.8, 26.9, 26.3.

(S)-tert-Butyl 2-azido-5-oxo-5-((9-oxo-9-((trityloxy)amino)nonyl)amino)pentanoate

(12d):

The α-azido L-glutamic acid α-tert-butyl ester **1** (0.2 g, 0.87 mmol) was coupled to **9f** (0.38 g, 0.87 mmol) in the presence of IBCF (0.12 g, 0.87 mmol) and NMM (0.27 g, 2.62 mmol) as described for the synthesis of **2**. Purification of the crude product was done by prep TLC in EtOAc:Hexanes (1:1) resulting in **12d** (0.34g, 60% yield). ¹H NMR (500 MHz, CDCl₃) δ 7.59 – 7.27 (m, 15H), 3.89 (ddd, *J* = 42.9, 8.9, 4.8 Hz, 1H), 3.31 – 3.12 (m, 2H), 2.29 (t, *J* = 7.1 Hz, 2H), 2.25 – 2.16 (m, 1H), 1.99 (dq, *J* = 14.3, 7.0 Hz, 1H), 1.93 – 1.79 (m, 1H), 1.60 (t, *J* = 20.4 Hz, 1H), 1.52 (s, 9H), 1.50 – 1.43 (m, 2H), 1.33 – 0.99 (m, 10H). ¹³C NMR (126 MHz, CDCl₃) δ 171.0, 169.1, 140.9, 128.9, 128.0, 82.9, 61.6, 39.4, 32.0, 29.4, 28.7, 27.9, 26.9, 26.5.

(S)-tert-Butyl 2-amino-5-oxo-5-((4-oxo-4-((trityloxy)amino)butyl)amino)pentanoate

(13a):

To a solution of **12a** (0.22 g, 0.39 mmol) in EtOH (6 mL) and H₂O (2 mL), NH₄Cl (0.094 g, 1.76 mmol) and zinc powder (0.12 g) were added and the resulting mixture was stirred under reflux for 2 h. After completion of the reaction, the mixture was filtered through a celite pad. Following the removal of the solvent, the crude product was purified by preparative TLC with DCM:MeOH:NH₄OH (10:1:0.1) yielding **13a** (0.097 g, 46% yield).

^1H NMR (400 MHz, CDCl_3) δ 7.51 – 7.19 (m, 15H), 3.24 (s, 1H), 3.09 – 2.84 (m, 2H), 2.21 (t, $J = 7.4$ Hz, 2H), 2.06 – 1.93 (m, 1H), 1.90 – 1.82 (m, 1H), 1.76 – 1.66 (m, 1H), 1.64 – 1.54 (m, 2H), 1.43 (s, 9H), 1.40 – 1.36 (m, 1H). ^{13}C NMR (101 MHz, CDCl_3) δ 176.9, 142.1, 140.9, 129.1, 128.1, 127.8, 127.6, 93.5, 81.2, 54.4, 39.2, 32.8, 30.4, 29.0, 28.0, 22.8.

(*S*)-*tert*-Butyl 2-amino-5-oxo-5-((7-oxo-7-((trityloxy)amino)heptyl)amino)pentanoate (13b):

Compound **12b** (0.28 g, 0.45 mmol) was reduced in the presence of NH_4Cl (0.058 g, 1.08 mmol) and zinc powder (0.042 g) as described for **13a**. Prep TLC with $\text{DCM}:\text{MeOH}:\text{NH}_4\text{OH}$ (10:1:0.1) yielded **13b** (0.25 g, 93% yield). ^1H NMR (400 MHz, CDCl_3) δ 7.52 – 7.10 (m, 15H), 3.59 – 3.40 (m, 1H), 3.21 – 3.01 (m, 2H), 2.43 – 2.24 (m, 2H), 2.21 – 2.06 (m, 1H), 1.96 – 1.77 (m, 2H), 1.62 – 1.52 (m, 1H), 1.44 (s, 9H), 1.40 – 1.34 (m, 3H), 1.23 – 1.05 (m, 5H). ^{13}C NMR (101 MHz, cdcl_3) δ 177.3, 172.2, 142.0, 141.1, 129.0, 128.1, 127.9, 127.8, 127.7, 93.3, 82.2, 54.0, 39.4, 32.6, 31.1, 29.1, 28.6, 28.0, 26.5, 24.9, 23.2.

(*S*)-*tert*-Butyl 2-amino-5-oxo-5-((8-oxo-8-((trityloxy)amino)octyl)amino)pentanoate (13c):

Compound **12c** (0.25 g, 0.39 mmol) was reduced in the presence of NH_4Cl (0.05 g, 0.94 mmol) and zinc powder (0.036 g) as described for **13a**. Prep TLC with $\text{DCM}:\text{MeOH}:\text{NH}_4\text{OH}$ (10:1:0.1) yielded **13c** (0.20 g, 85% yield). ^1H NMR (400 MHz, CDCl_3) δ 7.58 – 7.11 (m, 15H), 3.37 – 3.24 (m, 1H), 3.16 (dd, $J = 12.7, 6.4$ Hz, 2H), 2.28

(t, $J = 7.4$ Hz, 2H), 2.11 – 2.01 (m, 1H), 1.87 – 1.69 (m, 2H), 1.61 – 1.51 (m, 1H), 1.48 – 1.34 (m, 10H), 1.33 – 0.94 (m, 8H). ^{13}C NMR (101 MHz, CDCl_3) δ 177.3, 174.7, 172.3, 141.9, 141.1, 129.0, 128.1, 127.9, 93.3, 81.4, 54.3, 39.4, 33.0, 31.1, 30.3, 29.7, 29.4, 28.8, 28.0, 26.6, 23.2.

(S)-tert-Butyl 2-amino-5-oxo-5-((9-oxo-9-((trityloxy)amino)nonyl)amino)pentanoate (13d):

Compound **12d** (0.29 g, 0.45 mmol) was reduced in the presence of NH_4Cl (0.057 g, 1.07 mmol) and zinc powder (0.041 g) as described for **13a**. Prep TLC with $\text{DCM}:\text{MeOH}:\text{NH}_4\text{OH}$ (10:1:0.1) yielded **13c** (0.26 g, 92% yield). ^1H NMR (400 MHz, CDCl_3) δ 7.51 – 7.15 (m, 15H), 3.51 – 3.40 (m, 1H), 3.23 – 3.10 (m, 2H), 2.39 – 2.26 (m, 2H), 2.20 – 2.06 (m, 1H), 1.98 – 1.77 (m, 2H), 1.64 – 1.36 (m, 12H), 1.33 – 0.85 (m, 10H). ^{13}C NMR (101 MHz, CDCl_3) δ 177.4, 172.3, 141.9, 141.1, 129.0, 128.1, 127.9, 93.3, 82.0, 54.1, 39.5, 32.7, 31.2, 29.7, 29.4, 29.0, 28.8, 28.0, 26.7, 25.0, 23.3.

(S)-tert-Butyl 2-(4-(((2-amino-4-oxo-3,4-dihydropteridin-6-yl)methyl)amino)benzamido)-5-oxo-5-((4-oxo-4-((trityloxy)amino)butyl)amino)pentanoate (14a):

Compound **13a** (0.078 g, 0.14 mmol) was coupled to pteroyl azide (0.13 g, 0.29 mmol) in presence of TMG (0.05 g, 0.43 mmol) in DMSO as described for **5** to yield **14a** (0.035 g, 29% yield). ^1H NMR (500 MHz, $\text{DMSO}-d_6$) δ 8.66 (s, 1H), 7.64 (d, $J = 8.3$ Hz, 2H), 7.32 (s, 16H), 6.64 (d, $J = 8.4$ Hz, 2H), 4.49 (d, $J = 5.8$ Hz, 2H), 4.24 – 4.15 (m, 1H), 2.85 – 2.75 (m, 2H), 2.17 – 2.11 (m, 2H), 2.04 – 1.95 (m, 1H), 1.92 – 1.82 (m, 1H), 1.79 – 1.72

(m, 2H), 1.40 (s, 9H), 1.34 – 1.27 (m, 2H). HRMS (ESI) calcd for C₄₆H₅₀N₉O₇ [M+H]⁺ 840.3828 found 840.3828.

(S)-tert-Butyl 2-(4-(((2-amino-4-oxo-3,4-dihydropteridin-6-yl)methyl)amino)benzamido)-5-oxo-5-((7-oxo-7-((trityloxy)amino)heptyl)amino)pentanoate (14b):

Compound **13b** (0.22 g, 0.38 mmol) was coupled to pteroyl azide (0.16 g, 0.49 mmol) in presence of TMG (0.086 g, 0.75 mmol) in DMSO as described for **5** to yield **14b** (0.08 g, 24% yield). ¹H NMR (400 MHz, DMSO-*d*₆) δ 8.62 (s, 1H), 7.62 (d, *J* = 8.7 Hz, 2H), 7.30 (s, 19H), 6.61 (d, *J* = 8.9 Hz, 2H), 4.46 (d, *J* = 5.9 Hz, 2H), 4.24 – 4.13 (m, 1H), 2.97 – 2.88 (m, 2H), 2.18 – 2.10 (m, 2H), 2.02 – 1.93 (m, 1H), 1.92 – 1.82 (m, 1H), 1.74 (t, *J* = 7.7 Hz, 2H), 1.44 – 1.34 (m, 11H), 1.28 – 1.18 (m, 4H), 0.95 – 0.88 (m, 2H). HRMS (ESI) calcd for C₄₉H₅₆N₉O₇ [M+H]⁺ 882.4297 found 882.4295.

(S)-tert-Butyl 2-(4-(((2-amino-4-oxo-3,4-dihydropteridin-6-yl)methyl)amino)benzamido)-5-oxo-5-((8-oxo-8-((trityloxy)amino)octyl)amino)pentanoate (14c):

Compound **13c** (0.20 g, 0.34 mmol) was coupled to pteroyl azide (0.23 g, 0.50 mmol) in presence of TMG (0.097 g, 0.84 mmol) in DMSO as described for **5** to yield **14c** (0.070 g, 23% yield). ¹H NMR (400 MHz, DMSO-*d*₆) δ 8.62 (s, 1H), 7.62 (d, *J* = 8.7 Hz, 2H), 7.30 (s, 15H), 6.61 (d, *J* = 8.7 Hz, 2H), 4.46 (d, *J* = 5.8 Hz, 2H), 4.22 – 4.14 (m, 1H), 3.01 – 2.91 (m, 2H), 2.15 (dd, *J* = 13.8, 6.8 Hz, 2H), 2.02 – 1.93 (m, 1H), 1.92 – 1.81 (m,

1H), 1.74 (t, $J = 7.0$ Hz, 2H), 1.36 (s, 9H), 1.32 – 1.24 (m, 2H), 1.17 – 1.04 (m, 6H), 0.94 – 0.81 (m, 2H). HRMS (ESI) calcd for $C_{50}H_{58}N_9O_7$ $[M+H]^+$ 896.4454 found 896.4447.

(S)-tert-Butyl 2-(4-(((2-amino-4-oxo-3,4-dihydropteridin-6-yl)methyl)amino)benzamido)-5-oxo-5-((9-oxo-9-((trityloxy)amino)nonyl)amino)pentanoate (14d):

Compound **13d** (0.25 g, 0.41 mmol) was coupled to pteroyl azide (0.21 g, 0.62 mmol) in presence of TMG (0.095 g, 0.82 mmol) in DMSO as described for **5** to yield **14d** (0.065 g, 17% yield). 1H NMR (400 MHz, $DMSO-d_6$) δ 8.62 (s, 1H), 7.62 (d, $J = 8.4$ Hz, 2H), 7.30 (s, 12H), 6.61 (d, $J = 8.5$ Hz, 2H), 4.46 (d, $J = 5.1$ Hz, 2H), 4.26 – 4.11 (m, 1H), 3.00 – 2.94 (m, 2H), 2.21 – 2.09 (m, 2H), 2.06 – 1.93 (m, 1H), 1.91 – 1.79 (m, 1H), 1.74 (t, $J = 8.6$ Hz, 2H), 1.37 (s, 8H), 1.33 – 1.26 (m, 2H), 1.17 – 1.03 (m, 8H), 0.97 – 0.84 (m, 2H). HRMS (ESI) calcd for $C_{51}H_{60}N_9O_7$ $[M+H]^+$ 910.4610 found 910.4603.

(S)-2-(4-(((2-Amino-4-oxo-3,4-dihydropteridin-6-yl)methyl)amino)benzamido)-5-((4-(hydroxyamino)-4-oxobutyl)amino)-5-oxopentanoic acid (15a):

Compound **14a** (0.035 g, 0.042 mmol) was dissolved in neat TFA (2 mL) and TIPS (0.5 mL) and the resulting mixture was stirred at room temperature for 2 h. The desired product **15a** (0.022 g, 96% yield) was obtained as described for the synthesis of **6**. 1H NMR (500 MHz, $DMSO-d_6$) δ 8.67 (s, 1H), 7.67 (d, $J = 8.7$ Hz, 2H), 6.65 (d, $J = 8.7$ Hz, 2H), 4.51 (s, 2H), 4.29 (t, $J = 10.8$ Hz, 1H), 3.01 (dt, $J = 13.2, 6.8$ Hz, 2H), 2.22 – 2.13 (m, 2H), 2.11 – 2.02 (m, 1H), 1.98 – 1.85 (m, 3H), 1.64 – 1.52 (m, 2H). ^{13}C NMR (126 MHz, $DMSO-d_6$) δ 174.1, 171.7, 169.1, 166.6, 161.0, 153.8, 151.0, 149.4, 148.8, 129.3,

128.2, 121.6, 111.5, 52.4, 46.2, 38.4, 32.3, 30.2, 26.9, 25.6. HRMS (ESI) calcd for $C_{23}H_{28}N_9O_7$ $[M+H]^+$ 542.2106 found 542.2097.

(S)-2-(4-(((2-Amino-4-oxo-3,4-dihydropteridin-6-yl)methyl)amino)benzamido)-5-((7-(hydroxyamino)-7-oxoheptyl)amino)-5-oxopentanoic acid (15b):

Compound **14b** (0.061 g, 0.069 mmol) was dissolved in neat TFA (2 mL) and TIPS (0.5 mL) and the resulting mixture was stirred at room temperature for 2 h. The desired product **15b** (0.043 g, quantitative yield) was obtained as described for the synthesis of **6**. 1H NMR (500 MHz, DMSO- d_6) δ 8.67 (s, 1H), 7.66 (d, $J = 8.3$ Hz, 2H), 6.65 (d, $J = 8.2$ Hz, 2H), 4.51 (s, 2H), 4.35 – 4.20 (m, 1H), 3.00 (dd, $J = 12.1, 6.1$ Hz, 2H), 2.22 – 2.14 (m, 2H), 2.11 – 2.01 (m, 1H), 1.97 – 1.85 (m, 3H), 1.52 – 1.41 (m, 2H), 1.39 – 1.30 (m, 2H), 1.28 – 1.16 (m, 4H). ^{13}C NMR (126 MHz, DMSO- d_6) δ 174.1, 171.6, 166.6, 153.9, 151.0, 148.8, 129.3, 128.3, 121.7, 111.5, 52.5, 46.2, 38.8, 32.5, 32.3, 29.3, 28.6, 26.9, 26.4, 25.3. HRMS (ESI) calcd for $C_{26}H_{34}N_9O_7$ $[M+H]^+$ 584.2576 found 584.2568.

(S)-2-(4-(((2-Amino-4-oxo-3,4-dihydropteridin-6-yl)methyl)amino)benzamido)-5-((8-(hydroxyamino)-8-oxooctyl)amino)-5-oxopentanoic acid (15c):

Compound **14c** (0.07 g, 0.078 mmol) was dissolved in neat TFA (2 mL) and TIPS (0.5 mL) and the resulting mixture was stirred at room temperature for 2 h. The desired product **15c** (0.058 g, quantitative yield) was obtained as described for the synthesis of **6**. 1H NMR (500 MHz, DMSO- d_6) δ 8.69 (s, 1H), 7.66 (d, $J = 8.8$ Hz, 2H), 6.65 (d, $J = 8.8$ Hz, 2H), 4.52 (s, 2H), 4.35 – 4.20 (m, 1H), 3.09 – 2.89 (m, 2H), 2.22 – 2.14 (m, 2H), 2.09 – 2.00 (m, 1H), 1.98 – 1.85 (m, 3H), 1.51 – 1.42 (m, 2H), 1.39 – 1.30 (m, 2H), 1.27 –

1.16 (m, 6H). ^{13}C NMR (126 MHz, DMSO- d_6) δ 174.1, 171.6, 169.4, 166.5, 160.8, 153.6, 151.0, 149.8, 148.7, 129.2, 128.2, 121.7, 111.5, 52.6, 46.1, 38.8, 32.5, 32.3, 29.3, 28.8, 28.7, 26.9, 26.6, 25.4. HRMS (ESI) calcd for $\text{C}_{27}\text{H}_{36}\text{N}_9\text{O}_7$ $[\text{M}+\text{H}]^+$ 598.2732 found 598.2717.

(S)-2-(4-(((2-Amino-4-oxo-3,4-dihydropteridin-6-yl)methyl)amino)benzamido)-5-((9-(hydroxyamino)-9-oxononyl)amino)-5-oxopentanoic acid (15d):

Compound **14d** (0.065 g, 0.071 mmol) was dissolved in neat TFA (2 mL) and TIPS (2 mL) and the resulting mixture was stirred at room temperature for 2 h. The desired product **15d** (0.037 g, 84% yield) was obtained as described for the synthesis of **6**. ^1H NMR (500 MHz, DMSO- d_6) δ 8.67 (s, 1H), 7.66 (d, $J = 8.7$ Hz, 2H), 6.65 (d, $J = 8.7$ Hz, 2H), 4.51 (s, 2H), 4.34 – 4.20 (m, 1H), 3.00 (dd, $J = 12.8, 6.7$ Hz, 2H), 2.22 – 2.13 (m, 2H), 2.09 – 2.03 (m, 1H), 1.98 – 1.85 (m, 3H), 1.54 – 1.41 (m, 2H), 1.41 – 1.30 (m, 2H), 1.26 – 1.16 (m, 8H). ^{13}C NMR (126 MHz, DMSO- d_6) δ 174.1, 171.6, 169.4, 166.5, 161.1, 155.6, 153.9, 151.0, 148.8, 129.2, 128.2, 121.6, 111.5, 52.6, 46.2, 38.8, 32.5, 32.3, 29.4, 29.0, 28.9, 28.8, 26.9, 26.7, 25.4. HRMS (ESI) calcd for $\text{C}_{28}\text{H}_{38}\text{N}_9\text{O}_7$ $[\text{M}+\text{H}]^+$ 612.2889 found 612.2881.

tert-Butyl (2-amino-4-(thiophen-2-yl)phenyl)carbamate (17):

Zinc powder (4.75 g) was added to a solution of **16** (6.65 g, 20.74 mmol) in dioxane (180 mL) and H_2O (45 mL) and stirred overnight at 70°C . Upon completion, EtOAc was added and the mixture was washed with H_2O (3 x 100 mL) and brine (1 x 100 mL). The crude product was purified by column chromatography, eluting with EtOAc:Hexanes (2:1), to

obtain **17** (3.95 g, 54% yield). ^1H NMR (400 MHz, CDCl_3) δ 7.34 – 7.20 (m, 3H), 7.10 – 6.98 (m, 3H), 1.52 (s, 9H). ^{13}C NMR (101 MHz, CDCl_3) δ 153.7, 144.1, 139.9, 132.2, 127.9, 124.8, 124.4, 122.8, 117.5, 115.0, 80.7, 28.3.

***tert*-Butyl (2-(4-azidobutanamido)-4-(thiophen-2-yl)phenyl)carbamate (19a):**

The azido carboxylic acid **18a** (0.31 g, 2.41 mmol), EDCI (0.46 g, 2.41 mmol) and HOBT (0.33 g, 2.41 mmol) were dissolved in DMF and the mixture was stirred at room temperature for 30 min. Following the addition of **17** (0.5 g, 1.72 mmol), the reaction was allowed to stir at 70°C for 6 h. Once the reaction was completed, DCM was added and the mixture was washed with H_2O (3 x 50 mL), NaHCO_3 (1 x 50 mL), brine (1 x 50 mL) and dried with Na_2SO_4 . Solvent was evaporated off to give **19a** (0.64 g, 92% yield) which was used without further purification. ^1H NMR (400 MHz, CDCl_3) δ 7.42 – 7.31 (m, 2H), 7.28 – 7.19 (m, 2H), 7.04 (dd, $J = 5.1, 3.6$ Hz, 1H), 6.98 (s, 1H), 3.34 (t, $J = 6.6$ Hz, 2H), 2.42 (t, $J = 7.2$ Hz, 2H), 1.95 (p, $J = 6.9$ Hz, 2H), 1.51 (s, 9H). ^{13}C NMR (101 MHz, CDCl_3) δ 171.3, 154.1, 143.1, 131.5, 130.1, 129.8, 128.1, 124.9, 124.6, 123.7, 123.3, 122.6, 81.1, 50.7, 33.7, 28.3, 24.7.

***tert*-Butyl (2-(7-azidoheptanamido)-4-(thiophen-2-yl)phenyl)carbamate (19b):**

The azido carboxylic acid **18b** (0.41 g, 2.4 mmol) was coupled to **17** (0.5 g, 1.72 mmol) in the presence of EDCI (0.46 g, 2.41 mmol) and HOBT (0.33 g, 2.41 mmol) as described for **19a** to give **19b** (0.74 g, 98% yield) which was used without further purification. ^1H NMR (400 MHz, CDCl_3) δ 7.40 (d, $J = 8.4$ Hz, 1H), 7.33 (dd, $J = 8.4, 1.9$ Hz, 1H), 7.21 (ddd, $J = 12.5, 8.3, 4.9$ Hz, 3H), 7.07 – 6.95 (m, 1H), 3.22 (t, $J = 6.9$ Hz,

2H), 2.31 (t, $J = 7.5$ Hz, 2H), 1.74 – 1.61 (m, 2H), 1.60 – 1.51 (m, 2H), 1.49 (s, 9H), 1.34 (t, $J = 9.5$ Hz, 4H). ^{13}C NMR (101 MHz, CDCl_3) δ 172.6, 154.1, 143.2, 131.3, 130.3, 129.9, 128.0, 124.7, 124.6, 123.5, 123.2, 122.5, 80.8, 51.3, 36.9, 28.7, 28.3, 26.4, 25.4.

***tert*-Butyl (2-(8-azidooctanamido)-4-(thiophen-2-yl)phenyl)carbamate (19c):**

The azido carboxylic acid **18c** (0.45 g, 2.4 mmol) was coupled to **17** (0.5 g, 1.72 mmol) in the presence of EDCI (0.46 g, 2.41 mmol) and HOBT (0.33 g, 2.41 mmol) as described for **19a** to give **19c** (0.56 g, 72% yield) which was used without further purification. ^1H NMR (500 MHz, CDCl_3) δ 7.45 – 7.34 (m, 2H), 7.30 – 7.23 (m, 2H), 7.06 (dd, $J = 8.9, 5.0$ Hz, 2H), 3.27 (t, $J = 6.9$ Hz, 2H), 2.36 (t, $J = 7.5$ Hz, 2H), 1.76 – 1.66 (m, 2H), 1.65 – 1.56 (m, 2H), 1.53 (s, 9H), 1.42 – 1.31 (m, 6H). ^{13}C NMR (126 MHz, CDCl_3) δ 172.4, 154.0, 143.1, 131.4, 129.9, 127.9, 124.6, 124.5, 123.4, 123.1, 122.4, 80.8, 51.3, 36.9, 28.9, 28.7, 28.6, 28.1, 26.4, 25.3.

***tert*-Butyl (2-(9-azidononanamido)-4-(thiophen-2-yl)phenyl)carbamate (19d):**

The azido carboxylic acid **18d** (0.48 g, 2.41 mmol) was coupled to **17** (0.5 g, 1.72 mmol) in the presence of EDCI (0.46 g, 2.41 mmol) and HOBT (0.33 g, 2.41 mmol) as described for **19a**. The crude product was purified by column chromatography using DCM:Acetone (30:1) as eluent to obtain **19d** (0.56 g, 70% yield). ^1H NMR (400 MHz, CDCl_3) δ 7.29 (dt, $J = 8.4, 5.1$ Hz, 2H), 7.16 (ddd, $J = 5.5, 4.4, 1.1$ Hz, 2H), 7.02 – 6.91 (m, 2H), 3.18 (t, $J = 6.9$ Hz, 2H), 2.27 (t, $J = 7.5$ Hz, 2H), 1.67 – 1.57 (m, 2H), 1.55 – 1.48 (m, 2H), 1.43 (s, 8H), 1.33 – 1.18 (m, 8H). ^{13}C NMR (101 MHz, CDCl_3) δ 172.6, 154.1, 143.2, 131.5,

130.1, 128.0, 124.8, 124.7, 123.6, 123.2, 122.6, 80.9, 51.4, 37.1, 29.2, 29.1, 29.0, 28.8, 28.3, 26.7, 25.6.

***tert*-Butyl (2-(4-aminobutanamido)-4-(thiophen-2-yl)phenyl)carbamate (20a):**

To a solution of **19a** (0.53 g, 1.37 mmol) in EtOH (9 mL), EtOAc (3 mL) and H₂O (3 mL), NH₄Cl (0.18 g, 3.42 mmol) and zinc powder (0.23 g) were added and the resulting mixture was stirred under reflux for 2 h. After completion of the reaction, the mixture was filtered through a celite pad. The crude product was purified by preparative TLC with DCM:MeOH:NH₄OH (8.5:1.5:0.3) yielding **20a** (0.40 g, 78% yield). ¹H NMR (400 MHz, CDCl₃) δ 7.66 – 7.45 (m, 2H), 7.31 (d, *J* = 8.1 Hz, 1H), 7.15 (s, 2H), 6.97 (s, 1H), 2.80 – 2.53 (m, 2H), 2.42 – 2.29 (m, 2H), 1.86 – 1.69 (m, 2H), 1.52 – 1.38 (m, 9H). ¹³C NMR (101 MHz, CDCl₃) δ 172.8, 153.9, 143.3, 131.2, 130.6, 129.1, 128.0, 124.6, 124.0, 123.7, 123.0, 122.6, 80.6, 40.8, 34.4, 28.3, 27.3.

***tert*-Butyl (2-(7-aminoheptanamido)-4-(thiophen-2-yl)phenyl)carbamate (20b):**

Compound **19b** (0.55 g, 1.24 mmol) was reduced with NH₄Cl (0.16 g, 2.98 mmol) and zinc (0.21 g) as described for **20a** resulting in **20b** (0.38 g, 74% yield). ¹H NMR (400 MHz, CDCl₃) δ 7.58 (s, 1H), 7.41 (d, *J* = 8.4 Hz, 1H), 7.30 (d, *J* = 8.4 Hz, 1H), 7.17 (t, *J* = 3.8 Hz, 2H), 7.02 – 6.89 (m, 1H), 2.70 – 2.48 (m, 2H), 2.27 (t, *J* = 7.2 Hz, 2H), 1.67 – 1.53 (m, 2H), 1.45 (s, 9H), 1.36 (d, *J* = 5.6 Hz, 2H), 1.29 – 1.15 (m, 4H). ¹³C NMR (101 MHz, CDCl₃) δ 172.9, 154.1, 143.3, 131.1, 130.5, 130.0, 128.0, 124.7, 124.5, 123.4, 123.1, 122.5, 80.6, 41.7, 36.8, 32.7, 28.8, 28.3, 26.4, 25.5.

***tert*-Butyl (2-(8-aminooctanamido)-4-(thiophen-2-yl)phenyl)carbamate (20c):**

Compound **19c** (0.40 g, 0.87 mmol) was reduced with NH₄Cl (0.12 g, 2.19 mmol) and zinc (0.14 g) as described for **20a** resulting in **20c** (0.32 g, 86% yield). ¹H NMR (400 MHz, CDCl₃) δ 7.55 (s, 1H), 7.38 (d, *J* = 7.6 Hz, 1H), 7.26 (d, *J* = 3.4 Hz, 1H), 7.19 – 7.04 (m, 2H), 6.94 (s, 1H), 2.64 – 2.47 (m, 2H), 2.32 – 2.15 (m, 2H), 1.67 – 1.49 (m, 2H), 1.42 (s, 9H), 1.27 – 0.93 (m, 8H). ¹³C NMR (101 MHz, CDCl₃) δ 173.0, 154.1, 143.2, 131.1, 130.5, 130.0, 128.0, 124.6, 123.4, 123.0, 122.4, 80.5, 41.7, 36.9, 32.7, 28.9, 28.3, 26.5, 25.5.

***tert*-Butyl (2-(9-aminononanamido)-4-(thiophen-2-yl)phenyl)carbamate (20d):**

Compound **19d** (0.45 g, 0.95 mmol) was reduced with NH₄Cl (0.13 g, 2.39 mmol) and zinc (0.16 g) as described for **20a** resulting in **20d** (0.34 g, 79% yield). ¹H NMR (400 MHz, CDCl₃) δ 7.60 (s, 1H), 7.38 (d, *J* = 8.4 Hz, 1H), 7.30 (d, *J* = 8.2 Hz, 1H), 7.19 (d, *J* = 5.7 Hz, 2H), 7.04 – 6.91 (m, 1H), 2.63 (t, *J* = 8.7 Hz, 2H), 2.30 (t, *J* = 7.2 Hz, 2H), 1.73 – 1.56 (m, 2H), 1.46 (s, 9H), 1.41 (s, 2H), 1.24 (s, 8H). ¹³C NMR (101 MHz, CDCl₃) δ 172.9, 154.2, 143.3, 131.2, 130.4, 130.1, 128.0, 124.7, 124.6, 123.4, 123.1, 122.5, 80.6, 41.7, 37.0, 32.5, 29.1, 29.1, 29.0, 28.3, 26.7, 25.6.

(*S*)-*tert*-Butyl 2-azido-5-((4-((2-((*tert*-butoxycarbonyl)amino)-5-(thiophen-2-yl)phenyl)amino)-4-oxobutyl)amino)-5-oxopentanoate (21a):

The α-azido L-glutamic acid α-*tert*-butyl ester **1** (0.13 g, 0.56 mmol), EDCI (0.11 g, 0.56 mmol) and HOBT (0.076 g, 0.56 mmol) were dissolved in DMF and stirred at room temperature for 30 min. Compound **20a** (0.15 g, 0.34 mmol) was added and the mixture

allowed to stir overnight at room temperature. DCM was added to the reaction and then washed with H₂O (3 x 50 mL), NaHCO₃ (1 x 50 mL), brine (1 x 50 mL) and dried with Na₂SO₄. Solvent was evaporated off and the crude product was purified by preparative TLC using DCM:MeOH:NH₄OH (8.5:1.5:0.3) to yield **21a** (0.23g, 98% yield). ¹H NMR (400 MHz, CDCl₃) δ 7.59 – 7.49 (m, 2H), 7.36 (dd, *J* = 8.4, 1.7 Hz, 1H), 7.20 (t, *J* = 3.7 Hz, 2H), 7.00 (dd, *J* = 4.8, 3.8 Hz, 1H), 3.78 (dd, *J* = 8.7, 4.8 Hz, 1H), 3.29 – 3.20 (m, 2H), 2.36 (t, *J* = 11.1 Hz, 2H), 2.25 (t, *J* = 7.1 Hz, 2H), 2.18 – 2.04 (m, 1H), 2.00 – 1.89 (m, 1H), 1.86 – 1.75 (m, 2H), 1.47 (s, 9H), 1.45 (s, 9H). ¹³C NMR (101 MHz, CDCl₃) δ 172.4, 169.2, 153.9, 143.2, 131.0, 130.5, 129.5, 128.0, 124.7, 124.4, 123.6, 123.1, 122.3, 83.1, 80.7, 61.8, 38.7, 34.2, 32.1, 28.3, 28.0, 27.0, 25.9.

(*S*)-tert-Butyl 2-azido-5-((7-((2-((tert-butoxycarbonyl)amino)-5-(thiophen-2-yl)phenyl)amino)-7-oxoheptyl)amino)-5-oxopentanoate (21b**):**

Compound **1** (0.12 g, 0.50 mmol) was coupled to **20b** (0.15 g, 0.36 mmol) with EDCI (0.096 g, 0.50 mmol) and HOBT (0.068 g, 0.50 mmol) as described for **21a** to give **21b** (0.22 g, 98% yield). ¹H NMR (400 MHz, CDCl₃) δ 7.57 – 7.44 (m, 2H), 7.33 (d, *J* = 8.4 Hz, 1H), 7.18 (d, *J* = 4.5 Hz, 2H), 7.03 – 6.90 (m, 1H), 3.76 (dd, *J* = 8.9, 4.8 Hz, 1H), 3.10 (dd, *J* = 12.9, 6.6 Hz, 2H), 2.30 (t, *J* = 7.2 Hz, 2H), 2.22 (t, *J* = 7.2 Hz, 2H), 2.17 – 2.05 (m, 1H), 1.96 – 1.83 (m, 1H), 1.64 – 1.54 (m, 2H), 1.45 (s, 9H), 1.44 (s, 9H), 1.41 – 1.32 (m, 2H), 1.30 – 1.18 (m, 4H). ¹³C NMR (101 MHz, CDCl₃) δ 172.9, 171.6, 169.2, 154.0, 143.2, 131.1, 130.5, 129.8, 128.0, 124.7, 124.5, 123.4, 123.1, 122.5, 83.0, 80.7, 61.8, 39.3, 36.7, 32.1, 29.2, 28.5, 28.3, 27.9, 27.1, 26.3, 25.4.

(S)-tert-Butyl 2-azido-5-((8-((2-((tert-butoxycarbonyl)amino)-5-(thiophen-2-yl)phenyl)amino)-8-oxooctyl)amino)-5-oxopentanoate (21c):

Compound **1** (0.11 g, 0.49 mmol) was coupled to **20c** (0.15 g, 0.35 mmol) with EDCI (0.093 g, 0.49 mmol) and HOBT (0.066 g, 0.49 mmol) as described for **21a** to give **21c** (0.23 g, quantitative yield). ¹H NMR (400 MHz, CDCl₃) δ 7.53 – 7.41 (m, 2H), 7.39 – 7.30 (m, 1H), 7.18 (t, *J* = 3.8 Hz, 2H), 6.99 (dd, *J* = 4.9, 3.8 Hz, 1H), 3.76 (dd, *J* = 9.0, 4.8 Hz, 1H), 3.13 (dd, *J* = 13.4, 6.7 Hz, 2H), 2.32 (t, *J* = 7.3 Hz, 2H), 2.21 (t, *J* = 7.2 Hz, 2H), 2.15 – 2.03 (m, 1H), 1.89 (ddd, *J* = 15.6, 13.9, 6.9 Hz, 1H), 1.71 – 1.57 (m, 2H), 1.46 (s, 9H), 1.44 (s, 9H), 1.42 – 1.37 (m, 2H), 1.31 – 1.22 (m, 6H). ¹³C NMR (101 MHz, CDCl₃) δ 172.8, 171.5, 169.2, 154.0, 143.3, 131.1, 130.4, 129.9, 128.0, 124.7, 124.5, 123.4, 123.1, 122.5, 83.0, 80.7, 61.8, 39.4, 36.9, 32.1, 29.3, 28.8, 28.6, 28.3, 28.0, 27.1, 26.5, 25.4

(S)-tert-Butyl 2-azido-5-((9-((2-((tert-butoxycarbonyl)amino)-5-(thiophen-2-yl)phenyl)amino)-9-oxononyl)amino)-5-oxopentanoate (21d):

Compound **1** (0.087 g, 0.38 mmol) was coupled to **20b** (0.15 g, 0.27 mmol) with EDCI (0.072 g, 0.38 mmol) and HOBT (0.051 g, 0.38 mmol) as described for **21a** to give **21d** (0.20 g, quantitative yield). ¹H NMR (400 MHz, CDCl₃) δ 7.43 (dd, *J* = 15.0, 9.4 Hz, 2H), 7.34 (dd, *J* = 8.4, 2.0 Hz, 1H), 7.20 (dd, *J* = 4.1, 2.9 Hz, 2H), 7.00 (dd, *J* = 4.9, 3.7 Hz, 1H), 3.77 (dd, *J* = 9.0, 4.8 Hz, 1H), 3.16 (dd, *J* = 13.6, 6.5 Hz, 2H), 2.34 (t, *J* = 7.4 Hz, 2H), 2.22 (t, *J* = 7.1 Hz, 2H), 2.17 – 2.07 (m, 1H), 1.97 – 1.85 (m, 1H), 1.71 – 1.61 (m, 2H), 1.47 (s, 9H), 1.45 (s, 9H), 1.43 – 1.39 (m, 2H), 1.30 – 1.18 (m, 8H). ¹³C NMR (101 MHz, CDCl₃) δ 172.8, 171.4, 169.2, 154.0, 143.3, 131.2, 130.4, 130.0, 128.0, 124.7,

124.5, 123.5, 123.1, 122.5, 83.1, 80.7, 61.8, 39.5, 37.0, 32.1, 29.4, 28.9, 28.8, 28.3, 28.0, 27.1, 26.6, 25.5.

(S)-tert-Butyl 2-amino-5-((4-((2-((tert-butoxycarbonyl)amino)-5-(thiophen-2-yl)phenyl)amino)-4-oxobutyl)amino)-5-oxopentanoate (22a):

To a solution of **21a** (0.21 g, 0.37 mmol) in EtOH (9 mL) and H₂O (3 mL) was added NH₄Cl (0.049 g, 0.91 mmol) and zinc powder (0.06 g) and the resulting mixture was stirred under reflux for 3 h. After completion of the reaction, the mixture was filtered through a celite pad. The crude product was purified by preparative TLC with DCM:MeOH (10:1) yielding **22a** (0.13 g, 63% yield). ¹H NMR (400 MHz, CDCl₃) δ 7.72 (s, 1H), 7.55 (d, *J* = 8.3 Hz, 1H), 7.38 (d, *J* = 8.4 Hz, 1H), 7.23 (dd, *J* = 8.9, 8.1 Hz, 2H), 7.06 – 6.98 (m, 1H), 3.36 – 3.20 (m, 3H), 2.39 (t, *J* = 6.2 Hz, 2H), 2.32 – 2.24 (m, 2H), 2.14 – 2.06 (m, 1H), 1.93 – 1.83 (m, 2H), 1.79 – 1.70 (m, 1H), 1.49 (s, 9H), 1.43 (s, 9H). ¹³C NMR (101 MHz, CDCl₃) δ 172.3, 154.0, 143.4, 131.1, 130.4, 129.8, 128.0, 124.7, 123.6, 123.1, 122.4, 81.5, 80.6, 38.6, 34.3, 33.0, 28.3, 28.0, 26.1.

(S)-tert-Butyl 2-amino-5-((7-((2-((tert-butoxycarbonyl)amino)-5-(thiophen-2-yl)phenyl)amino)-7-oxoheptyl)amino)-5-oxopentanoate (22b):

Compound **21b** (0.22 g, 0.34 mmol) was reduced in the presence of NH₄Cl (0.046 g, 0.86 mmol) and zinc powder (0.056 g) as described for **22a** yielding **22b** (0.14 g, 68% yield). ¹H NMR (400 MHz, CDCl₃) δ 7.42 (dd, *J* = 31.0, 8.4 Hz, 3H), 7.29 – 7.18 (m, 2H), 7.10 – 6.94 (m, 1H), 3.29 – 3.07 (m, 2H), 2.37 (t, *J* = 5.5 Hz, 2H), 2.32 – 2.19 (m, 2H), 2.15 – 1.99 (m, 1H), 1.85 – 1.63 (m, 4H), 1.61 – 1.39 (m, 20H), 1.39 – 1.27 (m, 4H). ¹³C NMR

(101 MHz, CDCl₃) δ 172.5, 143.3, 131.5, 130.2, 128.0, 124.8, 123.6, 123.2, 122.6, 81.4, 80.8, 39.2, 36.8, 33.1, 29.3, 28.3, 28.0, 26.2, 25.3.

(S)-tert-butyl 2-amino-5-((8-((2-((tert-butoxycarbonyl)amino)-5-(thiophen-2-yl)phenyl)amino)-8-oxooctyl)amino)-5-oxopentanoate (22c):

Compound **21c** (0.23 g, 0.36 mmol) was reduced in the presence of NH₄Cl (0.086 g, 1.61 mmol) and zinc powder (0.11 g) as described for **22a** yielding **22c** (0.20 g, 90% yield). ¹H NMR (400 MHz, CDCl₃) δ 7.59 (s, 1H), 7.45 (d, *J* = 8.4 Hz, 1H), 7.34 (d, *J* = 8.3 Hz, 1H), 7.20 (d, *J* = 4.3 Hz, 2H), 7.06 – 6.93 (m, 1H), 3.20 – 3.07 (m, 2H), 2.99 – 2.75 (m, 2H), 2.35 (t, *J* = 7.1 Hz, 2H), 2.25 (t, *J* = 14.4 Hz, 2H), 2.04 (dd, *J* = 20.4, 9.4 Hz, 1H), 1.84 – 1.72 (m, 1H), 1.70 – 1.61 (m, 2H), 1.47 (s, 9H), 1.40 (s, 9H), 1.34 – 1.18 (m, 6H). ¹³C NMR (101 MHz, CDCl₃) δ 172.9, 154.1, 143.3, 131.2, 130.4, 130.1, 128.0, 125.0, 123.5, 123.1, 122.6, 82.0, 80.7, 77.4, 77.1, 76.8, 50.4, 39.4, 36.9, 32.7, 29.2, 28.7, 28.4, 28.3, 28.0, 26.4, 25.4.

(S)-tert-butyl 2-amino-5-((9-((2-((tert-butoxycarbonyl)amino)-5-(thiophen-2-yl)phenyl)amino)-9-oxononyl)amino)-5-oxopentanoate (22d):

Compound **21d** (0.20 g, 0.30 mmol) was reduced in the presence of NH₄Cl (0.073 g, 1.36 mmol) and zinc powder (0.089 g) as described for **22a** yielding **22d** (0.17 g, 88% yield). ¹H NMR (400 MHz, CDCl₃) δ 7.58 (s, 1H), 7.44 (t, *J* = 11.0 Hz, 1H), 7.32 (dd, *J* = 8.4, 1.6 Hz, 1H), 7.22 – 7.13 (m, 2H), 7.04 – 6.92 (m, 1H), 3.18 – 3.03 (m, 2H), 2.34 (t, *J* = 7.3 Hz, 2H), 2.31 – 2.20 (m, 2H), 2.10 – 1.94 (m, 1H), 1.87 – 1.70 (m, 1H), 1.71 – 1.60 (m, 2H), 1.46 (s, 9H), 1.41 (m, 10H), 1.36 – 1.15 (m, 9H). ¹³C NMR (101 MHz, CDCl₃) δ

173.0, 154.1, 143.3, 131.1, 130.5, 130.0, 128.0, 124.7, 124.5, 123.4, 123.1, 122.5, 81.9, 80.6, 39.4, 36.9, 32.7, 29.3, 28.8, 28.7, 28.3, 28.0, 26.5, 25.5.

(S)-tert-butyl 2-(4-(((2-amino-4-oxo-3,4-dihydropteridin-6-yl)methyl)amino)benzamido)-5-((4-((2-((tert-butoxycarbonyl)amino)-5-(thiophen-2-yl)phenyl)amino)-4-oxobutyl)amino)-5-oxopentanoate (23a):

Compound **22a** (0.12 g, 0.21 mmol) was coupled to pteroyl azide (0.19 g, 0.41 mmol) in the presence of TMG (0.071 g, 0.62 mmol) in DMSO as described for the synthesis of **5** to yield **23a** (0.045 g, 26% yield). ¹H NMR (500 MHz, DMSO-*d*₆) δ 8.66 (s, 1H), 7.75 (d, *J* = 1.9 Hz, 1H), 7.67 (d, *J* = 8.8 Hz, 2H), 7.62 (d, *J* = 8.5 Hz, 1H), 7.52 (dd, *J* = 5.1, 1.0 Hz, 1H), 7.48 – 7.38 (m, 2H), 7.12 (dd, *J* = 5.0, 3.6 Hz, 1H), 6.66 (dd, *J* = 14.6, 8.9 Hz, 2H), 4.49 (d, *J* = 6.0 Hz, 2H), 4.24 (dd, *J* = 12.3, 9.4 Hz, 1H), 3.15 – 3.08 (m, 2H), 2.38 (t, *J* = 7.3 Hz, 2H), 2.21 (dt, *J* = 14.2, 7.1 Hz, 2H), 2.09 – 1.99 (m, 1H), 1.97 – 1.87 (m, 1H), 1.74 (dd, *J* = 16.3, 9.0 Hz, 2H), 1.46 (s, 9H), 1.40 (s, 9H). HRMS (ESI) calcd for C₄₂H₅₁N₁₀O₈S [M+H]⁺ 855.3607 found 855.3607.

(S)-tert-butyl 2-(4-(((2-amino-4-oxo-3,4-dihydropteridin-6-yl)methyl)amino)benzamido)-5-((7-((2-((tert-butoxycarbonyl)amino)-5-(thiophen-2-yl)phenyl)amino)-7-oxoheptyl)amino)-5-oxopentanoate (23b):

Compound **22b** (0.12 g, 0.20 mmol) was coupled to pteroyl azide (0.18 g, 0.41 mmol) in the presence of TMG (0.07 g, 0.61 mmol) in DMSO as described for the synthesis of **5** to yield **23b** (0.038 g, 21% yield). ¹H NMR (500 MHz, DMSO-*d*₆) δ 8.66 (s, 1H), 7.73 (d, *J* = 1.9 Hz, 1H), 7.66 (d, *J* = 8.8 Hz, 2H), 7.61 (d, *J* = 8.4 Hz, 1H), 7.52 (dd, *J* = 5.1, 1.1

Hz, 1H), 7.47 – 7.40 (m, 2H), 7.13 (dd, $J = 4.5, 3.0$ Hz, 1H), 6.65 (d, $J = 8.8$ Hz, 2H), 4.49 (d, $J = 5.9$ Hz, 2H), 4.24 – 4.16 (m, 1H), 3.03 (dd, $J = 12.9, 6.7$ Hz, 2H), 2.40 – 2.35 (m, 2H), 2.24 – 2.12 (m, 2H), 2.06 – 1.97 (m, 1H), 1.94 – 1.85 (m, 1H), 1.65 – 1.54 (m, 2H), 1.47 (s, 10H), 1.42 – 1.36 (m, 12H), 1.35 – 1.27 (m, 4H). HRMS (ESI) calcd for $C_{45}H_{57}N_{10}O_8S$ $[M+H]^+$ 897.4076 found 897.4072.

(S)-tert-butyl 2-(4-(((2-amino-4-oxo-3,4-dihydropteridin-6-yl)methyl)amino)benzamido)-5-((8-((2-((tert-butoxycarbonyl)amino)-5-(thiophen-2-yl)phenyl)amino)-8-oxooctyl)amino)-5-oxopentanoate (23c):

Compound **22c** (0.17 g, 0.28 mmol) was coupled to pteroyl azide (0.25 g, 0.56 mmol) in the presence of TMG (0.097 g, 0.84 mmol) in DMSO as described for the synthesis of **5** to yield **23c** (0.070 g, 28% yield). 1H NMR (400 MHz, DMSO- d_6) δ 8.58 (s, 1H), 7.71 (s, 1H), 7.62 (d, $J = 8.6$ Hz, 2H), 7.58 (d, $J = 8.7$ Hz, 1H), 7.49 (d, $J = 4.5$ Hz, 1H), 7.44 – 7.37 (m, 2H), 7.12 – 7.08 (m, 1H), 6.61 (d, $J = 8.5$ Hz, 2H), 4.44 (d, $J = 6.0$ Hz, 2H), 4.23 – 4.12 (m, 1H), 3.03 – 2.94 (m, 2H), 2.34 (t, $J = 7.5$ Hz, 2H), 2.20 – 2.11 (m, 2H), 2.02 – 1.94 (m, 1H), 1.91 – 1.82 (m, 1H), 1.62 – 1.54 (m, 2H), 1.42 (s, 9H), 1.37 (s, 9H), 1.32 – 1.20 (m, 8H). HRMS (ESI) calcd for $C_{46}H_{59}N_{10}O_8S$ $[M+H]^+$ 911.4233 found 911.4217.

(S)-tert-butyl 2-(4-(((2-amino-4-oxo-3,4-dihydropteridin-6-yl)methyl)amino)benzamido)-5-((9-((2-((tert-butoxycarbonyl)amino)-5-(thiophen-2-yl)phenyl)amino)-9-oxononyl)amino)-5-oxopentanoate (23d):

Compound **22d** (0.17 g, 0.27 mmol) was coupled to pteroyl azide (0.24 g, 0.53 mmol) in the presence of TMG (0.091 g, 0.80 mmol) in DMSO as described for the synthesis of **5**

to yield **23d** (0.11 g, 46% yield). ^1H NMR (400 MHz, DMSO- d_6) δ 8.63 (s, 1H), 7.69 (d, $J = 2.1$ Hz, 1H), 7.63 (d, $J = 8.8$ Hz, 2H), 7.57 (d, $J = 8.5$ Hz, 1H), 7.49 (d, $J = 5.1$ Hz, 1H), 7.45 – 7.36 (m, 2H), 7.10 (dd, $J = 5.0, 3.7$ Hz, 1H), 6.62 (d, $J = 8.8$ Hz, 2H), 4.46 (d, $J = 6.0$ Hz, 2H), 4.23 – 4.12 (m, 1H), 3.02 – 2.94 (m, 2H), 2.34 (t, $J = 7.5$ Hz, 2H), 2.15 (dd, $J = 12.6, 6.6$ Hz, 2H), 2.01 – 1.93 (m, 1H), 1.91 – 1.83 (m, 1H), 1.64 – 1.54 (m, 2H), 1.44 (s, 9H), 1.41 – 1.38 (m, 2H), 1.37 (s, 9H), 1.32 – 1.21 (m, 8H). HRMS (ESI) calcd for $\text{C}_{47}\text{H}_{61}\text{N}_{10}\text{O}_8\text{S}$ $[\text{M}+\text{H}]^+$ 925.4389 found 925.4386.

(S)-2-(4-(((2-Amino-4-oxo-3,4-dihydropteridin-6-yl)methyl)amino)benzamido)-5-(((4-((2-amino-5-(thiophen-2-yl)phenyl)amino)-4-oxobutyl)amino)-5-oxopentanoic acid (24a):

Compound **23a** (0.032 g, 0.037 mmol) was dissolved in neat TFA (2 mL) and TIPS (0.5 mL) and stirred at room temperature for 2 h. The desired product **24a** (0.03 g, quantitative yield) was obtained as described for the synthesis of **6**. ^1H NMR (500 MHz, DMSO- d_6) δ 8.66 (s, 1H), 7.67 (d, $J = 8.5$ Hz, 2H), 7.50 (s, 1H), 7.36 (d, $J = 4.8$ Hz, 1H), 7.27 – 7.18 (m, 2H), 7.07 – 7.03 (m, 1H), 6.77 (d, $J = 8.3$ Hz, 1H), 6.65 (d, $J = 8.5$ Hz, 2H), 4.50 (s, 2H), 4.32 (t, $J = 10.6$ Hz, 1H), 3.11 (dt, $J = 12.8, 6.7$ Hz, 2H), 2.33 (t, $J = 7.4$ Hz, 2H), 2.22 (t, $J = 7.3$ Hz, 2H), 2.14 – 2.06 (m, 1H), 1.99 – 1.88 (m, 1H), 1.78 – 1.65 (m, 2H). ^{13}C NMR (126 MHz, DMSO- d_6) δ 174.1, 171.8, 171.4, 166.7, 153.9, 151.0, 148.8, 144.5, 129.3, 128.5, 124.1, 123.6, 123.5, 122.9, 121.6, 121.3, 116.6, 111.5, 65.2, 52.4, 46.2, 38.3, 33.4, 32.3, 31.0, 26.9, 25.6, 15.5. HRMS (ESI) calcd for $\text{C}_{33}\text{H}_{35}\text{N}_{10}\text{O}_6\text{S}$ $[\text{M}+\text{H}]^+$ 699.2456 found 699.2450.

(S)-2-(4-(((2-Amino-4-oxo-3,4-dihydropteridin-6-yl)methyl)amino)benzamido)-5-((7-((2-amino-5-(thiophen-2-yl)phenyl)amino)-7-oxoheptyl)amino)-5-oxopentanoic acid (24b):

Compound **23b** (0.039 g, 0.043 mmol) was dissolved in neat TFA (2 mL) and TIPS (0.5 mL) and stirred at room temperature for 2 h. The desired product **24b** (0.027 g, 84% yield) was obtained as described for the synthesis of **6**. ¹H NMR (500 MHz, DMSO-*d*₆) δ 8.67 (s, 1H), 7.67 (d, *J* = 8.6 Hz, 2H), 7.51 (d, *J* = 1.8 Hz, 1H), 7.36 (d, *J* = 4.9 Hz, 1H), 7.26 – 7.20 (m, 2H), 7.07 – 7.03 (m, 1H), 6.79 (d, *J* = 8.2 Hz, 1H), 6.65 (d, *J* = 8.6 Hz, 2H), 4.50 (s, 2H), 4.28 (t, *J* = 10.9 Hz, 1H), 3.08 – 2.99 (m, 2H), 2.34 (t, *J* = 7.4 Hz, 2H), 2.19 (t, *J* = 8.4 Hz, 2H), 2.08 – 2.02 (m, 1H), 1.97 – 1.88 (m, 1H), 1.65 – 1.53 (m, 2H), 1.43 – 1.34 (m, 2H), 1.35 – 1.25 (m, 4H). ¹³C NMR (126 MHz, DMSO-*d*₆) δ 174.1, 171.6, 166.6, 151.0, 148.8, 144.5, 129.3, 128.5, 128.2, 123.6, 122.7, 121.6, 121.4, 111.5, 65.2, 52.6, 46.2, 38.8, 36.1, 32.3, 29.3, 28.7, 26.9, 26.5, 25.4, 15.5. HRMS (ESI) calcd for C₃₆H₄₁N₁₀O₆S [M+H]⁺ 741.2926 found 741.2922.

(S)-2-(4-(((2-Amino-4-oxo-3,4-dihydropteridin-6-yl)methyl)amino)benzamido)-5-((8-((2-amino-5-(thiophen-2-yl)phenyl)amino)-8-oxooctyl)amino)-5-oxopentanoic acid (24c):

Compound **23c** (0.032 g, 0.035 mmol) was dissolved in neat TFA (2 mL) and TIPS (0.5 mL) and stirred at room temperature for 2 h. The desired product **24c** (0.025 g, 93% yield) was obtained as described for the synthesis of **6**. ¹H NMR (500 MHz, DMSO-*d*₆) δ 8.67 (s, 1H), 7.66 (d, *J* = 8.8 Hz, 2H), 7.51 (d, *J* = 1.9 Hz, 1H), 7.37 (d, *J* = 4.6 Hz, 1H), 7.27 – 7.21 (m, 2H), 7.07 – 7.03 (m, 2H), 6.79 (t, *J* = 7.3 Hz, 1H), 6.65 (d, *J* = 8.8 Hz,

2H), 4.51 (s, 2H), 4.32 – 4.23 (m, 1H), 3.08 – 2.99 (m, 2H), 2.34 (dd, $J = 9.4, 5.4$ Hz, 2H), 2.22 – 2.15 (m, 2H), 2.08 – 2.01 (m, 1H), 1.98 – 1.87 (m, 1H), 1.65 – 1.57 (m, 2H), 1.44 – 1.25 (m, 8H). ^{13}C NMR (126 MHz, DMSO- d_6) δ 174.1, 171.8, 171.6, 171.1, 171.0, 166.5, 161.0, 153.8, 151.0, 149.3, 148.8, 144.5, 129.2, 128.5, 128.2, 124.5, 123.7, 123.6, 123.4, 122.6, 121.7, 121.5, 121.4, 117.0, 111.5, 52.6, 46.2, 36.1, 32.3, 30.9, 29.4, 29.3, 29.0, 28.8, 26.9, 26.6, 25.4. HRMS (ESI) calcd for $\text{C}_{37}\text{H}_{43}\text{N}_{10}\text{O}_6 \text{S}$ $[\text{M}+\text{H}]^+$ 755.3082 found 755.3075.

(S)-2-(4-(((2-Amino-4-oxo-3,4-dihydropteridin-6-yl)methyl)amino)benzamido)-5-((9-((2-amino-5-(thiophen-2-yl)phenyl)amino)-9-oxononyl)amino)-5-oxopentanoic acid (24d):

Compound **23d** (0.034 g, 0.037 mmol) was dissolved in neat TFA (2 mL) and TIPS (0.5 mL) and stirred at room temperature for 2 h. The desired product **24d** (0.022 g, 79% yield) was obtained as described for the synthesis of **6**. ^1H NMR (500 MHz, DMSO- d_6) δ 8.67 (s, 1H), 7.66 (d, $J = 8.4$ Hz, 2H), 7.51 (s, 1H), 7.37 (d, $J = 5.0$ Hz, 1H), 7.28 – 7.21 (m, 2H), 7.08 – 7.02 (m, 1H), 6.80 (d, $J = 8.3$ Hz, 1H), 6.65 (d, $J = 8.4$ Hz, 2H), 4.51 (s, 2H), 4.35 – 4.25 (m, 1H), 3.05 – 2.97 (m, 2H), 2.34 (t, $J = 7.3$ Hz, 2H), 2.19 (t, $J = 11.0$ Hz, 2H), 2.11 – 2.00 (m, 1H), 1.97 – 1.86 (m, 1H), 1.67 – 1.54 (m, 2H), 1.40 – 1.22 (m, 10H). ^{13}C NMR (126 MHz, DMSO- d_6) δ 174.1, 171.8, 171.6, 166.5, 161.0, 153.8, 151.0, 148.8, 144.4, 129.2, 128.5, 128.2, 123.7, 123.4, 122.6, 121.7, 121.5, 111.5, 52.6, 46.2, 36.1, 32.3, 29.4, 29.1, 29.0, 26.9, 26.7, 25.5. HRMS (ESI) calcd for $\text{C}_{38}\text{H}_{45}\text{N}_{10}\text{O}_6 \text{S}$ $[\text{M}+\text{H}]^+$ 769.3239 found 769.3236.

3.11. References

1. Strausberg, R. L.; Simpson, A. J. G.; Old, L. J.; Riggins, G. J., Oncogenomics and the development of new cancer therapies. *Nature* **2004**, *429* (6990), 469-474.
2. Ma, W. W.; Adjei, A. A., Novel Agents on the Horizon for Cancer Therapy. *CA: A Cancer Journal for Clinicians* **2009**, *59* (2), 111-137.
3. Gryder, B. E.; Sodji, Q. H.; Oyelere, A. K., Targeted cancer therapy: giving histone deacetylase inhibitors all they need to succeed. *Future Medicinal Chemistry* **2012**, *4* (4), 505-524.
4. Butler, L. M.; Zhou, X.; Xu, W.-S.; Scher, H. I.; Rifkind, R. A.; Marks, P. A.; Richon, V. M., The histone deacetylase inhibitor SAHA arrests cancer cell growth, up-regulates thioredoxin-binding protein-2, and down-regulates thioredoxin. *Proceedings of the National Academy of Sciences* **2002**, *99* (18), 11700-11705.
5. Minucci, S.; Pelicci, P. G., Histone deacetylase inhibitors and the promise of epigenetic (and more) treatments for cancer. *Nature Review Cancer* **2006**, *6* (1), 38-51.
6. Dokmanovic, M.; Clarke, C.; Marks, P. A., Histone Deacetylase Inhibitors: Overview and Perspectives. *Molecular Cancer Research* **2007**, *5* (10), 981-989.
7. Witt, O.; Deubzer, H. E.; Milde, T.; Oehme, I., HDAC family: What are the cancer relevant targets? *Cancer Letters* **2009**, *277* (1), 8-21.
8. Ueki, N.; Lee, S.; Sampson, N. S.; Hayman, M. J., Selective cancer targeting with prodrugs activated by histone deacetylases and a tumour-associated protease. *Nature Communication* **2013**, *4*, 2735.
9. Weichert, W., HDAC expression and clinical prognosis in human malignancies. *Cancer Letters* **2009**, *280* (2), 168-176.
10. Porcu, P.; Wong, H. K., We Should Have a Dream: Unlocking the Workings of the Genome in Cutaneous T-Cell Lymphomas. *Clinical Lymphoma and Myeloma* **2009**, *9* (6), 409-411.
11. Mann, B. S.; Johnson, J. R.; Cohen, M. H.; Justice, R.; Pazdur, R., FDA Approval Summary: Vorinostat for Treatment of Advanced Primary Cutaneous T-Cell Lymphoma. *The Oncologist* **2007**, *12* (10), 1247-1252.
12. Subramanian, S.; Bates, S. E.; Wright, J. J.; Espinoza-Delgado, I.; Piekarczyk, R. L., Clinical Toxicities of Histone Deacetylase Inhibitors. *Pharmaceuticals* **2010**, *3* (9), 2751-2767.

13. de Bono, J. S.; Ashworth, A., Translating cancer research into targeted therapeutics. *Nature* **2010**, *467* (7315), 543-549.
14. Qiu, T. Z.; Zhou, L.; Zhu, W.; Wang, T. S.; Wang, J.; Shu, Y. Q.; Liu, P., Effects of treatment with histone deacetylase inhibitors in solid tumors: a review based on 30 clinical trials. *Future Oncology* **2013**, *9* (2), 255-269.
15. Grassadonia, A.; Cioffi, P.; Simiele, F.; Iezzi, L.; Zilli, M.; Natoli, C., Role of Hydroxamate-Based Histone Deacetylase Inhibitors (Hb-HDACi) in the Treatment of Solid Malignancies. *Cancers* **2013**, *5* (3), 919-942.
16. Bauer, J. A.; Morrison, B. H.; Grane, R. W.; Jacobs, B. S.; Dabney, S.; Gamero, A. M.; Carnevale, K. A.; Smith, D. J.; Drazba, J.; Seetharam, B.; Lindner, D. J., Effects of Interferon β on Transcobalamin II-Receptor Expression and Antitumor Activity of Nitrosylcobalamin. *Journal of the National Cancer Institute* **2002**, *94* (13), 1010-1019.
17. Russell-Jones, G.; McTavish, K.; McEwan, J.; Rice, J.; Nowotnik, D., Vitamin-mediated targeting as a potential mechanism to increase drug uptake by tumours. *Journal of Inorganic Biochemistry* **2004**, *98* (10), 1625-1633.
18. Mantovani, L. T.; Miotti, S.; Ménard, S.; Canevari, S.; Raspagliesi, F.; Bottini, C.; Bottero, F.; Colnaghi, M. I., Folate binding protein distribution in normal tissues and biological fluids from ovarian carcinoma patients as detected by the monoclonal antibodies MOv18 and MOv19. *European Journal of Cancer* **1994**, *30* (3), 363-369.
19. Parker, N.; Turk, M. J.; Westrick, E.; Lewis, J. D.; Low, P. S.; Leamon, C. P., Folate receptor expression in carcinomas and normal tissues determined by a quantitative radioligand binding assay. *Analytical Biochemistry* **2005**, *338* (2), 284-293.
20. Weitman, S. D.; Lark, R. H.; Coney, L. R.; Fort, D. W.; Frasca, V.; Zurawski, V. R.; Kamen, B. A., Distribution of the Folate Receptor GP38 in Normal and Malignant Cell Lines and Tissues. *Cancer Research* **1992**, *52* (12), 3396-3401.
21. Xia, W.; Low, P. S., Folate-Targeted Therapies for Cancer. *Journal of Medicinal Chemistry* **2010**, *53* (19), 6811-6824.
22. Lu, Y.; Low, P. S., Folate-mediated delivery of macromolecular anticancer therapeutic agents. *Advanced Drug Delivery Reviews* **2012**, *64*, Supplement (0), 342-352.
23. Low, P. S.; Kularatne, S. A., Folate-targeted therapeutic and imaging agents for cancer. *Current Opinion in Chemical Biology* **2009**, *13* (3), 256-262.

24. Vlahov, I. R.; Leamon, C. P., Engineering Folate–Drug Conjugates to Target Cancer: From Chemistry to Clinic. *Bioconjugate Chemistry* **2012**, *23* (7), 1357-1369.
25. Low, P. S.; Henne, W. A.; Doorneweerd, D. D., Discovery and Development of Folic-Acid-Based Receptor Targeting for Imaging and Therapy of Cancer and Inflammatory Diseases. *Accounts of Chemical Research* **2007**, *41* (1), 120-129.
26. Matherly, L.; Hou, Z.; Deng, Y., Human reduced folate carrier: translation of basic biology to cancer etiology and therapy. *Cancer Metastasis Reviews* **2007**, *26* (1), 111-128.
27. Leamon, C. P.; DePrince, R. B.; Hendren, R. W., Folate-mediated drug delivery: Effect of alternative conjugation chemistry. *Journal of Drug Targeting* **1999**, *7* (3), 157-169.
28. Ke, C.-Y.; Mathias, C. J.; Green, M. A., Targeting the Tumor-Associated Folate Receptor with an ¹¹¹In–DTPA Conjugate of Pteric Acid. *Journal of the American Chemical Society* **2005**, *127* (20), 7421-7426.
29. Barton, A. K.; Capdevila, A., Receptor-Mediated Folate Accumulation is Regulated by the Cellular Folate Content. *Proceedings of the National Academy of Sciences of the United States of America* **1986**, *83* (16), 5983-5987.
30. Lundquist; Pelletier, J. C., Improved Solid-Phase Peptide Synthesis Method Utilizing α -Azide-Protected Amino Acids. *Organic Letters* **2001**, *3* (5), 781-783.
31. Han, S.-Y.; Kim, Y.-A., Recent development of peptide coupling reagents in organic synthesis. *Tetrahedron* **2004**, *60* (11), 2447-2467.
32. Lin, W.; Zhang, X.; He, Z.; Jin, Y.; Gong, L.; Mi, A., REDUCTION OF AZIDES TO AMINES OR AMIDES WITH ZINC AND AMMONIUM CHLORIDE AS REDUCING AGENT. *Synthetic Communications* **2002**, *32* (21), 3279-3284.
33. Luo, J.; Smith, M. D.; Lantrip, D. A.; Wang, S.; Fuchs, P. L., Efficient Syntheses of Pyrofolic Acid and Pteroyl Azide, Reagents for the Production of Carboxyl-Differentiated Derivatives of Folic Acid. *Journal of the American Chemical Society* **1997**, *119* (42), 10004-10013.
34. Mehta, A.; Jaouhari, R.; Benson, T. J.; Douglas, K. T., Improved efficiency and selectivity in peptide synthesis: Use of triethylsilane as a carbocation scavenger in deprotection of t-butyl esters and t-butoxycarbonyl-protected sites. *Tetrahedron Letters* **1992**, *33* (37), 5441-5444.

35. Patil, V.; Sodji, Q. H.; Kornacki, J. R.; Mrksich, M.; Oyelere, A. K., 3-Hydroxypyridin-2-thione as Novel Zinc Binding Group for Selective Histone Deacetylase Inhibition. *Journal of Medicinal Chemistry* **2013**.
36. Sodji, Q. H.; Patil, V.; Kornacki, J. R.; Mrksich, M.; Oyelere, A. K., Synthesis and Structure–Activity Relationship of 3-Hydroxypyridine-2-thione-Based Histone Deacetylase Inhibitors. *Journal of Medicinal Chemistry* **2013**, *56* (24), 9969-9981.
37. Gryder, B. E.; Akbashev, M. J.; Rood, M. K.; Raftery, E. D.; Meyers, W. M.; Dillard, P.; Khan, S.; Oyelere, A. K., Selectively Targeting Prostate Cancer with Antiandrogen Equipped Histone Deacetylase Inhibitors. *ACS Chemical Biology* **2013**, *8* (11), 2550-2560.
38. Wallace, K. J.; Hanes, R.; Anslyn, E.; Morey, J.; Kilway, K. V.; Siegel, J., Preparation of 1,3,5-Tris(aminomethyl)-2,4,6-triethylbenzene from Two Versatile 1,3,5-Tri(halosubstituted) 2,4,6-Triethylbenzene Derivatives. *Synthesis* **2005**, *2005* (12), 2080-2083.
39. Schäfer, S.; Saunders, L.; Eliseeva, E.; Velena, A.; Jung, M.; Schwienhorst, A.; Strasser, A.; Dickmanns, A.; Ficner, R.; Schlimme, S.; Sippl, W.; Verdin, E.; Jung, M., Phenylalanine-containing hydroxamic acids as selective inhibitors of class IIb histone deacetylases (HDACs). *Bioorganic & Medicinal Chemistry* **2008**, *16* (4), 2011-2033.
40. Raje, N.; Hari, P. N.; Vogl, D. T.; Jagannath, S.; Orłowski, R. Z.; Supko, J. G.; Stephenson, P.; Jones, S. S.; Wheeler, C.; Lonial, S., Rocilinostat (ACY-1215), a Selective HDAC6 Inhibitor, Alone and in Combination with Bortezomib in Multiple Myeloma: Preliminary Results From the First-in-Humans Phase I/II Study. *Blood* **2012**, *120* (21).
41. Methot, J. L.; Chakravarty, P. K.; Chenard, M.; Close, J.; Cruz, J. C.; Dahlberg, W. K.; Fleming, J.; Hamblett, C. L.; Hamill, J. E.; Harrington, P.; Harsch, A.; Heidebrecht, R.; Hughes, B.; Jung, J.; Kenific, C. M.; Kral, A. M.; Meinke, P. T.; Middleton, R. E.; Ozerova, N.; Sloman, D. L.; Stanton, M. G.; Szewczak, A. A.; Tyagarajan, S.; Witter, D. J.; Paul Secrist, J.; Miller, T. A., Exploration of the internal cavity of histone deacetylase (HDAC) with selective HDAC1/HDAC2 inhibitors (SHI-1:2). *Bioorganic & Medicinal Chemistry Letters* **2008**, *18* (3), 973-978.
42. Kumar, P.; Lokanatha Rai, K., Reduction of aromatic nitro compounds to amines using zinc and aqueous chelating ethers: Mild and efficient method for zinc activation. *Chemical Papers* **2012**, *66* (8), 772-778.

43. Paulos, C. M.; Reddy, J. A.; Leamon, C. P.; Turk, M. J.; Low, P. S., Ligand Binding and Kinetics of Folate Receptor Recycling in Vivo: Impact on Receptor-Mediated Drug Delivery. *Molecular Pharmacology* **2004**, *66* (6), 1406-1414.
44. Chen, H.; Ahn, R.; Van den Bossche, J.; Thompson, D. H.; O'Halloran, T. V., Folate-mediated intracellular drug delivery increases the anticancer efficacy of nanoparticulate formulation of arsenic trioxide. *Molecular Cancer Therapeutics* **2009**, *8* (7), 1955-1963.
45. Suzuki, T.; Hisakawa, S.; Itoh, Y.; Suzuki, N.; Takahashi, K.; Kawahata, M.; Yamaguchi, K.; Nakagawa, H.; Miyata, N., Design, synthesis, and biological activity of folate receptor-targeted prodrugs of thiolate histone deacetylase inhibitors. *Bioorganic & Medicinal Chemistry Letters* **2007**, *17* (15), 4208-4212.
46. Simmons, G.; Rennekamp, A. J.; Chai, N.; Vandenberghe, L. H.; Riley, J. L.; Bates, P., Folate Receptor Alpha and Caveolae Are Not Required for Ebola Virus Glycoprotein-Mediated Viral Infection. *Journal of Virology* **2003**, *77* (24), 13433-13438.
47. Bergman, J. A.; Woan, K.; Perez-Villaruel, P.; Villagra, A.; Sotomayor, E. M.; Kozikowski, A. P., Selective Histone Deacetylase 6 Inhibitors Bearing Substituted Urea Linkers Inhibit Melanoma Cell Growth. *Journal of Medicinal Chemistry* **2012**, *55* (22), 9891-9899.
48. Senese, S.; Zaragoza, K.; Minardi, S.; Muradore, I.; Ronzoni, S.; Passafaro, A.; Bernard, L.; Draetta, G. F.; Alcalay, M.; Seiser, C.; Chiocca, S., Role for Histone Deacetylase 1 in Human Tumor Cell Proliferation. *Molecular and Cellular Biology* **2007**, *27* (13), 4784-4795.
49. Chen, C.; Ke, J.; Zhou, X. E.; Yi, W.; Brunzelle, J. S.; Li, J.; Yong, E.-L.; Xu, H. E.; Melcher, K., Structural basis for molecular recognition of folic acid by folate receptors. *Nature* **2013**, *advance online publication*.
50. Bantscheff, M.; Hopf, C.; Savitski, M. M.; Dittmann, A.; Grandi, P.; Michon, A.-M.; Schlegl, J.; Abraham, Y.; Becher, I.; Bergamini, G.; Boesche, M.; Delling, M.; Dumpelfeld, B.; Eberhard, D.; Huthmacher, C.; Mathieson, T.; Poeckel, D.; Reader, V.; Strunk, K.; Sweetman, G.; Kruse, U.; Neubauer, G.; Ramsden, N. G.; Drewes, G., Chemoproteomics profiling of HDAC inhibitors reveals selective targeting of HDAC complexes. *Nature Biotechnology* **2011**, *29* (3), 255-265.
51. Butler, K. V.; Kalin, J.; Brochier, C.; Vistoli, G.; Langley, B.; Kozikowski, A. P., Rational Design and Simple Chemistry Yield a Superior, Neuroprotective HDAC6 Inhibitor, Tubastatin A. *Journal of the American Chemical Society* **2010**, *132* (31), 10842-10846.

52. Zhao, R.; Min, S. H.; Wang, Y.; Campanella, E.; Low, P. S.; Goldman, I. D., A Role for the Proton-coupled Folate Transporter (PCFT-SLC46A1) in Folate Receptor-mediated Endocytosis. *Journal of Biological Chemistry* **2009**, *284* (7), 4267-4274.
53. Gurard-Levin, Z. A.; Scholle, M. D.; Eisenberg, A. H.; Mrksich, M., High-Throughput Screening of Small Molecule Libraries using SAMDI Mass Spectrometry. *ACS Combinatorial Science* **2011**, *13* (4), 347-350.
54. Gurard-Levin, Z. A.; Kilian, K. A.; Kim, J.; Bähr, K.; Mrksich, M., Peptide Arrays Identify Isoform-Selective Substrates for Profiling Endogenous Lysine Deacetylase Activity. *ACS Chemical Biology* **2010**, *5* (9), 863-873.
55. Trott, O.; Olson, A. J., AutoDock Vina: Improving the speed and accuracy of docking with a new scoring function, efficient optimization, and multithreading. *Journal of Computational Chemistry* **2010**, *31* (2), 455-461.
56. Gryder, B. E.; Rood, M. K.; Johnson, K. A.; Patil, V.; Raftery, E. D.; Yao, L.-P. D.; Rice, M.; Azizi, B.; Doyle, D. F.; Oyelere, A. K., Histone Deacetylase Inhibitors Equipped with Estrogen Receptor Modulation Activity. *Journal of Medicinal Chemistry* **2013**, *56* (14), 5782-5796.

CHAPTER 4

MECHANISM OF HDAC INHIBITOR RESISTANCE IN JURKAT

J- γ

4.1. Introduction

Histone deacetylase inhibitors (HDACi) by triggering a variety of cellular pathways have displayed significant potential as cancer chemotherapy agents. Responses to HDACi exposure in transformed cells include differentiation, cell cycle arrest, increased immunogenicity, apoptosis, and autophagy.^{1,2} These responses culminate in the decreased of tumor size and/or cell death. However, due to the ability of cancer cells to adapt to their microenvironments, various mechanisms of resistance to HDACi have been described.³ These drug-resistance mechanisms may explain the lack of efficacy of HDACi seen in certain clinical trials. Furthermore, the understanding of such mechanisms can result in the development of combination therapies with other cytotoxic agents capable of potentiating the clinical effects of HDACi.

4.2. Mechanisms of Resistance to HDACi

4.2.1. Efflux pumps

P-Glycoproteins including multidrug resistance proteins are upregulated in malignant cells upon exposure to cytotoxic agents.⁴ These efflux pumps whose substrates encompass a wide range of molecules exclude chemotherapeutics from malignant cells thus minimizing exposure of the drugs to their intracellular targets.⁵ Although various HDACi such as sodium butyrate, FK228 (Romidepsin), valproic acid and TSA were found to increase the expression of the P-glycoprotein, only FK228 (Romidepsin) is a

substrate of these efflux pumps.^{6,7,8} These pumps do not constitute an important mechanism of resistance to HDACi treatment as hydroxamate and carboxylic acid based inhibitors are not the substrates of such pumps.⁹

4.2.2. Changes in HDAC expression level

Although this mechanism has not been proven clinically, it has been observed in various cell lines upon exposure to HDACi. Following exposure to a inhibitor, cancer cells can upregulate their HDACs expression enabling them to compensate for the HDACi's presence. In melanoma cells, resistance to sodium butyrate was achieved by the overexpression of HDAC1.¹⁰ Furthermore, in HL-60 leukemia cells lacking HDAC6, higher levels of HDAC1, 2, and 4 were detected.¹¹

4.2.3. Expression of apoptosis related proteins

The induction of apoptosis is a balancing act between the expression of pro-apoptotic genes (Bax, Bak, Bim, Bmf and caspases) and anti-apoptotic genes (BCL2, BCL-X_L and XIAP).¹² HDACi treatment, by promoting the expression of pro-apoptotic genes, induce cancer cell death.¹³ However, this response is blunted when anti-apoptotic genes products are overexpressed.¹⁴

4.2.4. Increased antioxidant production

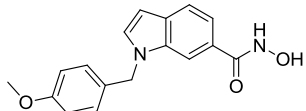
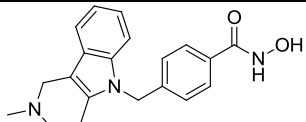
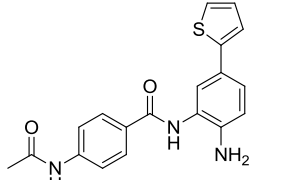
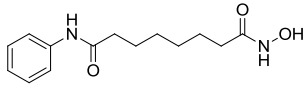
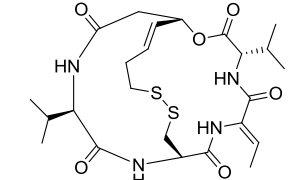
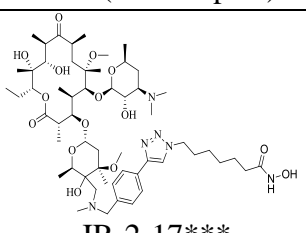
Increase in reactive oxygen species (ROS) is important in HDACi-induced cytotoxicity.¹⁵ The upregulation of ROS production has been linked to a disruption of the mitochondrial membrane, a decreased production of the antioxidant thioredoxin and the

upregulation of thioredoxin-binding protein 2 (TBP-2) which is a negative regulator of thioredoxin.^{1,16} As such, an increase in antioxidant production such as glutathione can mitigate the damages due to the ROS production upon exposure of cancer to HDACi.¹⁷

4.3. Novel mechanism of resistance to HDACi

Balasubramanian et al discovered that in T-cells, the HDAC8 selective inhibitor PCI-34051, induces apoptosis through a Ca^{2+} signaling pathway involving the phospholipase C- γ 1 (PLC- γ 1).¹⁸ Upon exposure to PCI-34051, Ca^{2+} is released from the endoplasmic reticulum (ER), resulting in the release of mitochondrial cytochrome c. The cytochrome c in turn binds to the inositol 1,4,5 triphosphate receptors (IP₃R) enabling the activation of PLC- γ 1 leading to further release of Ca^{2+} and mitochondrial cytochrome c through a positive feedback mechanism.^{19,20} In Jurkat J γ , a mutant Jurkat cell line with no detectable PLC- γ 1 activity, the HDAC8 selective PCI-34051 did not induce cell death, suggesting the crucial role of PLC- γ 1 in HDAC8 inhibitor induced apoptosis. We decided to examine the requirement of PLC- γ 1 in the apoptosis induced by selective HDACi (HDAC1 and 6), pan-inhibitors including IR-2-17 and the clinically approved SAHA and FK228 (Romidepsin) in Jurkat J γ (Table 4.1).

Table 4.1: Structures and HDAC inhibition profile of selected HDAC inhibitors.

Compound	IC ₅₀ (μM)					
	HDAC1	HDAC2	HDAC3	HDAC6	HDAC8	HDAC10
 PCI-34051*	4	> 50	> 50	2.9	0.01	13
 Tubastatin A†	16.4	> 30	> 30	0.015	0.854	> 30
 SHI1:2‡	0.007	0.049	10	> 10	> 10	-
 SAHA*	0.028	0.06	0.044	0.022	0.41	0.04
 FK228 (Romidepsin)**	0.036	0.047	NT	14	NT	NT
 IR-2-17***	0.024	NT	NT	0.003	1.84	NT

*Ref. ¹⁸; †Ref. ²¹; ‡Ref. ²²; **Ref. ²³; ***synthesized by Idris Raji; NT: Not tested

4.3.1. Anticancer activity of selected compounds against wild type Jurkat and the Jurkat subline J γ

The wild type Jurkat and its mutant subline J γ were exposed to tubastatin A and selected compounds aforementioned in Table 4.1. Against the wild type Jurkat, all the tested compounds were very potent with FK228 (Romidepsin) having a single digit nanomolar IC₅₀ (Table 4.2). In Jurkat J γ , the potency of all the compounds was diminished, however, the degree of resistance of Jurkat J γ cells varied from one compound to the other. The isoform selective HDACi, Tubastatin A (HDAC6) and SHI1:2 (HDAC1), and SAHA did not show any anticancer activity at the highest tested concentration of 20 μ M, whereas FK228 and IR-2-17 had IC₅₀s of 830 nM and 17.34 μ M respectively suggesting the crucial role of PLC- γ 1 in the apoptosis potentiation of these compounds (Table 4.2). The single digit nanomolar IC₅₀ of FK228 against the wild Jurkat is in agreement with previous studies which established FK228 as a potent drug against leukemia cells.²⁴ This observed potency is attributable to the reduced form of FK228 (red-FK228) which ensues following the cellular uptake of FK228 (Figure 4.1). Not only is red-FK228 a much more potent HDACi than FK228, but its formation also results in the depletion of cellular antioxidants such glutathione leading to an increased production of ROS.²⁵ The FK228-induced apoptosis is much more sensitive to the lack of PLC- γ 1 as its IC₅₀ was increased by 277 fold in J γ compared to 25 fold for IR-2-17 (Table 4.2). Although SHI1:2, tubastatin A and SAHA did not displayed any anticancer activity at 20 μ M, it is possible that these compounds may show anticancer activity at higher concentrations such as 25 times their IC₅₀s in wild type Jurkat.

Table 4.2: Anticancer activity of selected compounds (IC₅₀ in μM)

	Wild Jurkat	Jurkat Jγ	Resistance increase in Jγ compared to wild type Jurkat
SHI1:2	2.73 ± 0.35	NI	-
Tubastatin A	3.38 ± 0.26	NI	-
SAHA	1.49 ± 0.10	NI	-
FK228	0.003 ± 0.001	0.830 ± 0.100	277
IR-2-17	0.700 ± 0.140	17.34 ± 2.30	25

NI: No inhibition at 20 μM

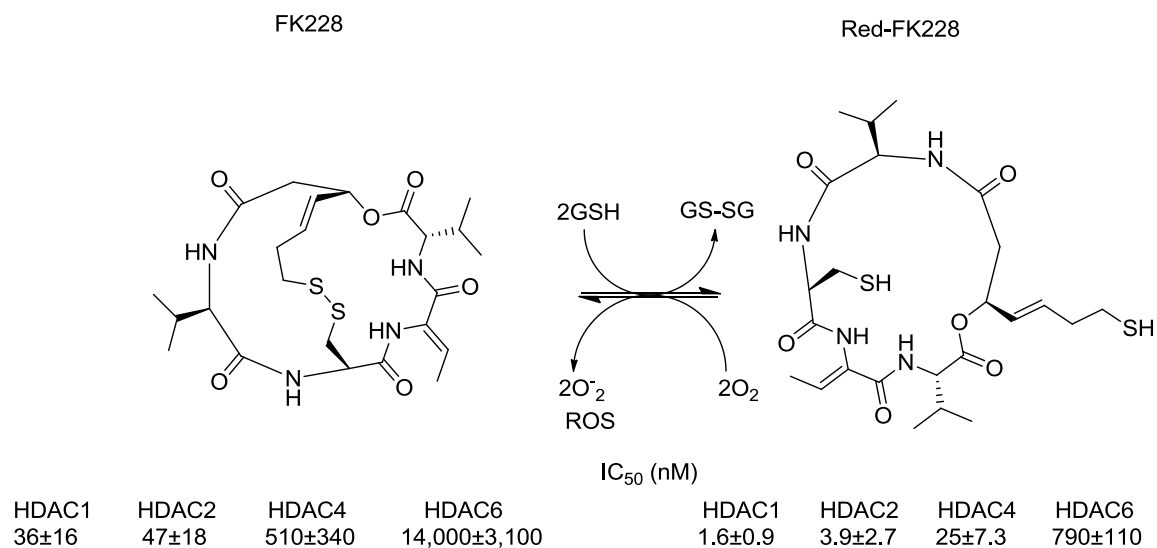


Figure 4.1: HDACs inhibition profile of FK228 and reduced FK228 (Red-FK228). IC₅₀ in nanomolar (nM).^{23,25}

4.3.2. Phospholipase C- γ 2 may be responsible for apoptosis potentiation in Jurkat J γ subline

PLC- γ 1 is a key player in potentiating both the intrinsic and extrinsic apoptotic pathways, however, its total loss in J γ does not render this cell line completely impervious to HDACi induced apoptosis though a degree of resistance is present. This observation points to the presence of other phospholipases capable of participating in all the pathways requiring PLC- γ 1. Indeed in T-cells, the phospholipase C- γ 2 (PLC- γ 2) is co-expressed along with PLC- γ 1 although in very small amount and possess identical activation pathways.²⁶

4.3.3. Mutations in PLC- γ 1 activation pathways as potentially novel mechanisms of HDACi resistance

Based on the resistance of Jurkat J γ cells (no PLC- γ 1 activity) to HDACi-induced apoptosis, it can be implied that mutations in malignant cells resulting in such phenotype (loss of PLC γ 1) can constitute a novel mechanism of resistance to HDACi. However, such mutations in any organism are lethal at the embryonic stage emphasizing the crucial role of PLC- γ 1 in processes such as embryogenesis, cellular homeostasis and potentially cancer.²⁷ Furthermore, the J γ subline is an artificial product of mutagenesis-mutant selection on the wild type Jurkat as opposed to a cell line isolated from a leukemia patient and whose survival is due to the residual expression of the PLC- γ 2.²⁷ Loss-of-function mutations of PLC- γ 1 have not been linked to tumorigenesis whereas multiple gain-of-

function mutations resulting in constitutive activation of PLC- γ 1 are implicated in cancer.^{28,29}

Although, loss-of-function mutations in PLC- γ 1 have not been described in cancer, mutations in the IP₃R (downstream of the PLC- γ 1 pathway) on the ER may result in resistance to apoptosis including HDACi-induced. As previously mentioned, initial Ca²⁺ release upon apoptosis induction triggers cytochrome c release from the mitochondria which potentiates further Ca²⁺ release from the ER upon binding to the IP₃R. Abrogation of the binding interactions between cytochrome c and IP₃R can prevent the late phase Ca²⁺ release upon apoptosis. This scenario has been described by Boehning and coworkers who showed that the mutation of key glutamic acids residues within the cytochrome c binding domain of IP₃R prevents the binding of cytochrome c resulting in resistance to apoptosis while retaining the ability of other cellular pathways to mobilize Ca²⁺ through PLC- γ 1 and IP₃R.³⁰

4.4. Conclusion

Through exposure of wild type Jurkat and Jurkat J γ cells to selected compounds we explored the indispensability of PLC- γ 1 in the potentiation of HDACi-induced apoptosis. Previous work by Balasubramanian suggested that the apoptotic pathway induced in Jurkat cells by an HDAC8 specific inhibitor requires the potentiation of PLC- γ 1. Based on this current work, I found that selective HDAC1 and HDAC6 inhibitors also have a similar PLC- γ 1 requirement in order to induce apoptosis in Jurkat cells. Furthermore, the lack of activity displayed by the pan-inhibitor and clinically approved SAHA, and the decreased potency of IR-2-17 (Macrolide-based pan-inhibitor) and

FK228 (clinically approved) in Jurkat J γ cells suggest that all HDACi-induced apoptosis in Jurkat cells is potentiated by PLC- γ 1. Although mutations resulting in the loss of PLC- γ 1 function have not been described in cancer, mutations abrogating the interactions of IP₃R with cytochrome c can constitute a novel mechanism of resistance to HDACi-induced apoptosis. The ensuing mutations will only prevent the late phase Ca²⁺ release upon apoptosis induction while maintaining the cell ability to mobilize cellular Ca²⁺ for other metabolic demands.

4.5. General procedures and experimental

Jurkat J. γ 1 were obtained from ATCC (Manassas, VA, USA), Jurkat wild type cell line was kindly donated by Dr. John McDonald and grown on recommended medium supplemented with 10% fetal bovine serum (Global Cell Solutions, Charlottesville, VA, USA) and 1% pen/Strep (Cellgro, Manassas, VA) at 37°C in an incubator with 5% CO₂. Tubastatin A was purchased from Sigma-Aldrich (St. Louis, MO, USA). FK228 was purchased from Medchemexpress (Princeton, NJ, USA). SHI1:2 was synthesized as previously reported.²² The CellTiter 96 AQueous One Solution Cell Proliferation assay (MTS) kit was purchased from Promega (Madison, WI, USA).

Cell viability assay

Jurkat and Jurkat J. γ 1 cells were maintained in RPMI 1640 supplemented with 10 % FBS and 1% pen/strep. These cells were incubated in media containing the various compounds for 72 hours. Cell viability was measured using the MTS assay according to manufacturer protocol. The DMSO concentration in the cell media during the cell viability experiment was maintained at 0.1%.

4.6. References

1. Johnstone, R. W., Histone-deacetylase inhibitors: novel drugs for the treatment of cancer. *Nature Review Drug Discovery* **2002**, *1* (4), 287-299.
2. Gammoh, N.; Lam, D.; Puente, C.; Ganley, I.; Marks, P. A.; Jiang, X., Role of autophagy in histone deacetylase inhibitor-induced apoptotic and nonapoptotic cell death. *Proceedings of the National Academy of Sciences of the United States of America* **2012**, *109* (17), 6561-6565.
3. Fantin, V. R.; Richon, V. M., Mechanisms of Resistance to Histone Deacetylase Inhibitors and Their Therapeutic Implications. *Clinical Cancer Research* **2007**, *13* (24), 7237-7242.
4. Haggmann, W.; Faissner, R.; Schnolzer, M.; Lohr, M.; Jesnowski, R., Membrane drug transporters and chemoresistance in human pancreatic carcinoma. *Cancers* **2010**, *3* (1), 106-25.
5. Borst, P.; Evers, R.; Kool, M.; Wijnholds, J., A Family of Drug Transporters: the Multidrug Resistance-Associated Proteins. *Journal of the National Cancer Institute* **2000**, *92* (16), 1295-1302.
6. Jin, S.; Scotto, K. W., Transcriptional Regulation of the MDR1 Gene by Histone Acetyltransferase and Deacetylase Is Mediated by NF- κ B. *Molecular and Cellular Biology* **1998**, *18* (7), 4377-4384.
7. Morrow, C. S.; Nakagawa, M.; Goldsmith, M. E.; Madden, M. J.; Cowan, K. H., Reversible transcriptional activation of mdrl by sodium butyrate treatment of human colon cancer cells. *Journal of Biological Chemistry* **1994**, *269* (14), 10739-46.
8. Lee, J. S.; Paull, K.; Alvarez, M.; Hose, C.; Monks, A.; Grever, M.; Fojo, A. T.; Bates, S. E., Rhodamine efflux patterns predict P-glycoprotein substrates in the National Cancer Institute drug screen. *Molecular Pharmacology* **1994**, *46* (4), 627-638.
9. Peart, M. J.; Tainton, K. M.; Ruefli, A. A.; Dear, A. E.; Sedelies, K. A.; O'Reilly, L. A.; Waterhouse, N. J.; Trapani, J. A.; Johnstone, R. W., Novel Mechanisms of Apoptosis Induced by Histone Deacetylase Inhibitors. *Cancer Research* **2003**, *63* (15), 4460-4471.
10. Bandyopadhyay, D.; Mishra, A.; Medrano, E. E., Overexpression of Histone Deacetylase 1 Confers Resistance to Sodium Butyrate-Mediated Apoptosis in Melanoma Cells through a p53-Mediated Pathway. *Cancer Research* **2004**, *64* (21), 7706-7710.

11. Fiskus, W.; Rao, R.; Fernandez, P.; Herger, B.; Yang, Y.; Chen, J.; Kolhe, R.; Mandawat, A.; Wang, Y.; Joshi, R.; Eaton, K.; Lee, P.; Atadja, P.; Peiper, S.; Bhalla, K., Molecular and biologic characterization and drug sensitivity of pan-histone deacetylase inhibitor-resistant acute myeloid leukemia cells. *Blood* **2008**, *112* (7), 2896-2905.
12. Bolden, J. E.; Peart, M. J.; Johnstone, R. W., Anticancer activities of histone deacetylase inhibitors. *Nature Review Drug Discovery* **2006**, *5* (9), 769-784.
13. Bolden, J. E.; Shi, W.; Jankowski, K.; Kan, C. Y.; Cluse, L.; Martin, B. P.; MacKenzie, K. L.; Smyth, G. K.; Johnstone, R. W., HDAC inhibitors induce tumor-cell-selective pro-apoptotic transcriptional responses. *Cell Death & Disease* **2013**, *4*, e519.
14. Robey, R. W.; Chakraborty, A. R.; Basseville, A.; Luchenko, V.; Bahr, J.; Zhan, Z. R.; Bates, S. E., Histone Deacetylase Inhibitors: Emerging Mechanisms of Resistance. *Molecular Pharmaceutics* **2011**, *8* (6), 2021-2031.
15. Ruefli, A. A.; Ausserlechner, M. J.; Bernhard, D.; Sutton, V. R.; Tainton, K. M.; Kofler, R.; Smyth, M. J.; Johnstone, R. W., The histone deacetylase inhibitor and chemotherapeutic agent suberoylanilide hydroxamic acid (SAHA) induces a cell-death pathway characterized by cleavage of Bid and production of reactive oxygen species. *Proceedings of the National Academy of Sciences* **2001**, *98* (19), 10833-10838.
16. Butler, L. M.; Zhou, X.; Xu, W.-S.; Scher, H. I.; Rifkind, R. A.; Marks, P. A.; Richon, V. M., The histone deacetylase inhibitor SAHA arrests cancer cell growth, up-regulates thioredoxin-binding protein-2, and down-regulates thioredoxin. *Proceedings of the National Academy of Sciences* **2002**, *99* (18), 11700-11705.
17. Xu, W.; Ngo, L.; Perez, G.; Dokmanovic, M.; Marks, P. A., Intrinsic apoptotic and thioredoxin pathways in human prostate cancer cell response to histone deacetylase inhibitor. *Proceedings of the National Academy of Sciences* **2006**, *103* (42), 15540-15545.
18. Balasubramanian, S.; Ramos, J.; Luo, W.; Sirisawad, M.; Verner, E.; Buggy, J. J., A novel histone deacetylase 8 (HDAC8)-specific inhibitor PCI-34051 induces apoptosis in T-cell lymphomas. *Leukemia* **2008**, *22* (5), 1026-1034.
19. Wozniak, A. L.; Wang, X.; Stieren, E. S.; Scarbrough, S. G.; Elferink, C. J.; Boehning, D., Requirement of biphasic calcium release from the endoplasmic reticulum for Fas-mediated apoptosis. *The Journal of Cell Biology* **2006**, *175* (5), 709-714.

20. Boehning, D.; Patterson, R. L.; Sedaghat, L.; Glebova, N. O.; Kurosaki, T.; Snyder, S. H., Cytochrome c binds to inositol (1,4,5) trisphosphate receptors, amplifying calcium-dependent apoptosis. *Nature Cell Biology* **2003**, *5* (12), 1051-1061.
21. Butler, K. V.; Kalin, J.; Brochier, C.; Vistoli, G.; Langley, B.; Kozikowski, A. P., Rational Design and Simple Chemistry Yield a Superior, Neuroprotective HDAC6 Inhibitor, Tubastatin A. *Journal of the American Chemical Society* **2010**, *132* (31), 10842-10846.
22. Methot, J. L.; Chakravarty, P. K.; Chenard, M.; Close, J.; Cruz, J. C.; Dahlberg, W. K.; Fleming, J.; Hamblett, C. L.; Hamill, J. E.; Harrington, P.; Harsch, A.; Heidebrecht, R.; Hughes, B.; Jung, J.; Kenific, C. M.; Kral, A. M.; Meinke, P. T.; Middleton, R. E.; Ozerova, N.; Sloman, D. L.; Stanton, M. G.; Szewczak, A. A.; Tyagarajan, S.; Witter, D. J.; Paul Secrist, J.; Miller, T. A., Exploration of the internal cavity of histone deacetylase (HDAC) with selective HDAC1/HDAC2 inhibitors (SHI-1:2). *Bioorganic & Medicinal Chemistry Letters* **2008**, *18* (3), 973-978.
23. Furumai, R.; Matsuyama, A.; Kobashi, N.; Lee, K.-H.; Nishiyama, M.; Nakajima, H.; Tanaka, A.; Komatsu, Y.; Nishino, N.; Yoshida, M.; Horinouchi, S., FK228 (Depsipeptide) as a Natural Prodrug That Inhibits Class I Histone Deacetylases. *Cancer Research* **2002**, *62* (17), 4916-4921.
24. Sasakawa, Y.; Naoe, Y.; Inoue, T.; Sasakawa, T.; Matsuo, M.; Manda, T.; Mutoh, S., Effects of FK228, a novel histone deacetylase inhibitor, on human lymphoma U-937 cells in vitro and in vivo. *Biochemical Pharmacology* **2002**, *64* (7), 1079-1090.
25. Mizutani, H.; Hiraku, Y.; Tada-Oikawa, S.; Murata, M.; Ikemura, K.; Iwamoto, T.; Kagawa, Y.; Okuda, M.; Kawanishi, S., Romidepsin (FK228), a potent histone deacetylase inhibitor, induces apoptosis through the generation of hydrogen peroxide. *Cancer Science* **2010**, *101* (10), 2214-2219.
26. Coggeshall, K. M.; McHugh, J. C.; Altman, A., Predominant expression and activation-induced tyrosine phosphorylation of phospholipase C-gamma 2 in B lymphocytes. *Proceedings of the National Academy of Sciences* **1992**, *89* (12), 5660-5664.
27. Irvin, B. J.; Williams, B. L.; Nilson, A. E.; Maynor, H. O.; Abraham, R. T., Pleiotropic Contributions of Phospholipase C- γ 1 (PLC- γ 1) to T-Cell Antigen Receptor-Mediated Signaling: Reconstitution Studies of a PLC- γ 1-Deficient Jurkat T-Cell Line. *Molecular and Cellular Biology* **2000**, *20* (24), 9149-9161.

28. Chung, S.-H.; Kim, S.-K.; Kim, J. K.; Yang, Y.-R.; Suh, P.-G.; Chang, J.-S., A double point mutation in PCL- γ 1 (Y509A/F510A) enhances Y783 phosphorylation and inositol phospholipid-hydrolyzing activity upon EGF stimulation. *Experimental and Molecular Medicine* **2010**, *42*, 216-222.
29. Everett, K. L.; Bunney, T. D.; Yoon, Y.; Rodrigues-Lima, F.; Harris, R.; Driscoll, P. C.; Abe, K.; Fuchs, H.; Hrabé de Angelis, M.; Yu, P.; Cho, W.; Katan, M., Characterization of Phospholipase C γ Enzymes with Gain-of-Function Mutations. *Journal of Biological Chemistry* **2009**, *284* (34), 23083-23093.
30. Boehning, D.; van Rossum, D. B.; Patterson, R. L.; Snyder, S. H., A peptide inhibitor of cytochrome c/inositol 1,4,5-trisphosphate receptor binding blocks intrinsic and extrinsic cell death pathways. *Proceedings of the National Academy of Sciences of the United States of America* **2005**, *102* (5), 1466-1471.

CHAPTER 5

COMPARISON OF HDAC INHIBITION PROFILE USING THE STANDARD FLUOROMETRIC ASSAY FLUOR DE LYS AND SELF-ASSEMBLED MONOLAYERS FOR MATRIX-ASSISTED LASER DESORPTION MASS SPECTROMETRY (SAMDI-MS)

5.1. Introduction

Protein acetylation and deacetylation are key regulatory mechanisms involved in the modulation of nearly 2,000 targets.¹ This has bolstered the importance in cellular homeostasis of histone acetyl transferase (HAT) and histone deacetylase (HDAC) which mediate protein acetylation and deacetylation respectively. HDACs are not only involved in the regulation of healthy cells' activity but have been linked to the pathogenesis of various illnesses including inflammatory, parasitic, neurodegenerative diseases and cancer.^{2,3,4} Although meaningful progresses have been made in understanding the involvement of all the different 18 human HDAC isoforms (Zinc and NAD⁺ dependent) in cellular functions and diseases, significant obstacles are still to be overcome. Such roadblocks include the development of a suitable HDAC activity assay with very low false positive possessing enough selectivity allowing the activity of a specific isoform to be distinguished from that of the other 17 isoforms in a cellular extract or milieu.^{5,6} This endeavor will enable us to parse out the role of each isoform and gain a better understanding of their mechanism of action. Furthermore, having an assay that can be automated thus compatible with high-throughput-screening (HTS) will make it an invaluable tool in the drug discovery field as HDAC inhibitors (HDACi) are emerging as potential therapeutics for various diseases.

A brief discussion will be included on sirtuins (NAD⁺ dependent HDAC) assays and I will focus on zinc dependent HDACs assays.

5.2. History of HDAC assays

5.2.1. Sirtuins assays

Class III histone deacetylase or sirtuins catalyze the deacetylation of histones and non-histone proteins using nicotinamide adenine dinucleotide (NAD⁺) as cofactor (Figure 5.1).^{7,8} Assays to measure the activity of these enzymes are based on a direct or indirect detection of the metabolites generated from the reaction. During the HPLC-based assay, the deacetylated product is separated from the acetylated substrate and quantified using HPLC. The use of radioactive substrate is not required making this assay safer for lab personnel. A limitation of the HPLC-based assay is the requirement for larger volume injection for samples with low peptide concentration.⁹ During the deacetylase assay, the acetate group is transferred from the lysine residue onto the NAD⁺ (Figure 5.1). Such acetyl moiety is hydrolyzed and isolated during the charcoal-binding assay unlike the substrates and other metabolites which are sequestered by the activated charcoal (Figure 5.2A). A [³H]acetylated substrate is needed as the [³H]acetate is quantified via scintillation count.⁹ The other by-products of the deacetylation, nicotinamide and O-Acetyl-ADP-Ribose can also be monitored and quantified using the TLC-based assay. The quantification of nicotinamide or O-Acetyl-ADP-Ribose using a densitometer involved the use of [¹⁴C]NAD⁺ or [³²P]NAD⁺ respectively as cofactor for the sirtuins reaction (Figure 5.2B).^{9,10} All the assays aforementioned are direct reporter of sirtuins activity, whereas indirect measurement assays have been recently developed including

the fluorogenic assay which relies on the release of a fluorophore coupled to a substrate. This assay can be used for all classes of HDACs and as such will be discussed in more detail in upcoming sections. Another assay that indirectly determine the sirtuins activity relies on an enzyme-coupled system in which the nicotinamide generated from the deacetylation reaction is metabolized by nicotinamidase into ammonia and nicotinic acid. Glutamate dehydrogenase transfers the ammonia thus generated to α -ketoglutarate in the presence of NAD(P)H yielding glutamate and NAD(P)⁺ which is monitored at 340nm (Figure 5.2C).¹¹ Other novel assays or monitoring approaches have been reviewed elsewhere.^{12,13}

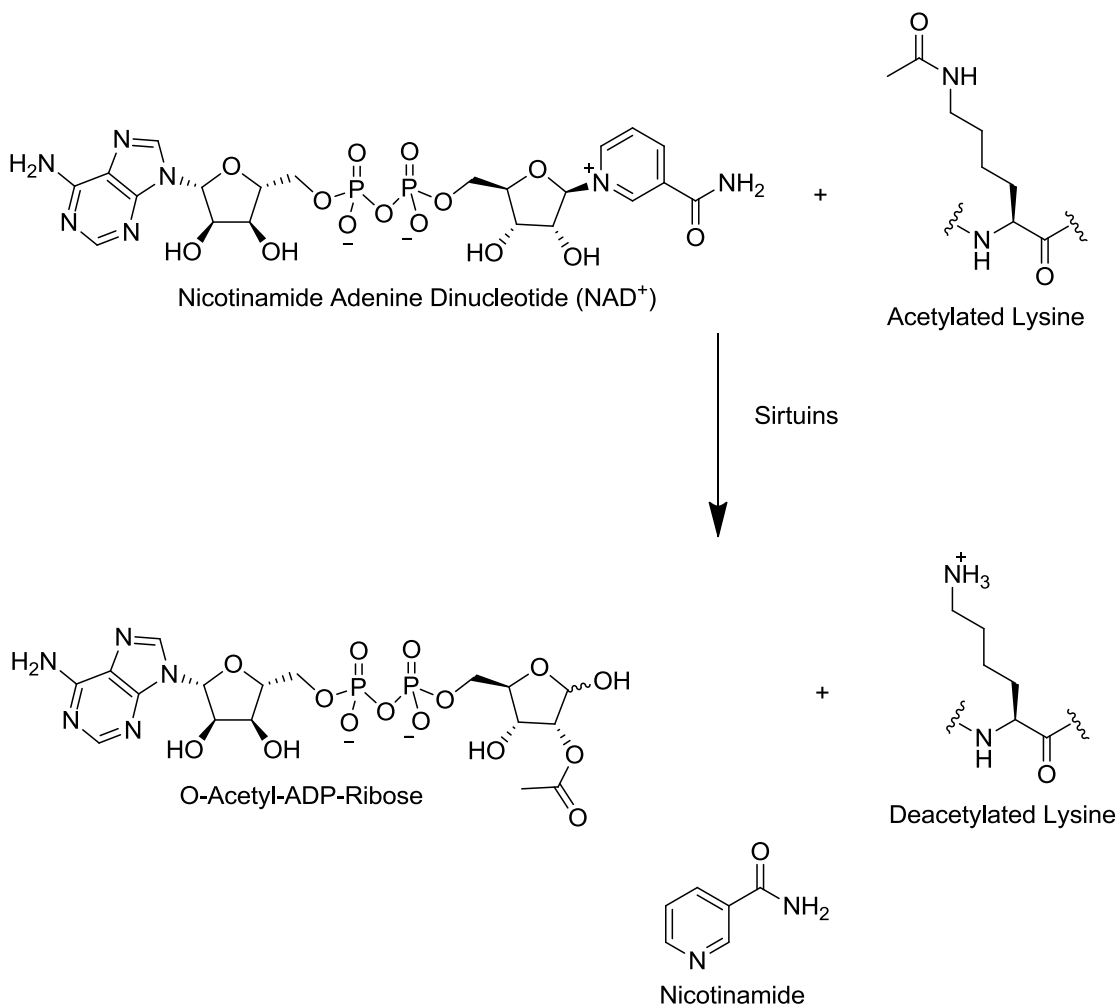


Figure 5.1: Schematic of Sirtuins mediated deacetylation.¹³

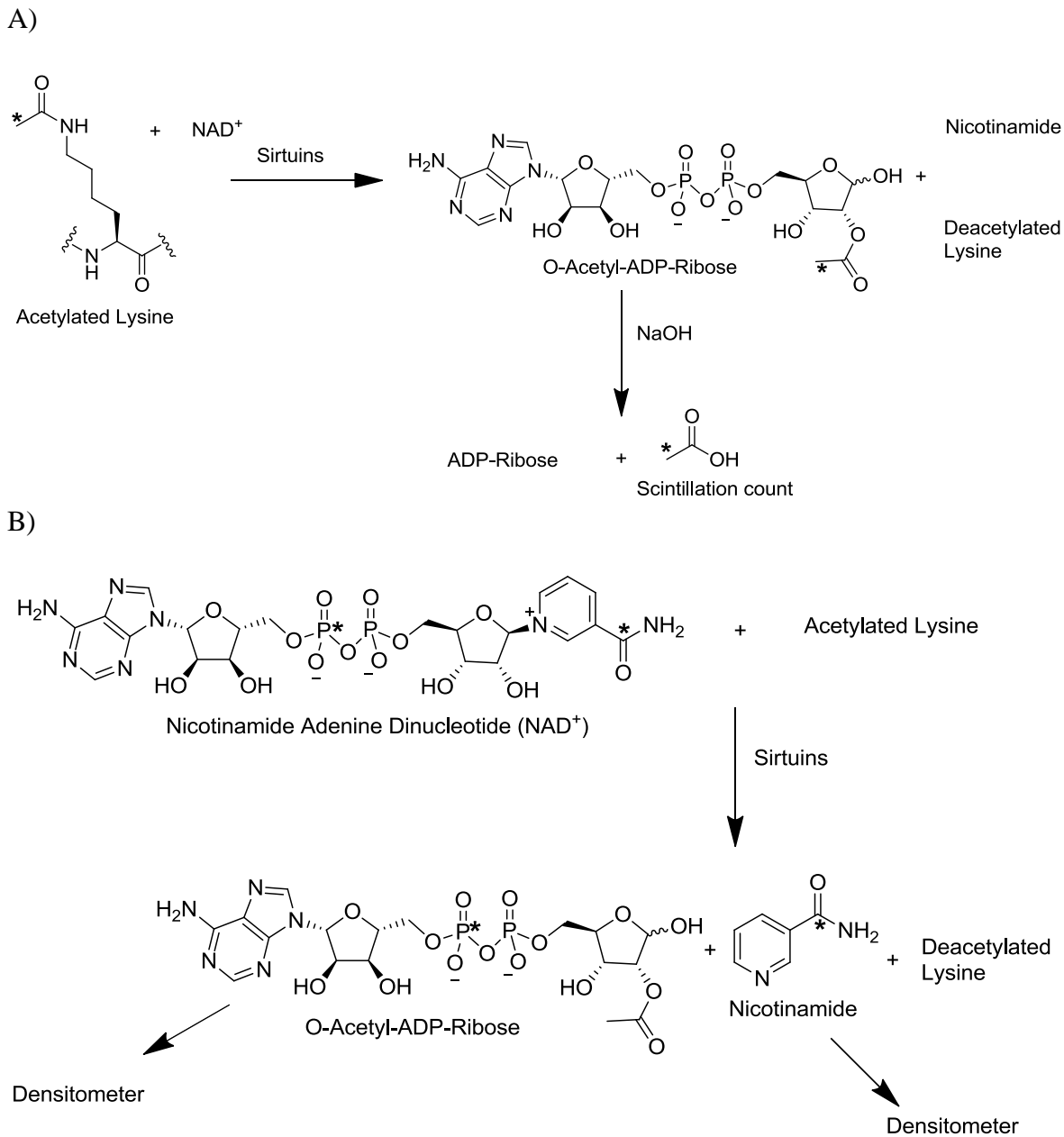


Figure 5.2: Schematic of selected sirtuins assays. * symbolizes radioactive labeling **A)** Charcoal-binding assay: radioactively labeled [³H]-acetate-lysine is used and [³H]-acetate quantified via scintillation count; **B)** TLC-based assay: For O-Acetyl-ADP-Ribose monitoring, [³²P]NAD⁺ is used, whereas for nicotinamide [¹⁴C]NAD⁺ is used; **C)** Enzyme-coupled detection of nicotinamide based on NH₃ release by nicotinamidase.^{9,11}

C)

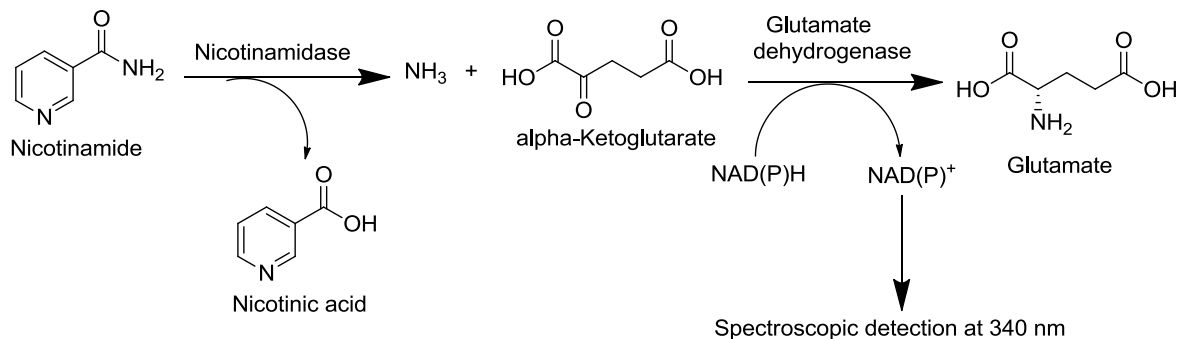


Figure 5.2: Schematic of selected sirtuins assays. * symbolizes radioactive labeling **A)** Charcoal-binding sirtuins assay: radioactively labeled [³H]-acetate-lysine is used and [³H]-acetate quantified via scintillation count; **B)** TLC-based assay: For O-Acetyl-ADP-Ribose monitoring, [³²P]NAD⁺ is used, whereas for nicotinamide [¹⁴C]NAD⁺ is used; **C)** Enzyme-coupled detection of nicotinamide based on NH₃ release by nicotinamidase.^{9,11}

5.2.2. Zinc dependent HDAC assays

The original assay widely used to measure HDAC activity relied on radioactively labeled acetylated histones as substrate. Following the incubation of the [³H]-acetyl-histone with HDAC and hydrolysis of the radioactively labeled acetate, the reaction mixture is extracted with organic solvent to collect the tritiated acetate group. Quantification of the released [³H]-acetate using scintillation count is correlated to the HDAC activity.¹⁴ Besides the radioactivity which can be problematic for laboratory personnel and the generation of highly toxic waste, obtaining the radioactively labeled histones is labor intensive as it involves repeated exposure of chickens to phenylhydrazine, followed by sacrificing them to collect their reticulocytes and labeling of their histone proteins with [³H]-acetic acid.¹⁵ Moreover, the organic extraction required for the [³H]-acetate quantification prevents the automation of this assay for HTS. The organic extraction was abrogated with the scintillation proximity assay, but the

protocol for histones labeling and isolation still stand as does the use of radioactive materials.¹⁶ Although immunoblotting of acetylated histone has been one of the first non-radioactive technique used to determine HDAC activity, all the labor involved does not make it an attractive technique, especially for drug discovery.¹⁷ These assays though labor intensive and not amenable to HTS, measure directly the HDAC activity using their natural acetylated histone substrates.

The first non-radioactive HDAC assay was developed by Hoffmann et al using a HPLC with a fluorescence detector to indirectly report HDAC activity (Figure 5.3). A 7-amino-4-methylcoumarin (AMC) tagged ϵ -acetylated lysine is used as a substrate which has a different retention time than the deacetylated AMC-Lys-NH₂ substrate on an HPLC trace (Figure 5.3A).¹⁸ Despite being easily synthesized, the AMC-Lys- ϵ -Acetyl substrate does not resemble the natural histone and possess a higher affinity to HDAC as demonstrated by K_M values of 0.68 μ M and 20 μ M respectively.¹⁸ Furthermore, the required HPLC renders its compatibility with HTS difficult.

5.3. Fluorogenic HDAC assay

This assay revolutionized the study of HDAC and their inhibition by allowing automation and adaptability with HTS. It built on advances made by Hoffmann and coworker by retaining the use of a fluorophore (AMC), but established the monitoring of the fluorophore as an indirect measurement of HDAC activity. A short peptide sequence, containing an ϵ -acetylated lysine residue and a C-terminus conjugated to a fluorophore such as AMC, is used as substrate. Upon incubation of this substrate (ϵ -Acetyl-Lys(AMC)-peptide) with the HDAC enzyme, the lysine residue is deacetylated and

subsequent addition of trypsin to the deacetylated substrate (NH₂-Lys(AMC)-peptide) releases AMC whose fluorescence can be measured (Figure 5.3B).¹⁹

A)

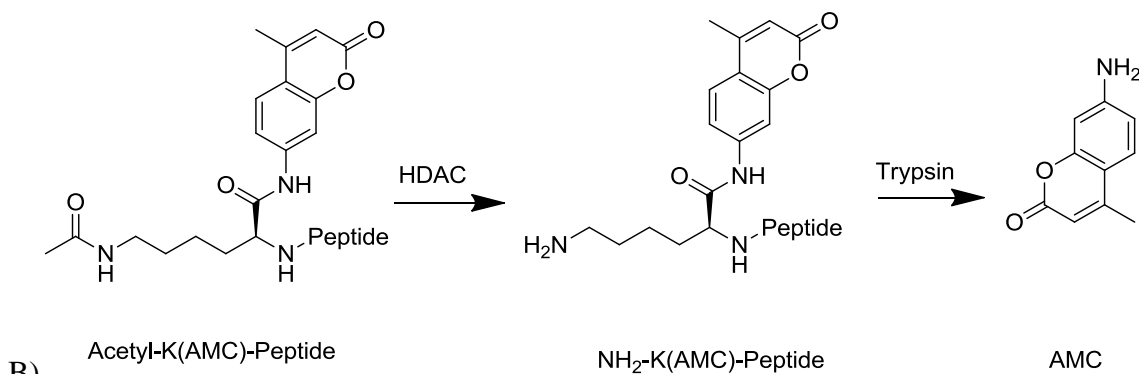
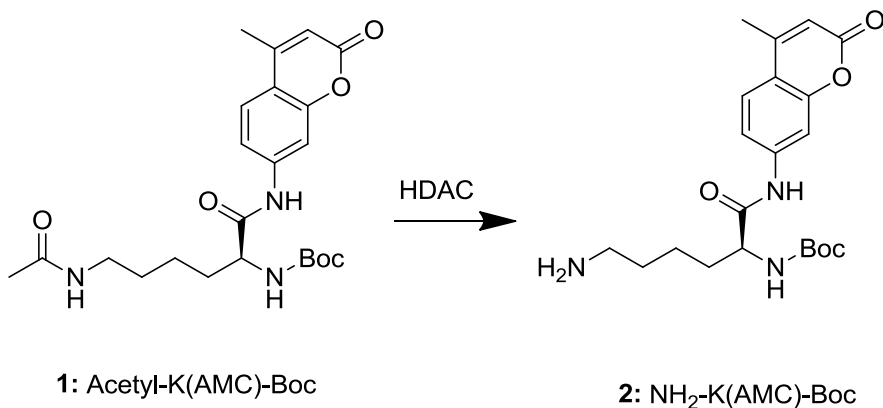


Figure 5.3: Schematic of the non-radioactive HDAC assay. **A)** HPLC monitoring of AMC as reporter of HDAC activity: **1** ($t_{\text{ret}} = 6.99$ min), **2** ($t_{\text{ret}} = 5.54$ min), flow rate = 1.2 mL/min, Multospher 100 RP-18, 250 X 4 mm, Phenomenex, acetonitrile/water (40:60), 0.01% trifluoroacetic acid.¹⁸ **B)** HDAC fluorogenic assay: fluorescence of AMC (fluorophore) as indirect reporter of HDAC activity **Step 1:** incubation of the substrate (ϵ -Acetyl-Lys(AMC)-peptide) containing a quenched fluorophore (AMC) with HDAC; **Step 2:** Incubation with trypsin releases the fluorophore from the peptide sequence. Free AMC has an excitation wavelength (λ_{ex}) of 390 nm and an emission (λ_{em}) of 460 nm.¹⁹

5.4. Pitfalls of the fluorogenic assay

The strategy of using a fluorescent reporter for various assay has been a popular one as it can be adapted easily to various systems, detected easily and used for HTS.²⁰ However, such labeling method can result in the perturbation of the enzymatic activity yielding false positive.⁶ The activation of sirtuins (SIRT) by resveratrol epitomized such effect. Using the Fluor de Lys-SIRT1 substrate linked to a fluorophore, resveratrol was found to activate SIRT1 resulting in various health benefits.²¹ Subsequent studies revealed that in the absence of the fluorophore, such activation was abrogated suggesting that the previously observed activation is an artifact due to the presence fluorophore.²² Furthermore, incorporation of the fluorophore decreased the affinity of the substrate for the SIRT1 and concomitant use of resveratrol yielded a tighter binding between the fluorophore-containing substrate and the enzyme.²³ The use of label-free substrate can resolve such issue and also eliminate the additional steps needed to label the substrate.²⁰

The fluorogenic assay requires the addition of trypsin to release the fluorophore. This added step increases the likelihood of error. Trypsin inhibitors can result in false positive during the said assay. Thus, a potent trypsin inhibitor with little to no HDAC inhibitory activity can prevent the release of the fluorophore. In this case, such compound will be reported as potent HDACi. A mandatory trypsin inhibition assay on potential HDACi has been suggested prior to running the HDAC fluorogenic assay to discriminate true HDAC inhibition from trypsin inhibitor-induced false positive.¹⁹ Reproducibility and accuracy can also be of a great concern as extra steps are added. Also, eliminating the extra steps needed for the indirect monitoring of HDAC activity minimize the rate of false positive and improve data accuracy. The second step in the conventional

fluorogenic can be abrogated by the use of the Caliper EZ reader II system which detects directly the fluorescence of the fluorophore tagged substrate and deacetylated product following electrophoretic separation.²⁴ Although additional step was no longer required for this assay, it still uses a fluorophore tagged substrate which can have a modified affinity for the enzyme and results in artificial sirtuins activation in the presence of resveratrol as previously described.²¹ This situation also stands to benefit from the use of label-free substrates as various alternative strategies are in place to monitor the changes resulting from the enzymatic activity.²⁵

5.5. HDAC assay using the self-assembled mono-layers for matrix assisted laser desorption ionization time-of-flight mass spectrometry (SAMDI-MS)

Fluorogenic HDAC assay which is to date the most used assay has two main challenges: finding an oligopeptide sequence resembling the natural substrate of each HDAC isoforms and directly measure the enzymatic activity. As a label-free method, SAMDI-MS can be used to measure the activity of various enzymes including HDAC, caspases and other enzymes.^{26,27} In the context of HDAC activity assay, the label-free peptide substrate with an acetylated lysine residue is immobilized onto a plate. Upon exposure to the HDAC, the loss of the acetyl group is detected by mass spectrometry as a change in the mass to charge ratio (m/z) of 42 (Figure 5.4), thus providing a direct measure of HDAC activity.²⁰ An alternative protocol involves conducting a solution-phase deacetylation reaction and immobilizing the product onto the plate followed by mass spectrometry.²⁸

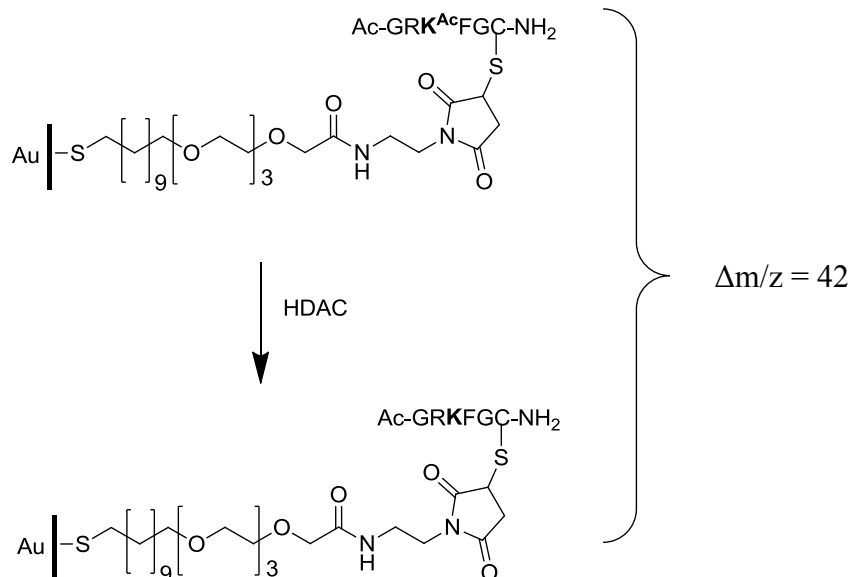


Figure 5.4: HDAC activity assay using SAMDI-MS. The acetylated substrate (Ac-GRK^{Ac}FGC-NH₂) is immobilized on a gold plate. Exposure of this substrate to HDAC results in the loss of the acetyl group indicated by a $\Delta m/z = 42$ (deacetylated substrate Ac-GRKFGC-NH₂).²⁰

The fluorogenic assay, due to its use of a relative few substrates not optimized for all HDAC isoforms, suffers from a lack of selectivity. In a milieu such as a cell lysate which contains multiple isozymes, one may not objectively measure the contribution of each isoform to the overall HDACs activity. The SAMDI-MS assay comes with specific substrates (amino acid sequences) for various HDACs, thus potentially addressing the problem of lack of specificity observed with the fluorogenic assay substrates (Table 5.1).²⁹

Table 5.1: Specific substrate of selected deacetylase enzymes.²⁹

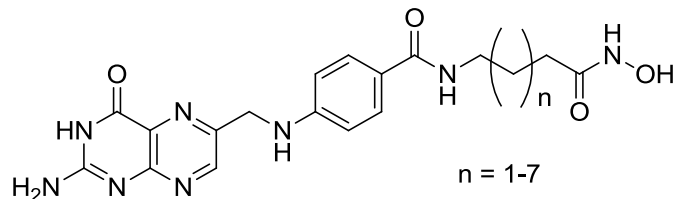
Enzyme	Substrate sequence
HDAC2	Ac-GRK ^{Ac} YWC-NH ₂
HDAC8	Ac-GRK ^{Ac} FPC-NH ₂
SIRT1	Ac-GRK ^{Ac} RVC-NH ₂

5.6. Comparison of the fluorogenic and SAMDI-MS for monitoring HDAC activity:

HDAC inhibition profile of pterotic hydroxamate based compounds

In our lab, we first experienced the dissimilarity between the fluorogenic and the SAMDI-MS assays by measuring the HDAC8 inhibition profile of selected ketolide-based HDACi.³⁰ Furthermore, using the fluorogenic assay, we were unable to elucidate the HDAC inhibition profile of 3-hydroxypyridin-2-thione based compounds due to the inconsistency of measured IC₅₀s (data not shown). Such inconsistencies were resolved using the SAMDI-MS assay.^{31,28} Based on these previous observations, we decided to conduct a detailed study by comparing the HDAC1, 6 and 8 inhibition profile of novel HDACi using the SAMDI-MS and commercial fluorogenic assays. Specifically, we synthesized pterotic acid based HDACi and measured their HDAC inhibitory profile using both Fluor de lys and the SAMDI-MS assays (Table 5.2). Overall, the IC₅₀ values obtained from both assays are not identical, however, similar trends are observable for HDAC1 and 6 inhibition.

Table 5.2: HDAC inhibition profile of pterioic acid based HDAC inhibitor: Fluorogenic assay vs SAMDI-MS.



n	HDAC1 IC ₅₀ (nM)		HDAC6 IC ₅₀ (nM)		HDAC8 IC ₅₀ (nM)	
	Fluor de lyst†	SAMDI‡	Fluor de lyst†	SAMDI‡	Fluor de lyst†	SAMDI‡
(1)	8000 ± 2000	22.1 ± 1.7%	4000	1460 ± 310	NI	25 ± 18%
(2)	190 ± 30	6150 ± 1320	52 ± 6	212 ± 15	7000 ± 2000	39 ± 6%
(3)	70 ± 8	79.6 ± 12.6	50 ± 5	43.6 ± 8.4	5400 ± 800	41 ± 17%
(4)	53 ± 7	23.4 ± 4.2	22 ± 3	12.2 ± 0.2	NI	1060 ± 320
(5)	11 ± 1	16.1 ± 2.8	76 ± 9	55.4 ± 2.2	NI	9380 ± 1720
(6)	104 ± 9	524 ± 36	4.9 ± 0.4	10.2 ± 1.0	NI	7590 ± 2120
(7)	270 ± 20	53 ± 7%	70 ± 10	476 ± 48	NI	40 ± 10%
SAHA	42 ± 3	38 ± 2	34 ± 2	144 ± 23	2800 ± 200	232 ± 19

% inhibition at 10 μ M; NI: No Inhibition at 10 μ M; †HDAC assay performed through a contractual agreement with BPS biosciences; ‡HDAC assay performed by James Kornacki from Northwestern University as previously reported.²⁸

All the compounds seem to be more active when their HDAC1 inhibition inhibitory profile is measured using the fluorogenic assay except for the 6-methylene compound (n=4). Furthermore, there is a great variation between the IC₅₀ values provided for the 4 and 9-methylene compounds by the SAMDI-MS and the fluorogenic assays, with the latter showing almost a 33-fold increase in the potency of these compounds against HDAC1 relative to the SAMDI-MS. Despite the discrepancy between the absolute IC₅₀ values afforded by both methodologies, the observed trend for the HDAC1 inhibition is similar. An increase in the linker length improves the anti-HDAC1 activity starting from 3-methylene linker with the optimum length being the 7-methylene spacer group.

Against HDAC6, both assays suggest that the 3-methylene linker compound is the least potent in the series, however, the fluorogenic assay reported an IC₅₀ 4-fold lower than that given by the SAMDI-MS. With increasing linker chain length, there is no observable trend in the IC₅₀s provided by both assays. The only silver lining is that both assays designated the 8-methylene compound as the most potent HDAC6 inhibitor followed by the 6-methylene and 5-methylene linker. Furthermore, the IC₅₀s of the three most active HDAC6 inhibitors obtained from both assays are nearly similar.

The dissimilarity between the two assays is made more glaring by the measurement of the HDAC8 inhibition activities of the pteric acid based HDACi. The fluorogenic assay revealed that only 2 compounds have measureable, though weak IC₅₀s. The inability to estimate the HDAC8 inhibitory activity of most of these compounds may be due to fluorophore label-induced change in the affinity of the substrate for the HDAC8 enzyme, analogous to the previous observation on HDAC8 and SIRT1.^{26,32} If the

fluorophore label increases the affinity of substrate for HDAC8, the pteric based inhibitors (weak HDAC8 inhibitors) may not be able to effectively compete against the said substrate.²³ Since the substrates for SAMDI-MS assay are not labeled, such artificial alteration in the substrates' HDAC binding affinities is quite unlikely. This may partly explain the determination of the HDAC8 inhibitory activities of these pteric acid based HDACi (Table 5.2). Based on the foregoing, fluorogenic assays, such as the one used here, may not be effective in gauging the HDAC8 inhibitory profile of these and possibly many HDACi. Moreover, Riester and coworkers demonstrated that HDAC8 is the most selective of all HDACs for its substrate,³³ hence, the substrate optimization performed prior to the SAMDI-MS may have been beneficial relative to the fluorogenic assay where such optimization was not done.

Using different substrates, tubastatin A was found by Butler et al to have an IC_{50} > 30 μ M against HDAC 2, whereas Wagner and coworkers reported an IC_{50} of 0.360 μ M against the same isoform. Such discrepancy can also be addressed by the standardization of isoform optimized substrates for all HDAC assays described in the literature. This will not only result in an increased reproducibility and accuracy of HDAC assays but also allow an objective comparison between HDACi developed by different laboratories.^{34,35}

The SAMDI-MS assay has addressed some of the problems seen with commonly used HDAC assays including fluorophore tag-induced perturbation of substrate binding affinities, false positive as seen with resveratrol and the indirect measurement of HDAC activity which can result in data inconsistency. However, a concern that it has not completely been addressed is the development of isoform specific substrates, though significant efforts have been made in that direction. Isoform specific substrates may not

be needed for closely related HDAC isoforms such as HDACs 1, 2 and 3. In fact attainment of substrate specificity among such closely related isoforms may not be feasible as they all have the same natural substrates, histones. On the other hand, substrate specificity may be achievable between the class I isoform (HDAC1, 2, 3) and the class IIb HDAC6 as these two classes have very distinct substrates: histones and cytoplasmic proteins respectively.³⁶ Obtaining a sub-class selective substrate can constitute the initial step towards the discovery of a class I selective HDACi devoid of any activity against class IIa HDAC isoforms. Such small molecule may prove to be advantageous for HDACi therapy as class I isoforms are overexpressed in many malignancies as opposed to class IIa which are cardioprotective.^{37,38}

5.7. Conclusion

The fluorogenic HDAC assay has been one of the most used to evaluate HDAC activity due to their ease and compatibility with automation screening platforms such as HTS. However, fluorophore labeled substrates have been shown to interfere with the HDAC enzymatic activities. Also, the limited substrate peptide sequences may not allow the distinction between the activities of various HDAC isozymes in a cellular lysate. Furthermore, the indirect measurement of HDAC activity heightens concern about data accuracy and the likelihood of false positive. On the other hand, the SAMDI-MS, a label-free technique, does not require any modifications to the substrate and enables a direct monitoring of HDAC activity. Furthermore, the substrate sequences have been optimized relative to the fluorogenic assay. These attributes confer a higher level of specificity and consistency to the SAMDI-MS data. In the examples cited, the major

discrepancy between SAMDI-MS and fluorogenic assays was seen with HDAC8, possibly due to the influence of the fluorophore label on substrate affinity. It is therefore possible that for compounds with lower anti-HDAC activity, the increased affinity of the substrate ensuing from the presence of the fluorophore can hinder the measurement of the HDAC activity using the fluorogenic assay.

5.8. References

1. Choudhary, C.; Kumar, C.; Gnad, F.; Nielsen, M. L.; Rehman, M.; Walther, T. C.; Olsen, J. V.; Mann, M., Lysine Acetylation Targets Protein Complexes and Co-Regulates Major Cellular Functions. *Science* **2009**, 325 (5942), 834-840.
2. Yang, X. J.; Seto, E., HATs and HDACs: from structure, function and regulation to novel strategies for therapy and prevention. *Oncogene* **2007**, 26 (37), 5310-5318.
3. Gryder, B. E.; Sodji, Q. H.; Oyelere, A. K., Targeted cancer therapy: giving histone deacetylase inhibitors all they need to succeed. *Future Medicinal Chemistry* **2012**, 4 (4), 505-524.
4. Haigis, M. C.; Sinclair, D. A., Mammalian Sirtuins: Biological Insights and Disease Relevance. *Annual Review of Pathology: Mechanisms of Disease* **2010**, 5 (1), 253-295.
5. Bradner, J. E.; West, N.; Grachan, M. L.; Greenberg, E. F.; Haggarty, S. J.; Warnow, T.; Mazitschek, R., Chemical phylogenetics of histone deacetylases. *Nature Chemical Biology* **2010**, 6 (3), 238-243.
6. Kaeberlein, M.; McDonagh, T.; Heltweg, B.; Hixon, J.; Westman, E. A.; Caldwell, S. D.; Napper, A.; Curtis, R.; DiStefano, P. S.; Fields, S.; Bedalov, A.; Kennedy, B. K., Substrate-specific Activation of Sirtuins by Resveratrol. *Journal of Biological Chemistry* **2005**, 280 (17), 17038-17045.
7. Sanders, B. D.; Jackson, B.; Marmorstein, R., Structural basis for sirtuin function: What we know and what we don't. *Biochimica et Biophysica Acta (BBA) - Proteins and Proteomics* **2010**, 1804 (8), 1604-1616.
8. Sauve, A. A., Sirtuin chemical mechanisms. *Biochimica et Biophysica Acta (BBA) - Proteins and Proteomics* **2010**, 1804 (8), 1591-1603.
9. Borra, M. T.; Denu, J. M., Quantitative Assays for Characterization of the Sir2 Family of NAD⁺-Dependent Deacetylases. In *Methods in Enzymology*, Allis, C. D.; Carl, W., Eds. Academic Press: 2003; Vol. Volume 376, pp 171-187.
10. Landry, J.; Sutton, A.; Tafrov, S. T.; Heller, R. C.; Stebbins, J.; Pillus, L.; Sternglanz, R., The silencing protein SIR2 and its homologs are NAD-dependent protein deacetylases. *Proceedings of the National Academy of Sciences* **2000**, 97 (11), 5807-5811.
11. Smith, B. C.; Hallows, W. C.; Denu, J. M., A continuous microplate assay for sirtuins and nicotinamide-producing enzymes. *Analytical Biochemistry* **2009**, 394 (1), 101-109.

12. Landry, J.; Sternglanz, R., Enzymatic assays for NAD-dependent deacetylase activities. *Methods* **2003**, *31* (1), 33-39.
13. Schutkowski, M.; Fischer, F.; Roessler, C.; Steegborn, C., New assays and approaches for discovery and design of Sirtuin modulators. *Expert Opinion on Drug Discovery* **2014**, *9* (2), 183-199.
14. Hay, C. W.; Candido, E. P., Histone deacetylase. Association with a nuclease resistant, high molecular weight fraction of HeLa cell chromatin. *Journal of Biological Chemistry* **1983**, *258* (6), 3726-3734.
15. Kölle, D.; Brosch, G.; Lechner, T.; Lusser, A.; Loidl, P., Biochemical Methods for Analysis of Histone Deacetylases. *Methods* **1998**, *15* (4), 323-331.
16. Nare, B.; Allocco, J. J.; Kuningas, R.; Galuska, S.; Myers, R. W.; Bednarek, M. A.; Schmatz, D. M., Development of a Scintillation Proximity Assay for Histone Deacetylase Using a Biotinylated Peptide Derived from Histone-H4. *Analytical Biochemistry* **1999**, *267* (2), 390-396.
17. Zhang, Y.; LeRoy, G.; Seelig, H.-P.; Lane, W. S.; Reinberg, D., The Dermatomyositis-Specific Autoantigen Mi2 Is a Component of a Complex Containing Histone Deacetylase and Nucleosome Remodeling Activities. *Cell* **1998**, *95* (2), 279-289.
18. Hoffmann, K.; Jung, M.; Brosch, G.; Loidl, P., A non-isotopic assay for histone deacetylase activity. *Nucleic Acids Research* **1999**, *27* (9), 2057-2058.
19. Wegener, D.; Wirsching, F.; Riester, D.; Schwienhorst, A., A Fluorogenic Histone Deacetylase Assay Well Suited for High-Throughput Activity Screening. *Chemistry & Biology* **2003**, *10* (1), 61-68.
20. Gurard-Levin, Z. A.; Scholle, M. D.; Eisenberg, A. H.; Mrksich, M., High-Throughput Screening of Small Molecule Libraries using SAMDI Mass Spectrometry. *ACS Combinatorial Science* **2011**, *13* (4), 347-350.
21. Howitz, K. T.; Bitterman, K. J.; Cohen, H. Y.; Lamming, D. W.; Lavu, S.; Wood, J. G.; Zipkin, R. E.; Chung, P.; Kisielewski, A.; Zhang, L.-L.; Scherer, B.; Sinclair, D. A., Small molecule activators of sirtuins extend *Saccharomyces cerevisiae* lifespan. *Nature* **2003**, *425* (6954), 191-196.
22. Pacholec, M.; Bleasdale, J. E.; Chrunyk, B.; Cunningham, D.; Flynn, D.; Garofalo, R. S.; Griffith, D.; Griffor, M.; Loulakis, P.; Pabst, B.; Qiu, X.; Stockman, B.; Thanabal, V.; Varghese, A.; Ward, J.; Withka, J.; Ahn, K., SRT1720, SRT2183, SRT1460, and Resveratrol Are Not Direct Activators of SIRT1. *Journal of Biological Chemistry* **2010**, *285* (11), 8340-8351.

23. Borra, M. T.; Smith, B. C.; Denu, J. M., Mechanism of Human SIRT1 Activation by Resveratrol. *Journal of Biological Chemistry* **2005**, *280* (17), 17187-17195.
24. Schroeder, F. A.; Lewis, M. C.; Fass, D. M.; Wagner, F. F.; Zhang, Y.-L.; Hennig, K. M.; Gale, J.; Zhao, W.-N.; Reis, S.; Barker, D. D.; Berry-Scott, E.; Kim, S. W.; Clore, E. L.; Hooker, J. M.; Holson, E. B.; Haggarty, S. J.; Petryshen, T. L., A Selective HDAC1/2 Inhibitor Modulates Chromatin and Gene Expression in Brain and Alters Mouse Behavior in Two Mood-Related Tests. *Plos One* **2013**, *8* (8).
25. Shiau, A. K.; Massari, M. E.; Ozbal, C. C., Back to basics: label-free technologies for small molecule screening. *Combinatorial Chemistry & High Throughput Screening* **2008**, *11* (3), 231-237.
26. Gurard-Levin, Z. A.; Kim, J.; Mrksich, M., Combining Mass Spectrometry and Peptide Arrays to Profile the Specificities of Histone Deacetylases. *ChemBioChem* **2009**, *10* (13), 2159-2161.
27. Su, J.; Rajapaksha, T. W.; Peter, M. E.; Mrksich, M., Assays of Endogenous Caspase Activities: A Comparison of Mass Spectrometry and Fluorescence Formats. *Analytical Chemistry* **2006**, *78* (14), 4945-4951.
28. Sodji, Q. H.; Patil, V.; Kornacki, J. R.; Mrksich, M.; Oyelere, A. K., Synthesis and Structure–Activity Relationship of 3-Hydroxypyridine-2-thione-Based Histone Deacetylase Inhibitors. *Journal of Medicinal Chemistry* **2013**, *56* (24), 9969-9981.
29. Gurard-Levin, Z. A.; Kilian, K. A.; Kim, J.; Bähr, K.; Mrksich, M., Peptide Arrays Identify Isoform-Selective Substrates for Profiling Endogenous Lysine Deacetylase Activity. *ACS Chemical Biology* **2010**, *5* (9), 863-873.
30. Mwakwari, S. C.; Guerrant, W.; Patil, V.; Khan, S. I.; Tekwani, B. L.; Gurard-Levin, Z. A.; Mrksich, M.; Oyelere, A. K., Non-Peptide Macrocyclic Histone Deacetylase Inhibitors Derived from Tricyclic Ketolide Skeleton. *Journal of Medicinal Chemistry* **2010**, *53* (16), 6100-6111.
31. Patil, V.; Sodji, Q. H.; Kornacki, J. R.; Mrksich, M.; Oyelere, A. K., 3-Hydroxypyridin-2-thione as Novel Zinc Binding Group for Selective Histone Deacetylase Inhibition. *Journal of Medicinal Chemistry* **2013**.
32. Beher, D.; Wu, J.; Cumine, S.; Kim, K. W.; Lu, S.-C.; Atangan, L.; Wang, M., Resveratrol is Not a Direct Activator of SIRT1 Enzyme Activity. *Chemical Biology & Drug Design* **2009**, *74* (6), 619-624.

33. Riestler, D.; Hildmann, C.; Grünewald, S.; Beckers, T.; Schwienhorst, A., Factors affecting the substrate specificity of histone deacetylases. *Biochemical and Biophysical Research Communications* **2007**, *357* (2), 439-445.
34. Butler, K. V.; Kalin, J.; Brochier, C.; Vistoli, G.; Langley, B.; Kozikowski, A. P., Rational Design and Simple Chemistry Yield a Superior, Neuroprotective HDAC6 Inhibitor, Tubastatin A. *Journal of the American Chemical Society* **2010**, *132* (31), 10842-10846.
35. Wagner, F. F.; Olson, D. E.; Gale, J. P.; Kaya, T.; Weïwer, M.; Aidoud, N.; Thomas, M.; Davoine, E. L.; Lemercier, B. C.; Zhang, Y.-L.; Holson, E. B., Potent and Selective Inhibition of Histone Deacetylase 6 (HDAC6) Does Not Require a Surface-Binding Motif. *Journal of Medicinal Chemistry* **2013**, *56* (4), 1772-1776.
36. Dokmanovic, M.; Clarke, C.; Marks, P. A., Histone Deacetylase Inhibitors: Overview and Perspectives. *Molecular Cancer Research* **2007**, *5* (10), 981-989.
37. Weichert, W., HDAC expression and clinical prognosis in human malignancies. *Cancer Letters* **2009**, *280* (2), 168-176.
38. Backs, J.; Olson, E. N., Control of Cardiac Growth by Histone Acetylation/Deacetylation. *Circulation Research* **2006**, *98* (1), 15-24.

CHAPTER 6

CONCLUSION AND FUTURE PERSPECTIVES

HDACs have emerged as valid targets for cancer therapy. This resulted in the development of HDACi and the FDA approvals of SAHA and FK228 (Romidepsin) for CTCL. However, these drugs, as pan-inhibitors of HDACs, target isoforms not involved in tumorigenesis as well. They are also associated with various side effects including cardiotoxicity and have not been efficacious against solid tumors. Two strategies have been suggested to boost the therapeutic effects of HDACi: the design of isoform selective inhibitors, and the targeted delivery of HDACs pan-inhibitors to malignant cells.

To this end, I explored the potential of isoform-selective HDACi as anticancer agents by synthesizing and testing 3-hydroxypyridin-2-thione (3HPT) based HDACi which were selective for HDAC6 and/or HDAC8. Selected 3HPT based compounds displayed anticancer activity against various cancer cell lines including DU145, LNCaP, Jurkat and the Jurkat subline J- γ which is resistant to SAHA-induced apoptosis. Although the 3HPT based inhibitors are active against certain cancer cells lines and lack cytotoxicity against healthy cells, they may not fared well in clinical trials just as other isoform-selective HDACi such as MS275. This suggests that isoform-selective HDACi may not be clinically indicated as monotherapy for cancer patients. However, these selective HDACi can still be considered as standalone therapy for other illnesses involving HDACs.

In light of the lack of clinical efficacy observed with isoform selective HDACi, I selectively delivered HDAC pan-inhibitors to FR(+) cancer cells using folic or pterioic acids as homing devices. Among the folic- and pterioic-based HDACi, only the pterioic-based had anticancer activities due to their inhibition of HDAC1. I devised a novel

approach which combined both isoform selectivity and targeting, resulting in the targeted delivery of isoform selective HDACi. This led to the design, synthesis and testing of folate-based biaryl benzamide HDACi selective for HDAC1. These biaryl benzamide compounds did not however displayed any anticancer activity against KB or HeLa cells. FR as a delivery system has a low efficiency (15-25%), suggesting that for a drug to display cellular activity through this pathway, it must be highly potent against its primary target.¹ The observed lack of cytotoxicity of the benzamide-based HDACi may reside in their diminished efficacy against HDAC1. It can be implied from the folate/pteroic targeting of HDACi that only compounds with IC₅₀ below 20 nM against a HDAC isoform may be the only HDACi to show cellular activity through this delivery system. Other targeting ligands which may possess higher delivery efficiencies may constitute viable alternative to FR targeting of HDACi. Such endeavor has been attempted by the Oyelere et al. using macrolide antibiotic to selectively delivered HDACi to lung tissues.²

I also attempted to understand the mechanism of resistance of HDACi-induced apoptosis in Jurkat J- γ . This work showed that phospholipase C is crucial for HDACi-induced apoptosis. Identifying the key players in the apoptotic pathway cannot only provide an understanding of the mechanisms of apoptosis but also identify the possible sites where mutations can result in resistance to apoptosis in general but to HDACi in particular. This endeavor can lead to an appropriate choice of chemotherapy agents to be use in combination with HDACi which can target those resistance pathways.

Therapeutic future of HDACi

The clinical trials conducted thus far on isoform-selective HDACi suggest their safety in patients.^{3,4} However, these molecules are also not efficacious as monotherapeutic agents against many malignancies.⁵ For isoform-selective HDACi to be further considered as anticancer drugs, they must be used in combination with other chemotherapy drugs. The additive effect ensuing from such combination can lead to a reduction in the posology of the chemotherapeutic agents including that of HDACi. Careful considerations should be made prior to the selection of the combination therapy. Exposure of cancer cells to certain HDACi result in the up-regulation of the P-Glycoproteins (P-gp) which can efflux drugs from cancer cells.⁶ To avoid a premature resistance to the chemotherapy regiment, one should select a HDACi that does not up-regulate the P-gp. Alternatively, the adjunct chemotherapy agent should not be a substrate of these P-gp pumps if the selected HDACi up-regulate these efflux pumps. Furthermore, the dosing schedule of each component of the combination therapy has to be studied, to optimize the impact of the said combination. For example, the combination of HDACi and topoisomerase inhibitors has been shown to be efficacious only when the HDACi is administered prior to the topoisomerase inhibitors.⁷

The only currently approved HDACi for cancer therapy are pan-inhibitors.⁵ Thus pan-inhibitors may be the only way forward for HDACi as monotherapy against cancer. Although the pan-inhibition of HDACs may prove to be more effective against cancer cells, it also can result in increased adverse reactions. A potential solution to this dilemma is the targeted delivery of these pan-inhibitors to malignant cells. Such targeted delivery

can also result in an increased accumulation of the HDACi in the tumor, potentially boosting their potency against solid tumors.

HDACi have also displayed therapeutic application in other illnesses including neurodegenerative, parasitic, and inflammatory diseases. In such instances, isoform-selective HDACi can be efficacious as monotherapy. For example, leishmania has been shown to be sensitive to selective HDAC6 inhibition (unpublished data).

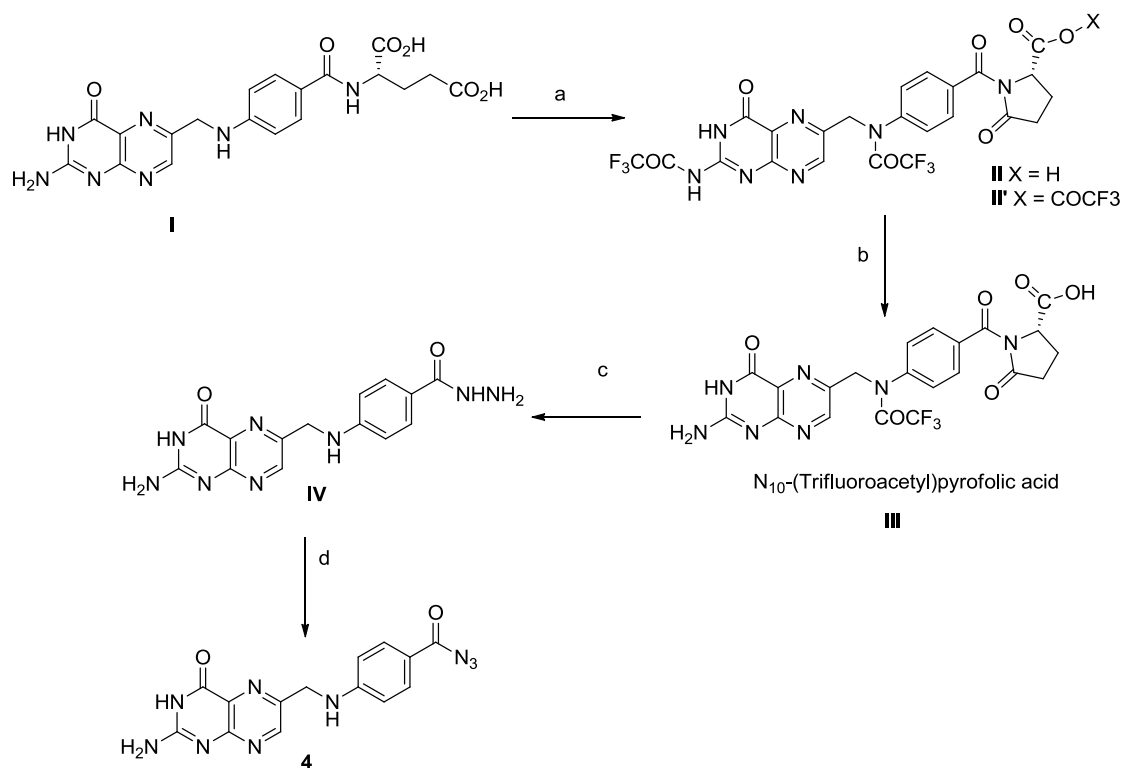
HDACi have the potential to be elixirs for many diseases including cancer. To reach such status, these molecules should be used as part of personalized medicine. This implies that the selection of a specific HDACi for the treatment of a patient's disease should be based on biomarkers from the patient, and the condition to be treated: targeted pan-inhibitors for cancer and isoform-selective inhibitors for other diseases.

References

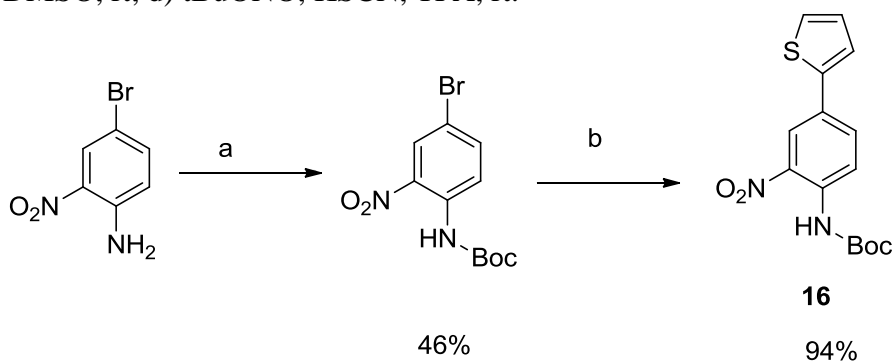
1. Lu, Y.; Low, P. S., Folate-mediated delivery of macromolecular anticancer therapeutic agents. *Advanced Drug Delivery Reviews* **2012**, *64*, Supplement (0), 342-352.
2. Mwakwari, S. C.; Guerrant, W.; Patil, V.; Khan, S. I.; Tekwani, B. L.; Gurard-Levin, Z. A.; Mrksich, M.; Oyelere, A. K., Non-Peptide Macrocyclic Histone Deacetylase Inhibitors Derived from Tricyclic Ketolide Skeleton. *Journal of Medicinal Chemistry* **2010**, *53* (16), 6100-6111.
3. Gojo, I.; Jiemjit, A.; Trepel, J. B.; Sparreboom, A.; Figg, W. D.; Rollins, S.; Tidwell, M. L.; Greer, J.; Chung, E. J.; Lee, M.-J.; Gore, S. D.; Sausville, E. A.; Zwiebel, J.; Karp, J. E., Phase 1 and pharmacologic study of MS-275, a histone deacetylase inhibitor, in adults with refractory and relapsed acute leukemias. *Blood* **2007**, *109* (7), 2781-2790.
4. Raje, N.; Hari, P. N.; Vogl, D. T.; Jagannath, S.; Orłowski, R. Z.; Supko, J. G.; Stephenson, P.; Jones, S. S.; Wheeler, C.; Lonial, S., Rocilinostat (ACY-1215), a Selective HDAC6 Inhibitor, Alone and in Combination with Bortezomib in Multiple Myeloma: Preliminary Results From the First-in-Humans Phase I/II Study. *Blood* **2012**, *120* (21).
5. Gryder, B. E.; Sodji, Q. H.; Oyelere, A. K., Targeted cancer therapy: giving histone deacetylase inhibitors all they need to succeed. *Future Medicinal Chemistry* **2012**, *4* (4), 505-524.
6. Xu, Y.; Jiang, Z.; Yin, P.; Li, Q.; Liu, J., Role for Class I histone deacetylases in multidrug resistance. *Experimental Cell Research* **2012**, *318* (3), 177-186.
7. Gray, J.; Cubitt, C. L.; Zhang, S.; Chiappori, A., Combination of HDAC and topoisomerase inhibitors in small cell lung cancer. *Cancer Biology & Therapy* **2012**, *13* (8), 614-622.

Appendix

Synthesis scheme of pteroyl azide and ^1H and ^{13}C NMR characterization of folate and pteronic acid based HDACi (Chapter 3)

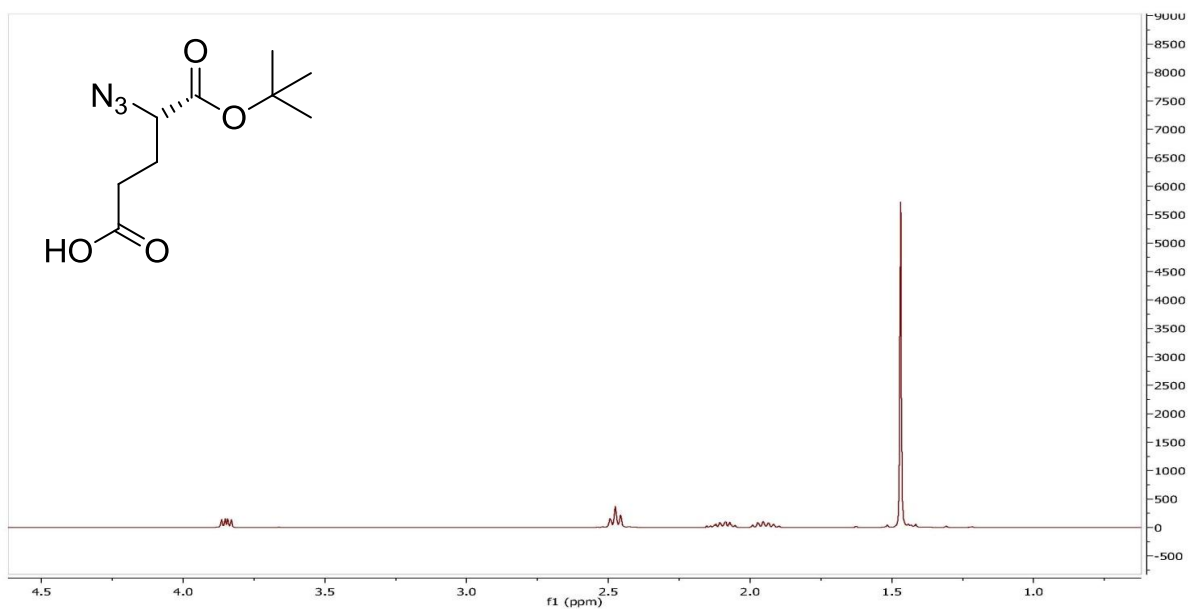


Scheme S1: Synthesis of pteroyl azide **4**. a) TFAA, THF rt; b) THF, ice; c) Hydrazine, DMSO, rt; d) tBuONO, KSCN, TFA, rt.

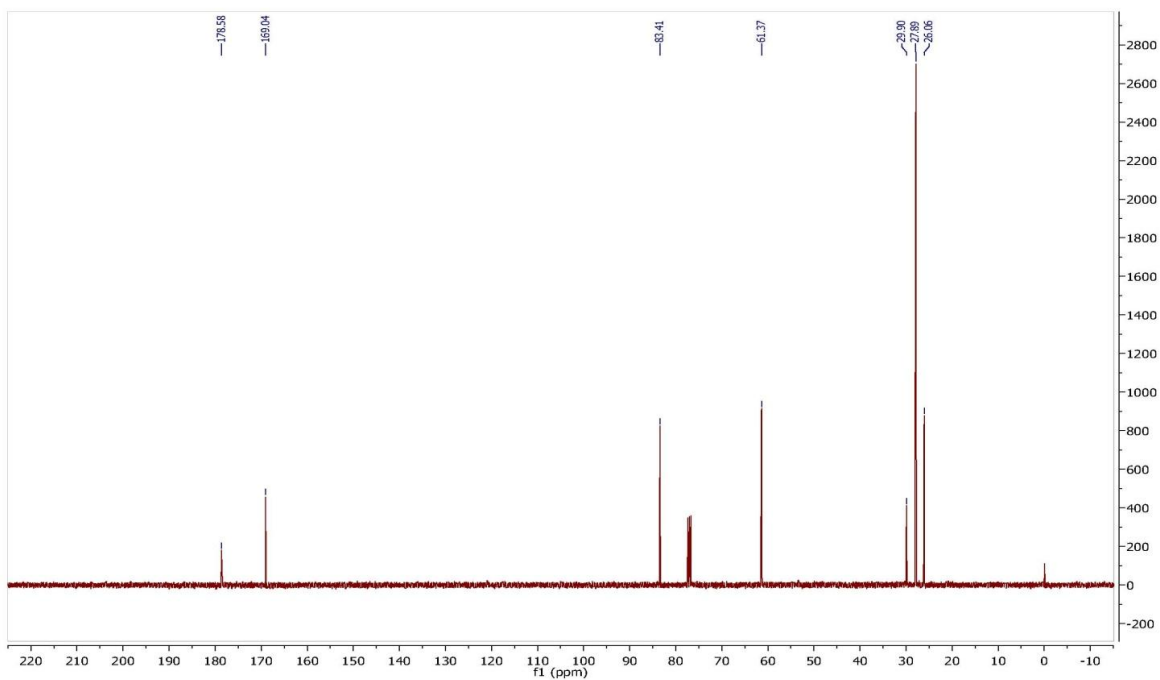


Scheme S2: Synthesis of **16**: a) Boc₂O, Et₃N, DCM; b) 2-thienyl-B(OH)₂, K₂CO₃, Pd(PPh₃)₄, THF.

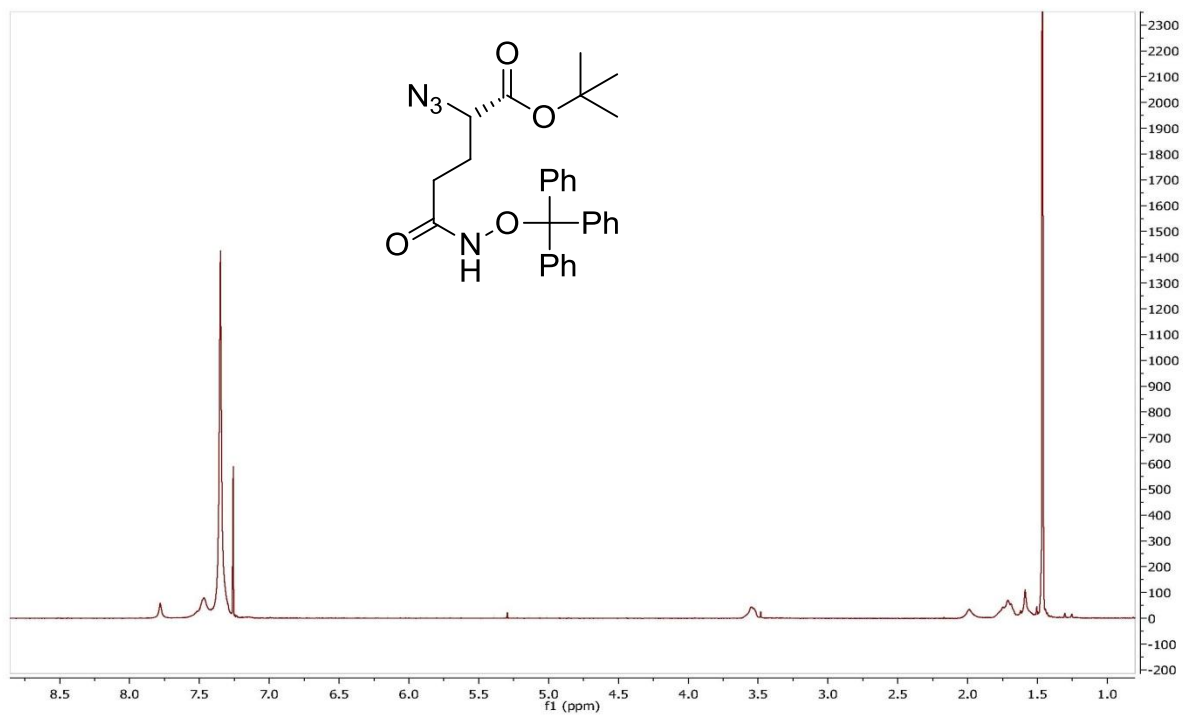
^1H NMR of **1**:



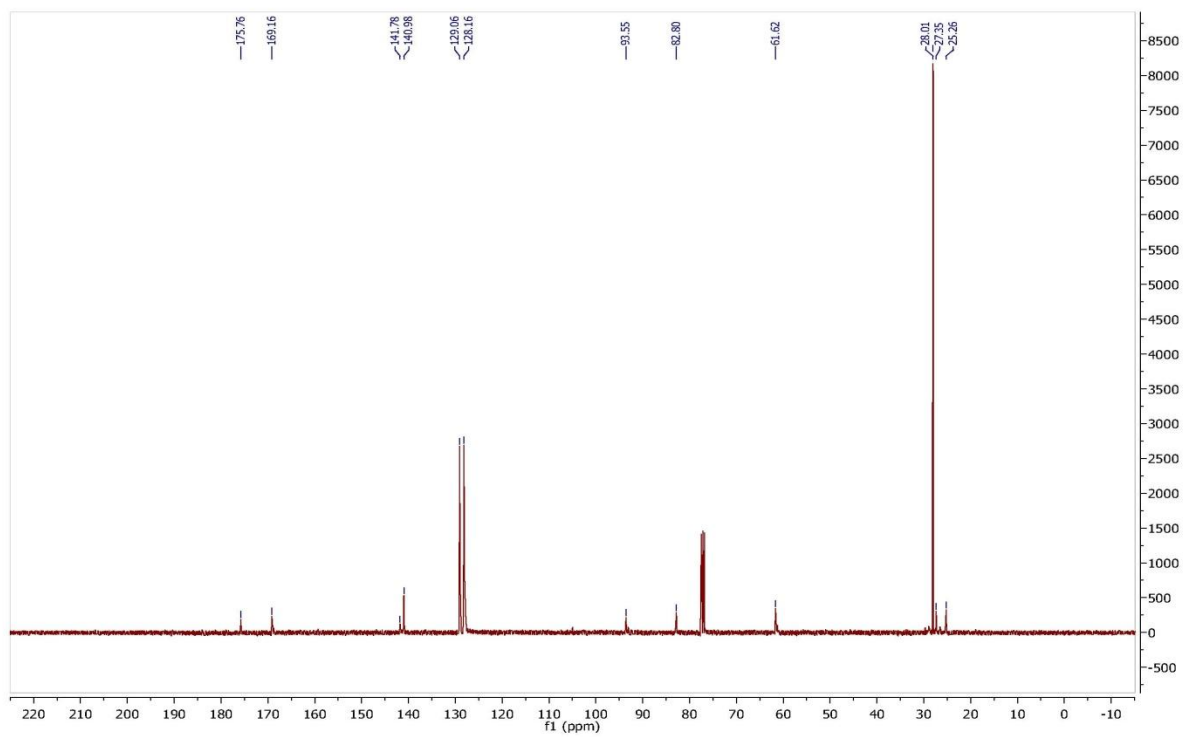
^{13}C NMR of **1**:



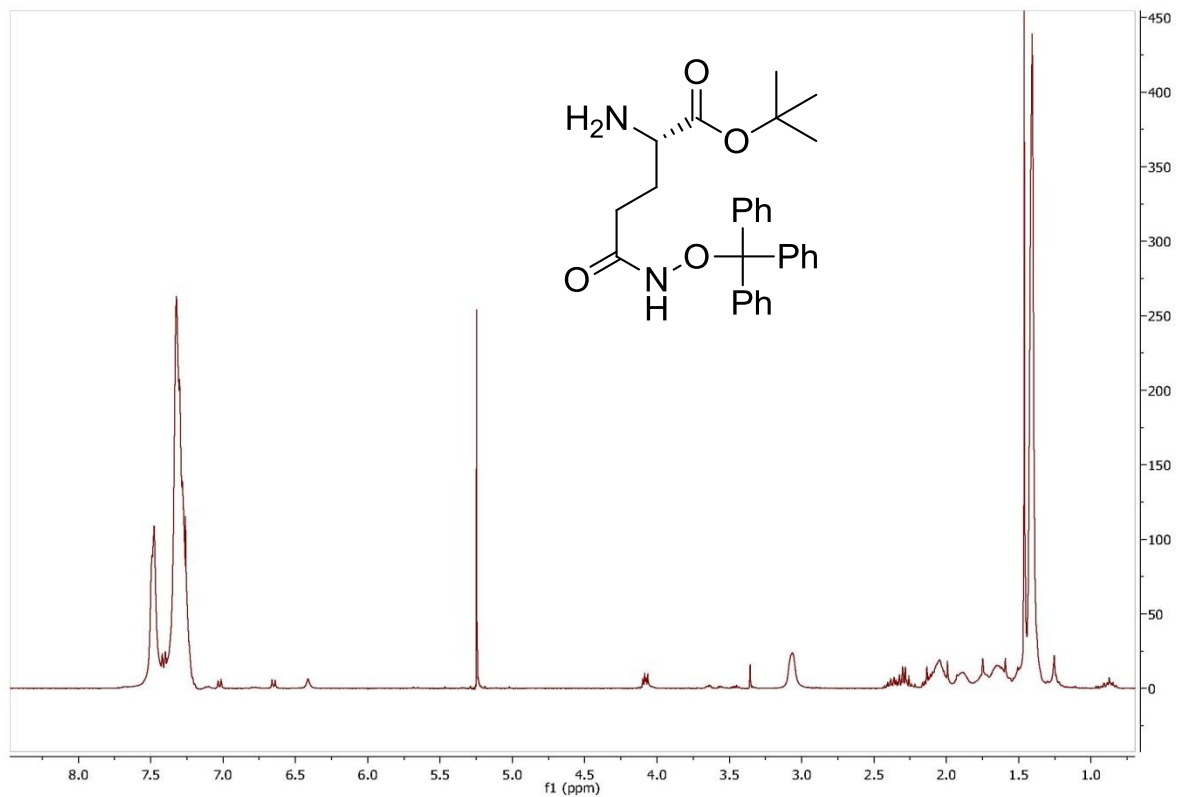
^1H NMR of **2**:



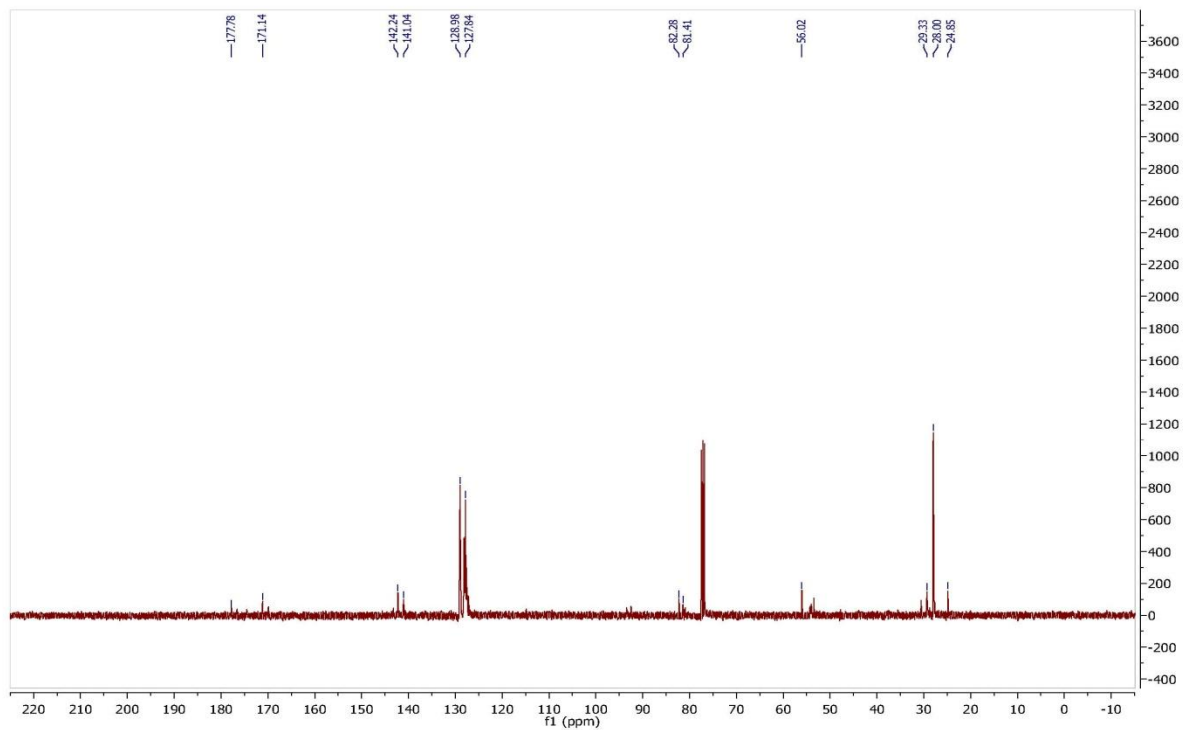
^{13}C NMR of **2**:



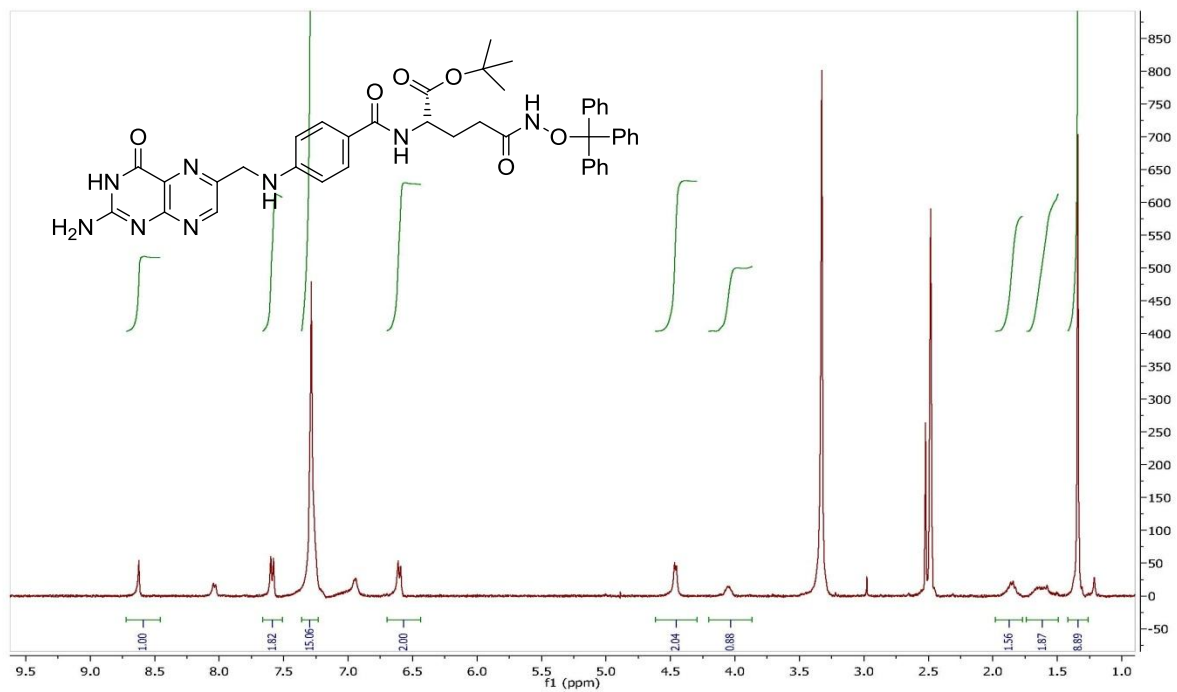
^1H NMR of **3**:



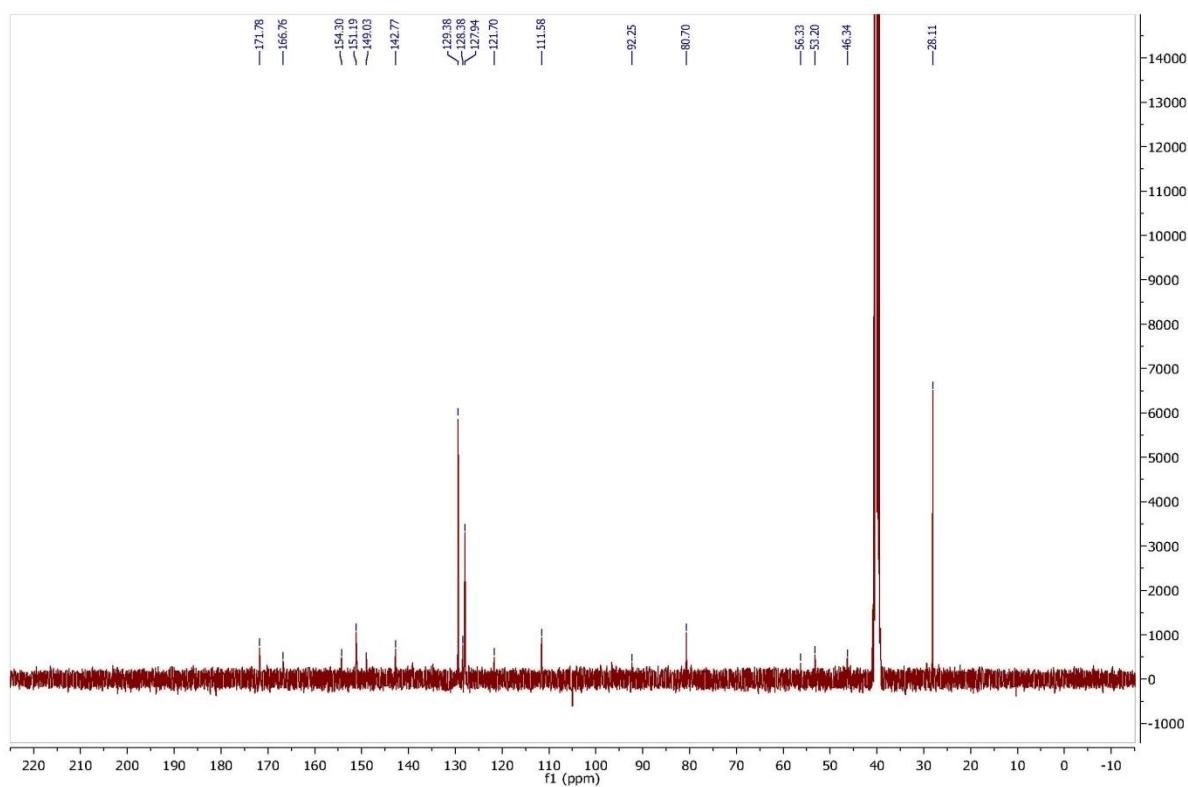
^{13}C NMR of **3**:



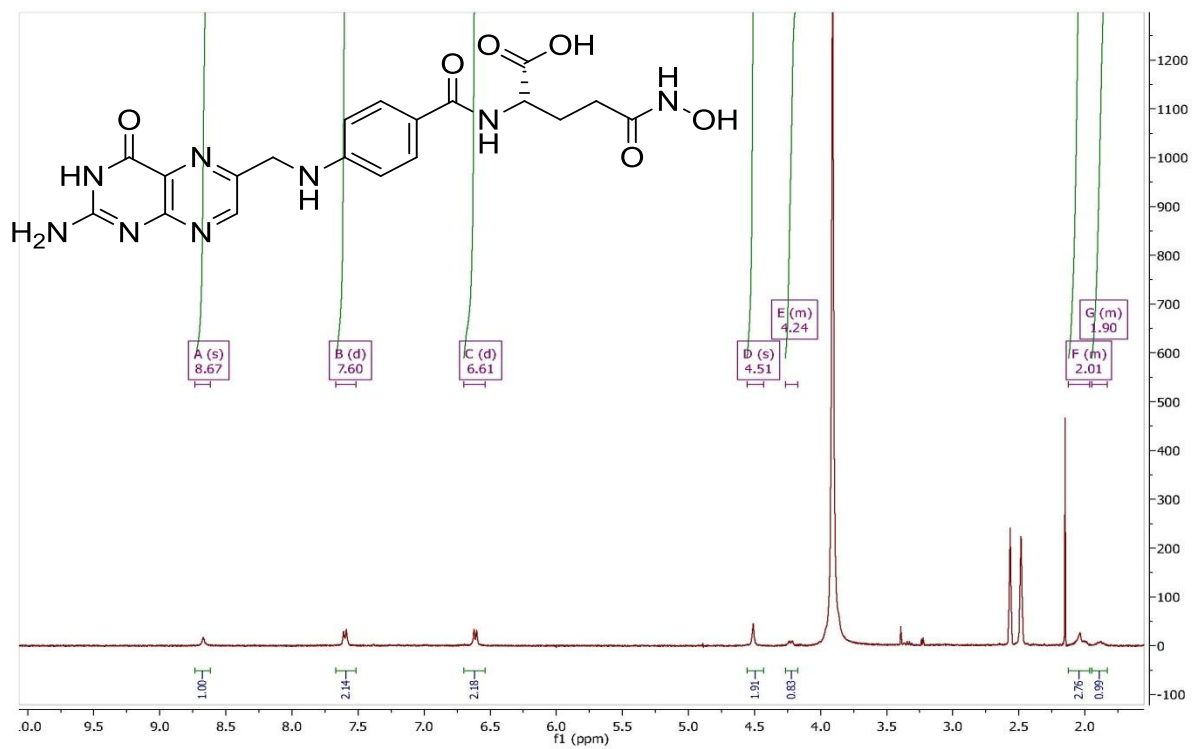
¹H NMR of **5**:



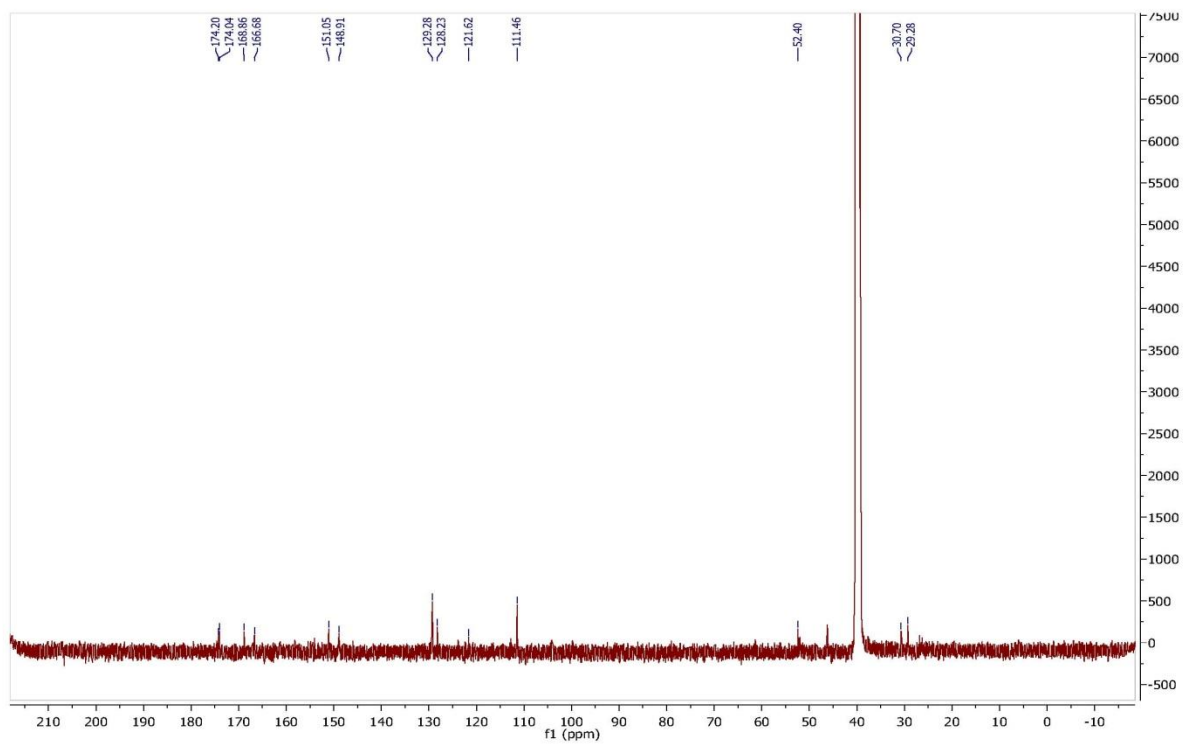
¹³C NMR of **5**:



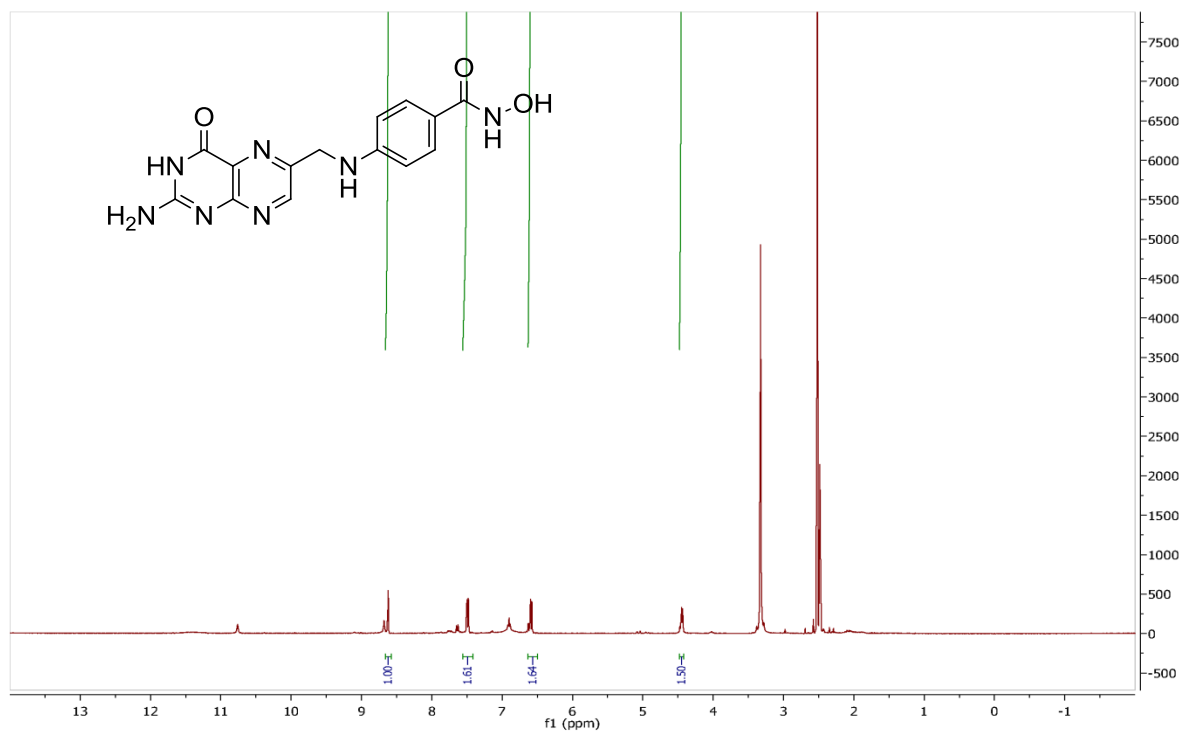
¹H NMR of 6:



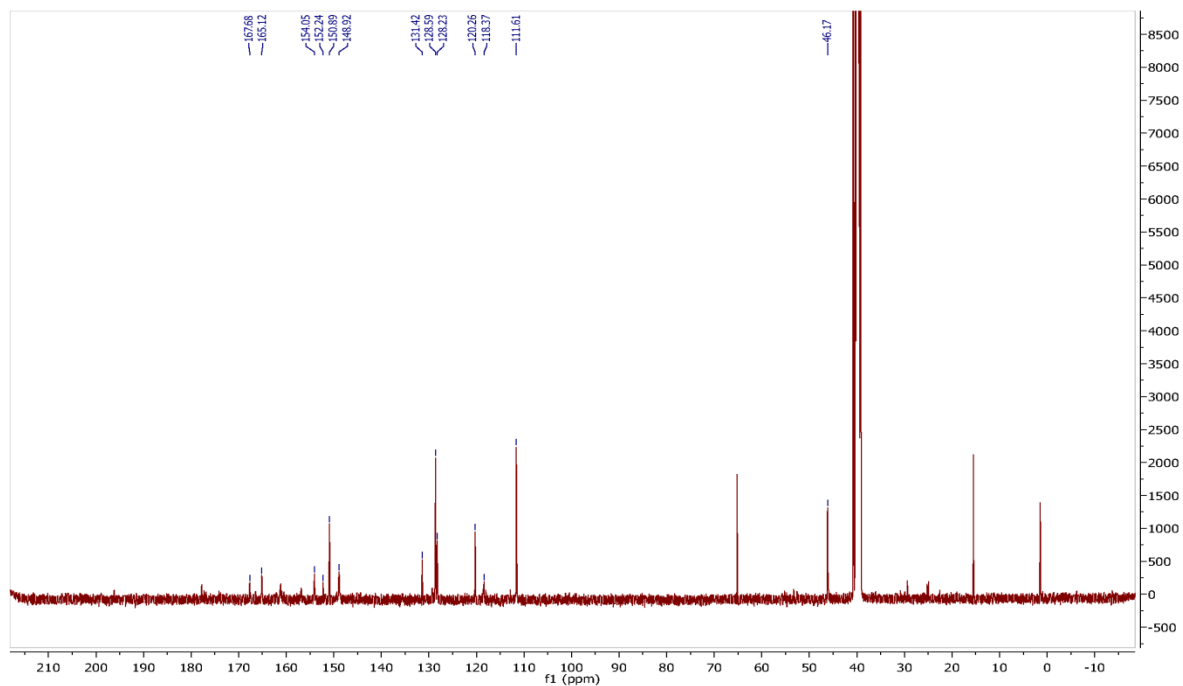
¹³C NMR of 6:



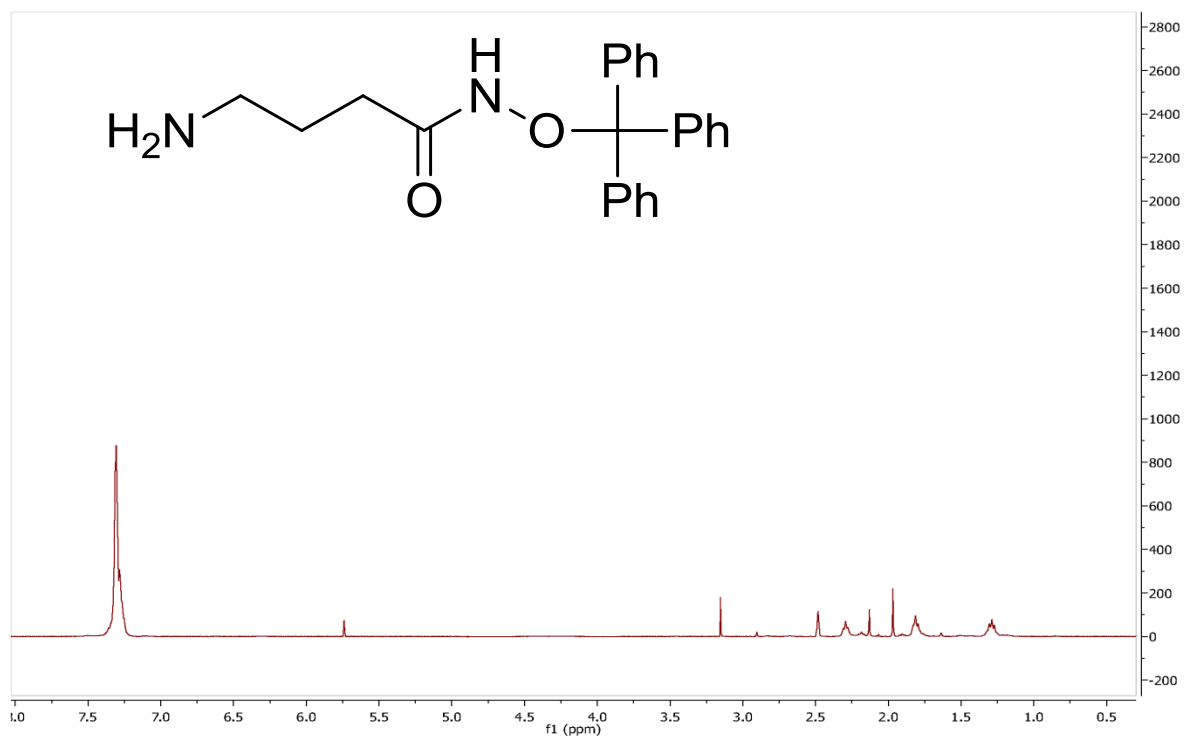
¹H NMR of 7:



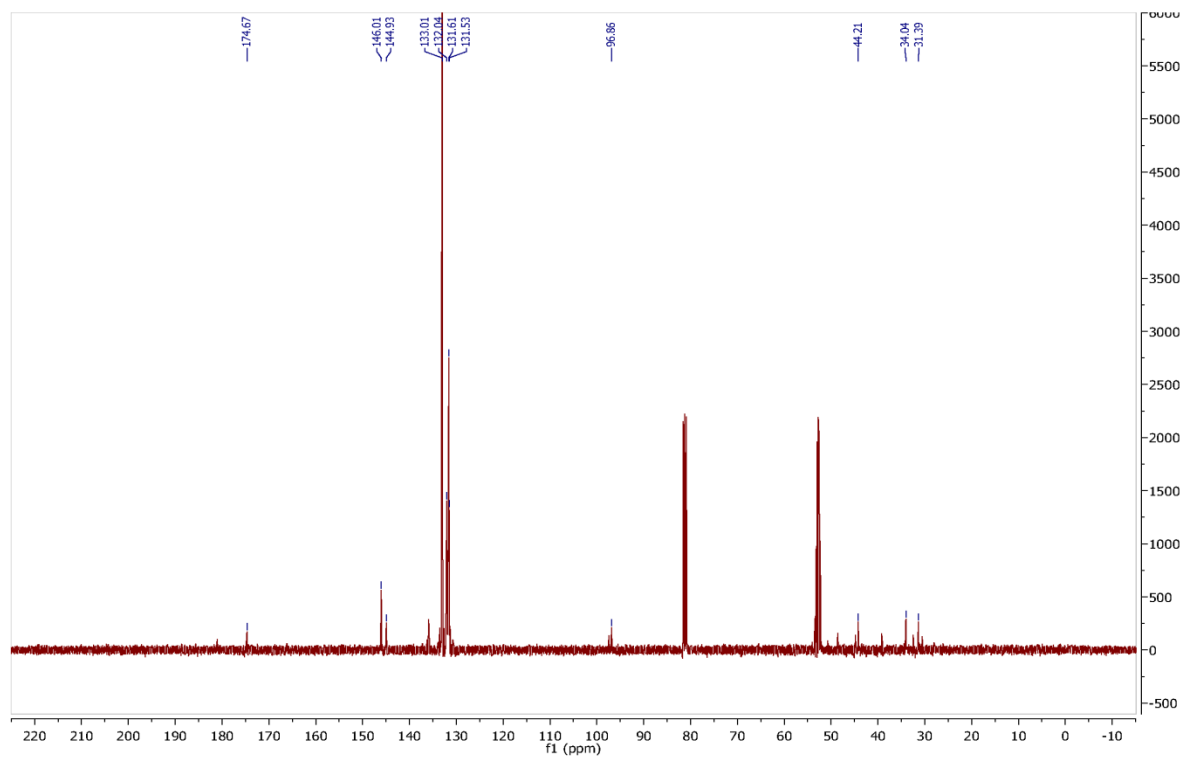
¹³C NMR of 7:



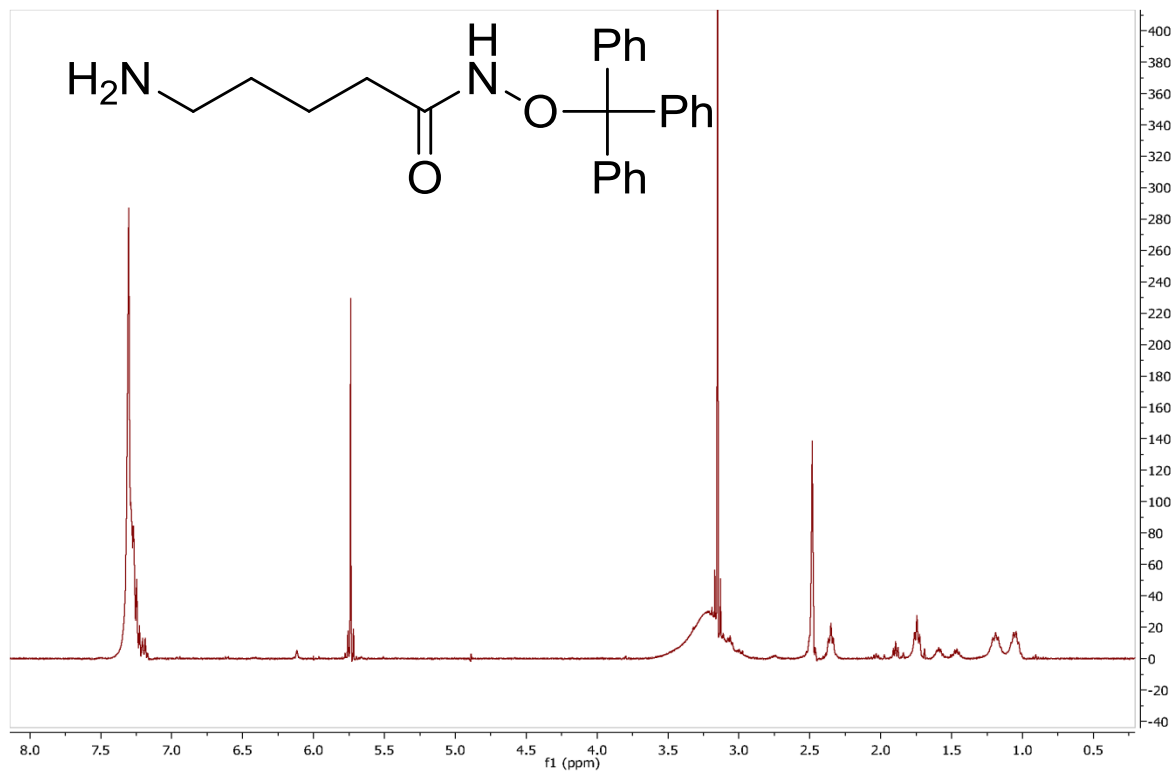
^1H NMR of **9a**:



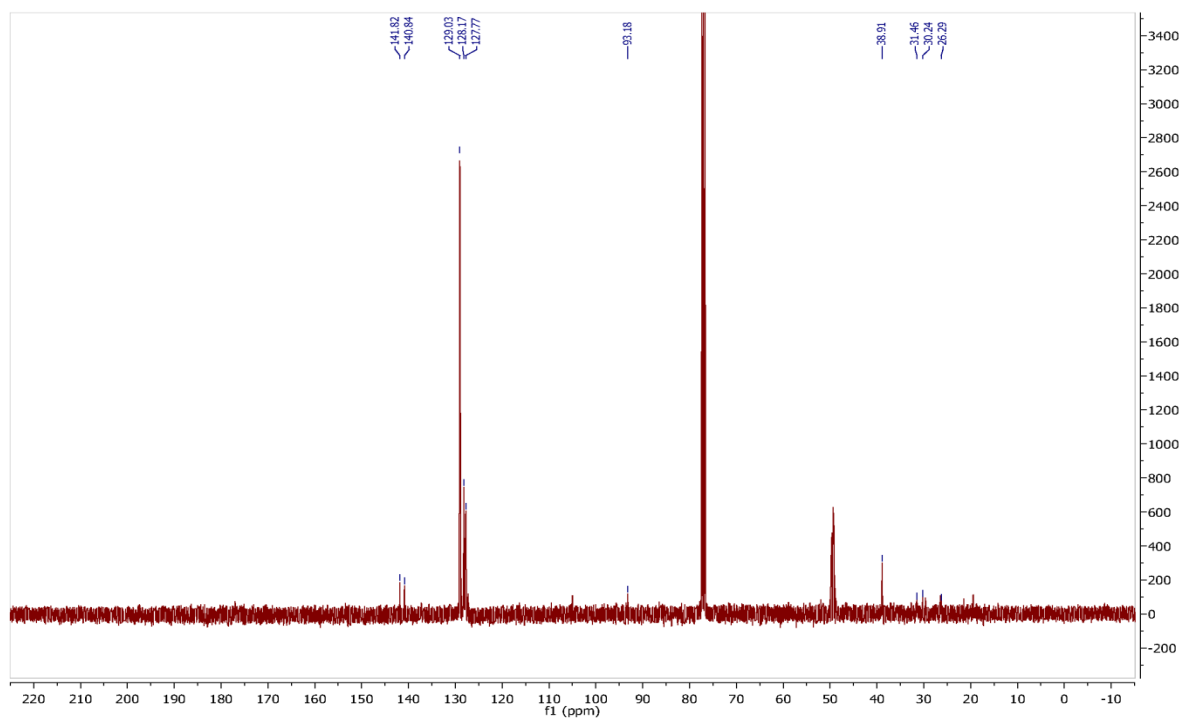
^{13}C NMR of **9a**:



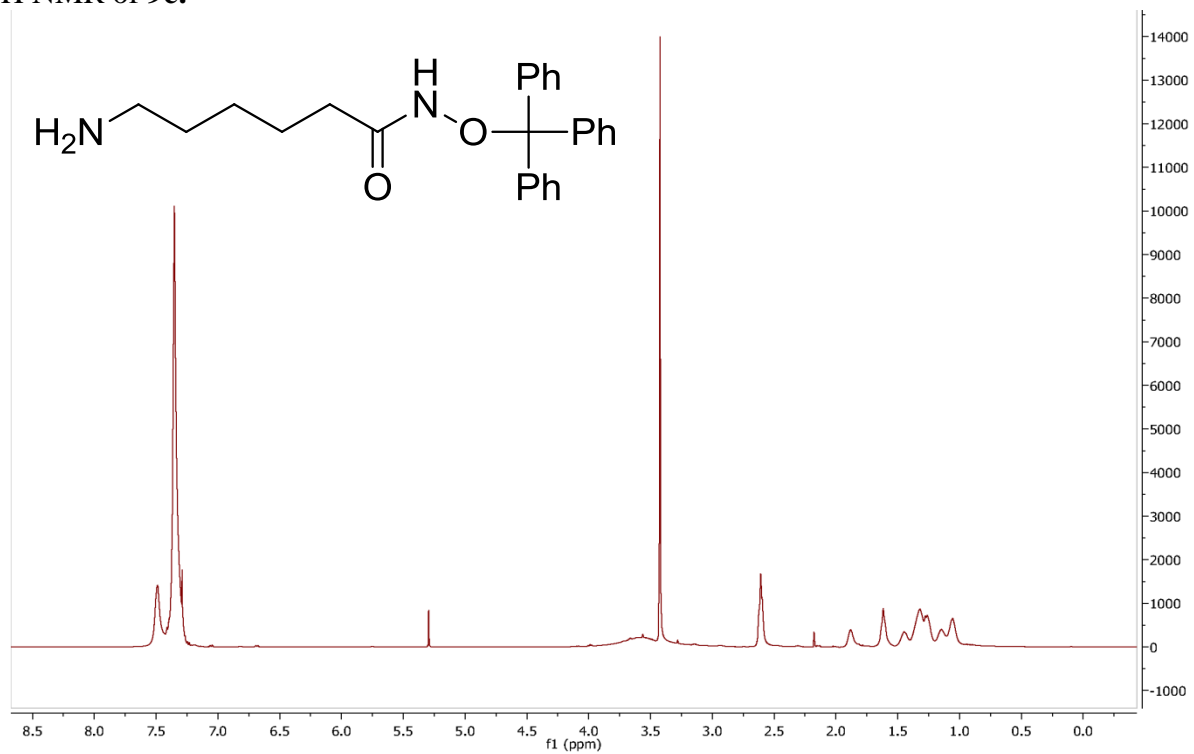
¹H NMR of **9b**:



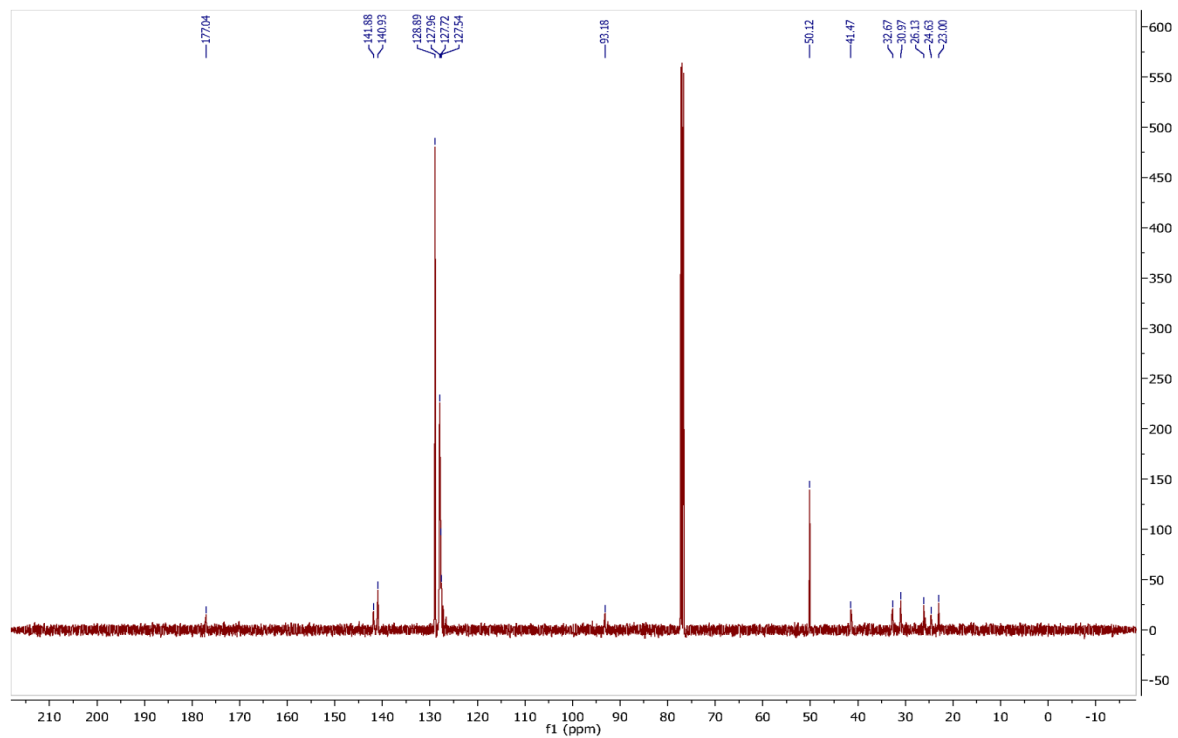
¹³C NMR of **9b**:



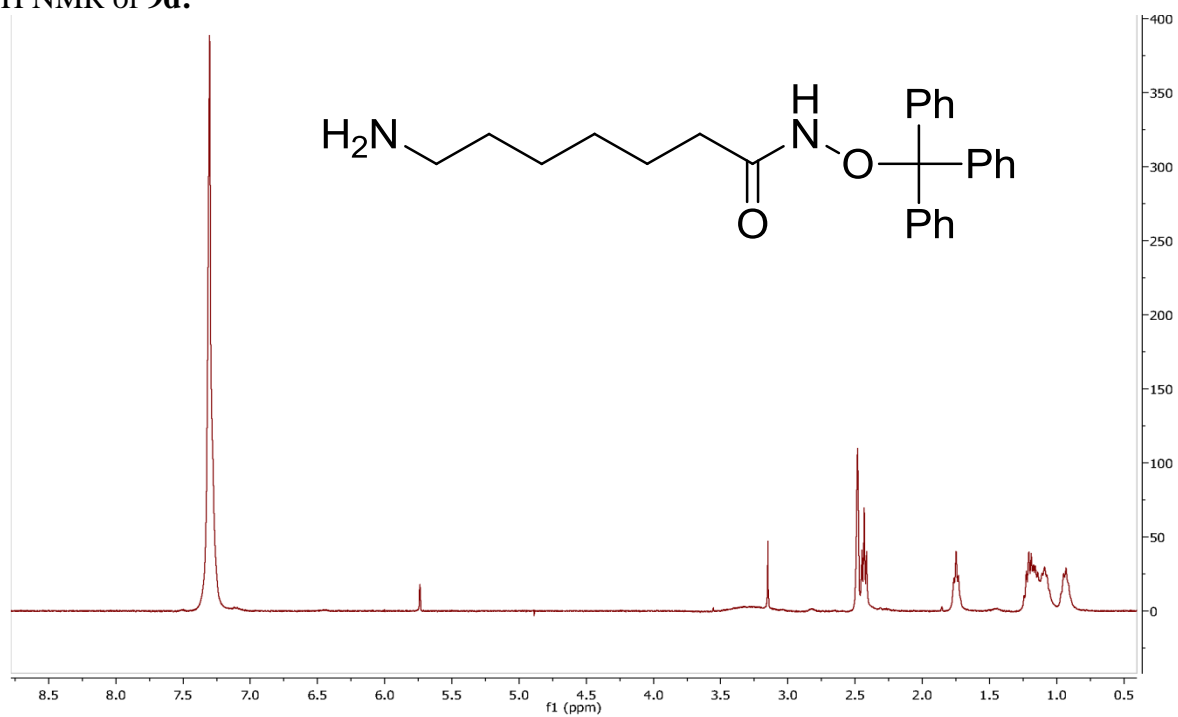
¹H NMR of **9c**:



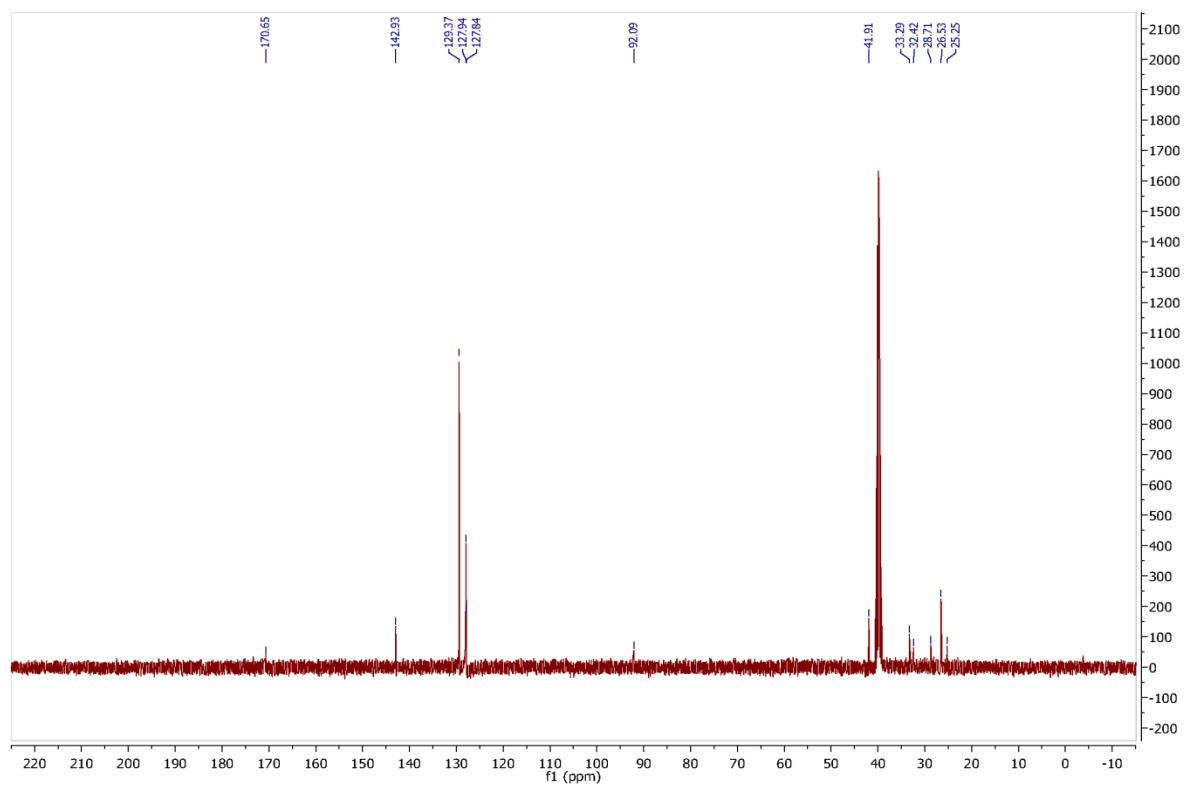
¹³C NMR of **9c**:



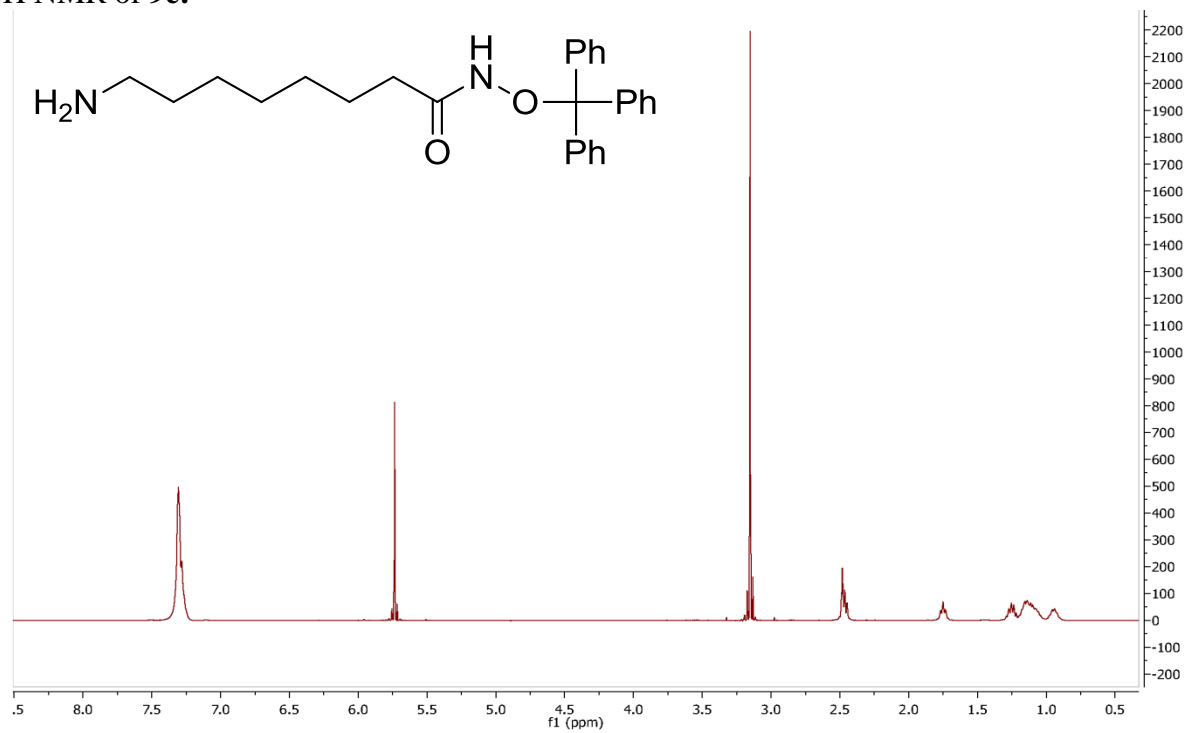
¹H NMR of **9d**:



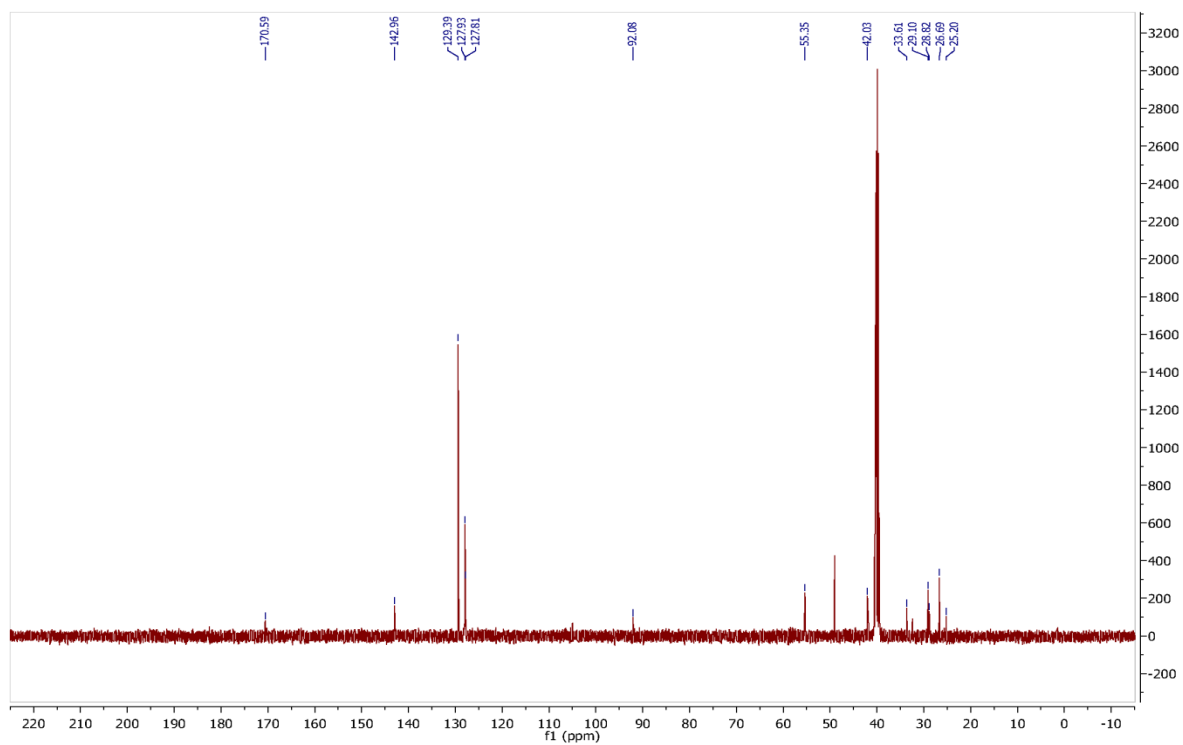
¹³C NMR of **9d**:



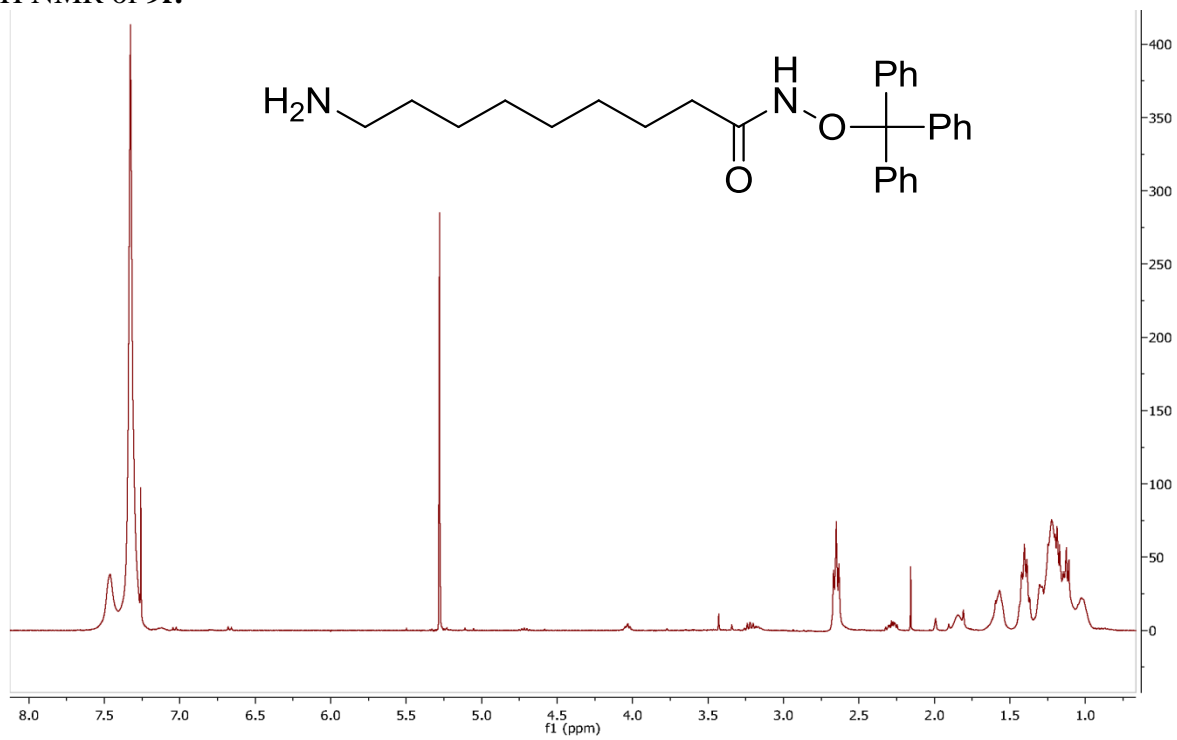
^1H NMR of **9e**:



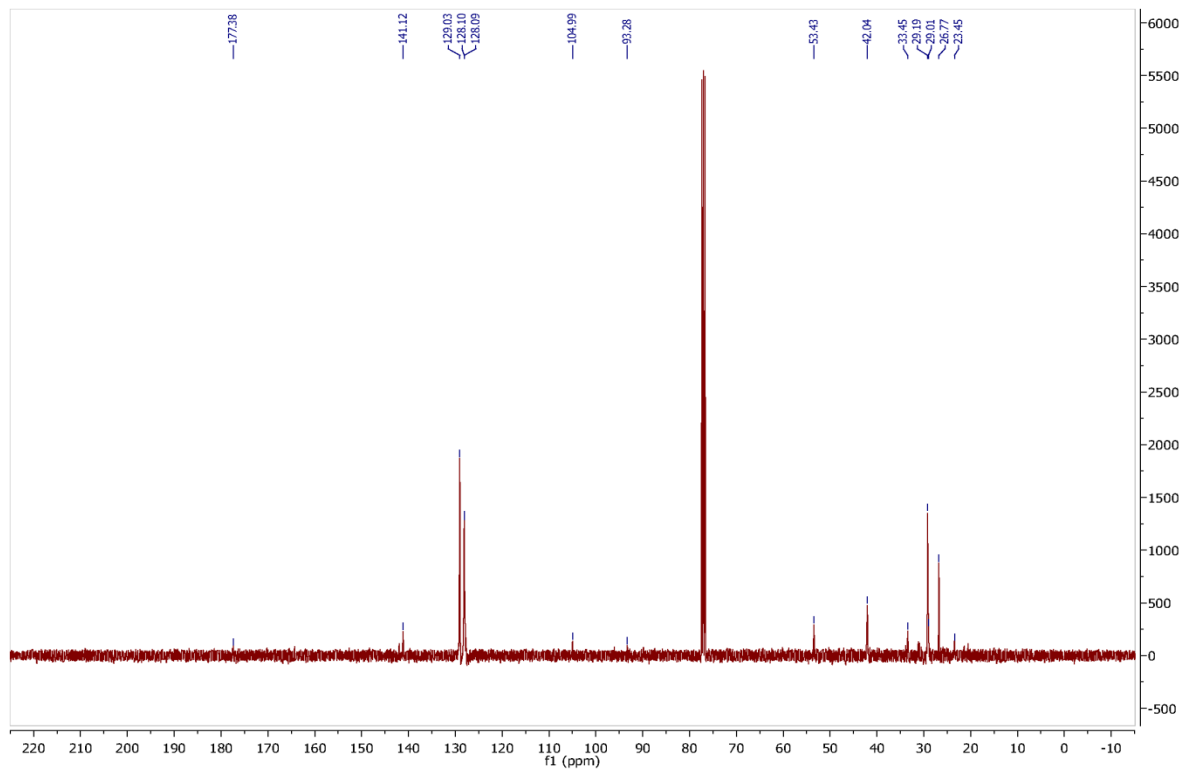
^{13}C NMR of **9e**:



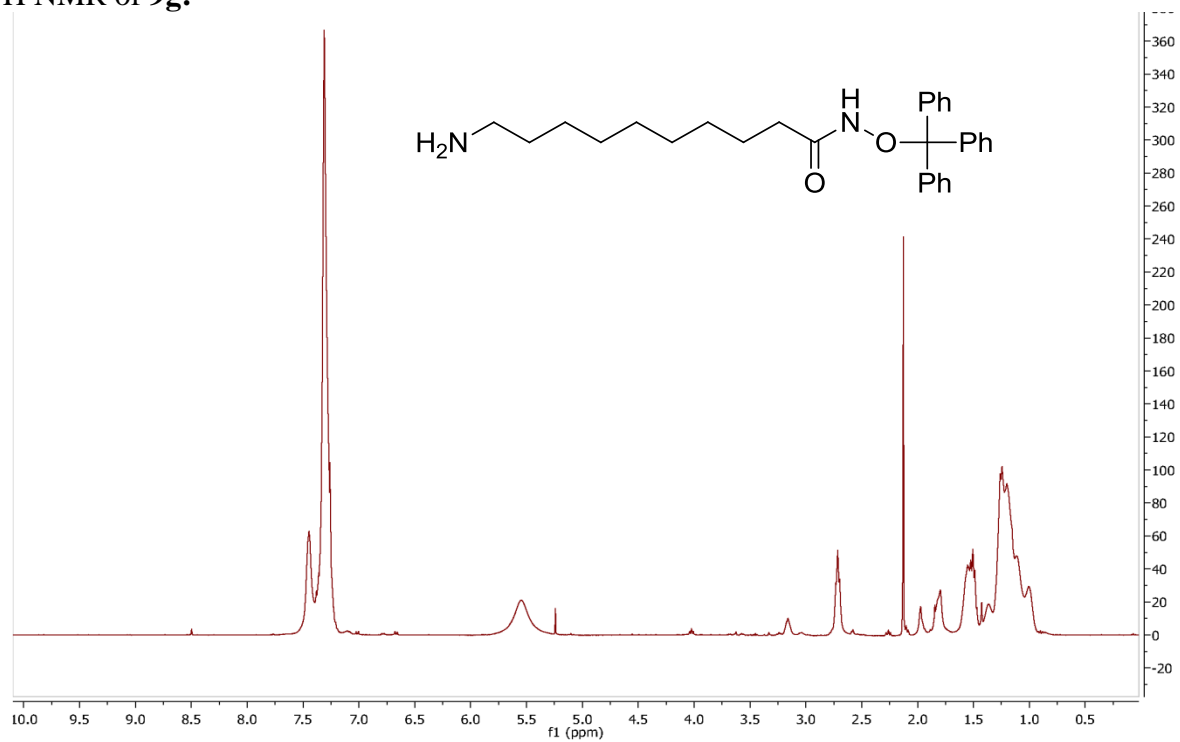
^1H NMR of **9f**:



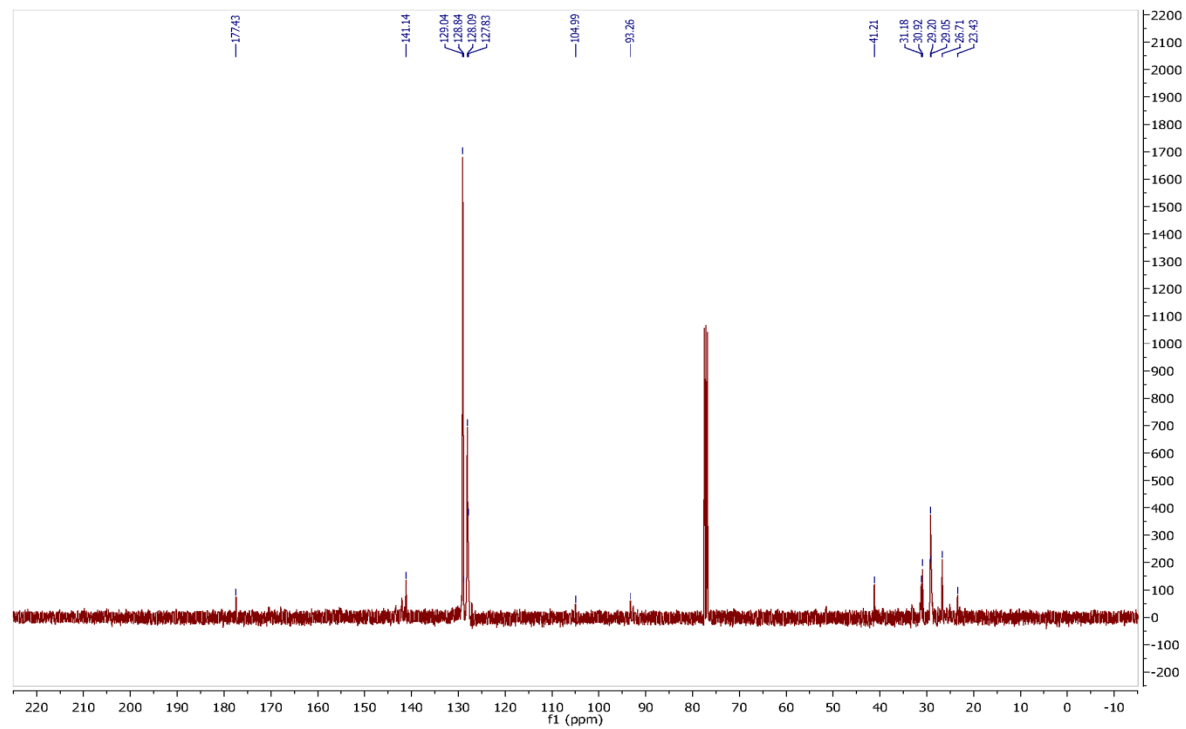
^{13}C NMR of **9f**:



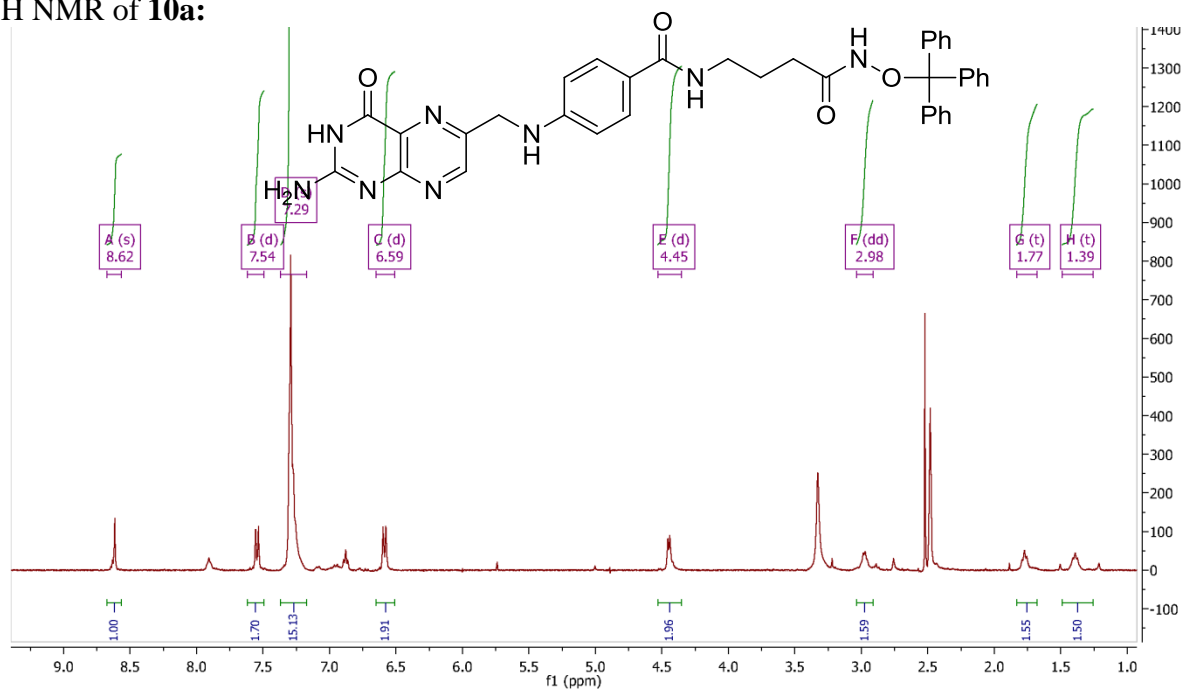
^1H NMR of **9g**:



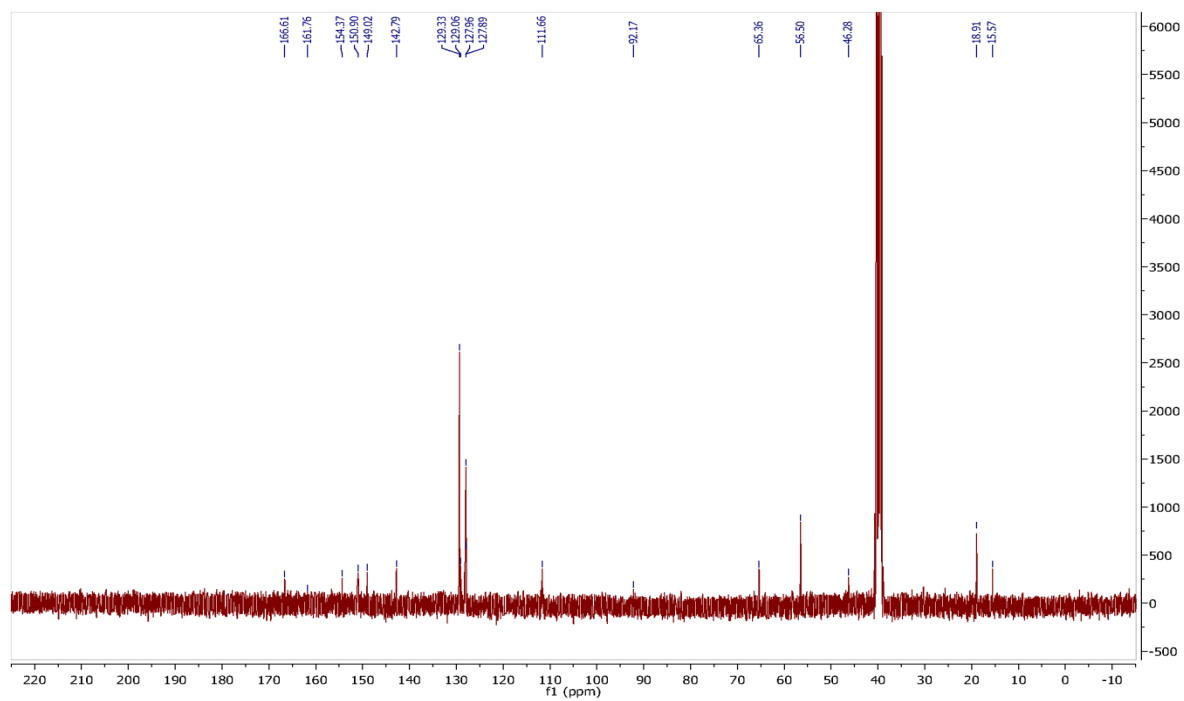
^{13}C NMR of **9g**:



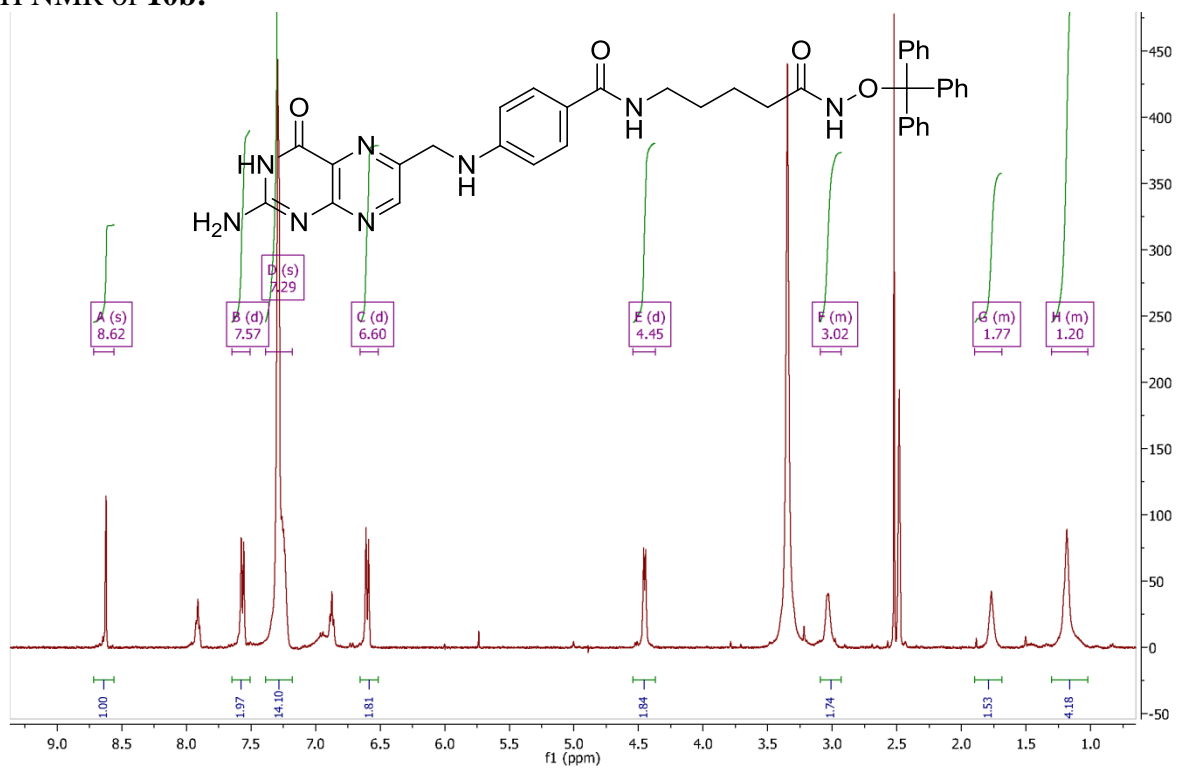
¹H NMR of 10a:



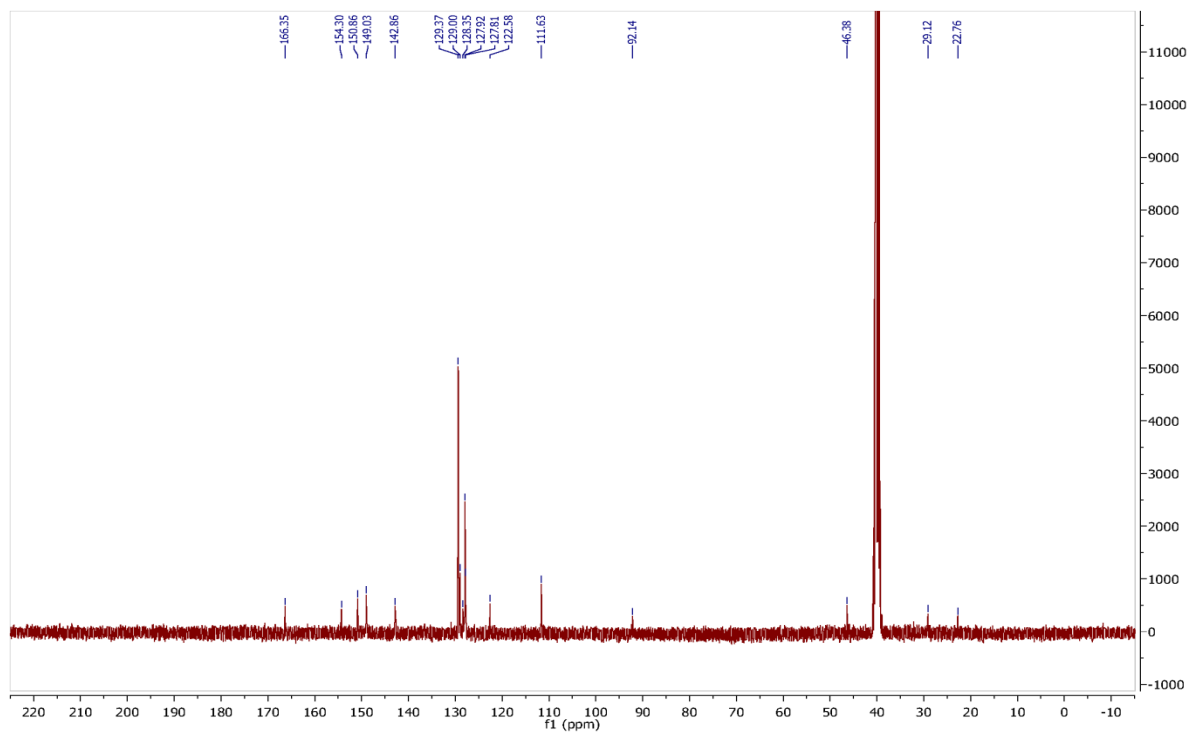
¹³C NMR of 10a:



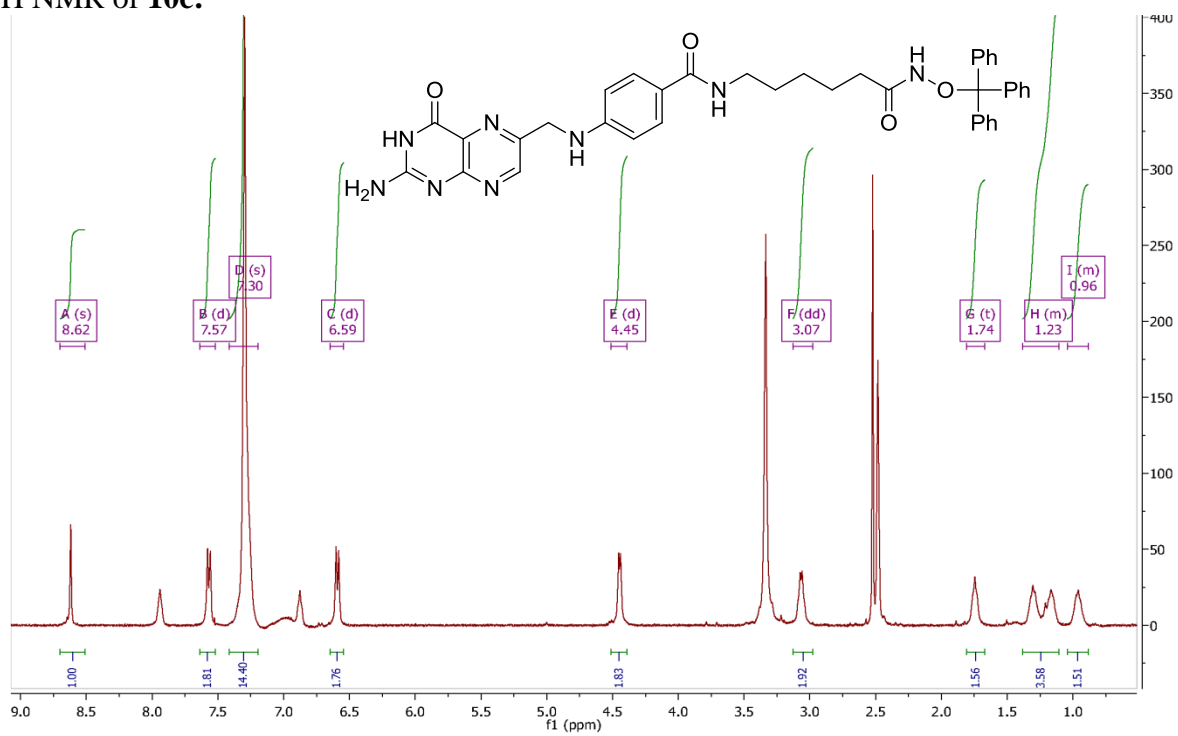
¹H NMR of **10b**:



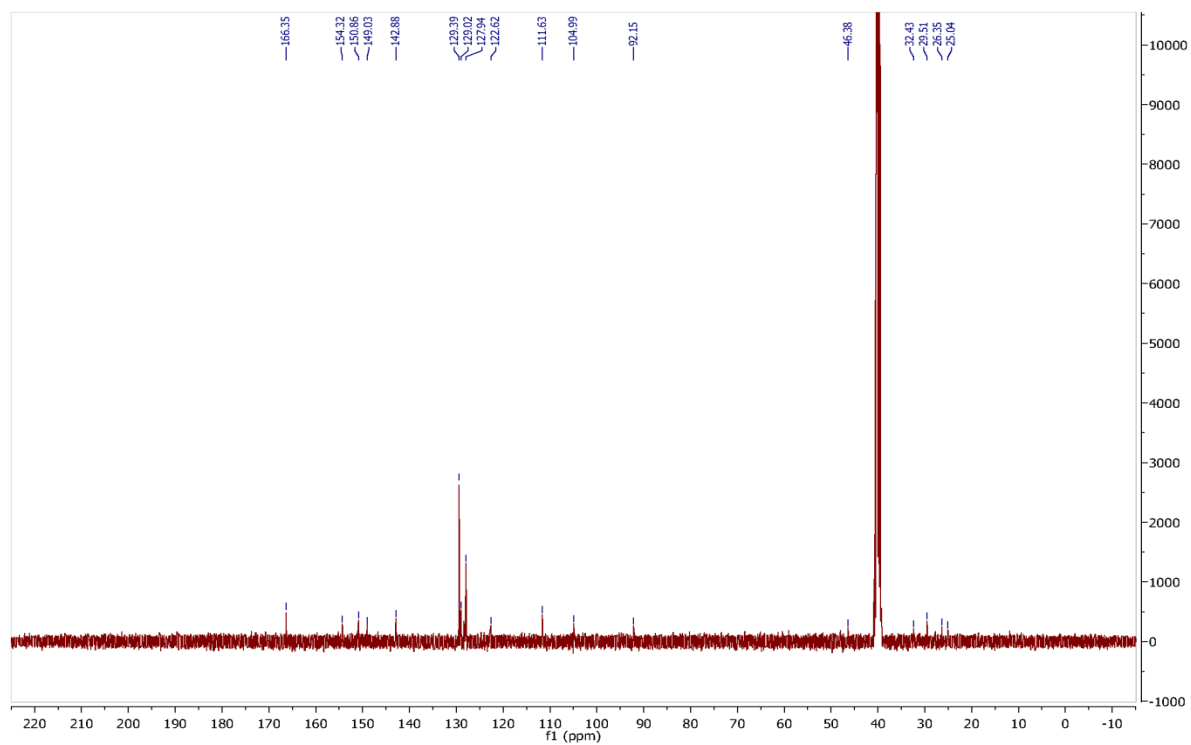
¹³C NMR of **10b**:



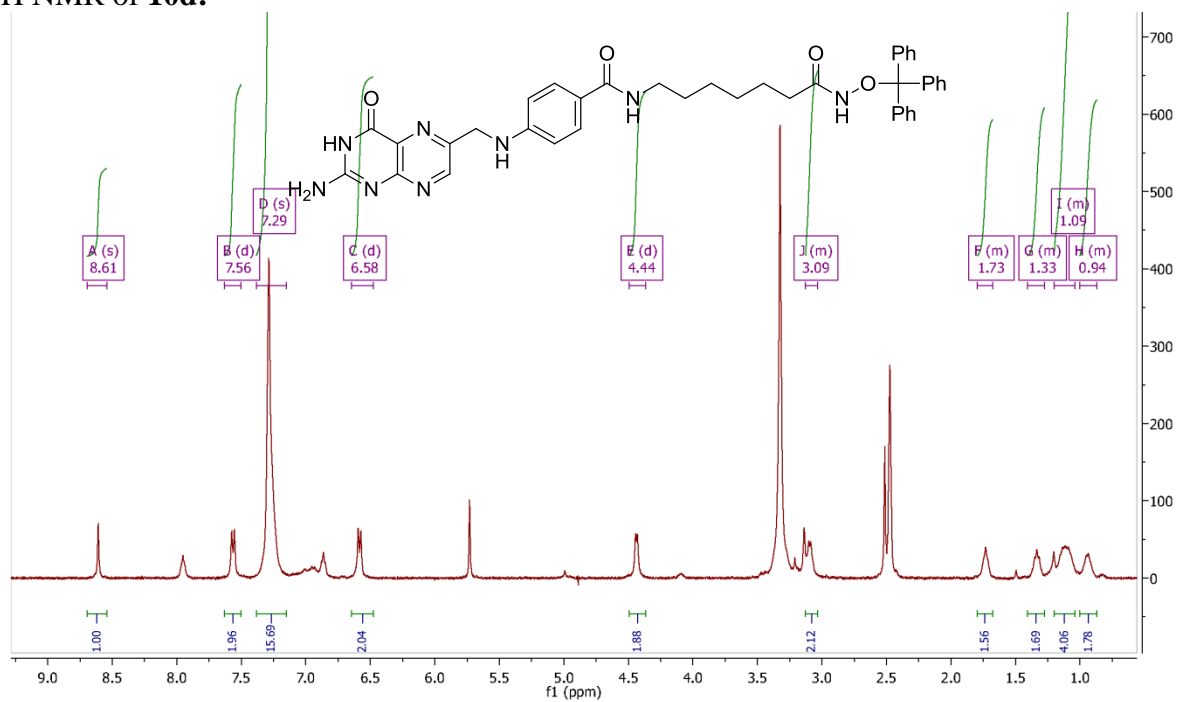
¹H NMR of 10c:



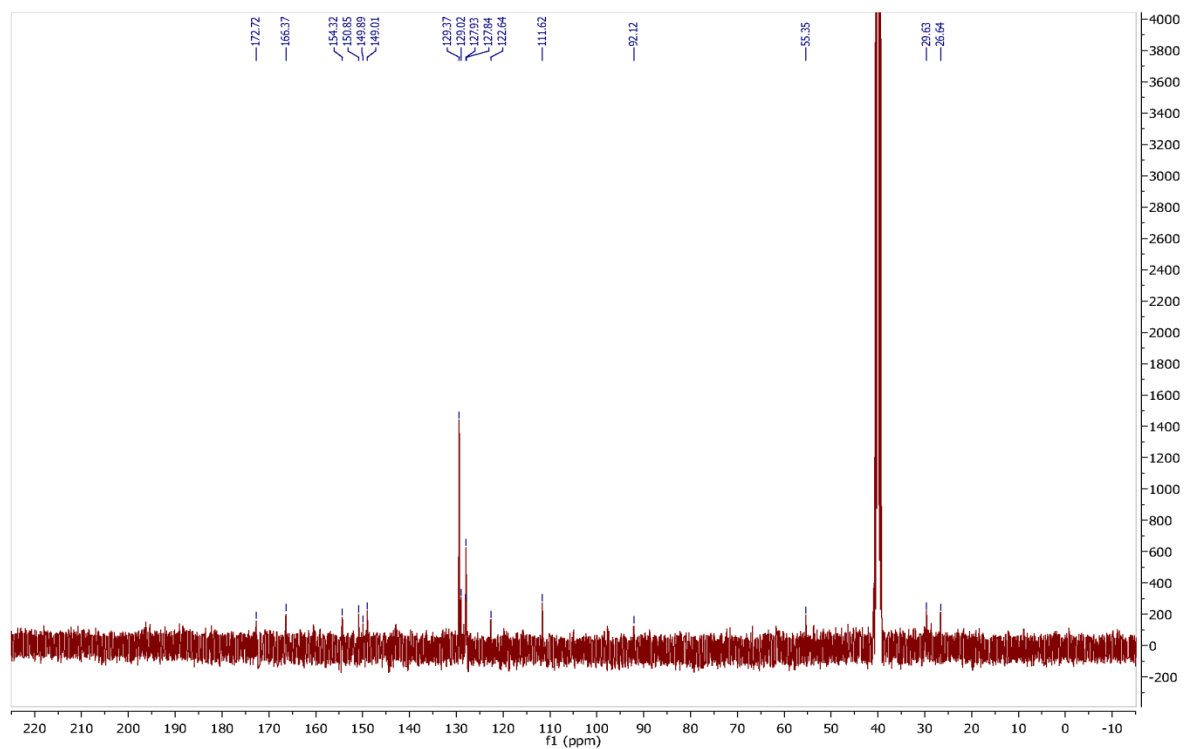
¹³C NMR of 10c:



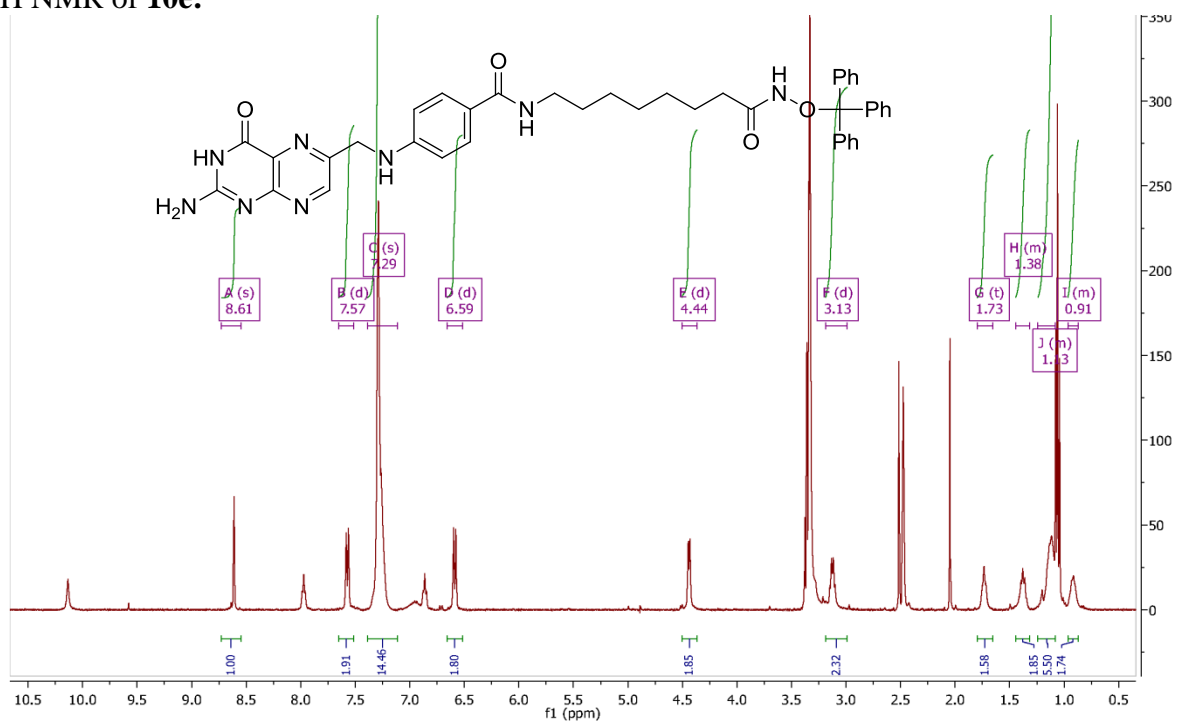
¹H NMR of **10d**:



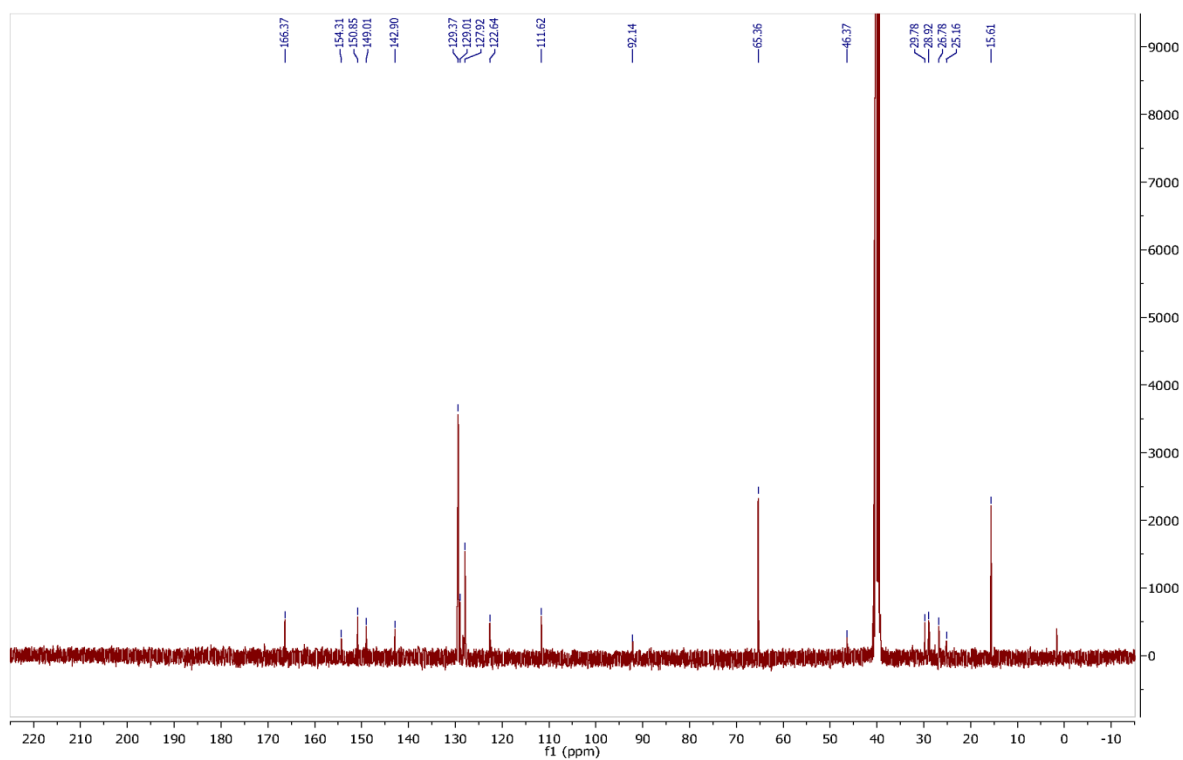
¹³C NMR of **10d**:



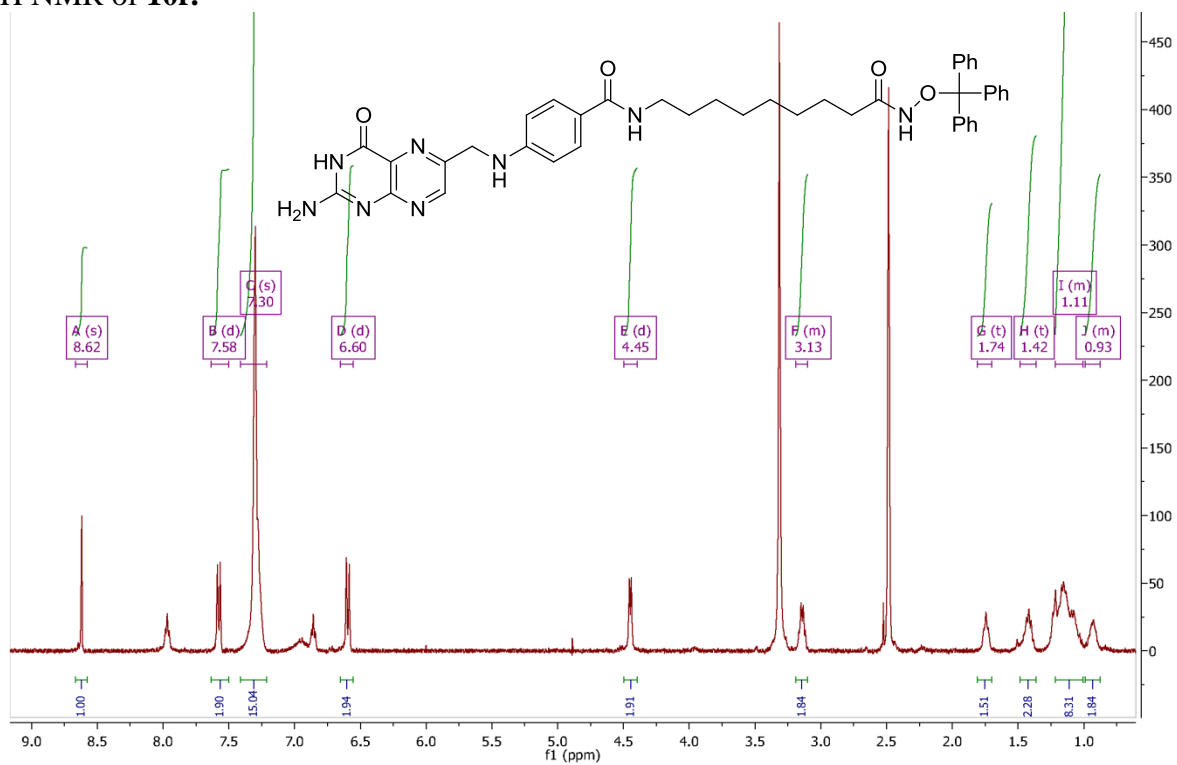
¹H NMR of 10e:



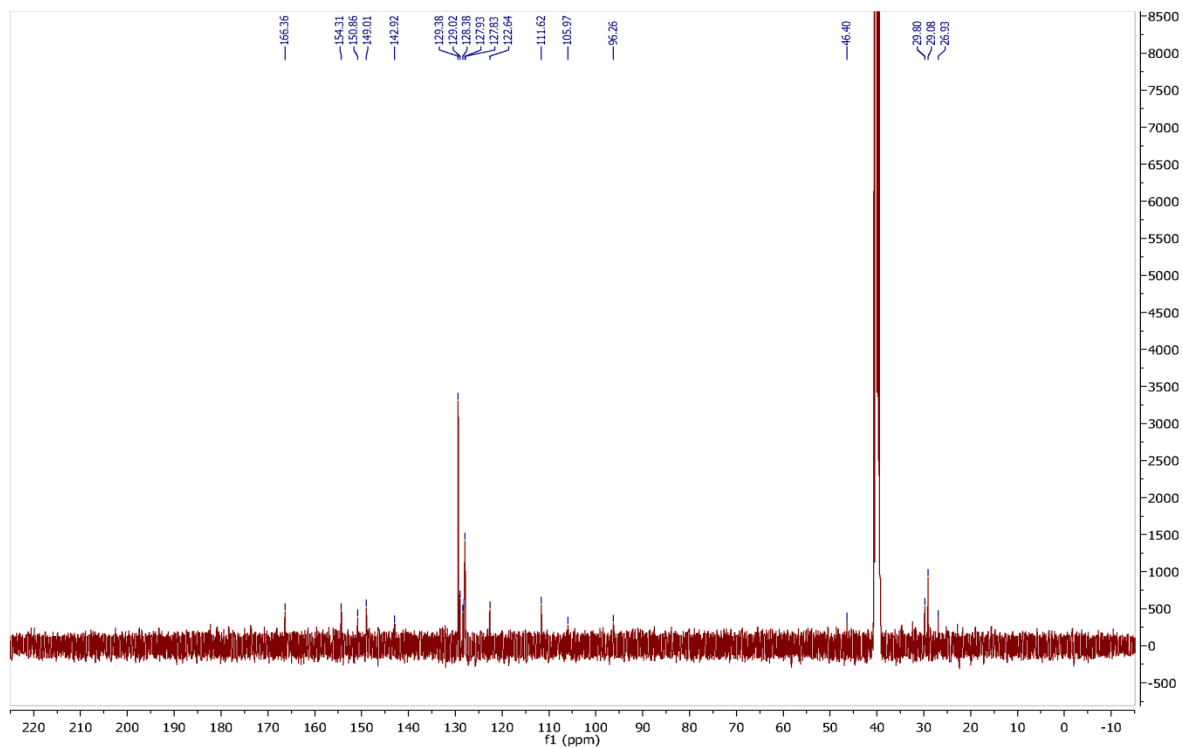
¹³C NMR of 10e:



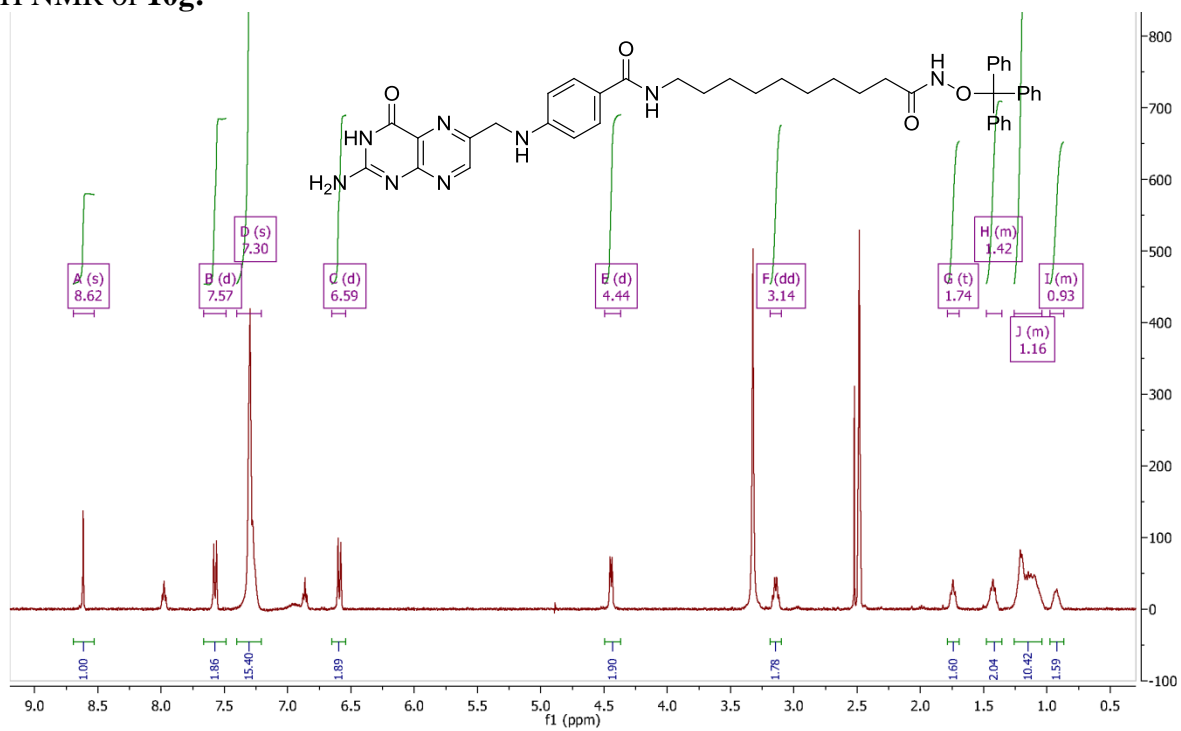
¹H NMR of **10f**:



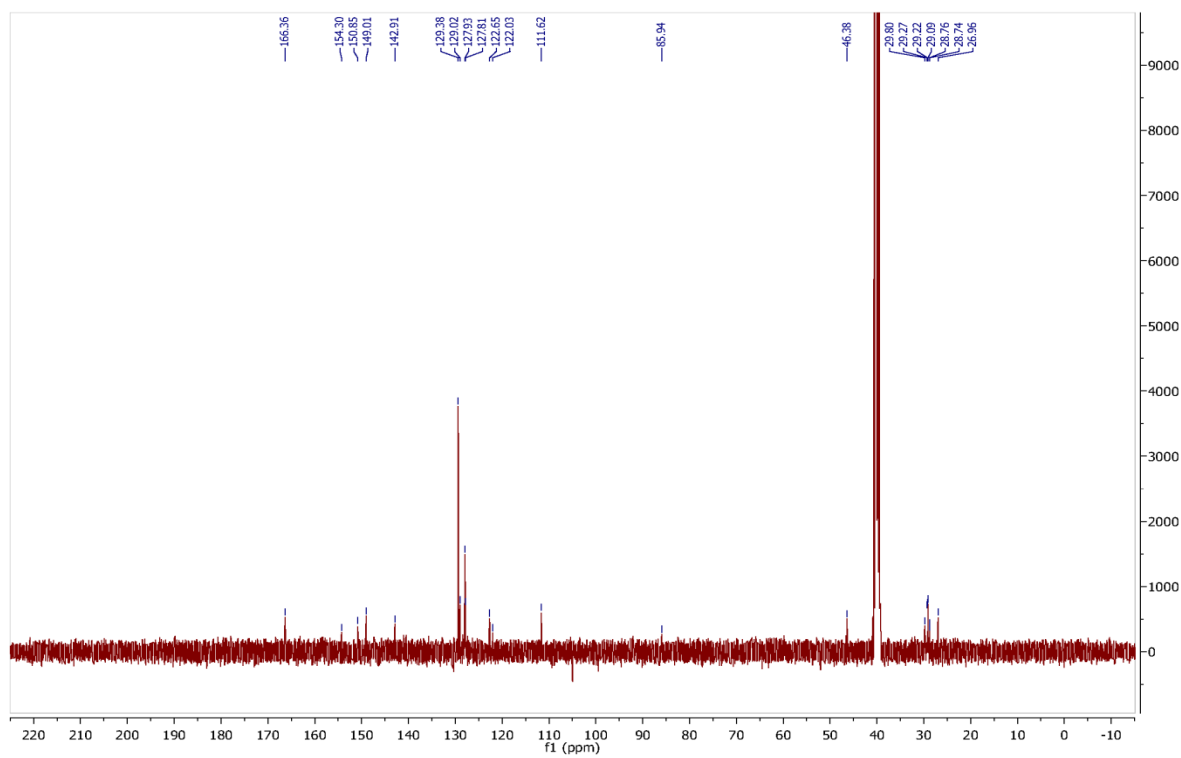
¹³C NMR of **10f**:



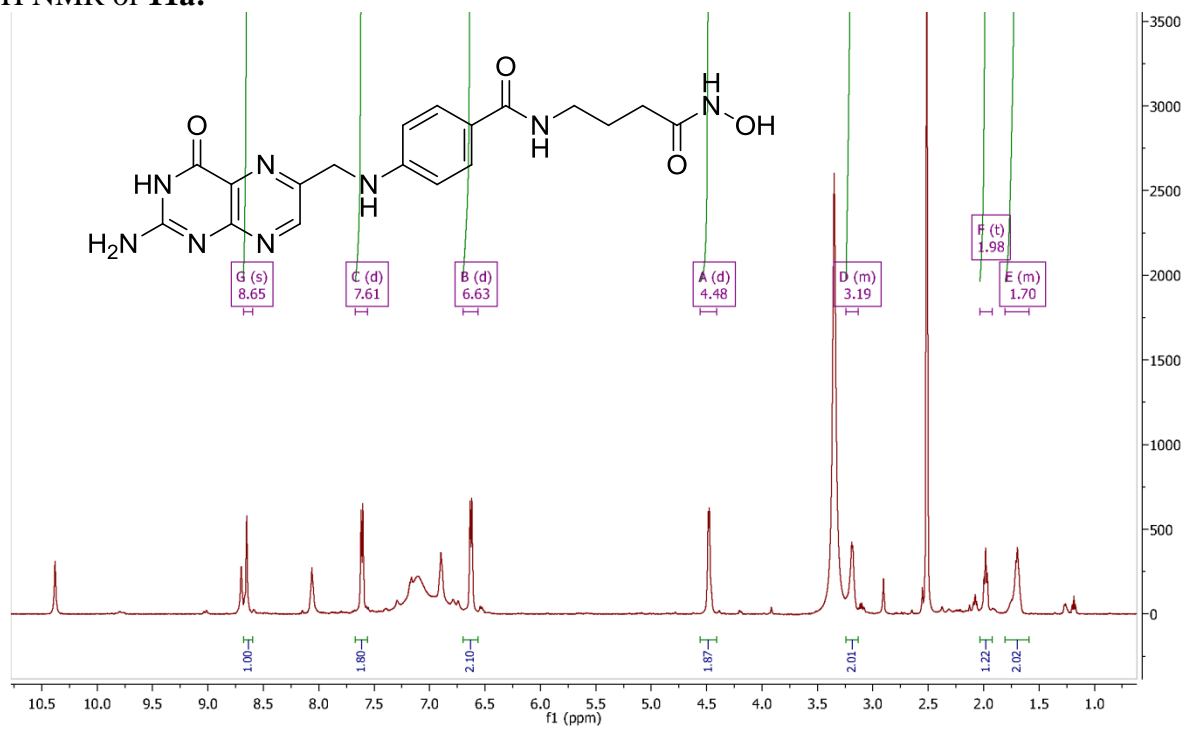
¹H NMR of 10g:



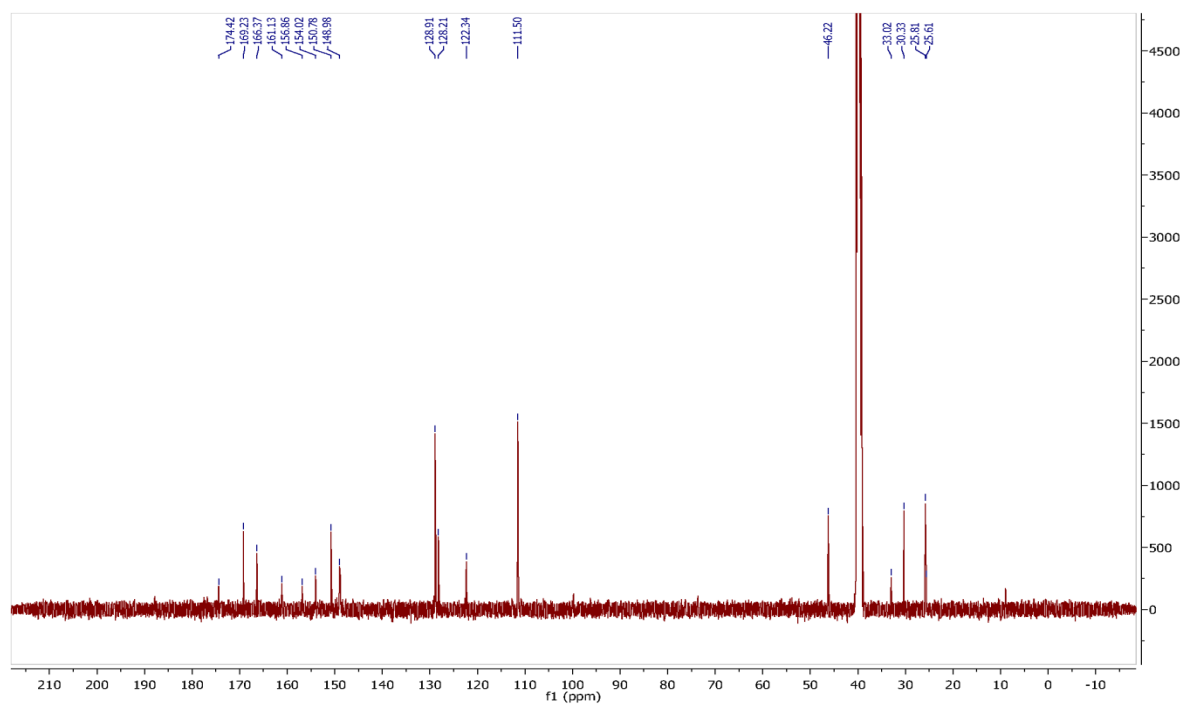
¹³C NMR of 10g:



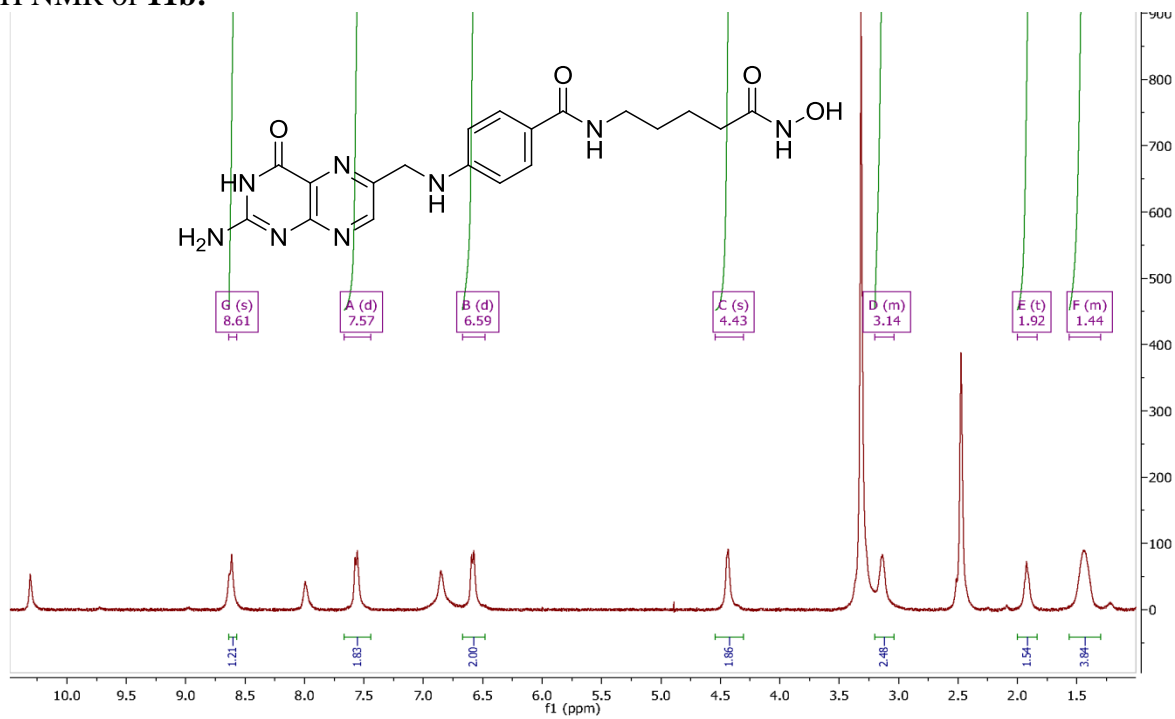
¹H NMR of **11a**:



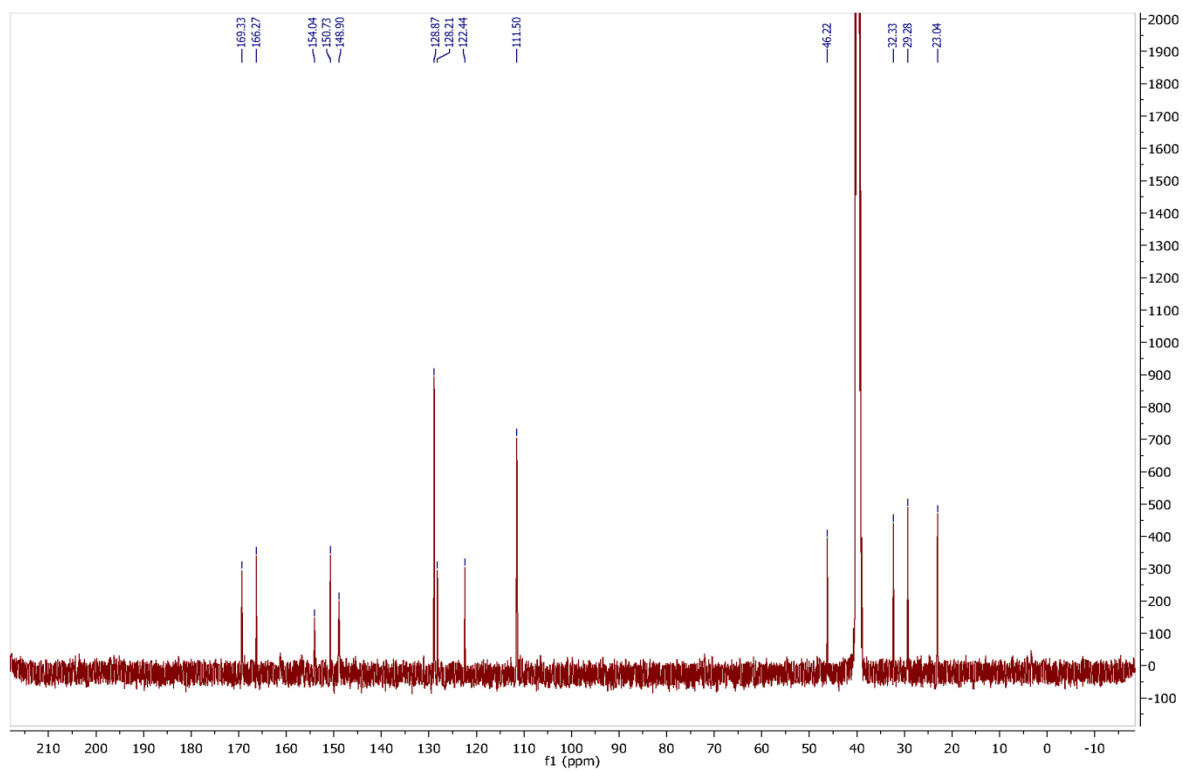
¹³C NMR of **11a**:



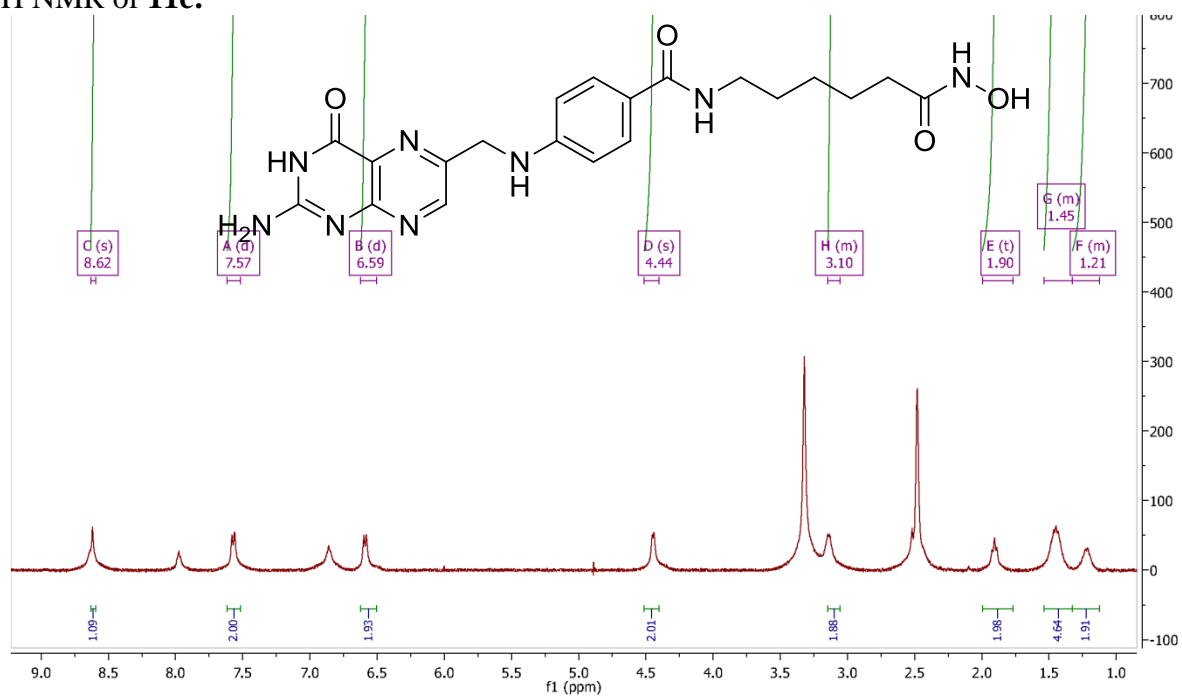
¹H NMR of **11b**:



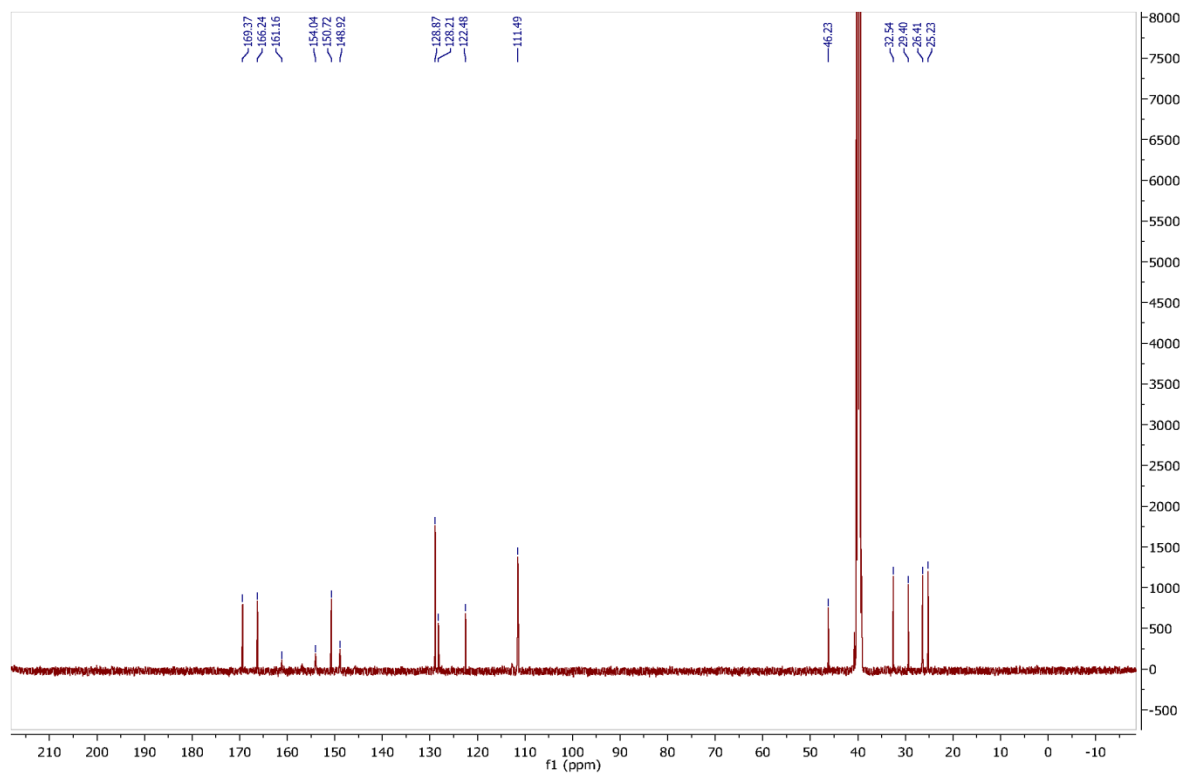
¹³C NMR of **11b**:



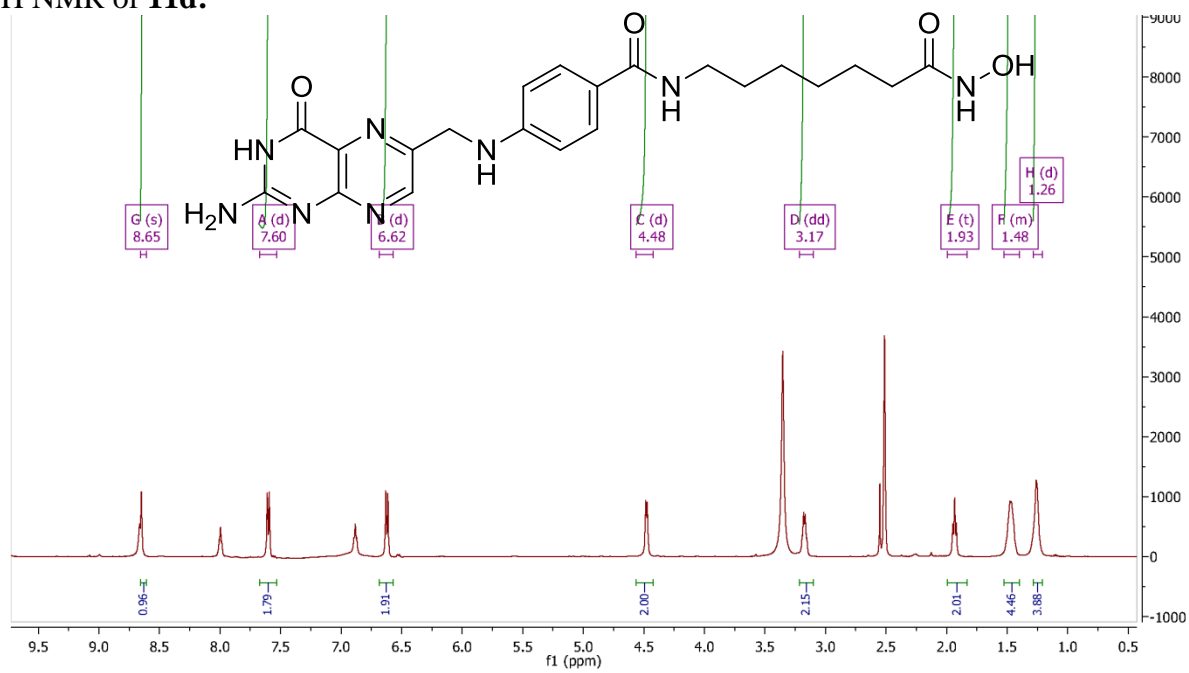
¹H NMR of **11c**:



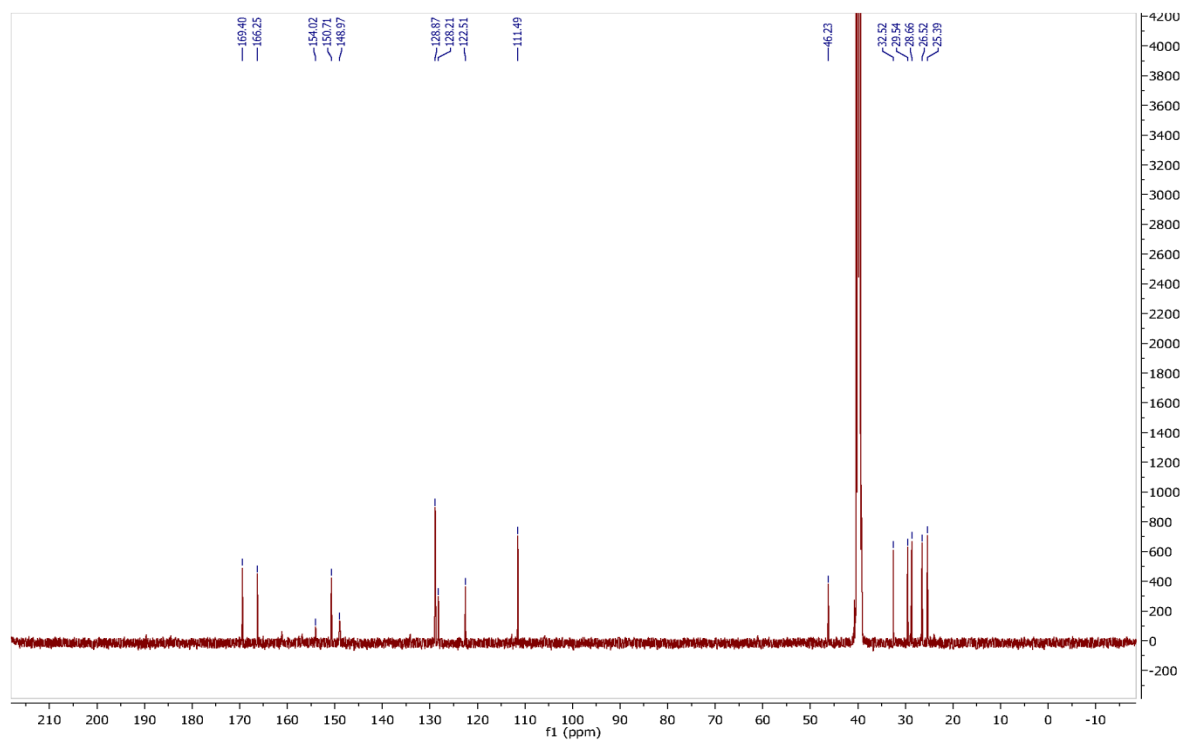
¹³C NMR of **11c**:



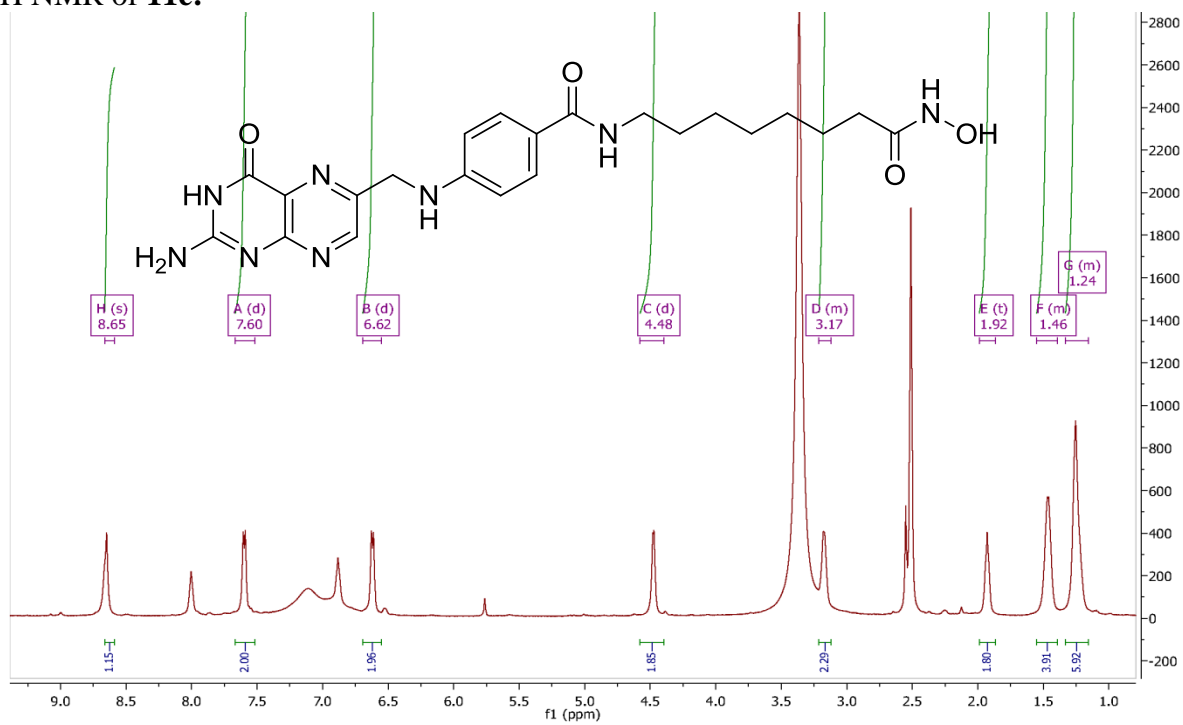
¹H NMR of **11d**:



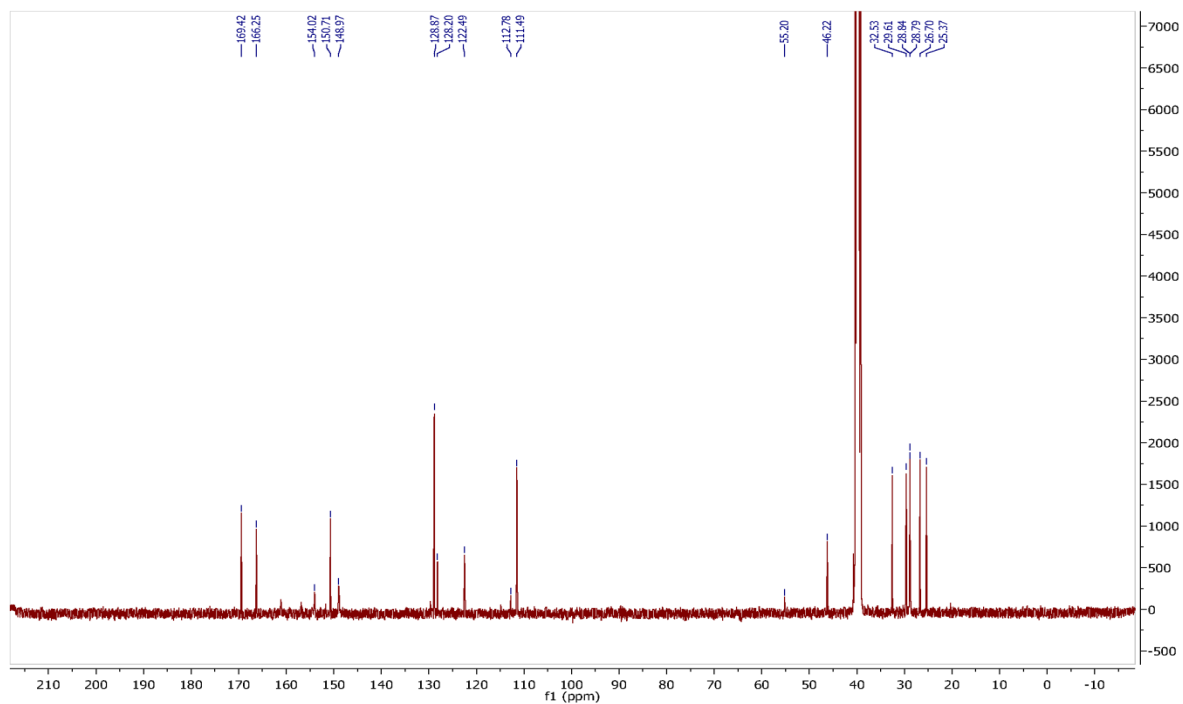
¹³C NMR of **11d**:



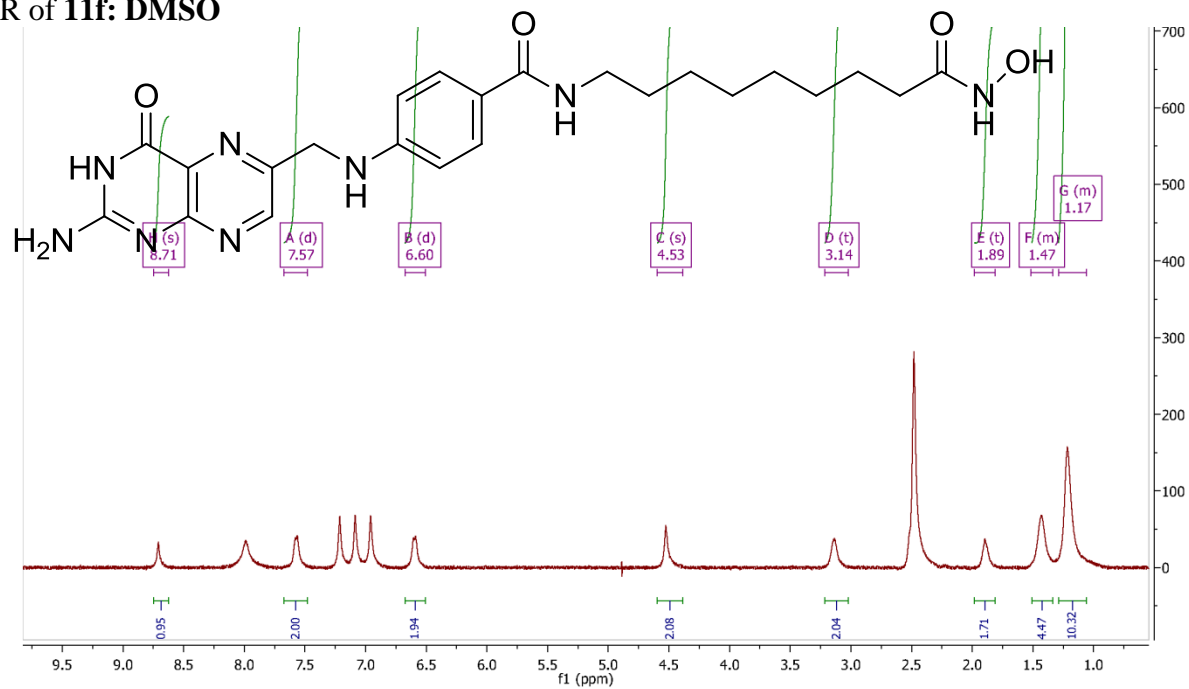
¹H NMR of **11e**:



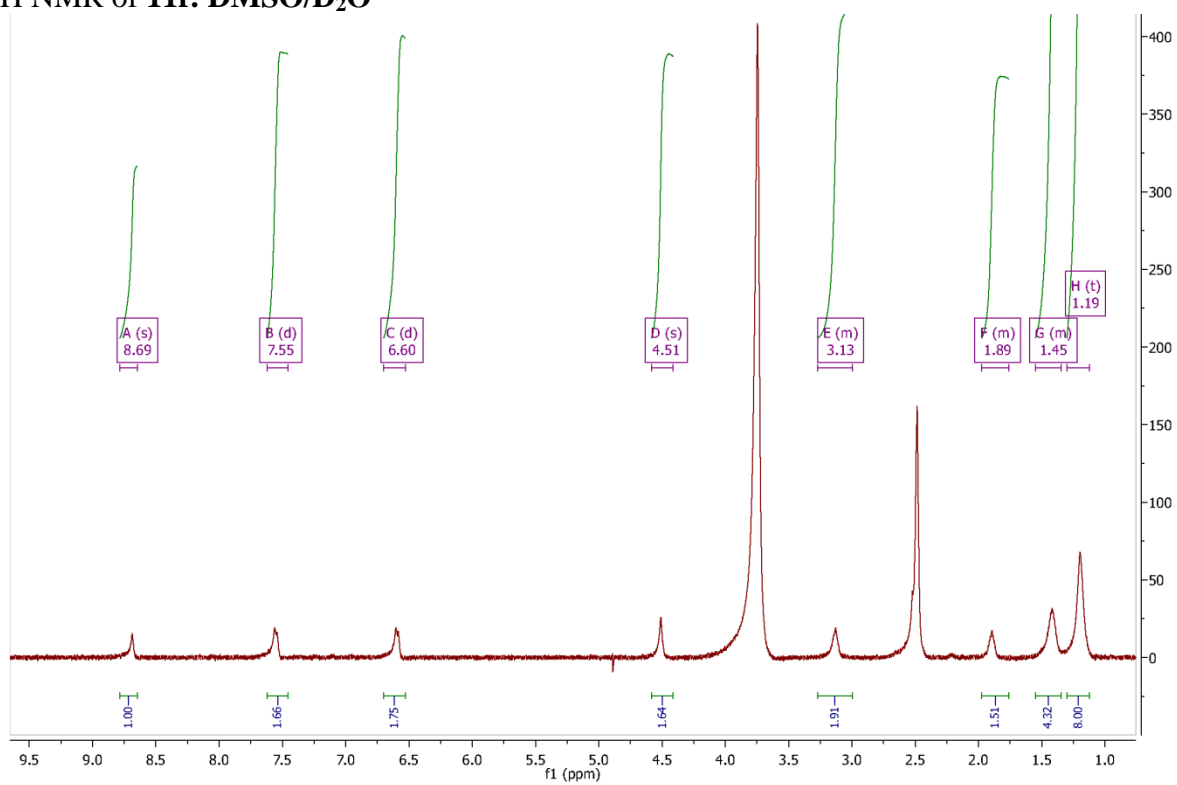
¹³C NMR of **11e**:



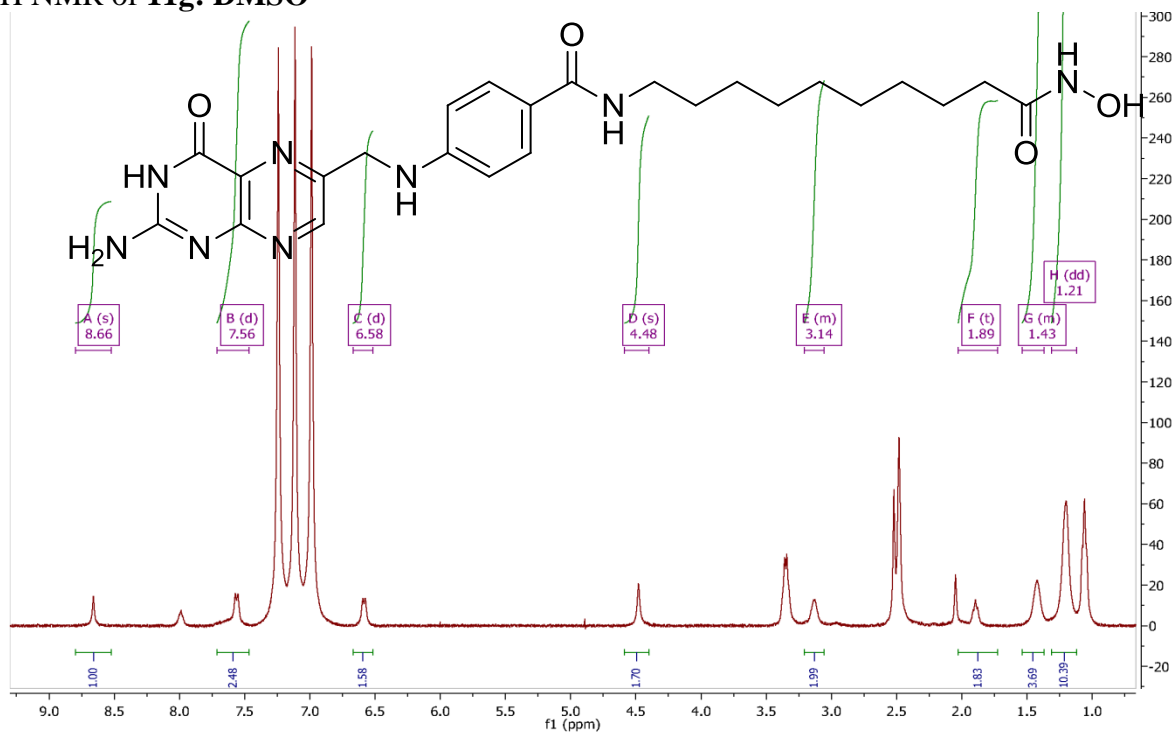
¹H NMR of 11f: DMSO



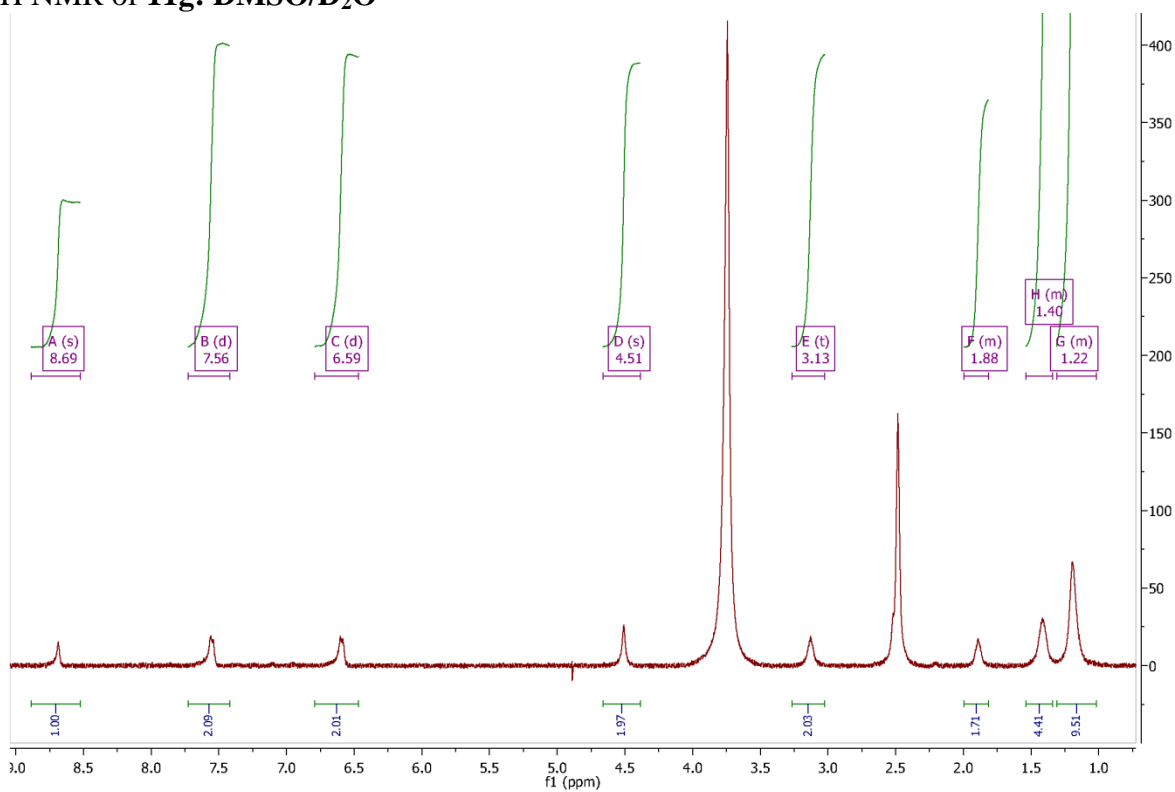
¹H NMR of 11f: DMSO/D₂O



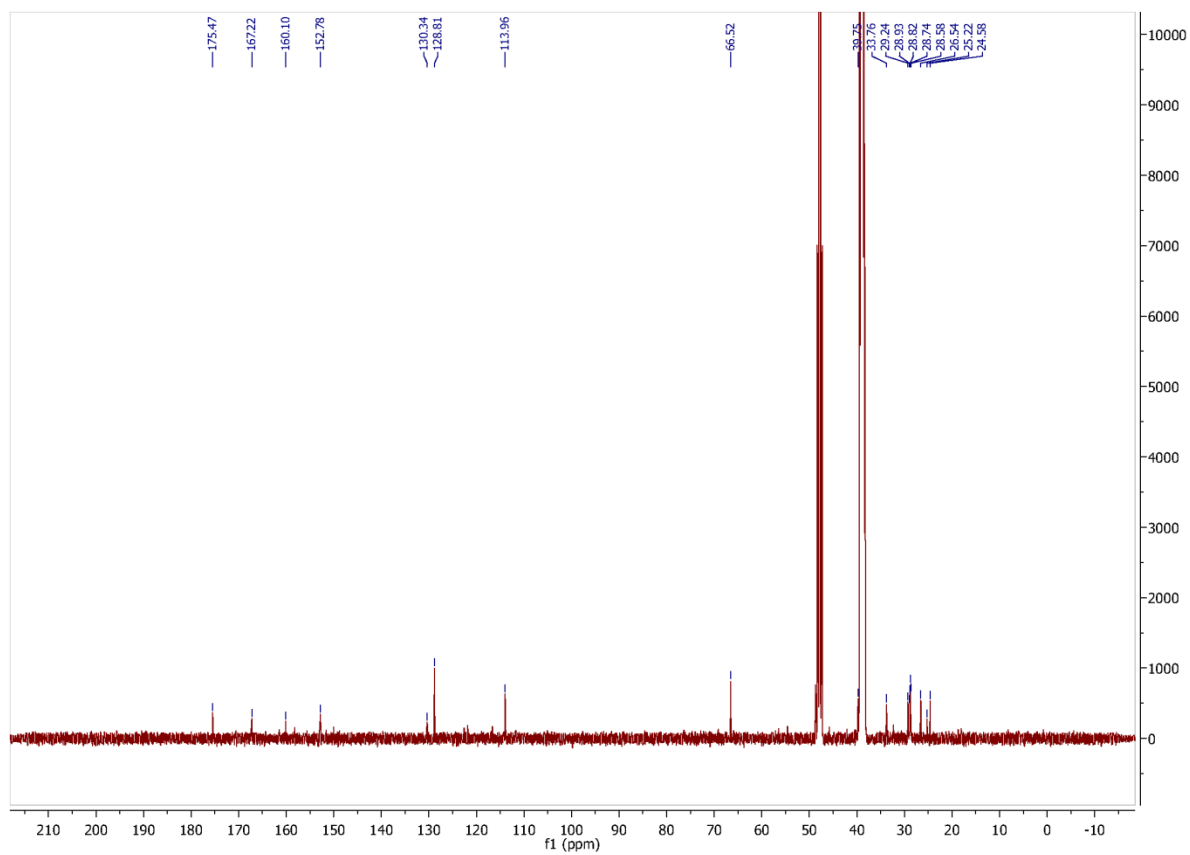
¹H NMR of 11g: DMSO



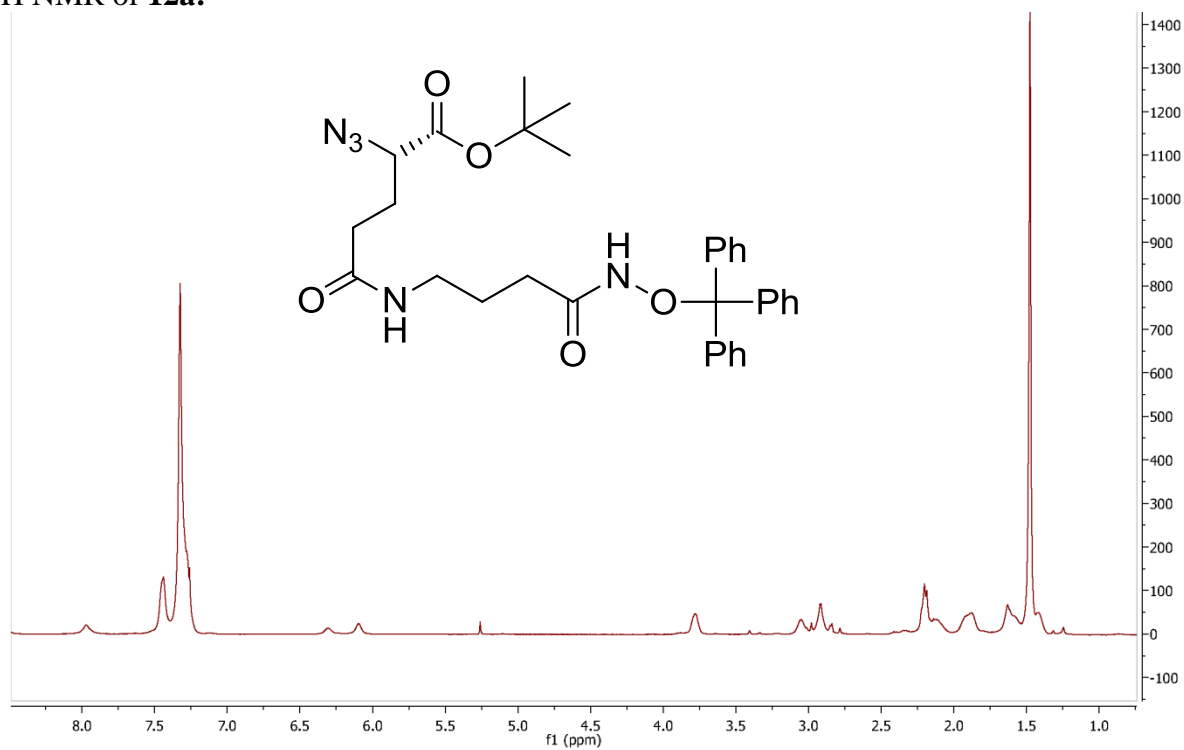
¹H NMR of 11g: DMSO/D₂O



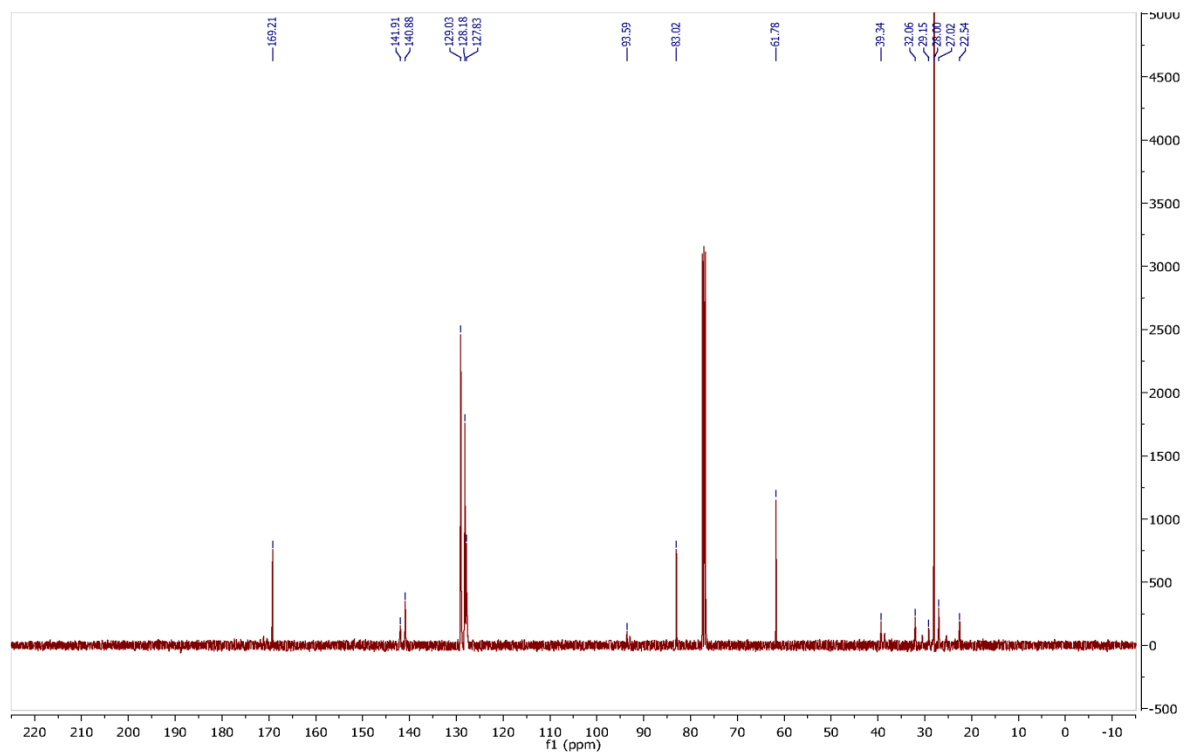
^{13}C NMR of **11g**:



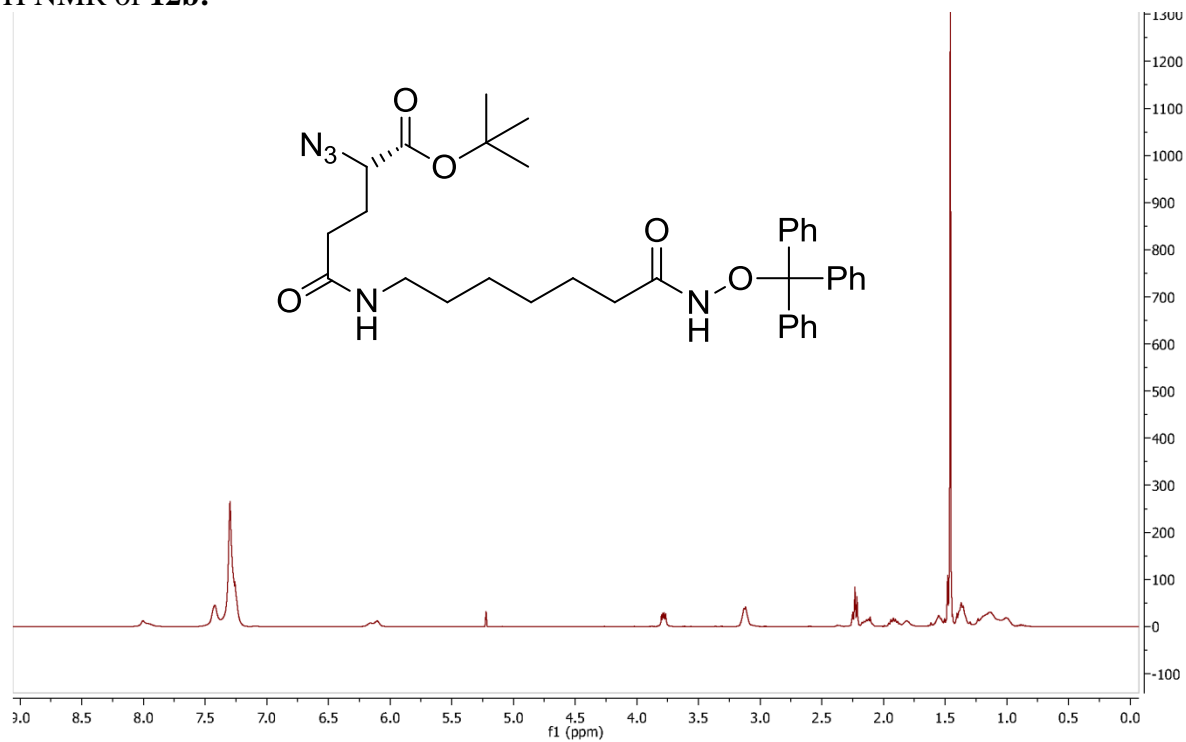
¹H NMR of **12a**:



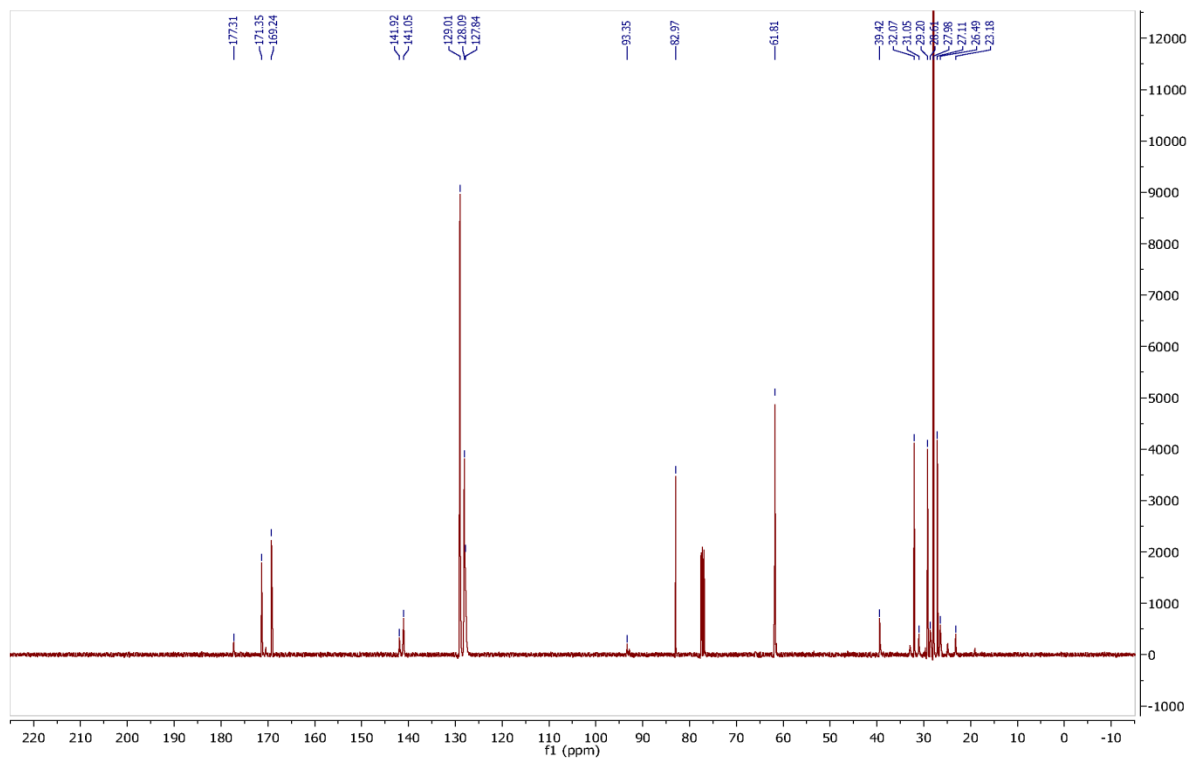
¹³C NMR of **12a**:



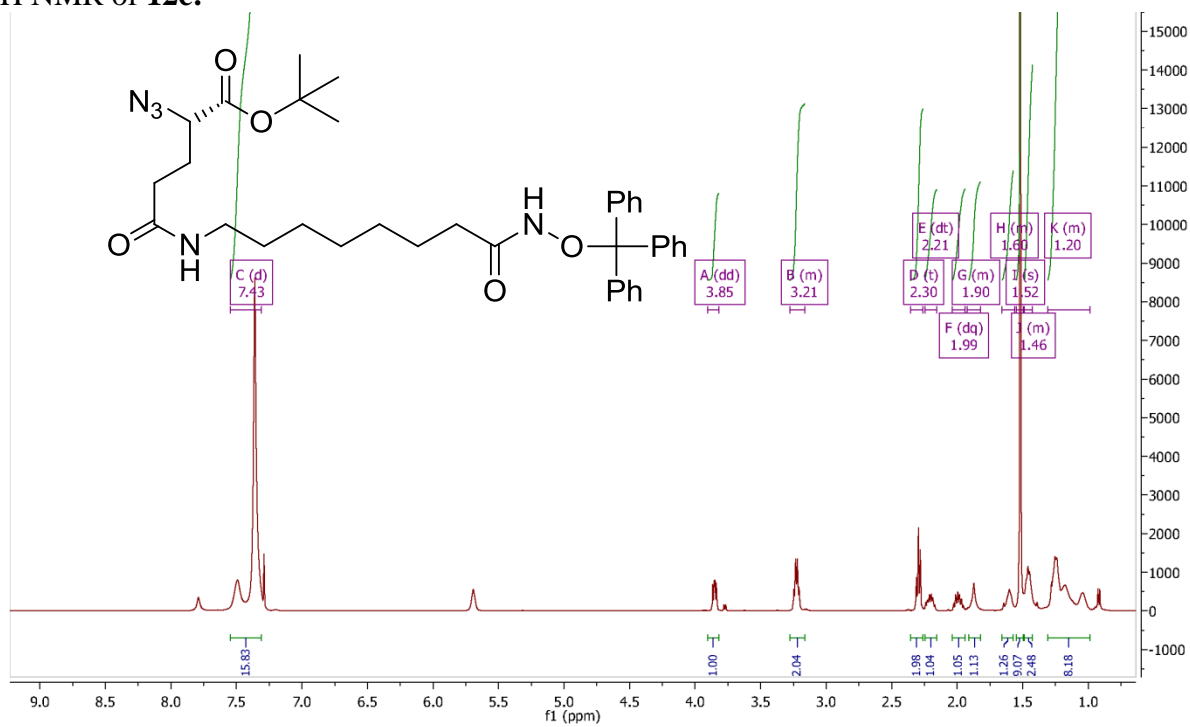
¹H NMR of **12b**:



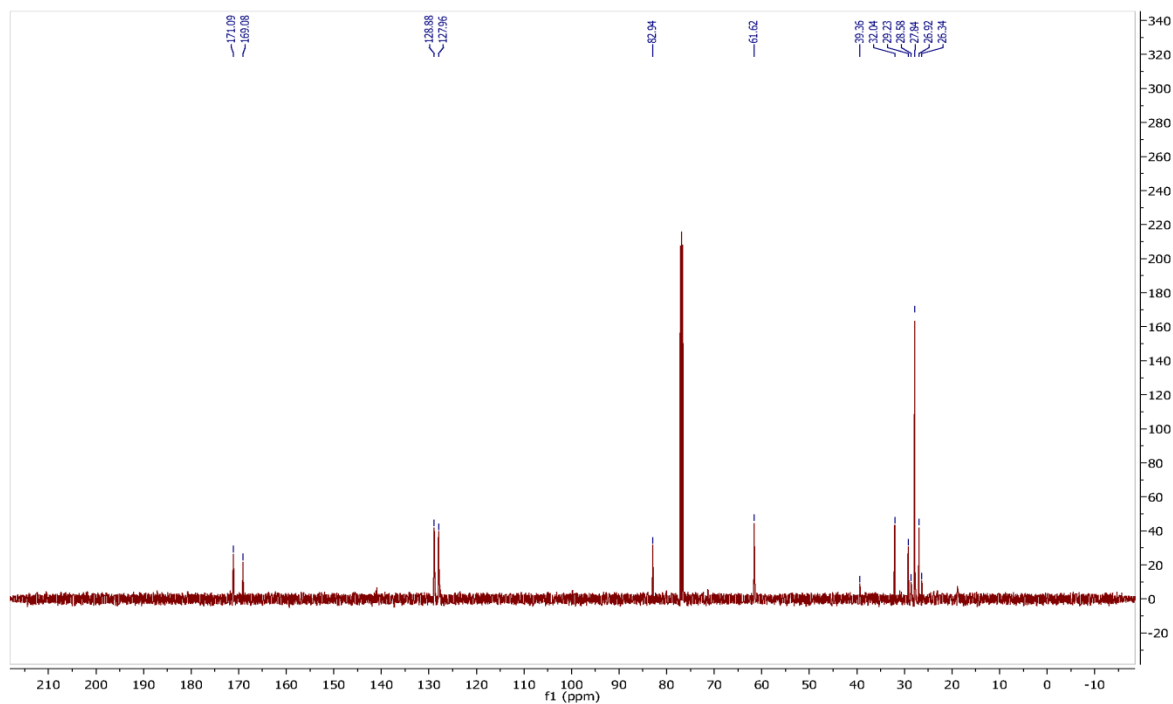
¹³C NMR of **12b**:



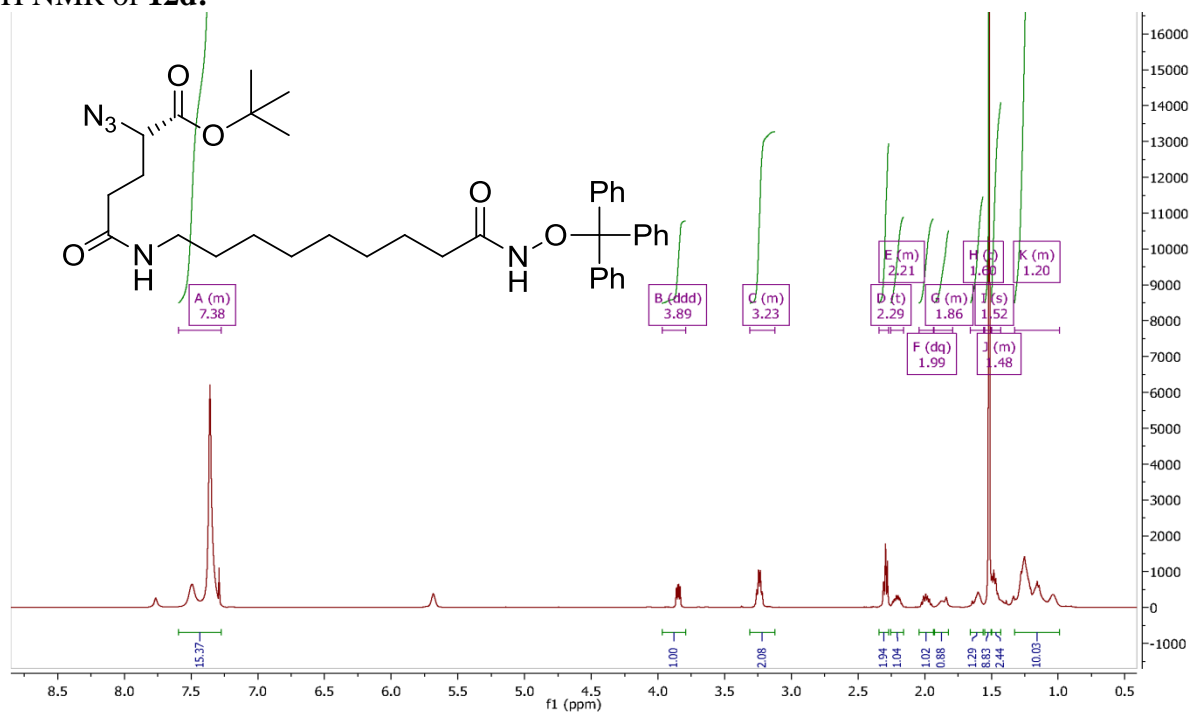
¹H NMR of **12c**:



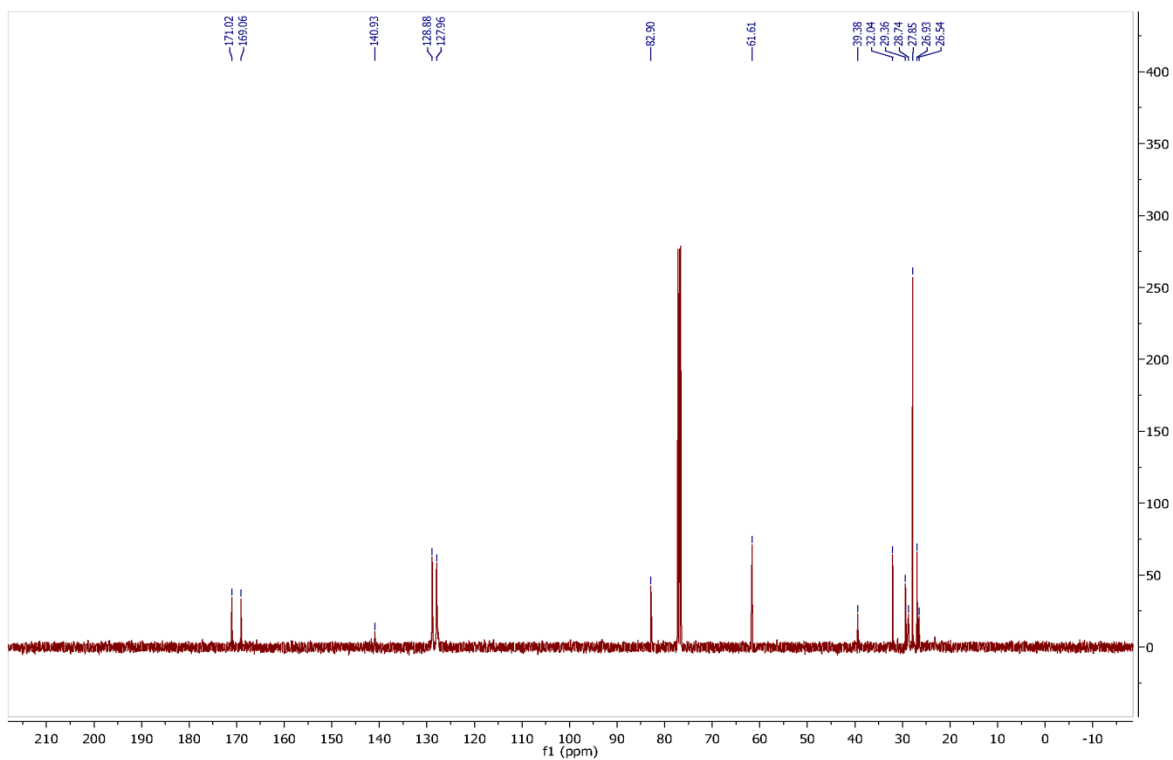
¹³C NMR of **12c**:



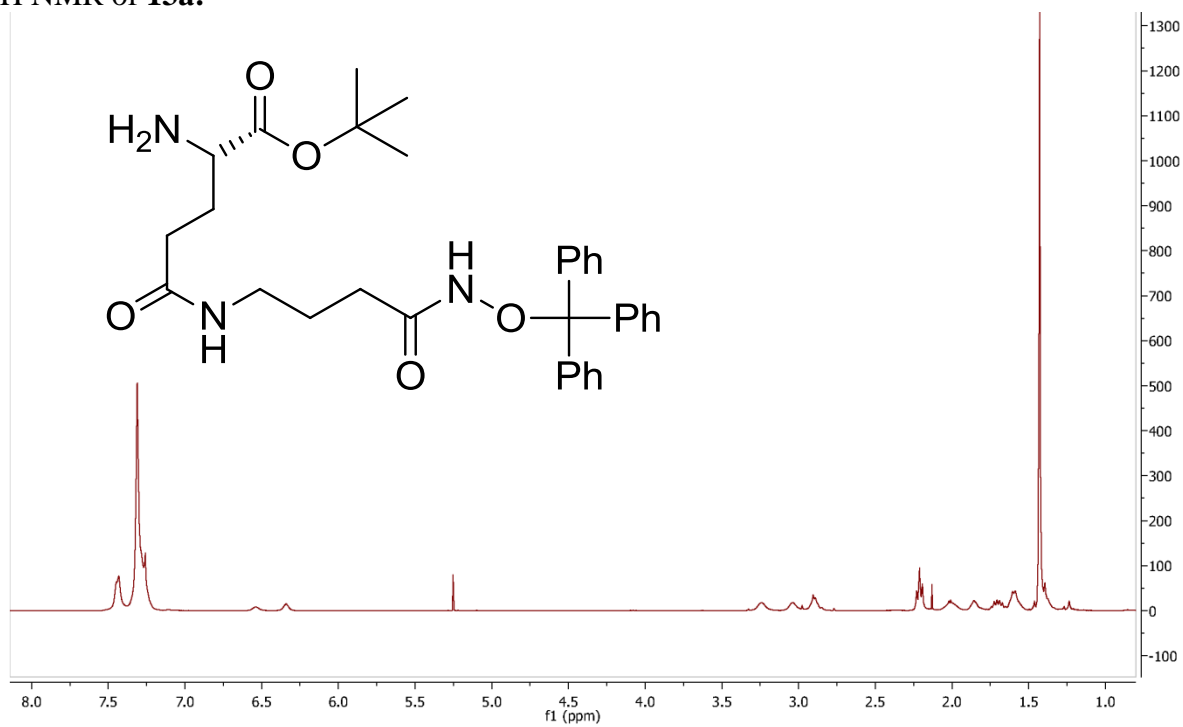
¹H NMR of **12d**:



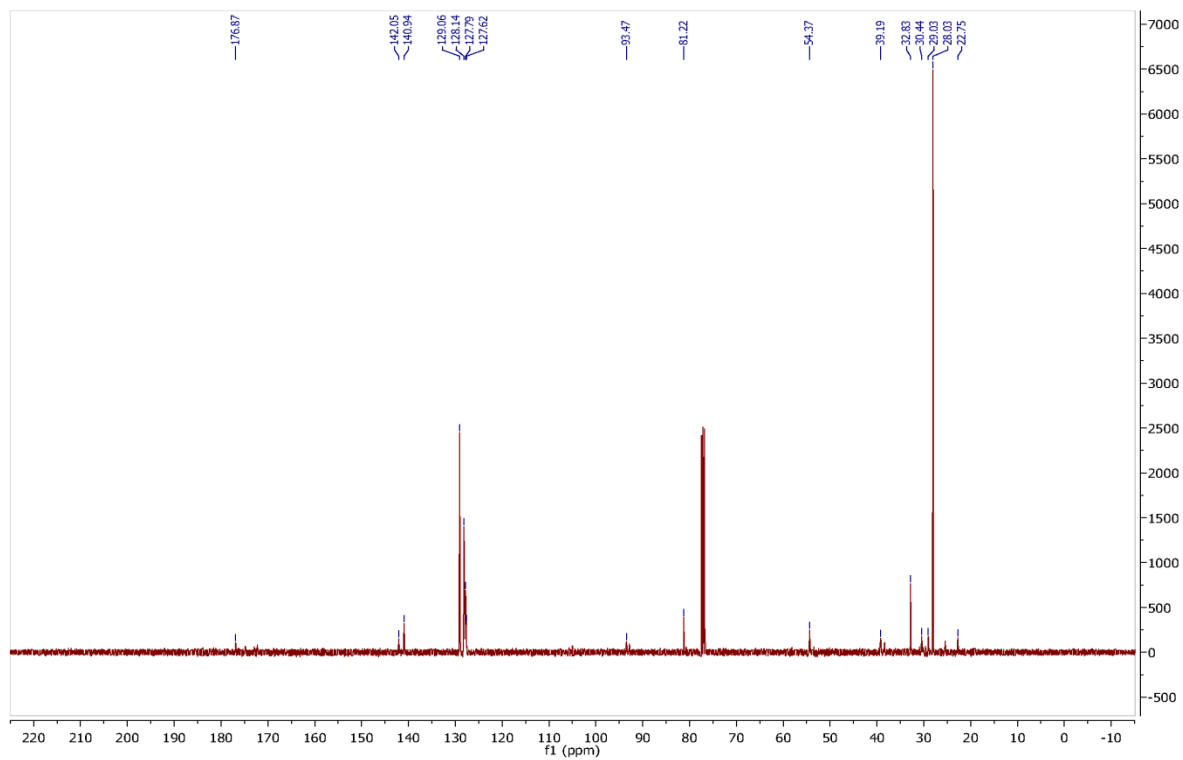
¹³C NMR of **12d**:



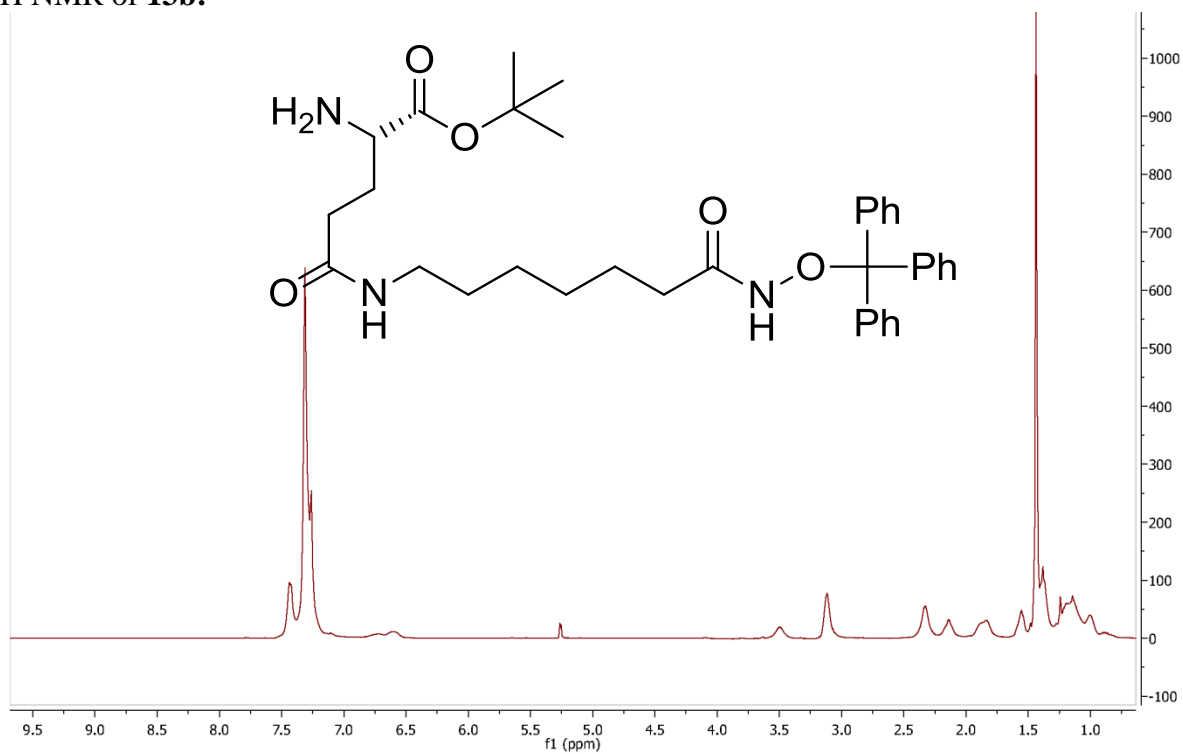
¹H NMR of **13a**:



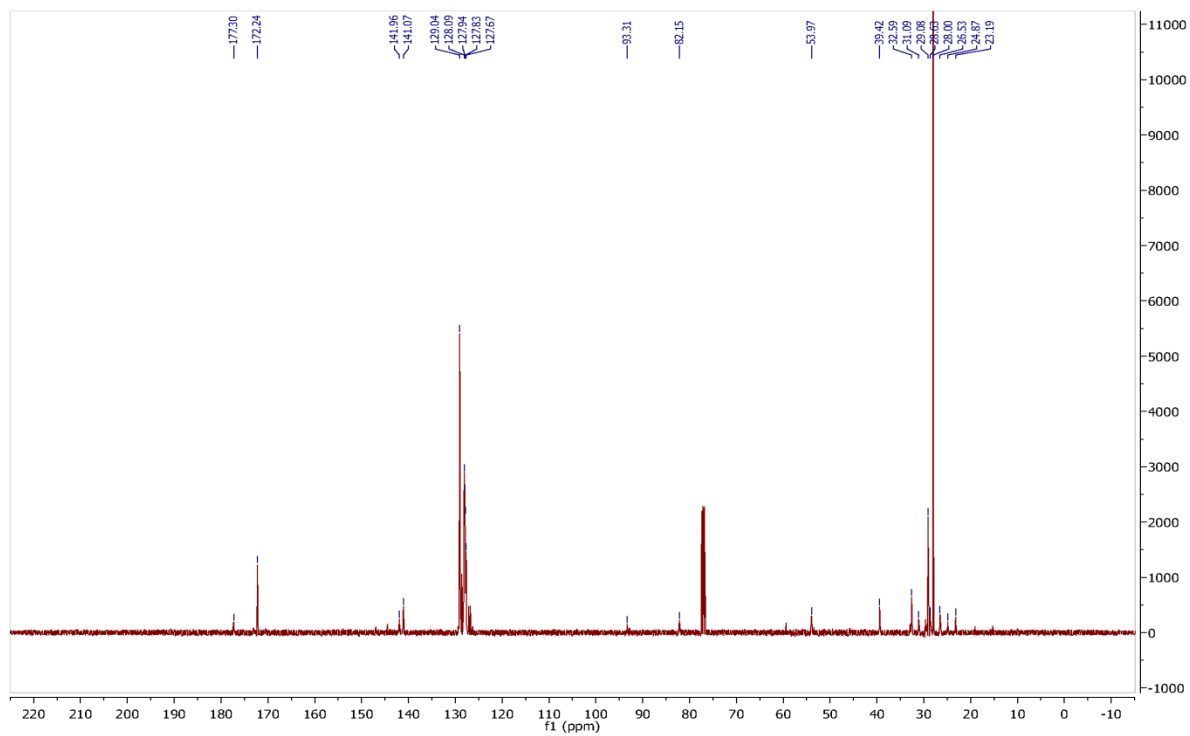
¹³C NMR of **13a**:



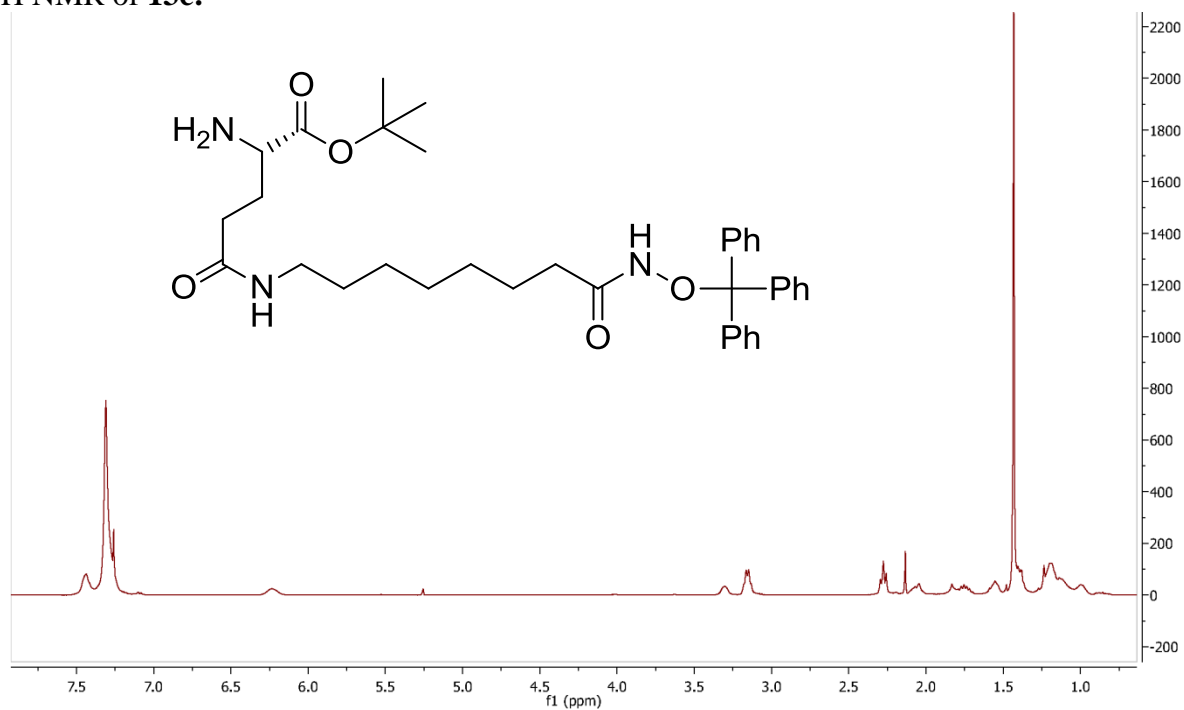
¹H NMR of **13b**:



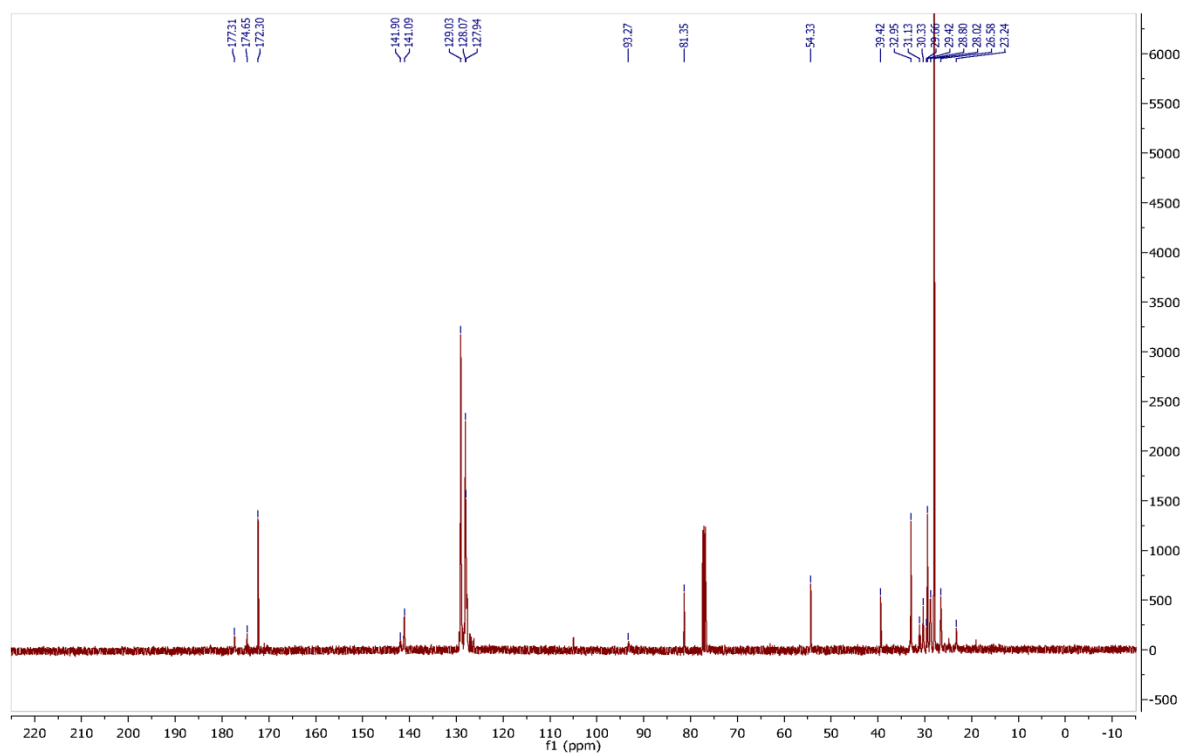
¹³C NMR of **13b**:



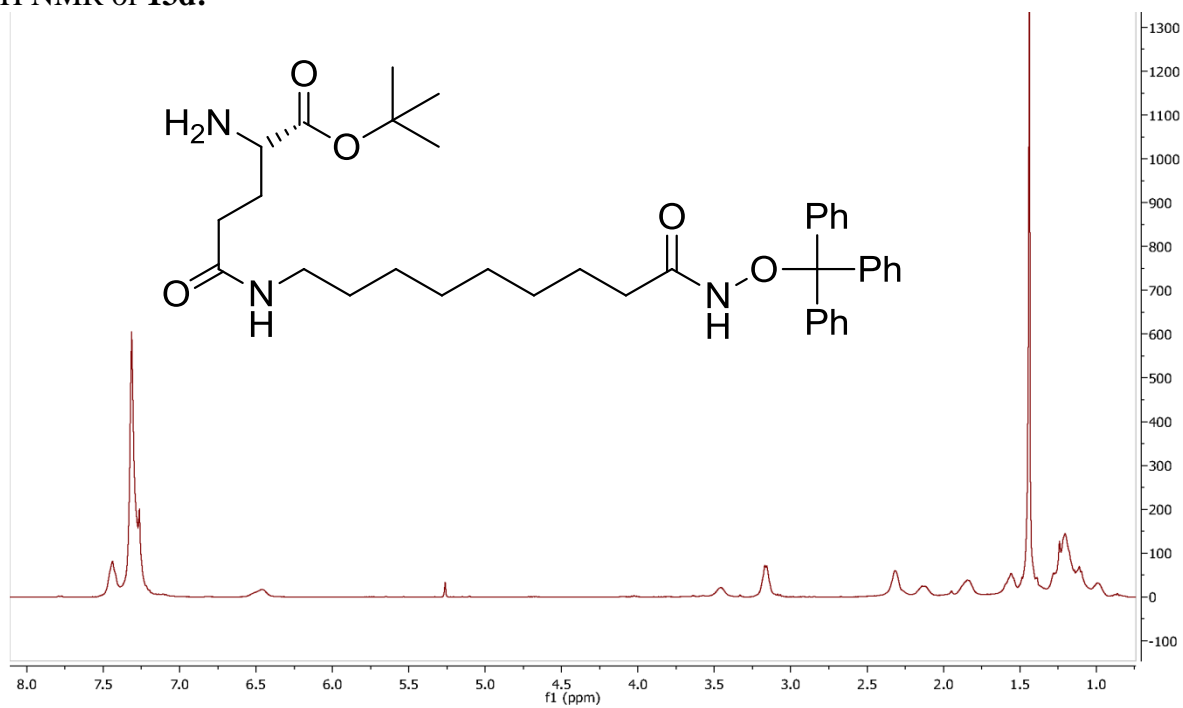
¹H NMR of **13c**:



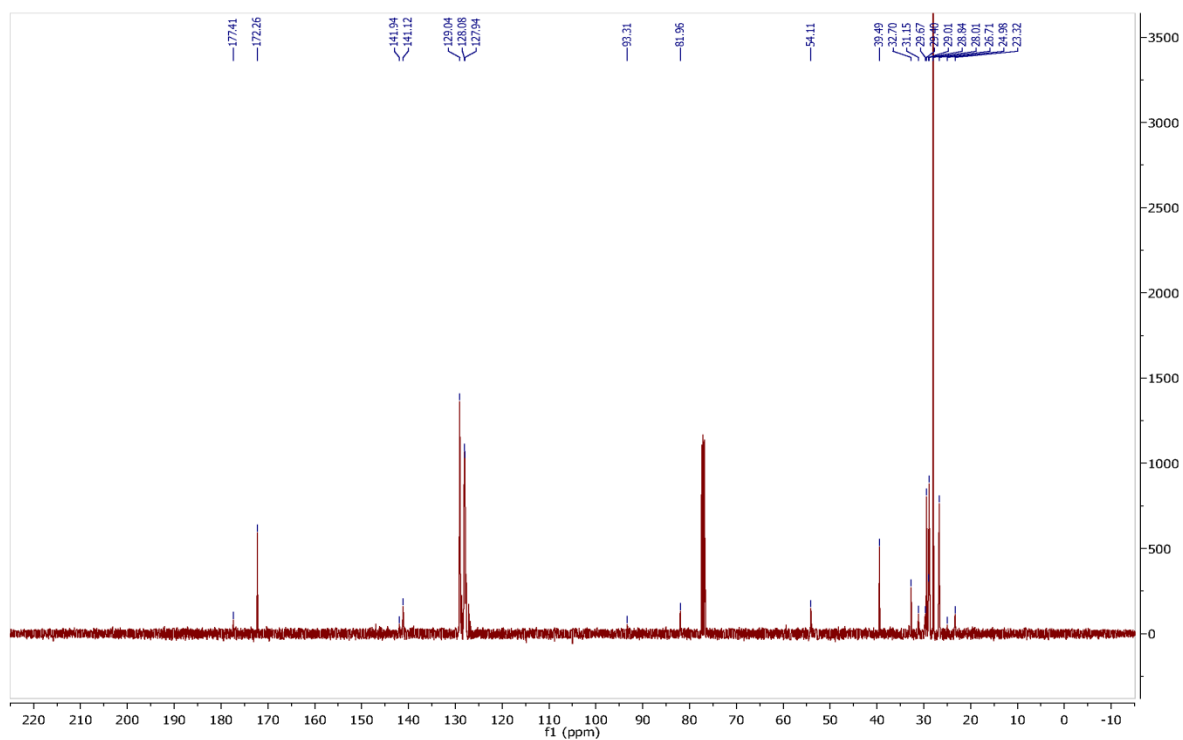
¹³C NMR of **13c**:



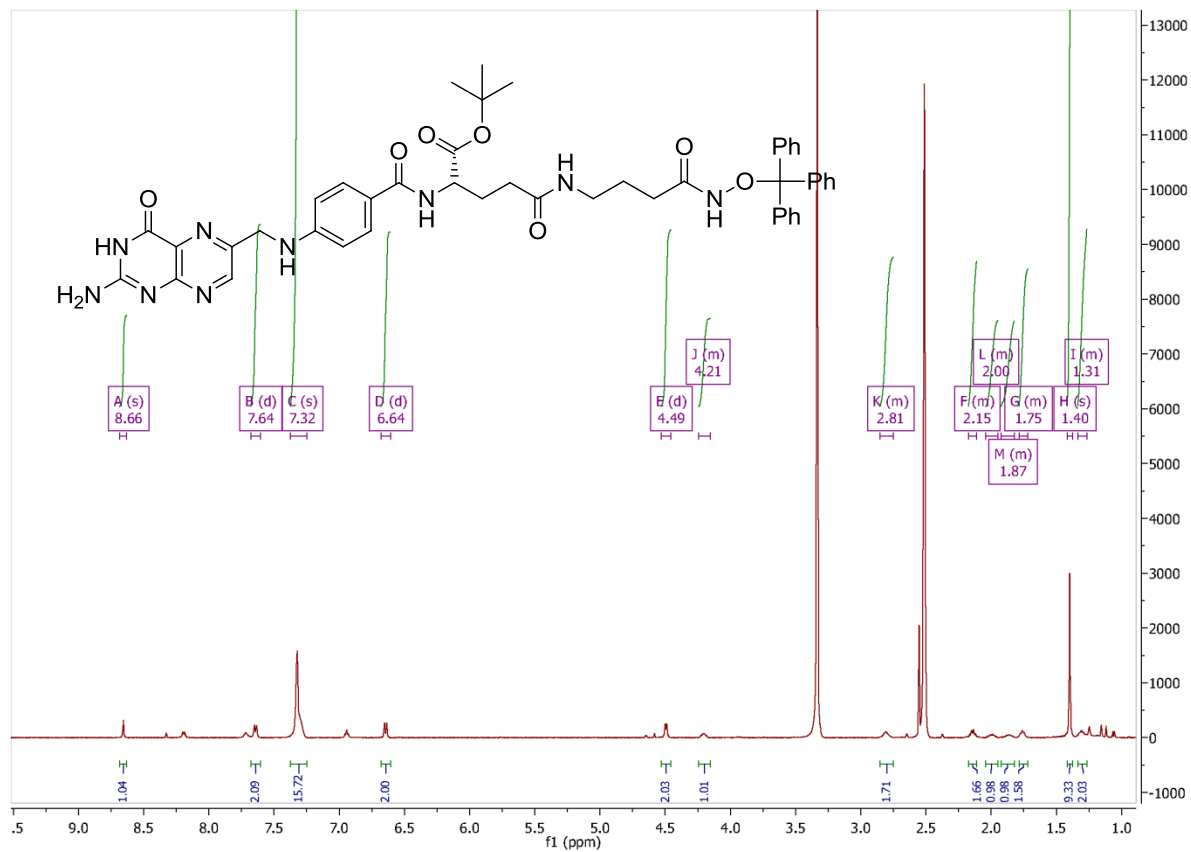
¹H NMR of **13d**:



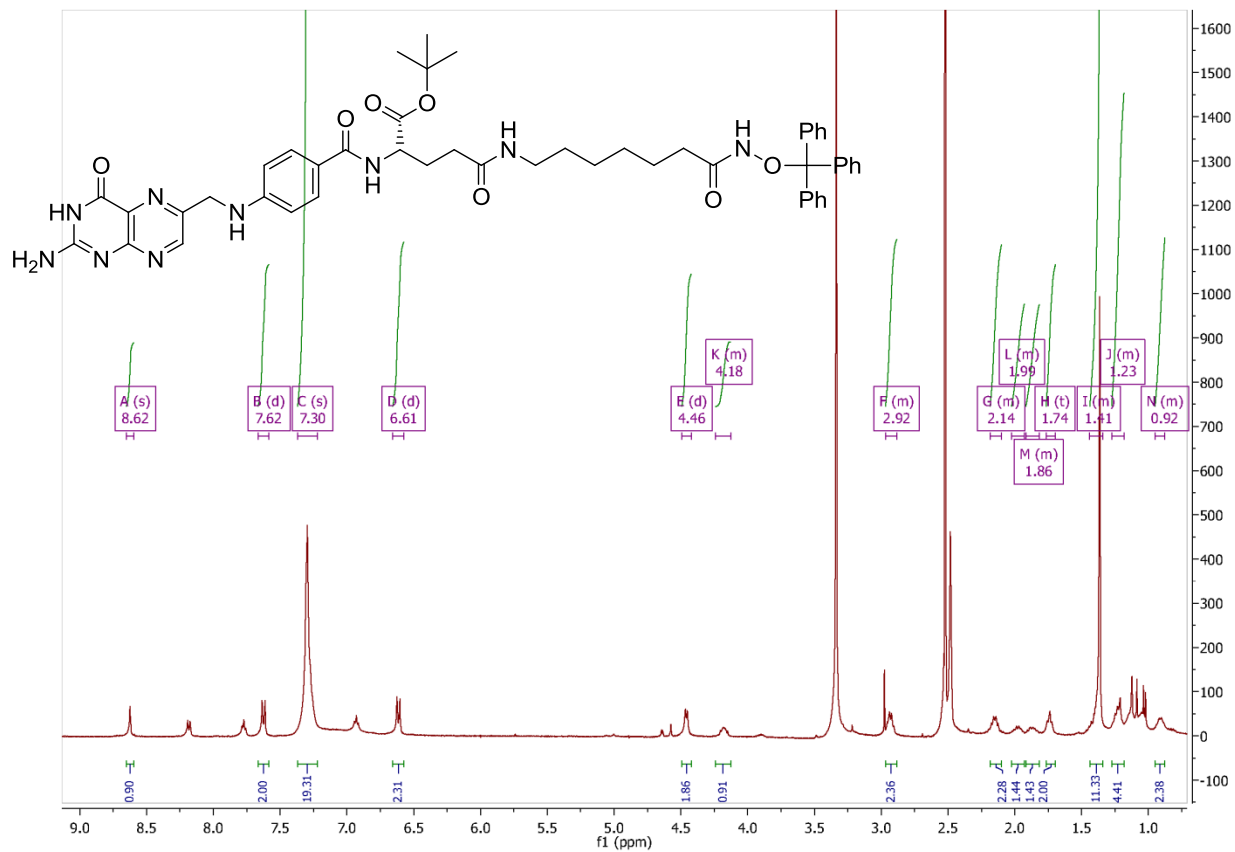
¹³C NMR of **13d**:



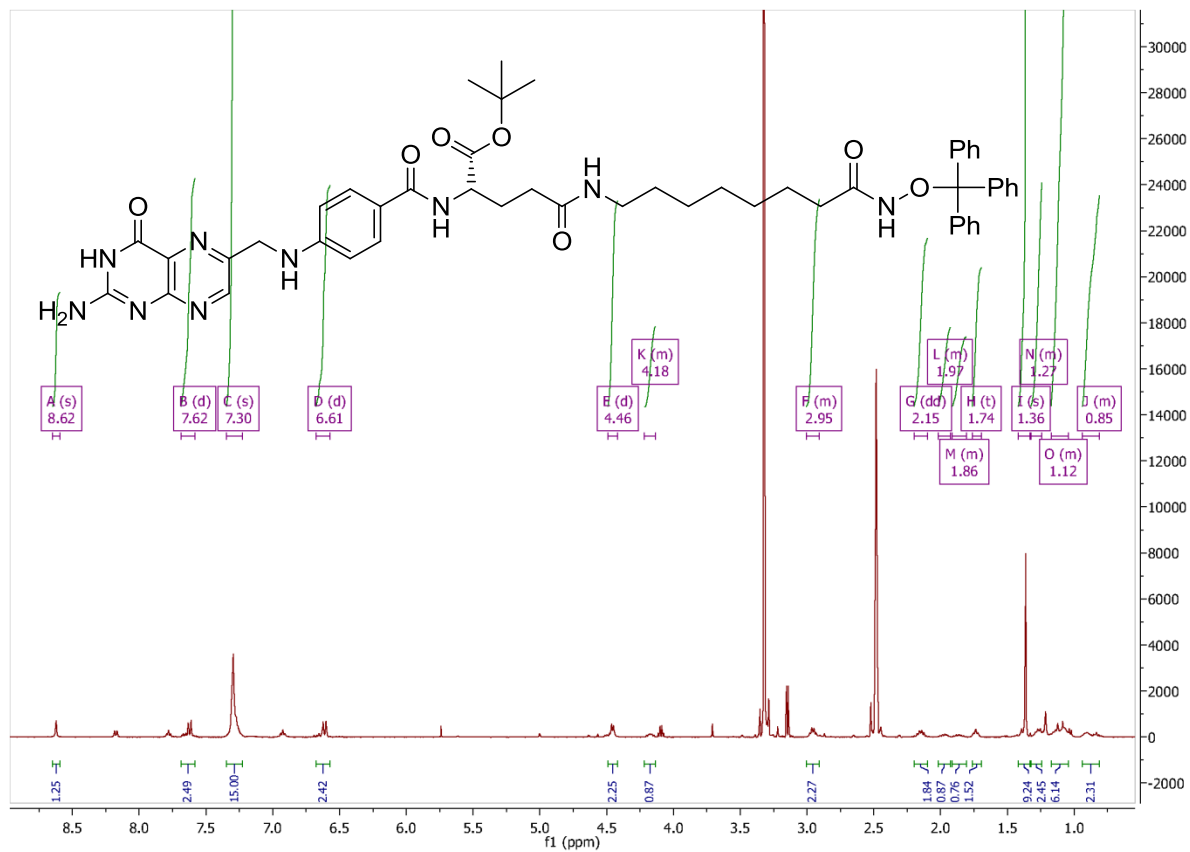
¹H NMR of **14a**:



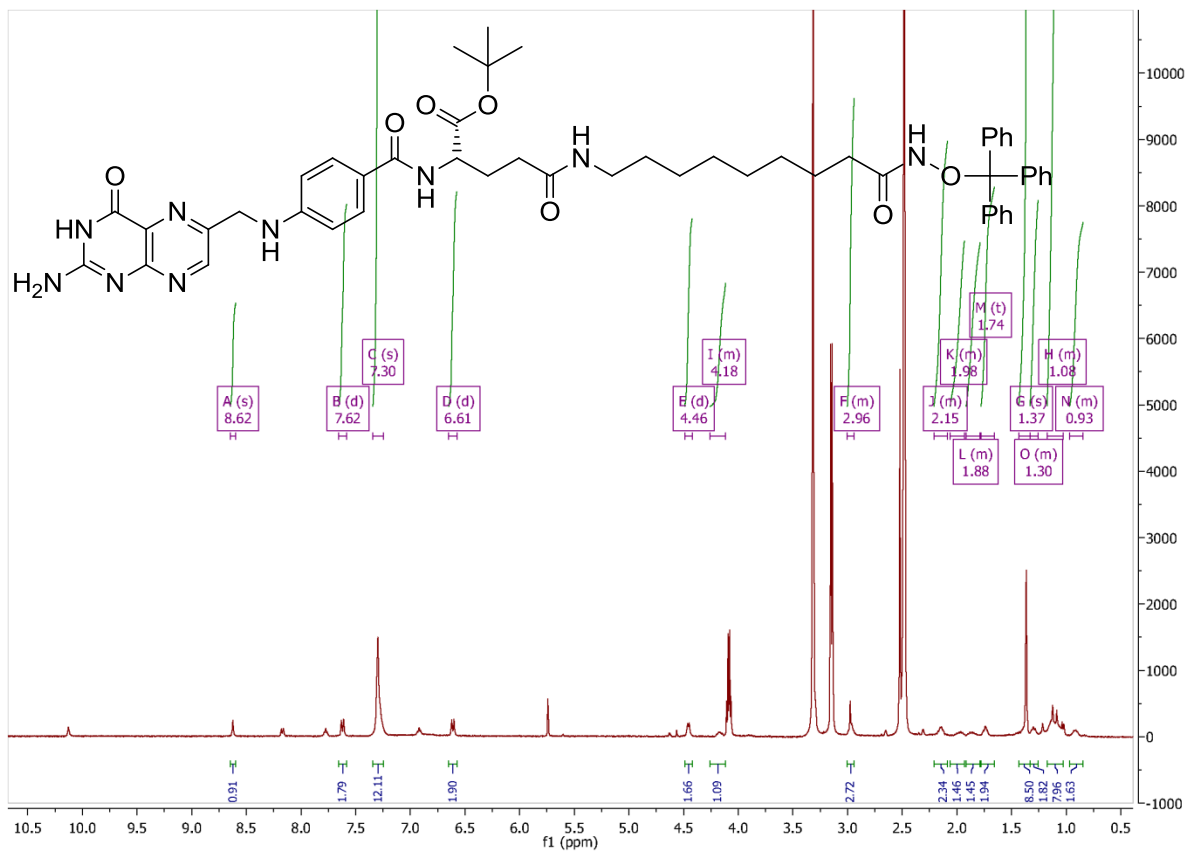
¹H NMR of **14b**:



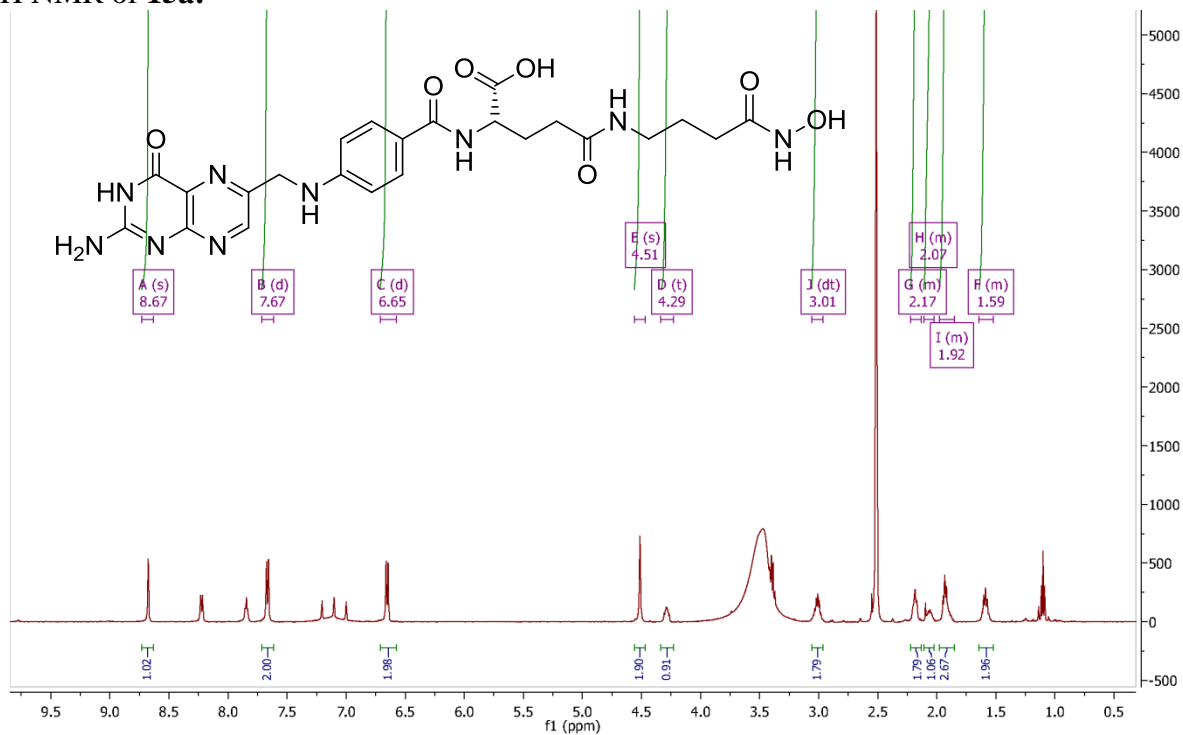
¹H NMR of **14c**:



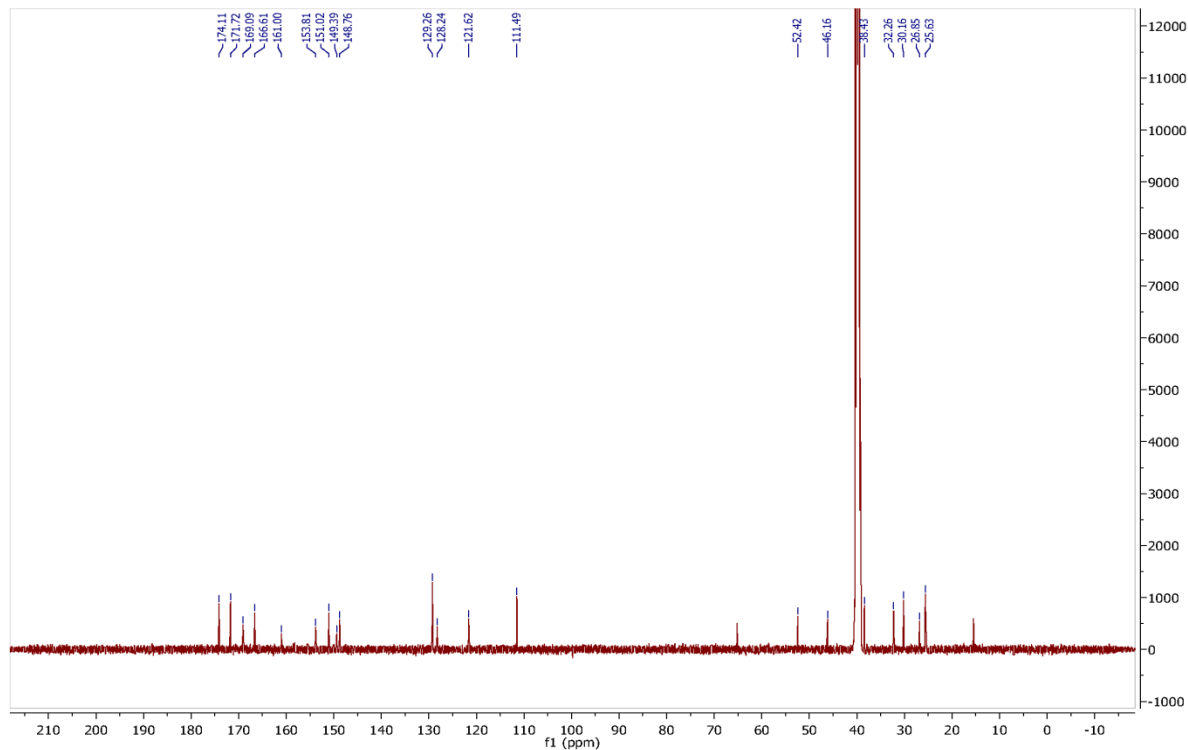
¹H NMR of **14d**:



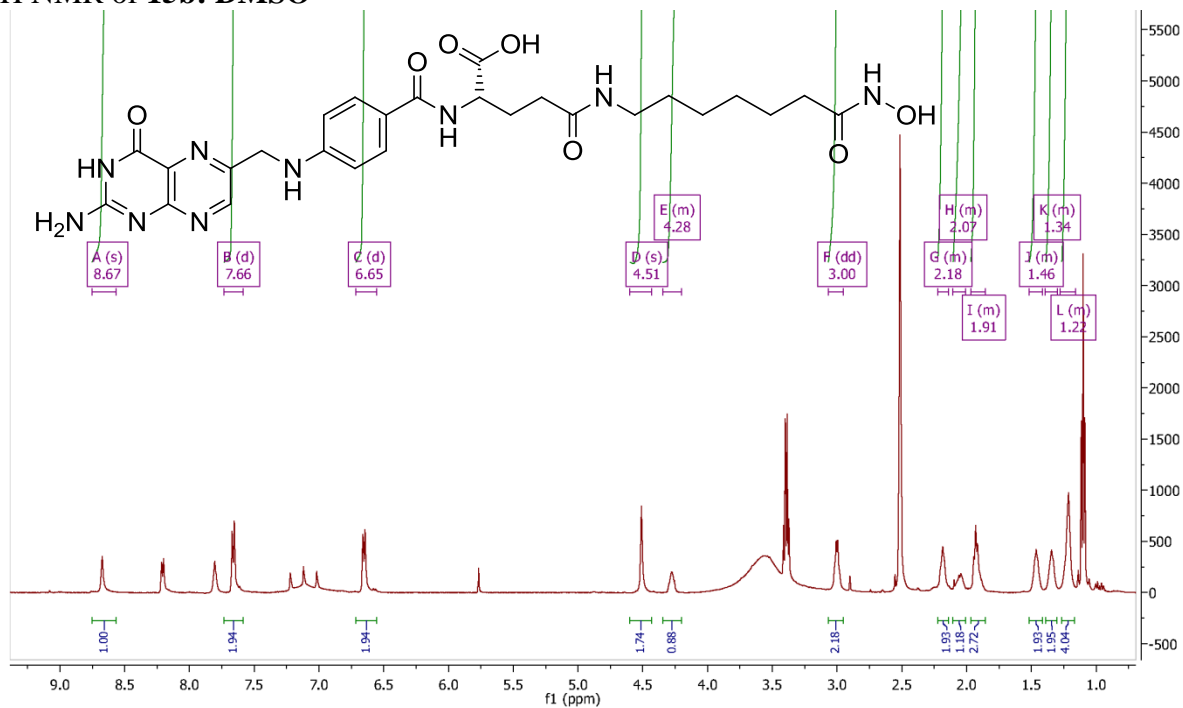
¹H NMR of **15a**:



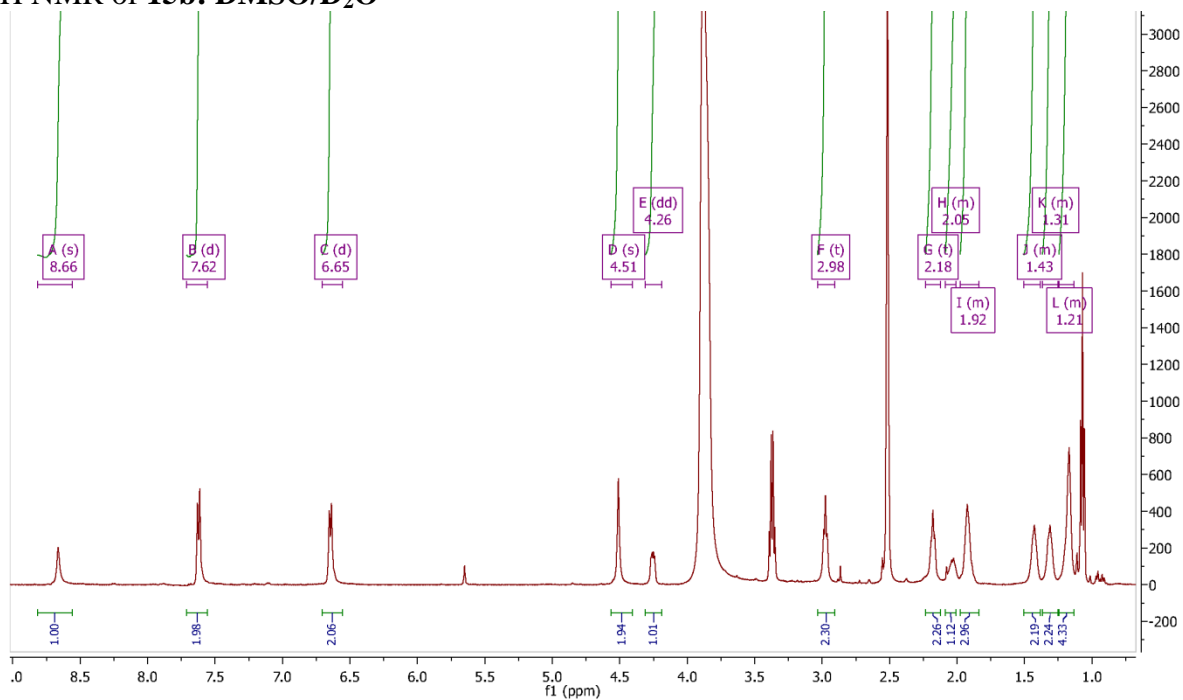
¹³C NMR of **15a**:



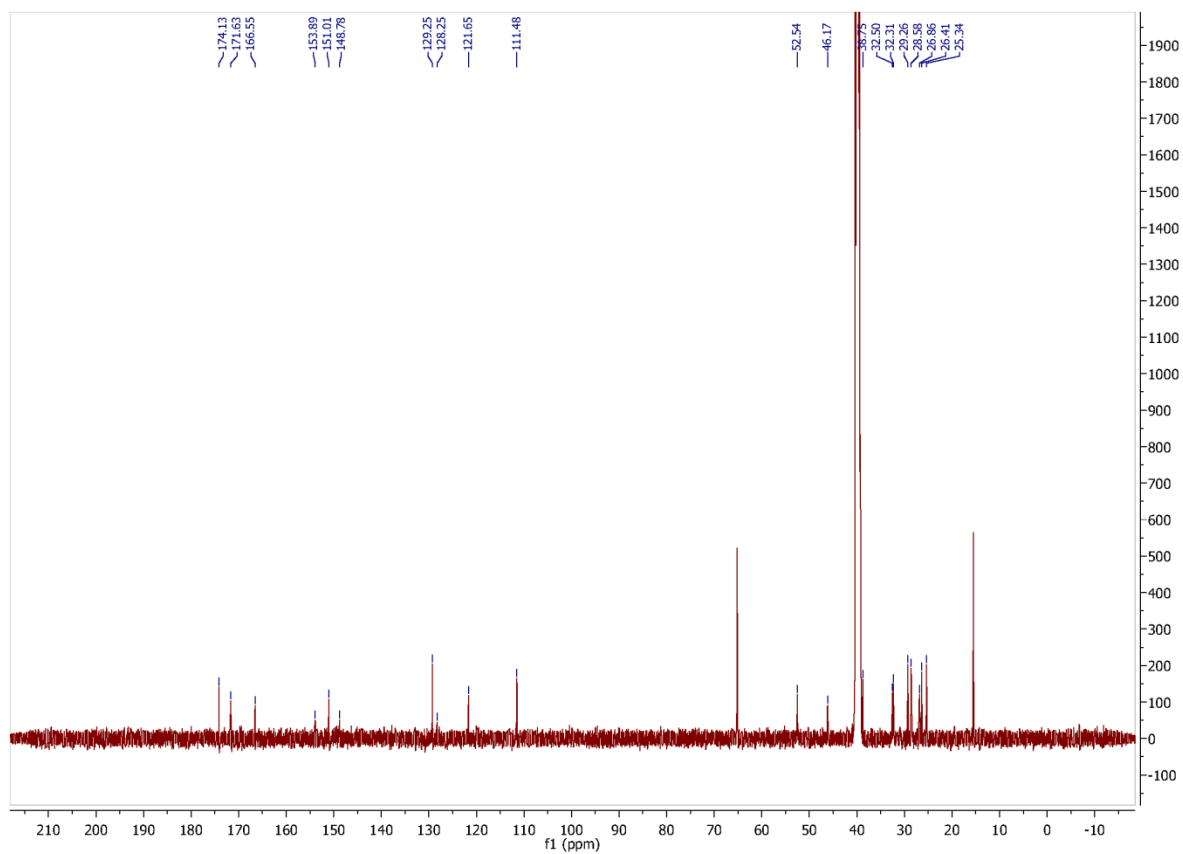
¹H NMR of 15b: DMSO



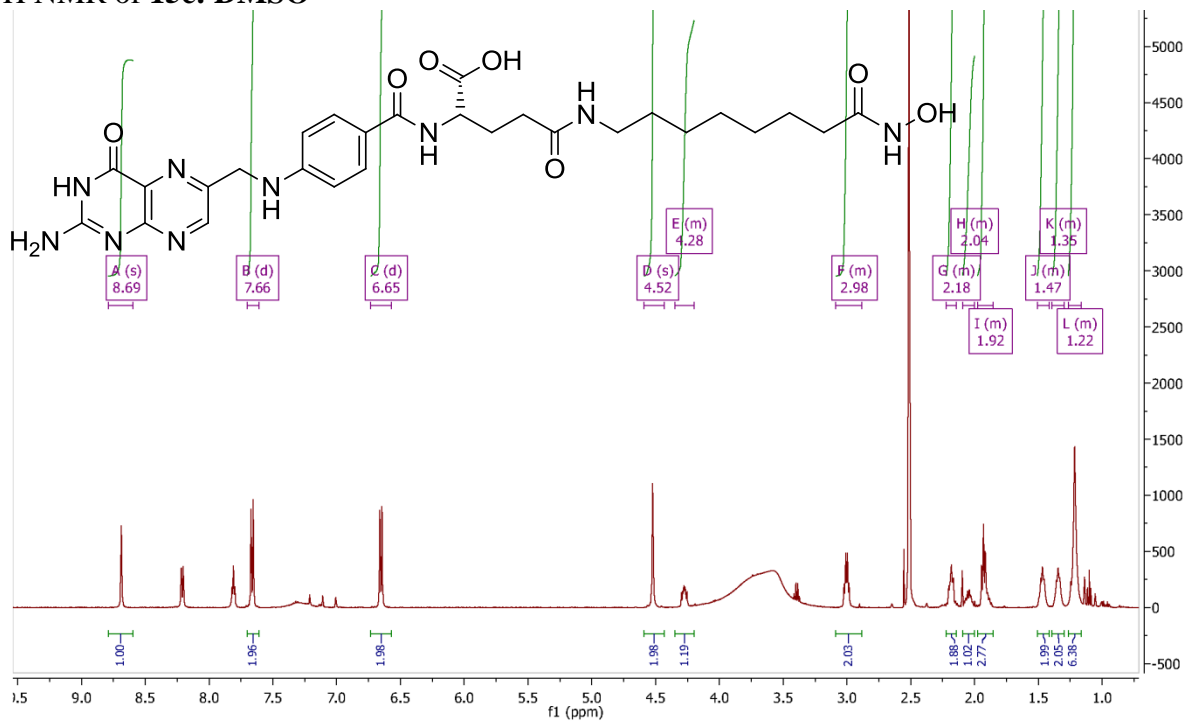
¹H NMR of 15b: DMSO/D₂O



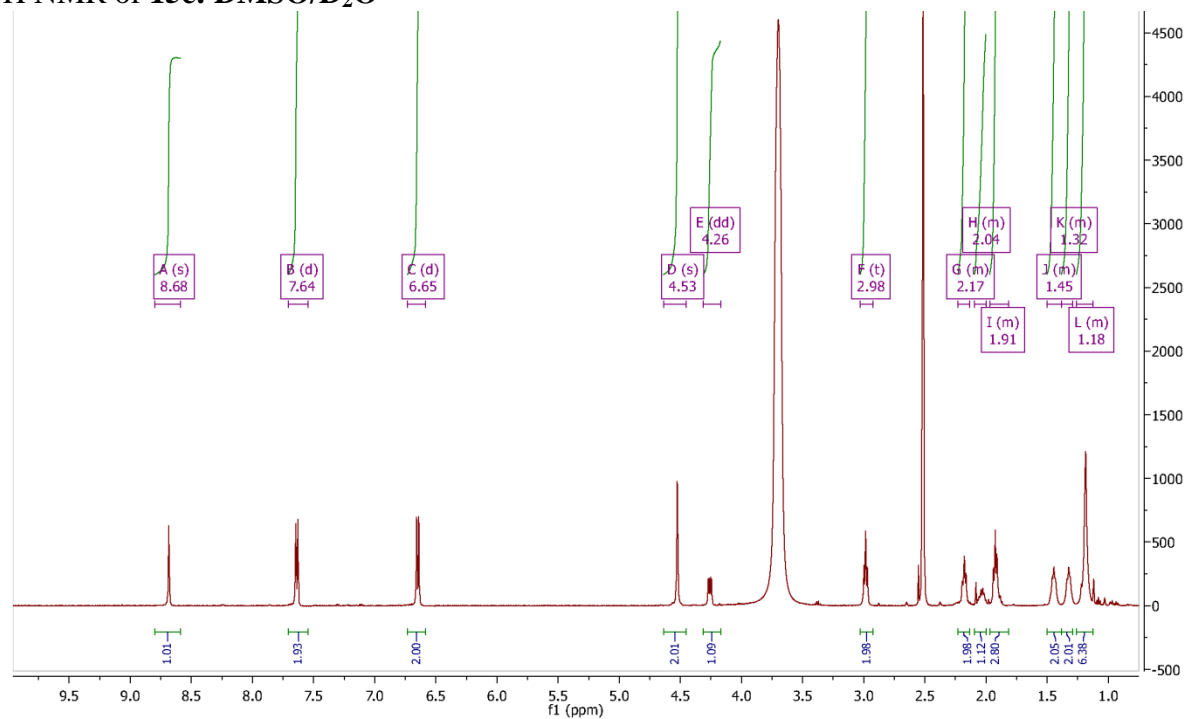
^{13}C NMR of **15b**:



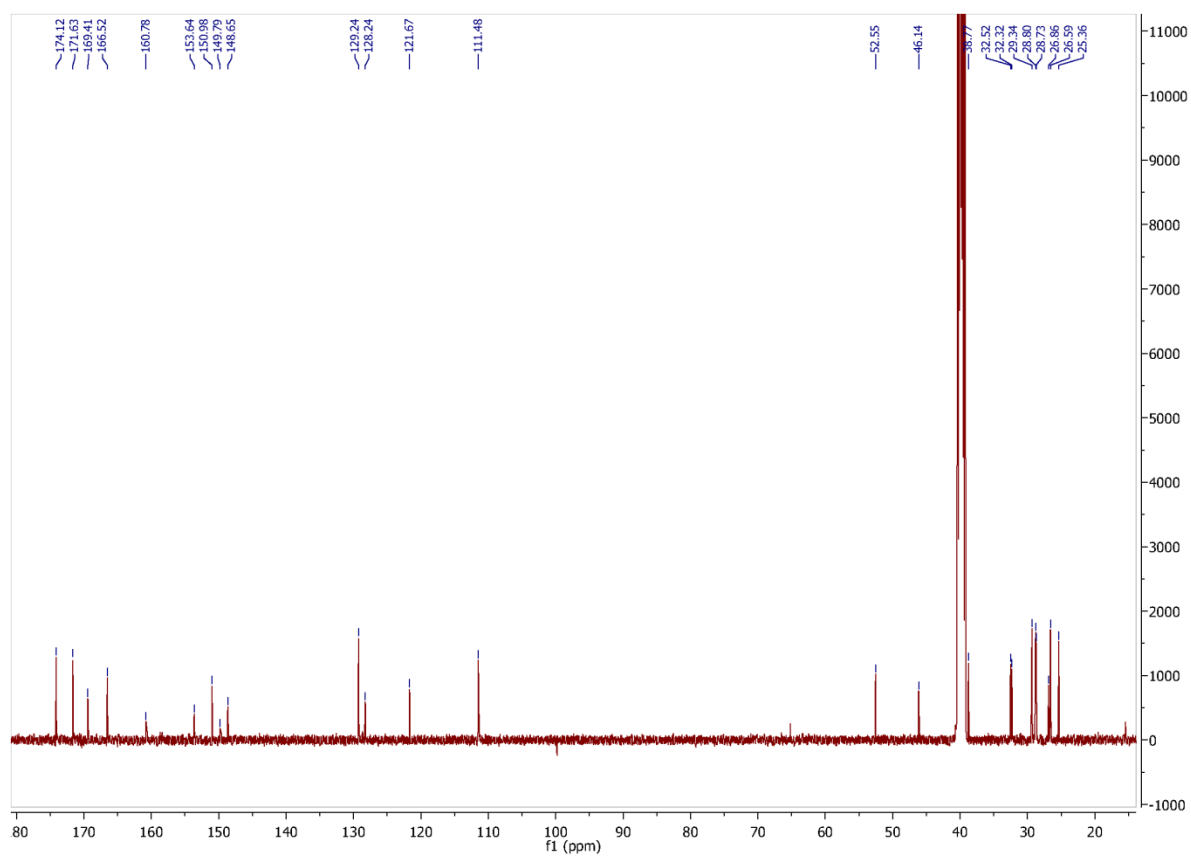
¹H NMR of 15c: DMSO



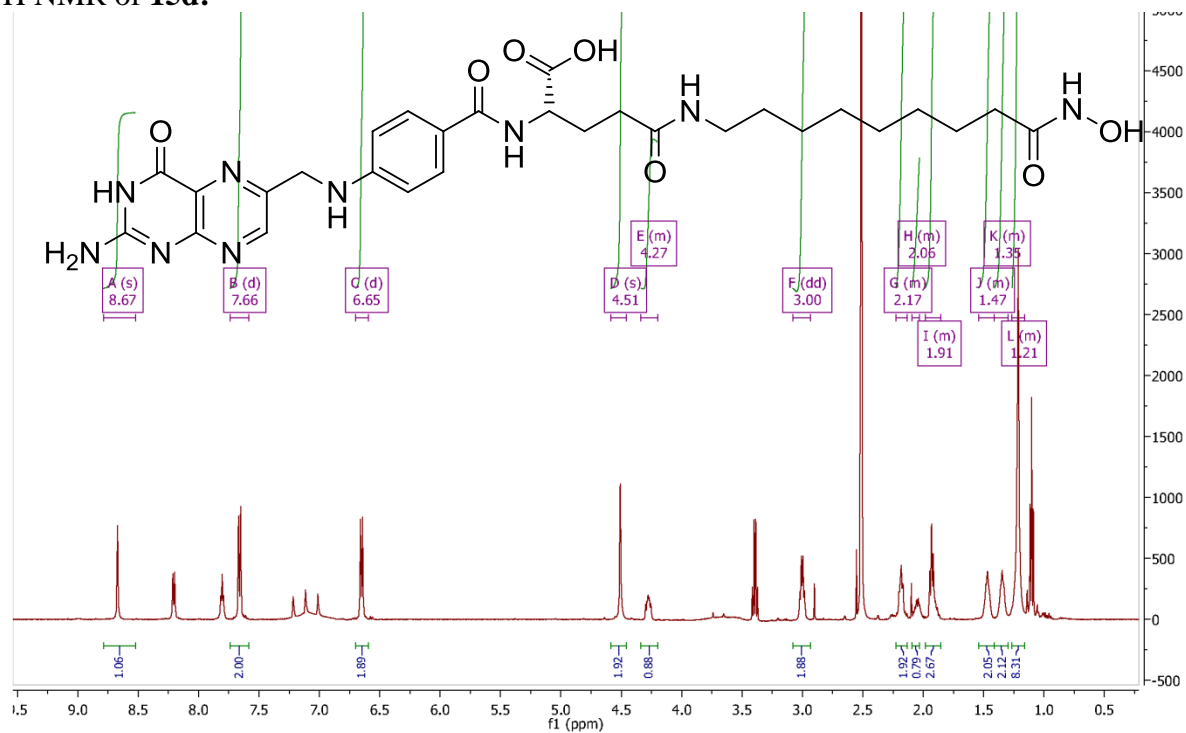
¹H NMR of 15c: DMSO/D₂O



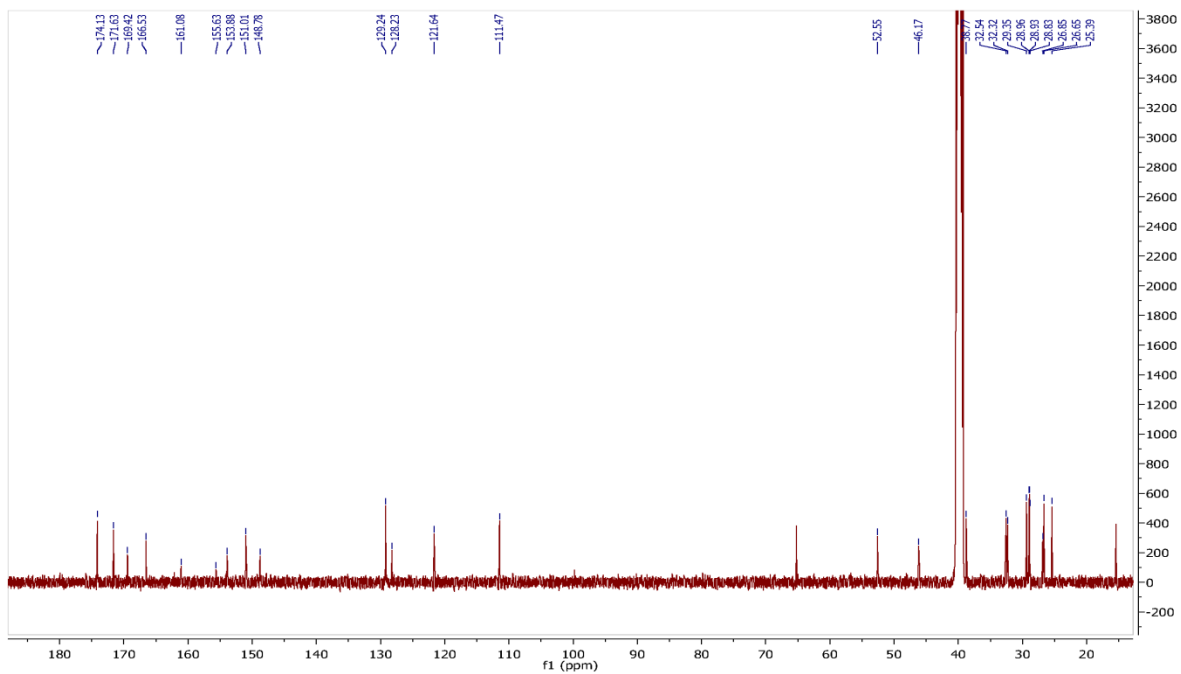
^{13}C NMR of **15c**:



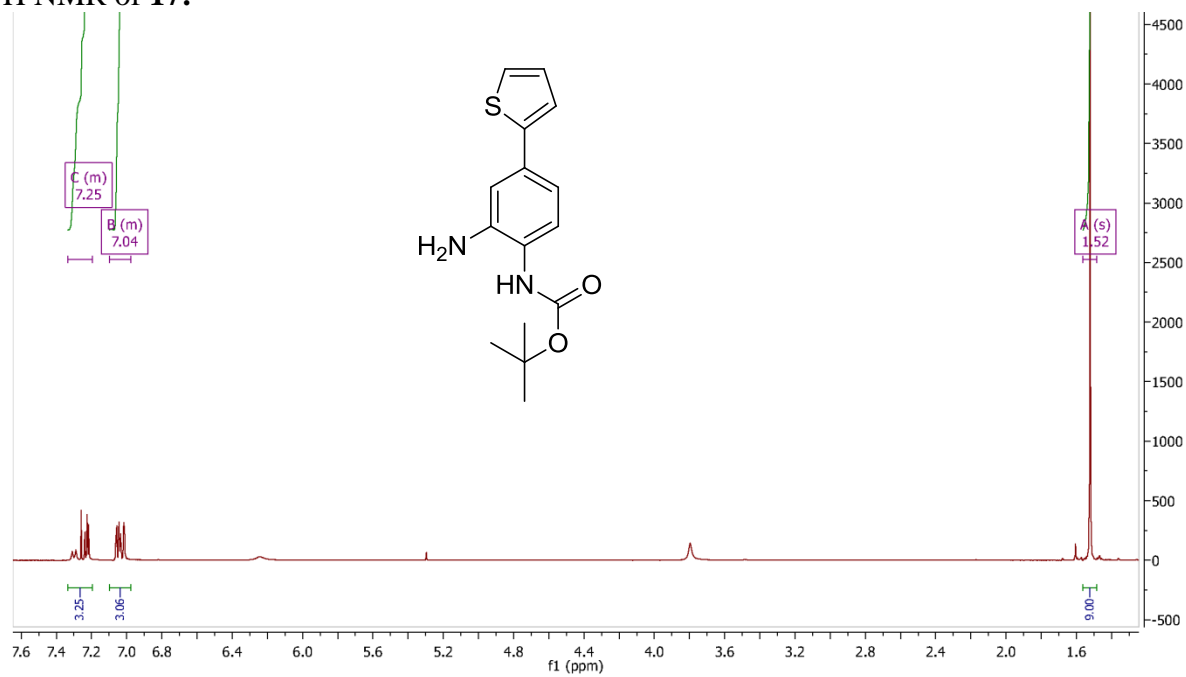
¹H NMR of **15d**:



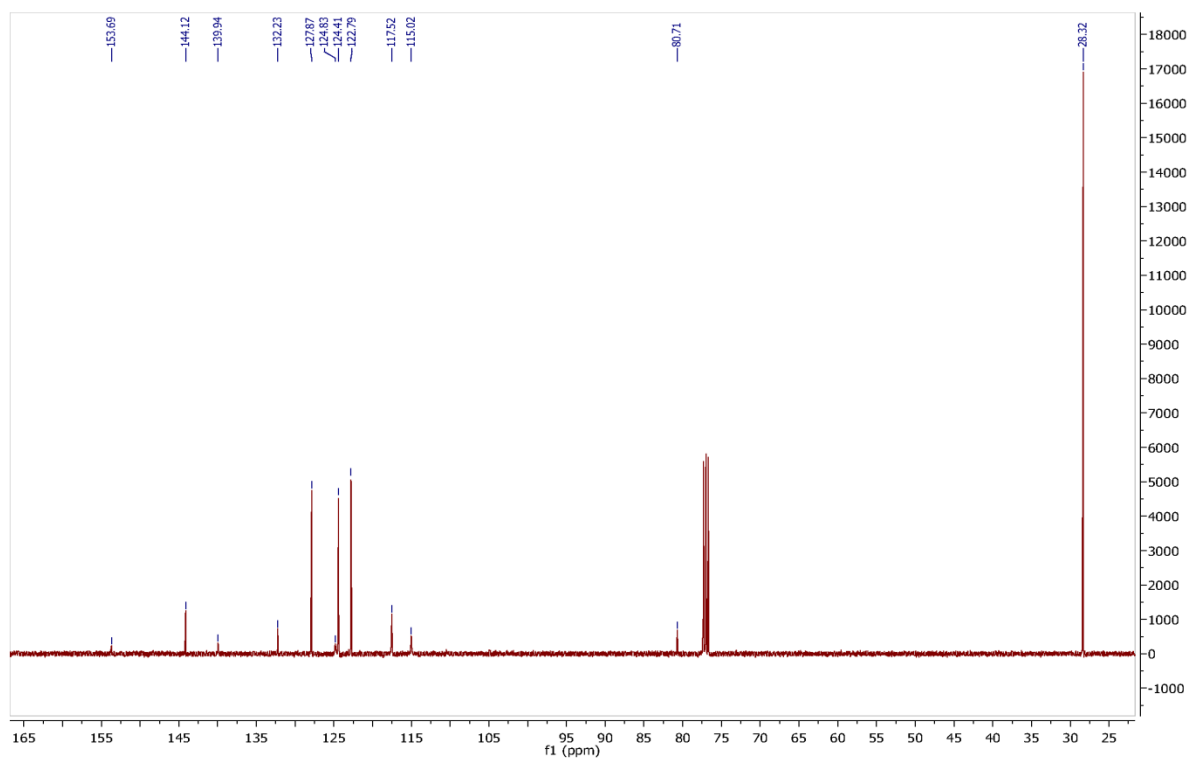
¹³C NMR of **15d**:



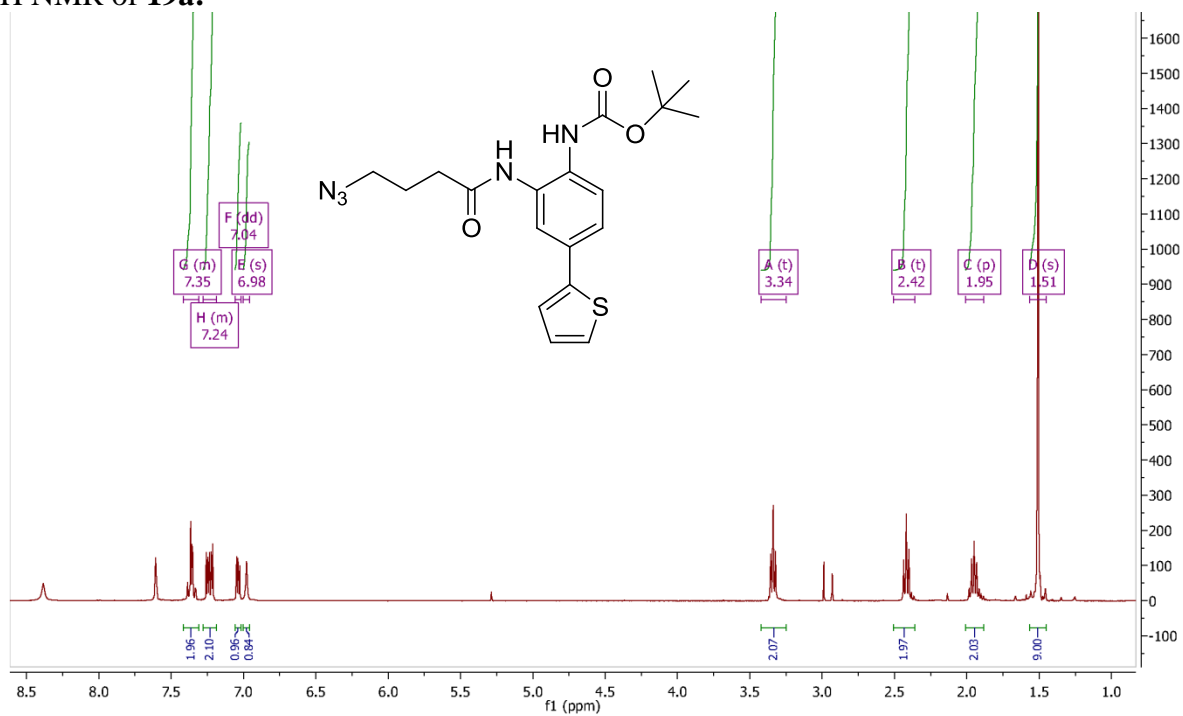
¹H NMR of 17:



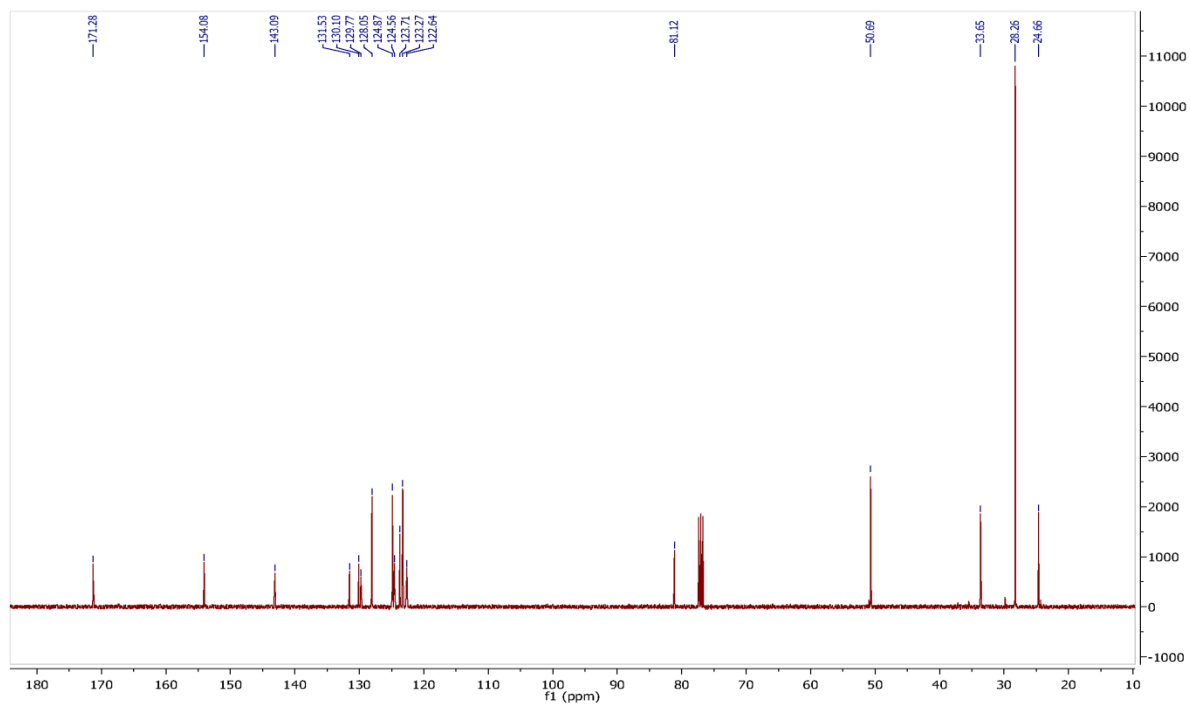
¹³C NMR of 17:



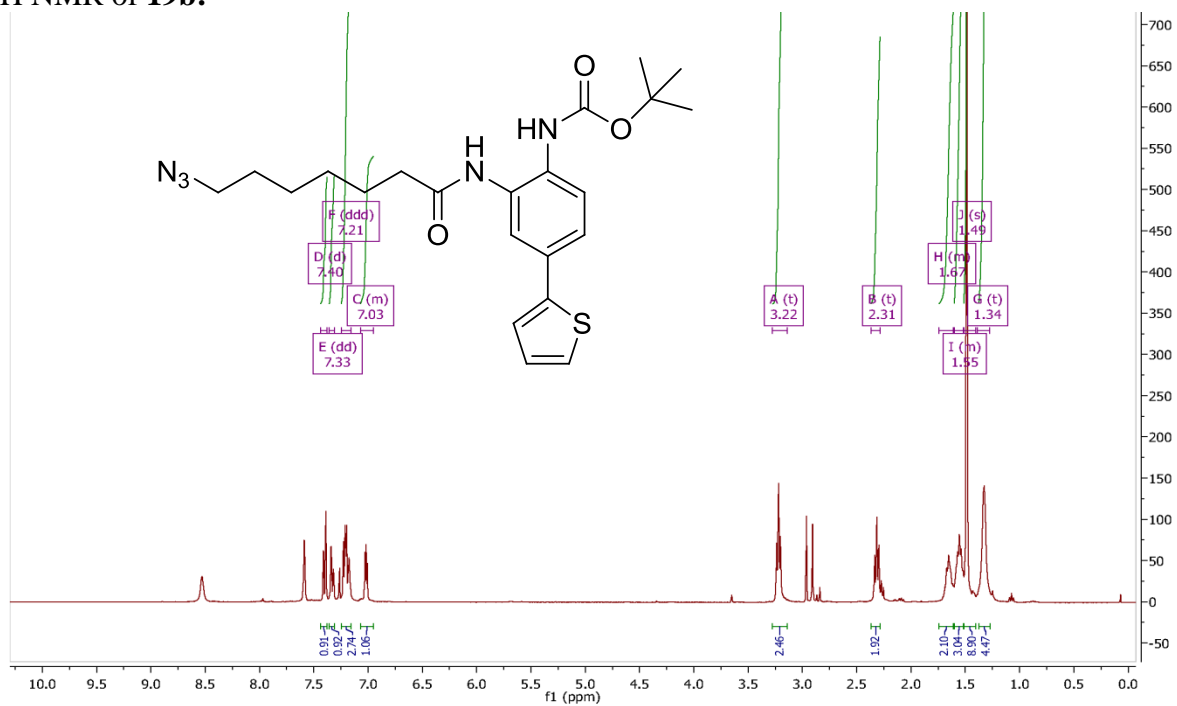
¹H NMR of **19a**:



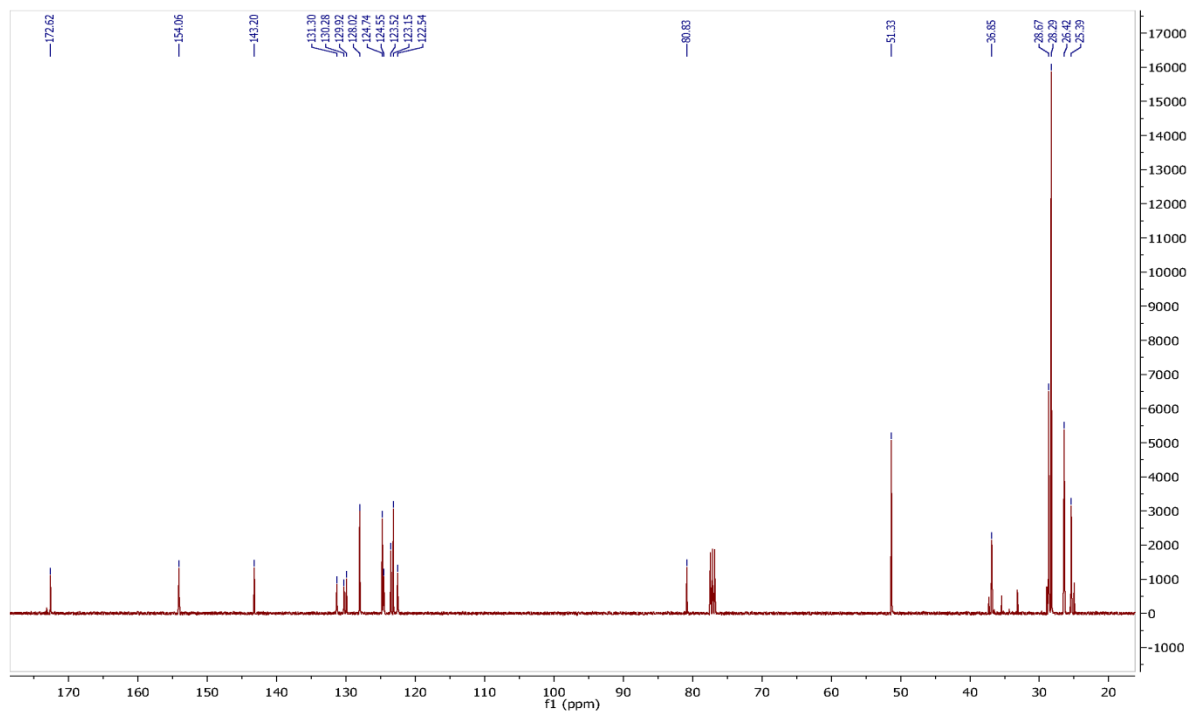
¹³C NMR of **19a**:



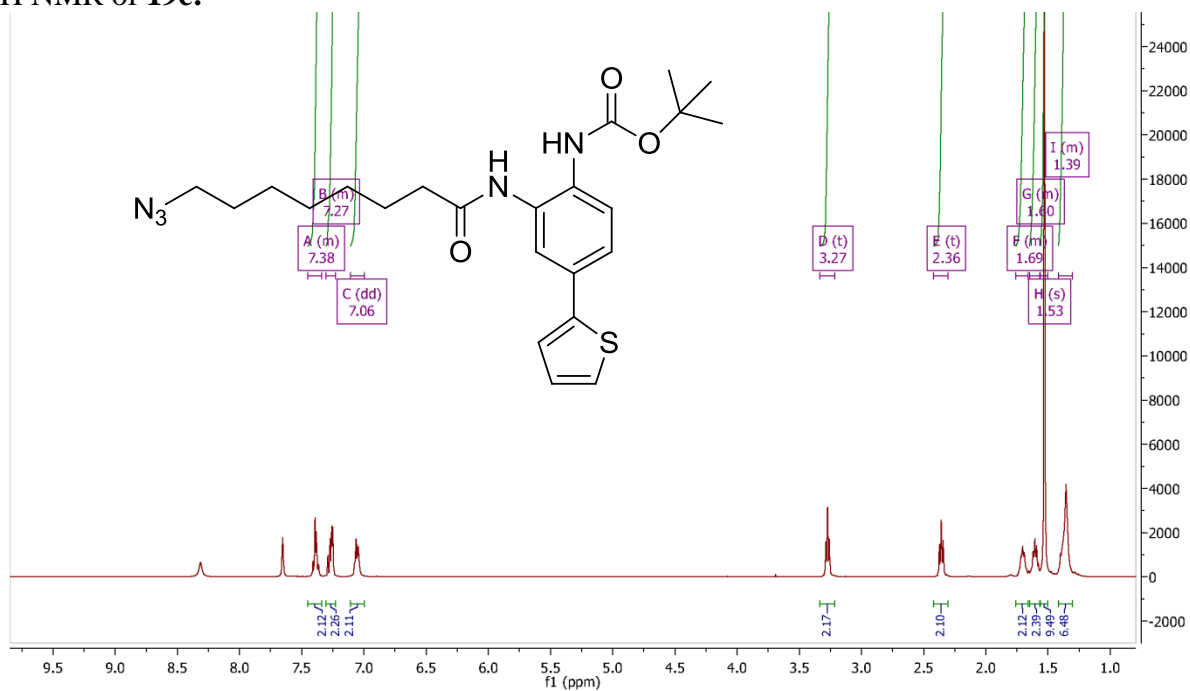
¹H NMR of **19b**:



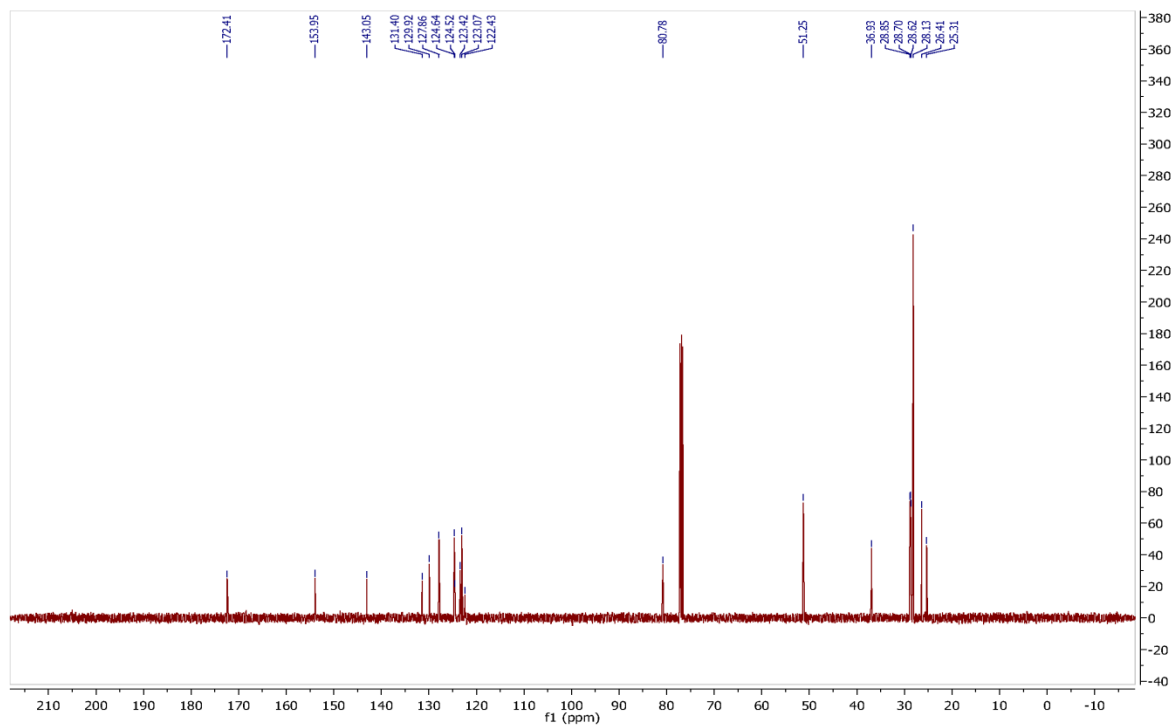
¹³C NMR of **19b**:



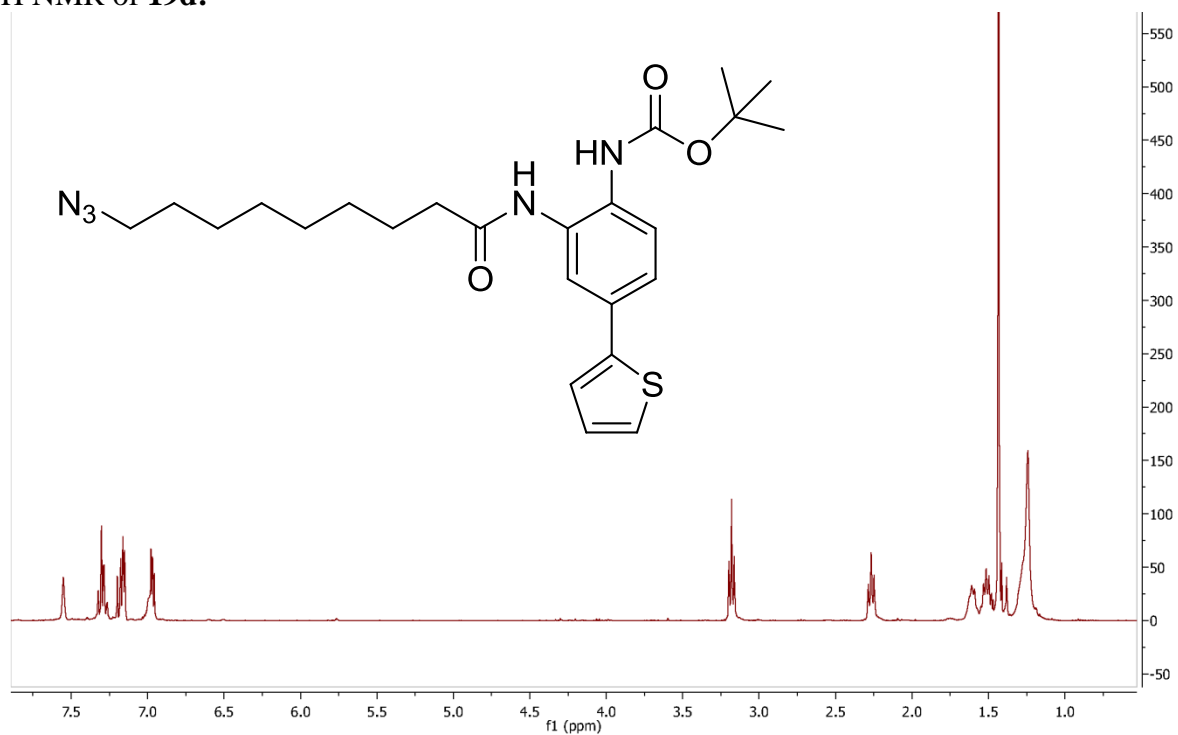
¹H NMR of **19c**:



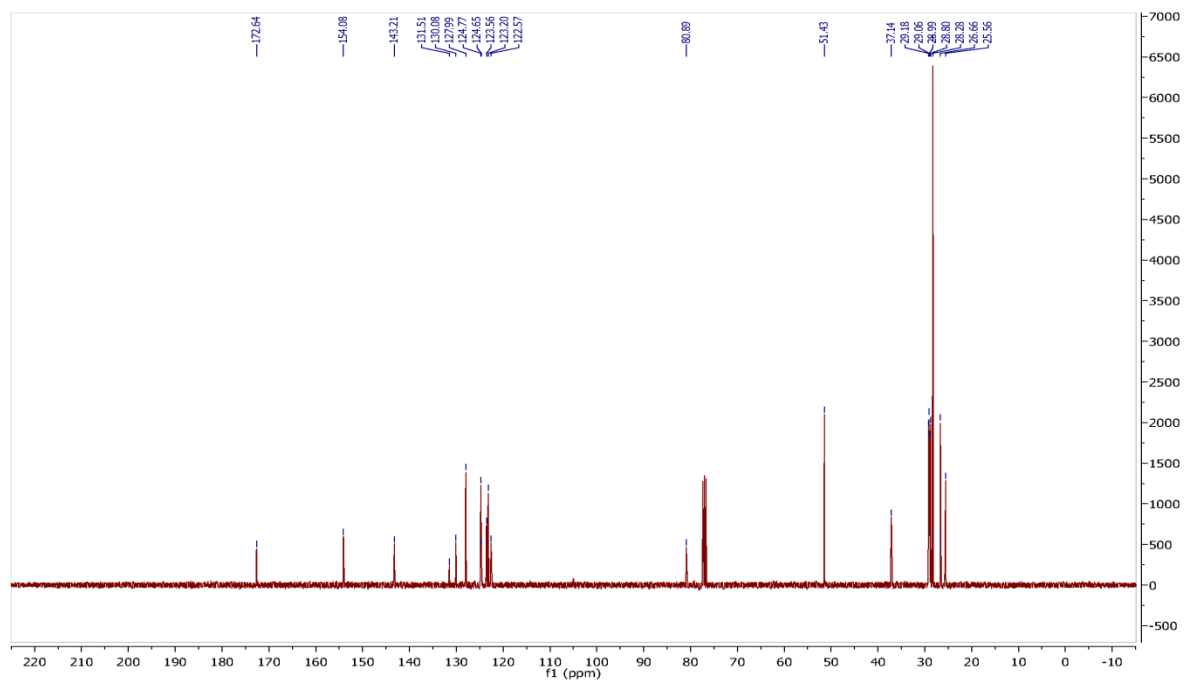
¹³C NMR of **19c**:



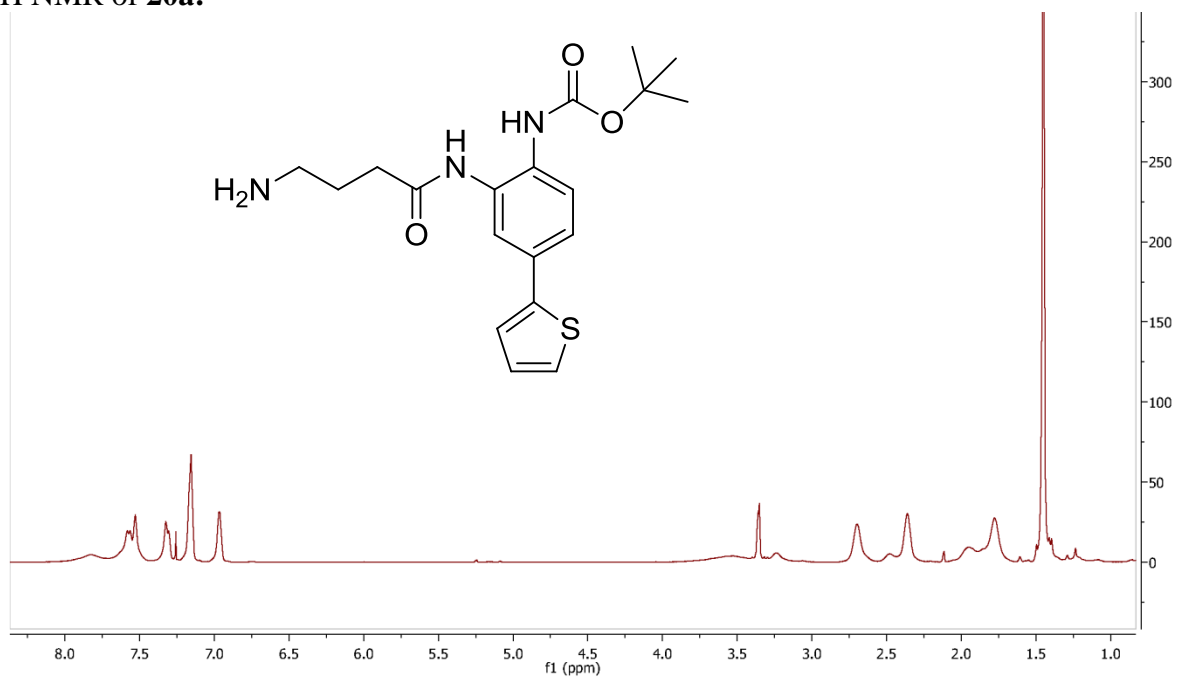
¹H NMR of **19d**:



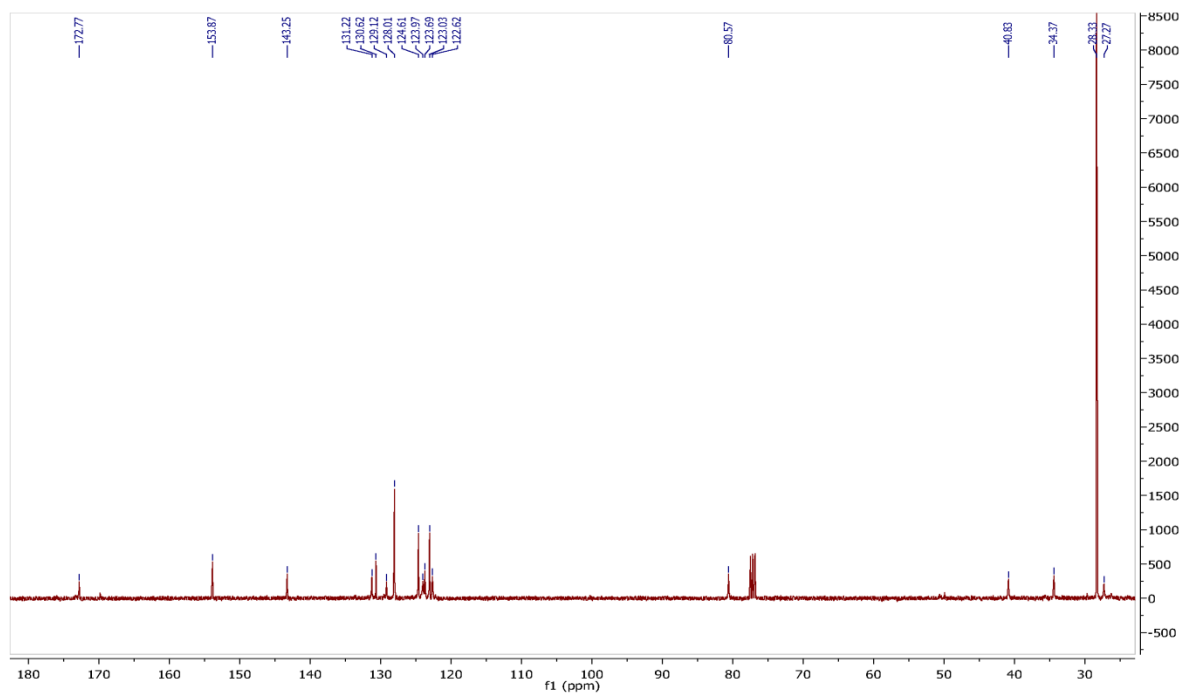
¹³C NMR of **19d**:



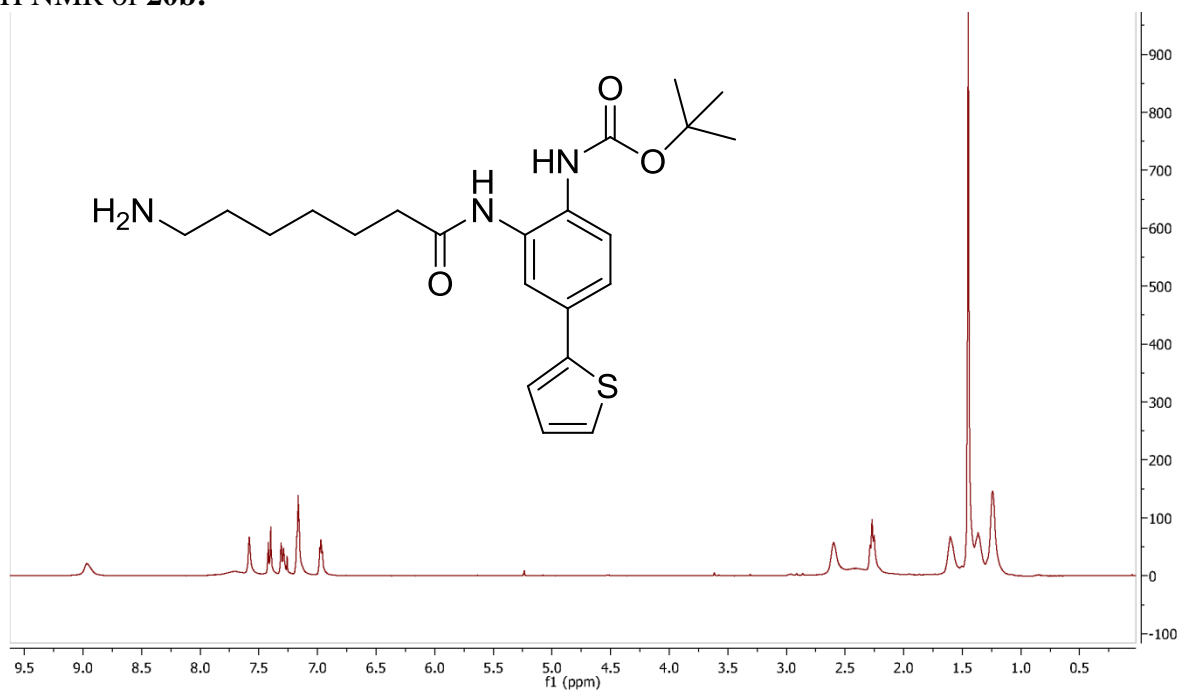
¹H NMR of **20a**:



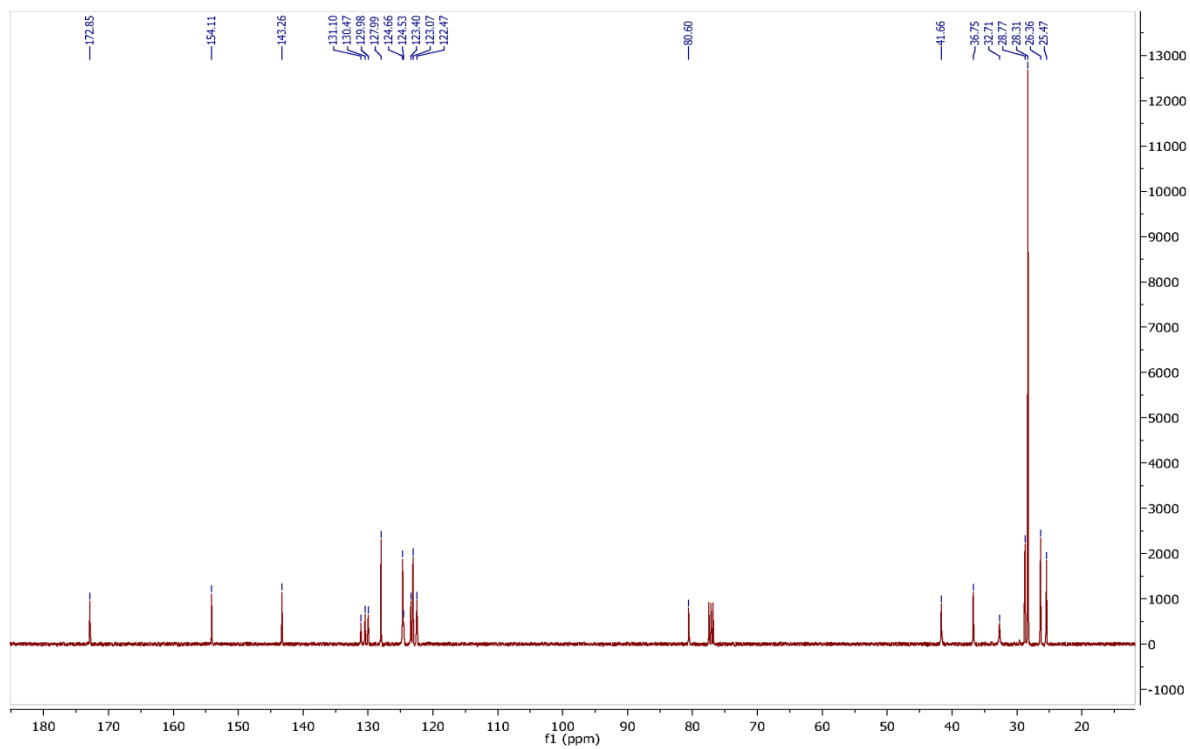
¹³C NMR of **20a**:



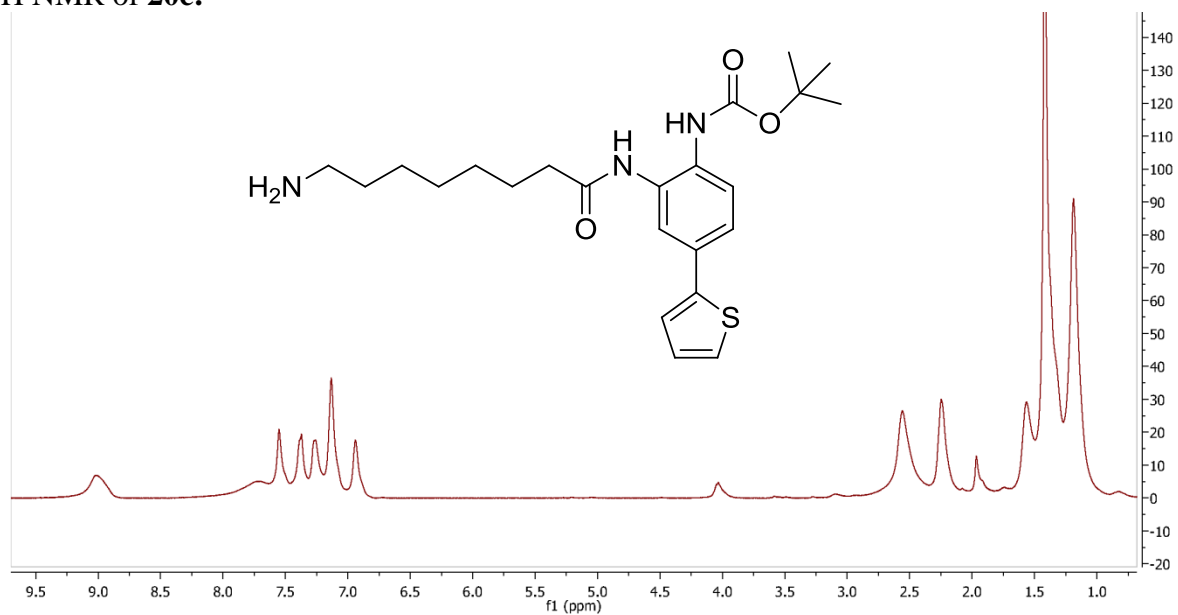
¹H NMR of **20b**:



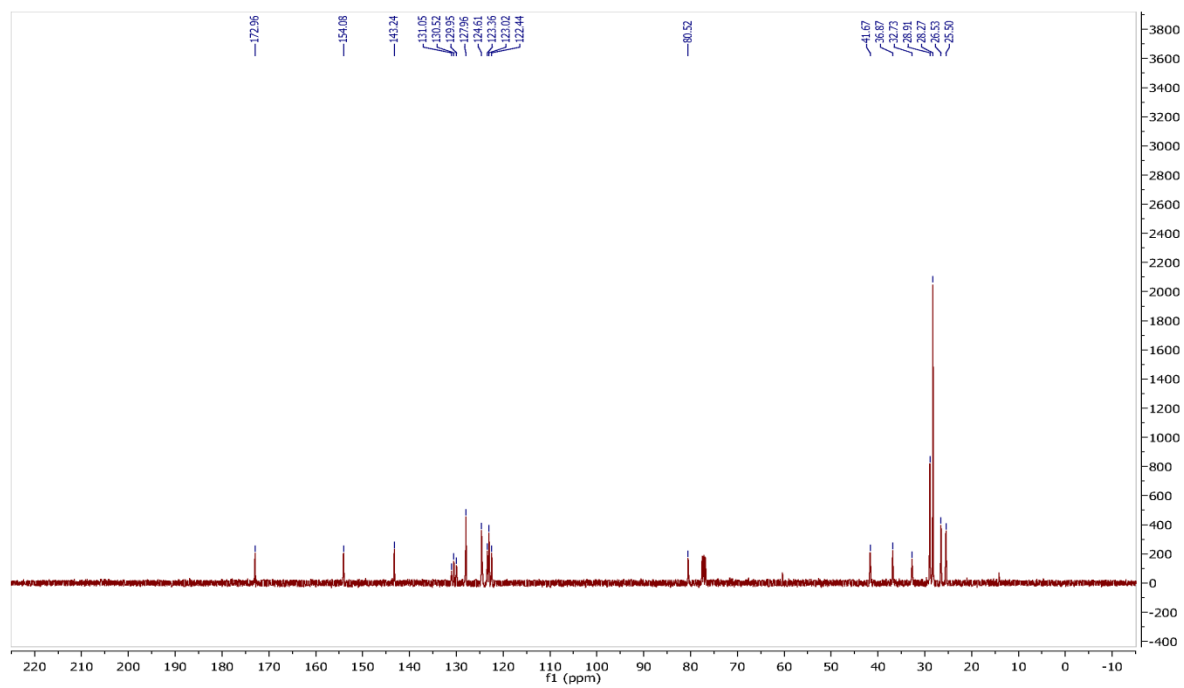
¹³C NMR of **20b**:



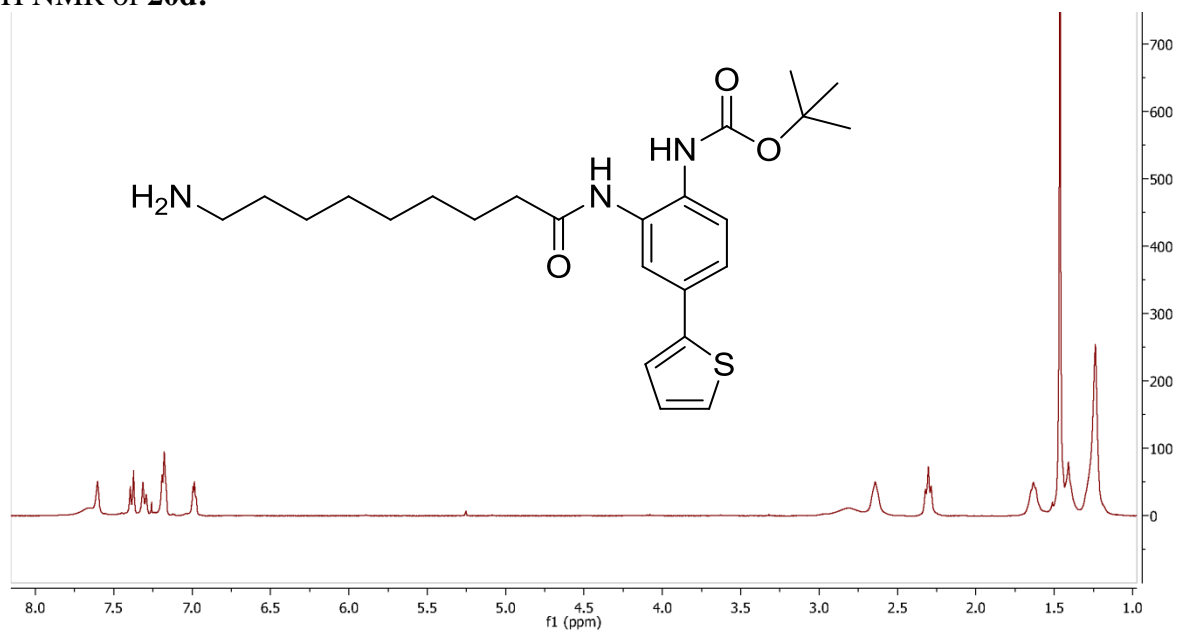
¹H NMR of **20c**:



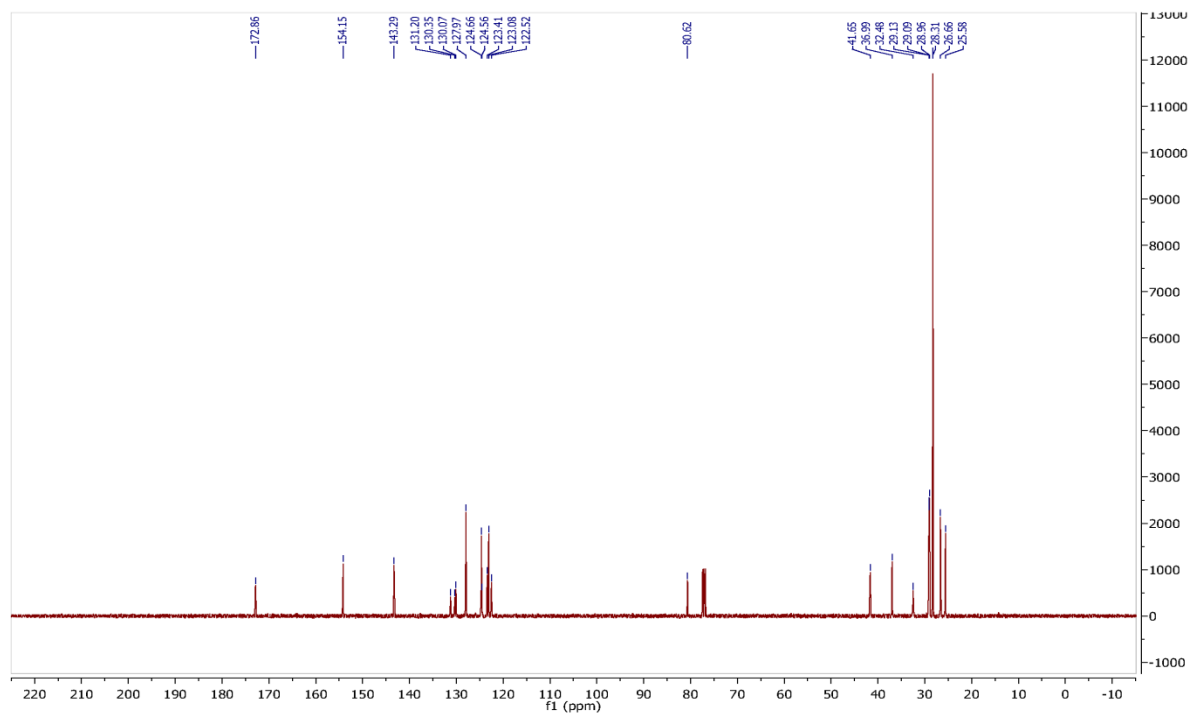
¹³C NMR of **20c**:



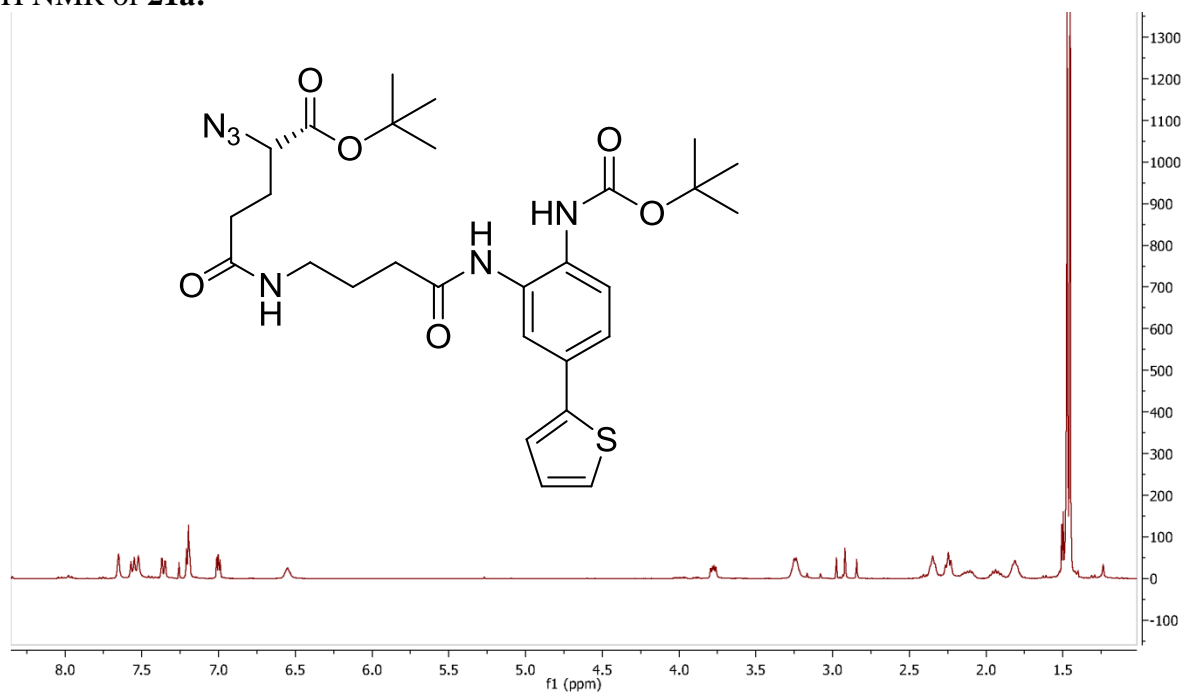
¹H NMR of **20d**:



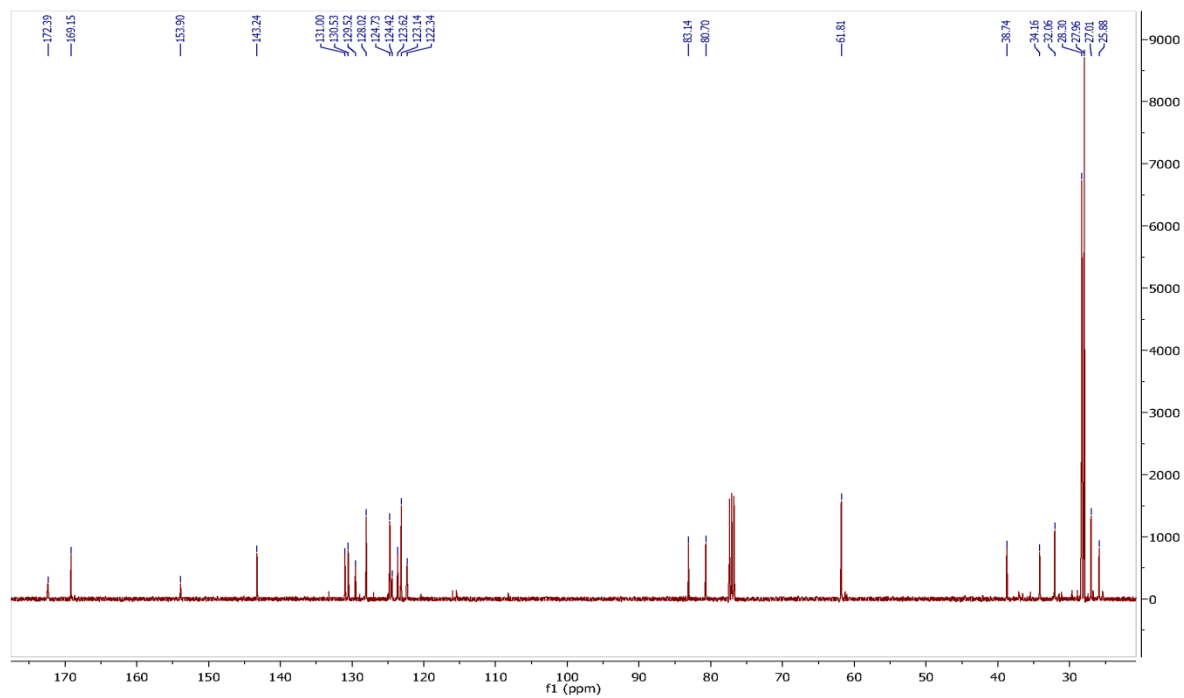
¹³C NMR of **20d**:



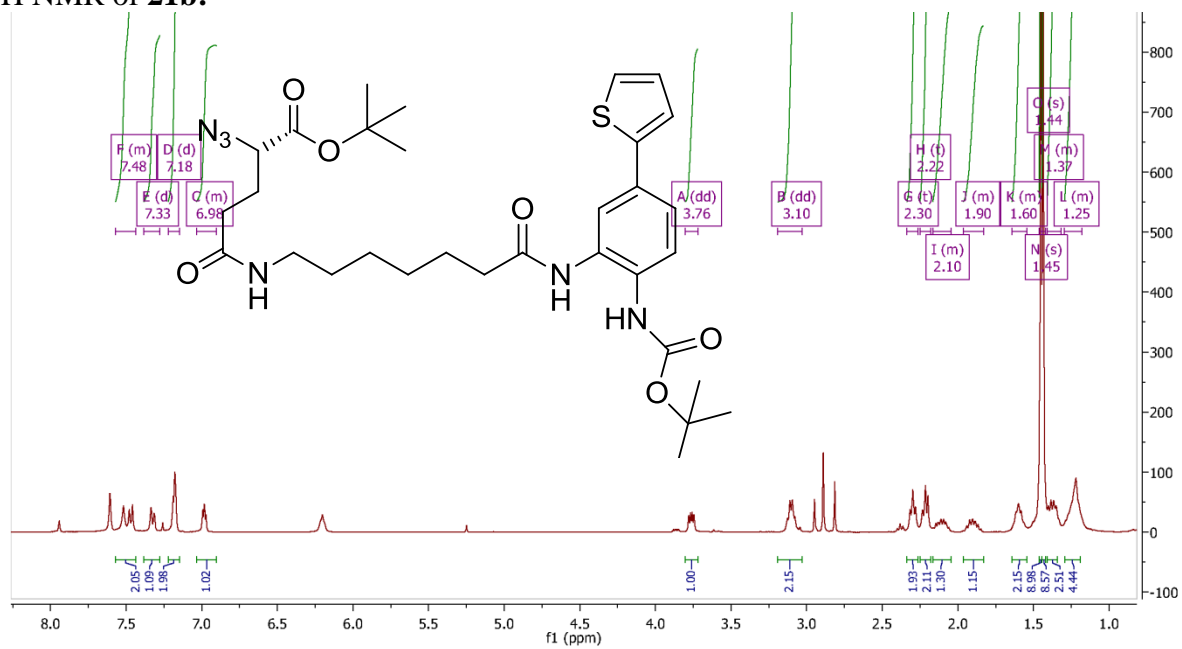
¹H NMR of **21a**:



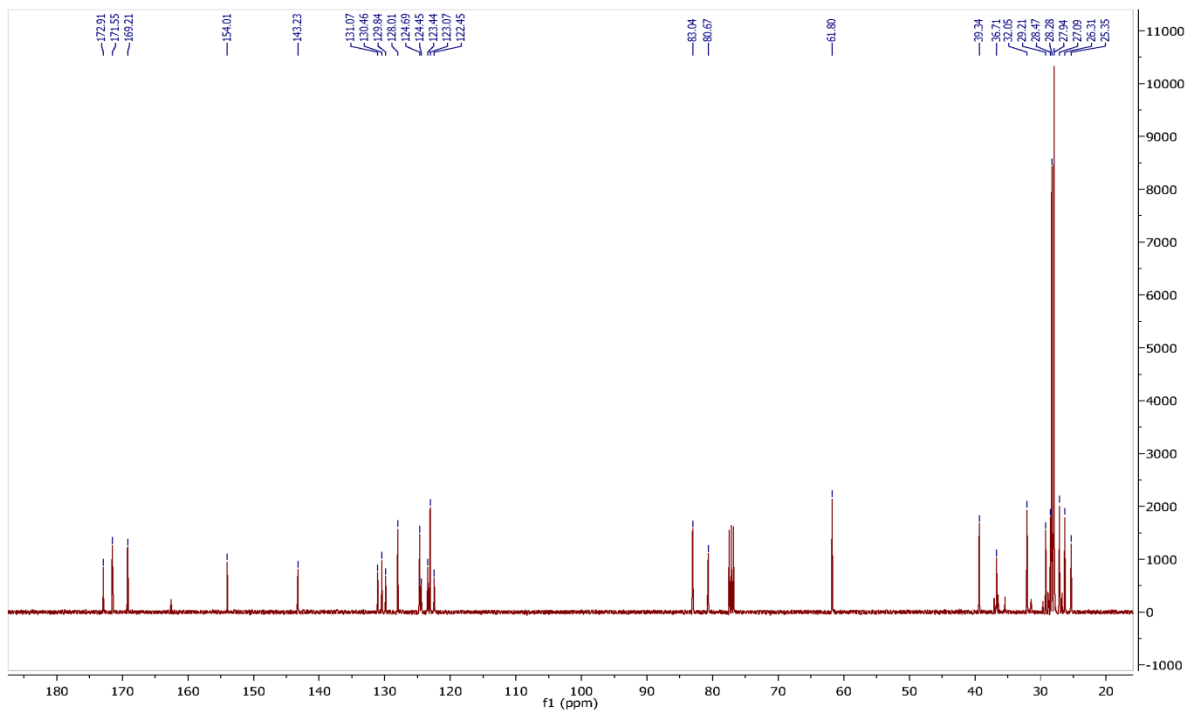
¹³C NMR of **21a**:



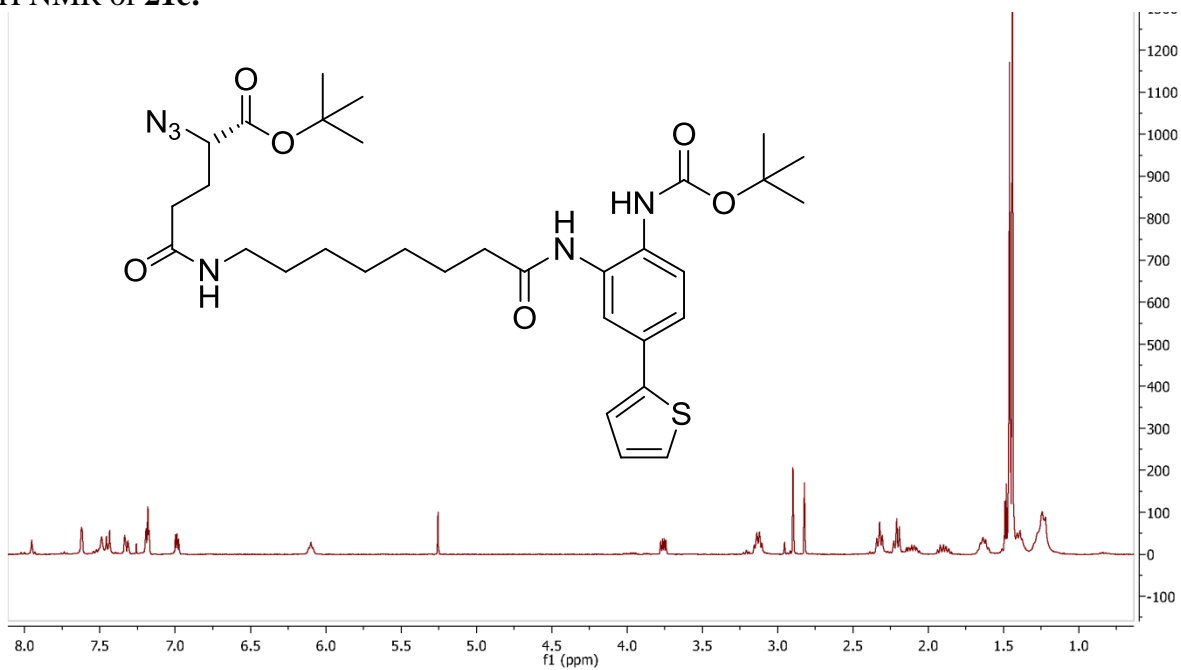
¹H NMR of **21b**:



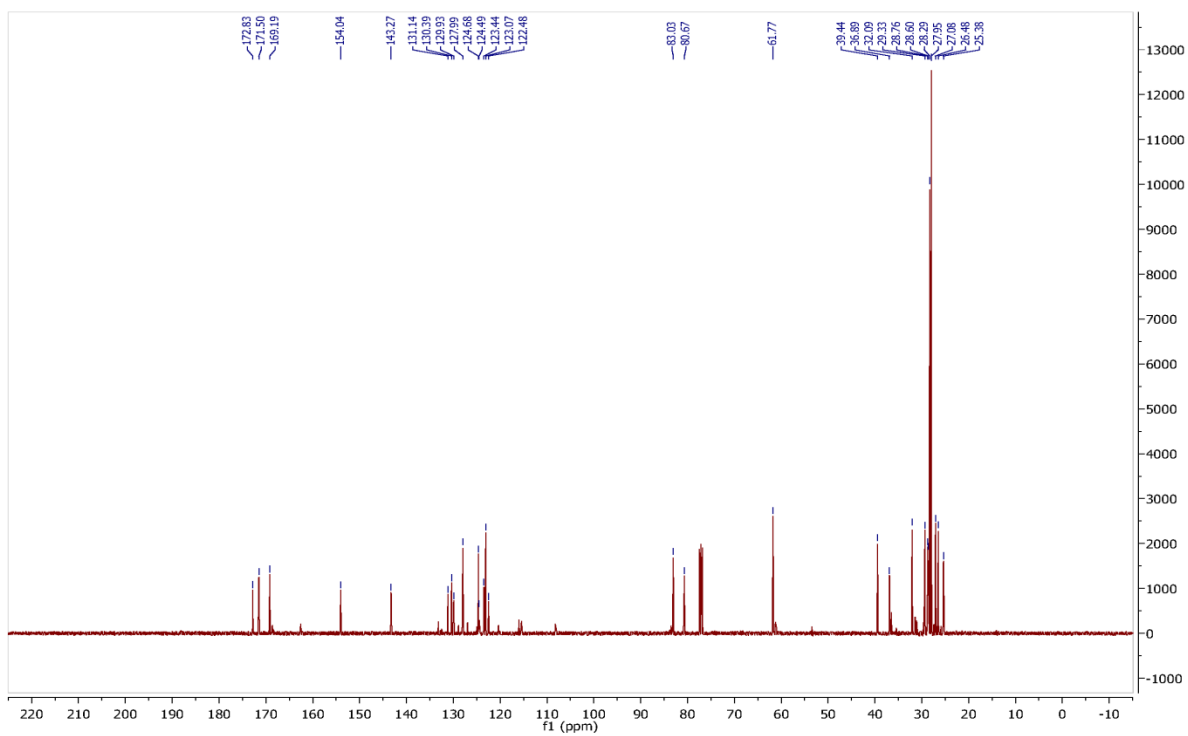
¹³C NMR of **21b**:



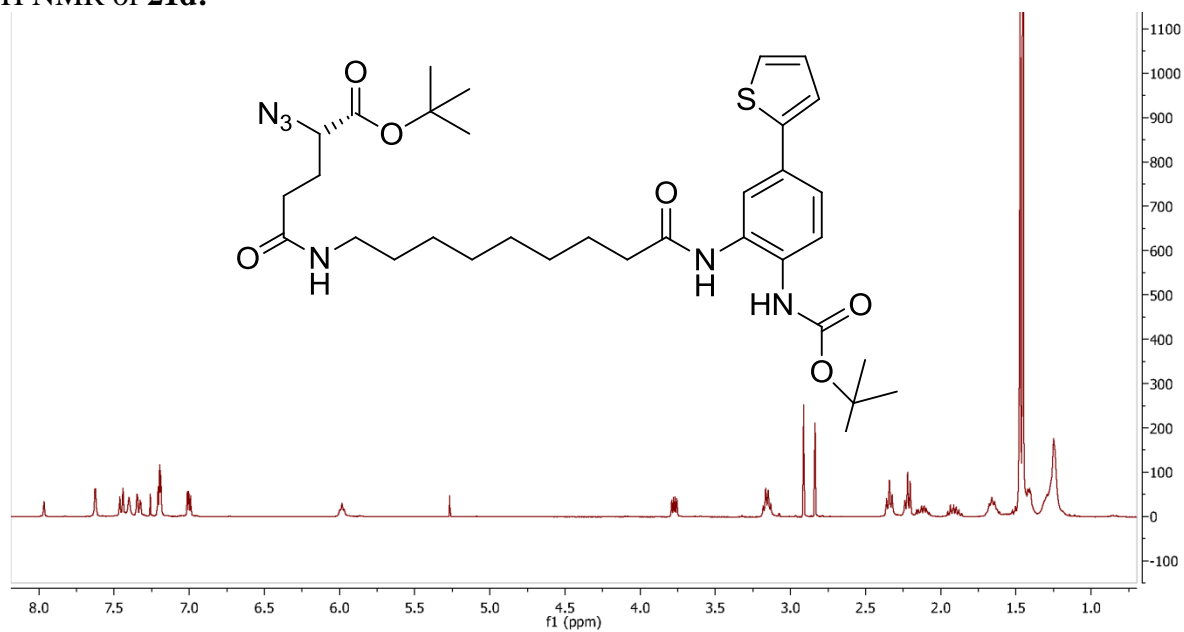
¹H NMR of **21c**:



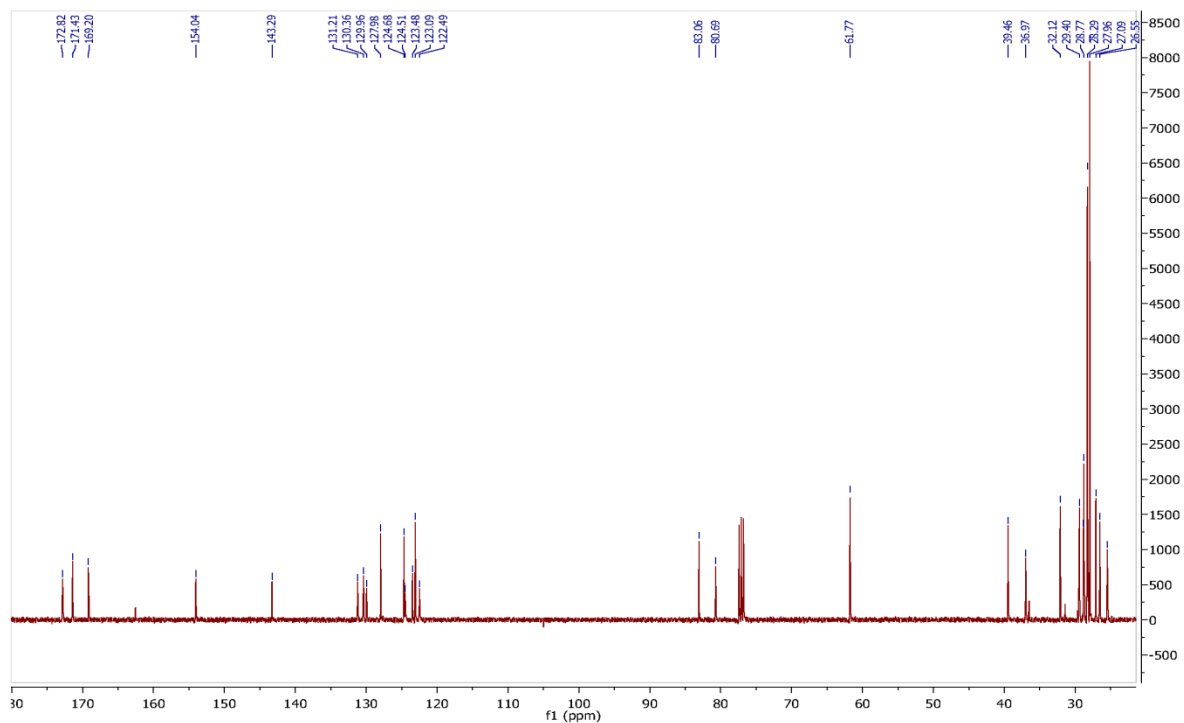
¹³C NMR of **21c**:



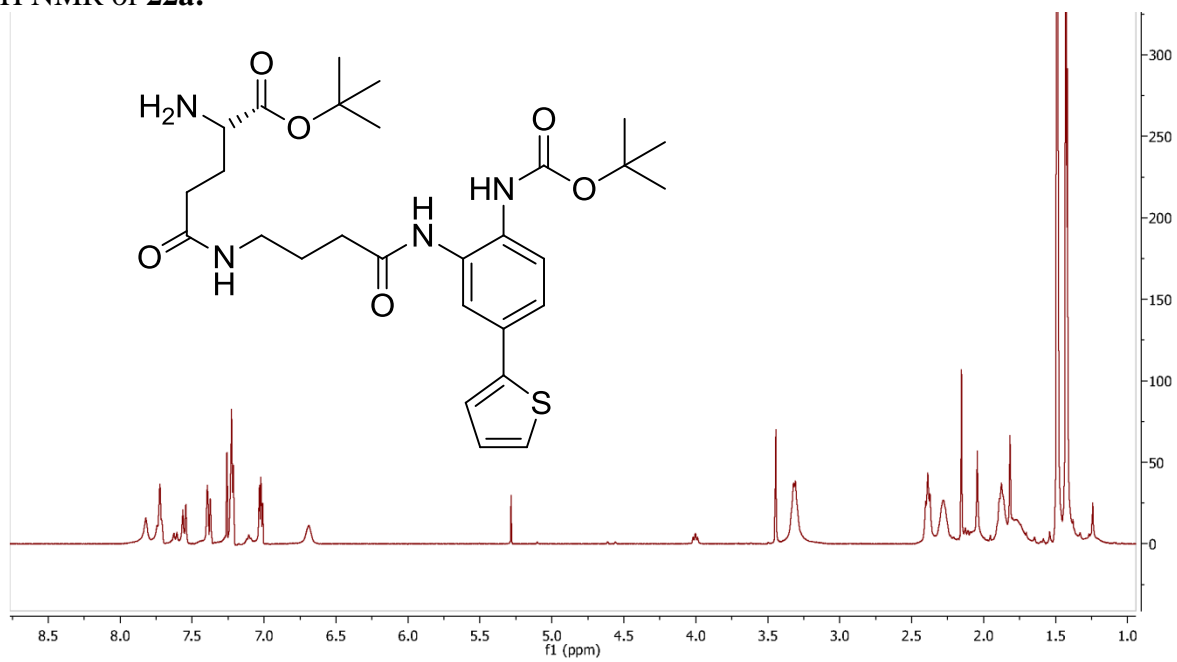
¹H NMR of **21d**:



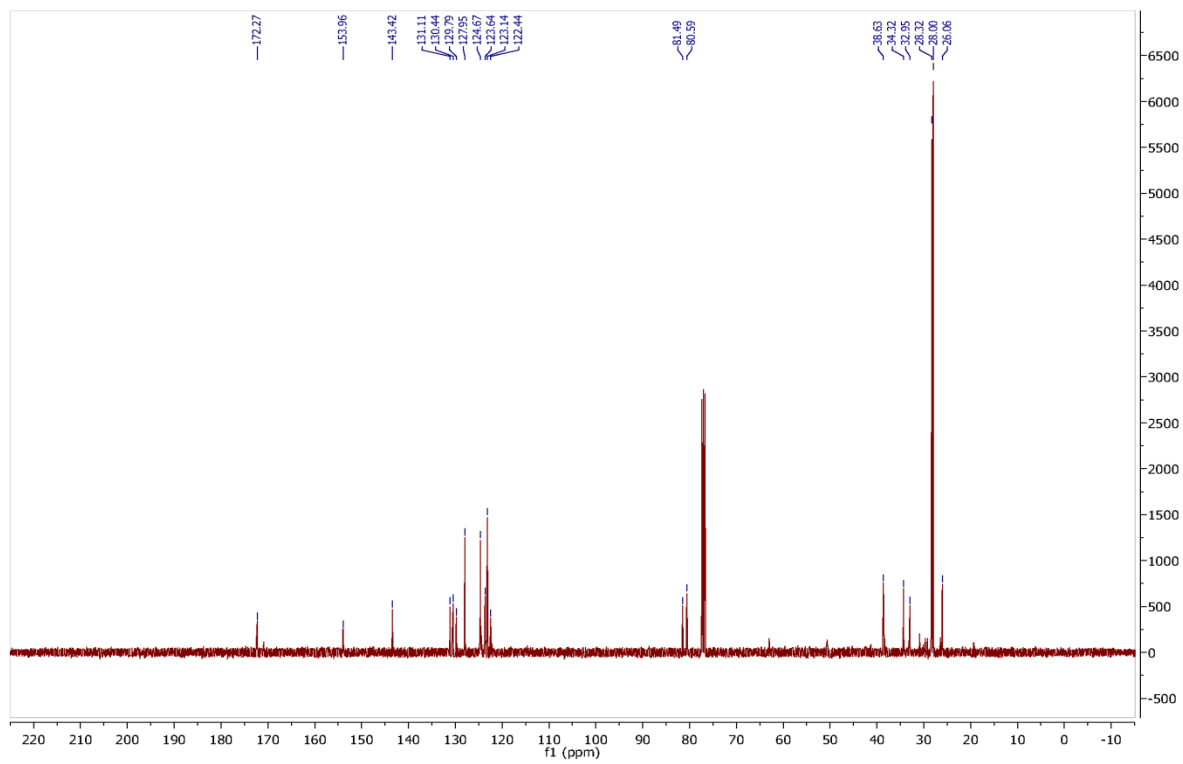
¹³C NMR of **21d**:



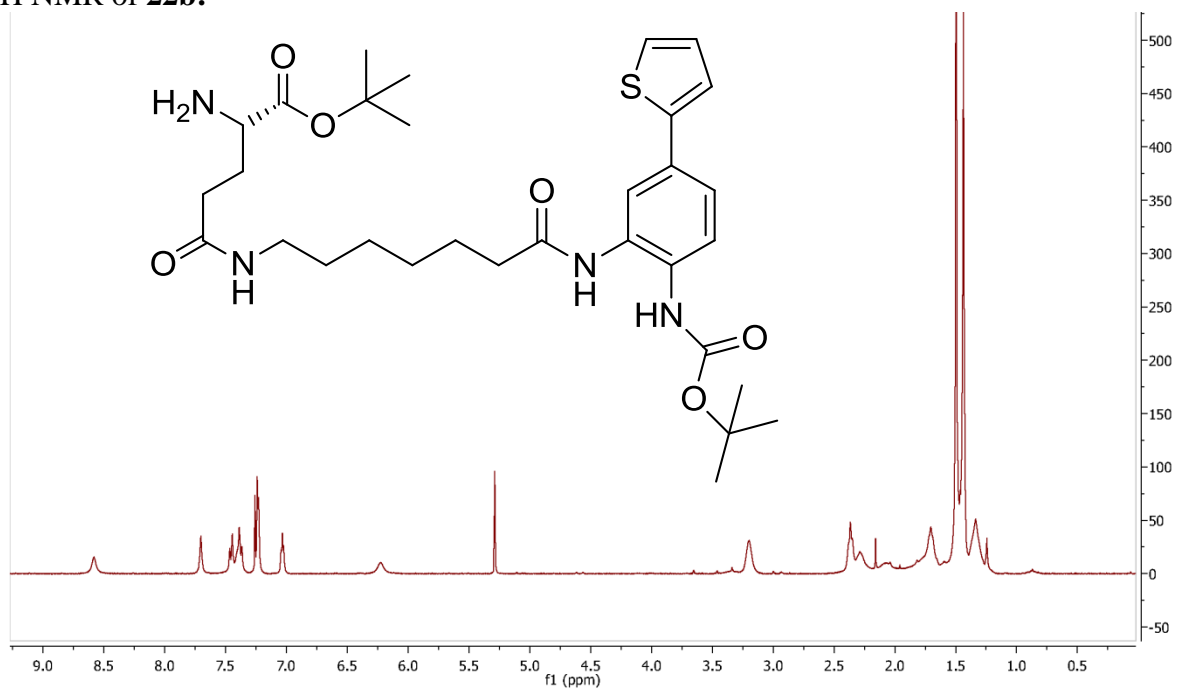
^1H NMR of **22a**:



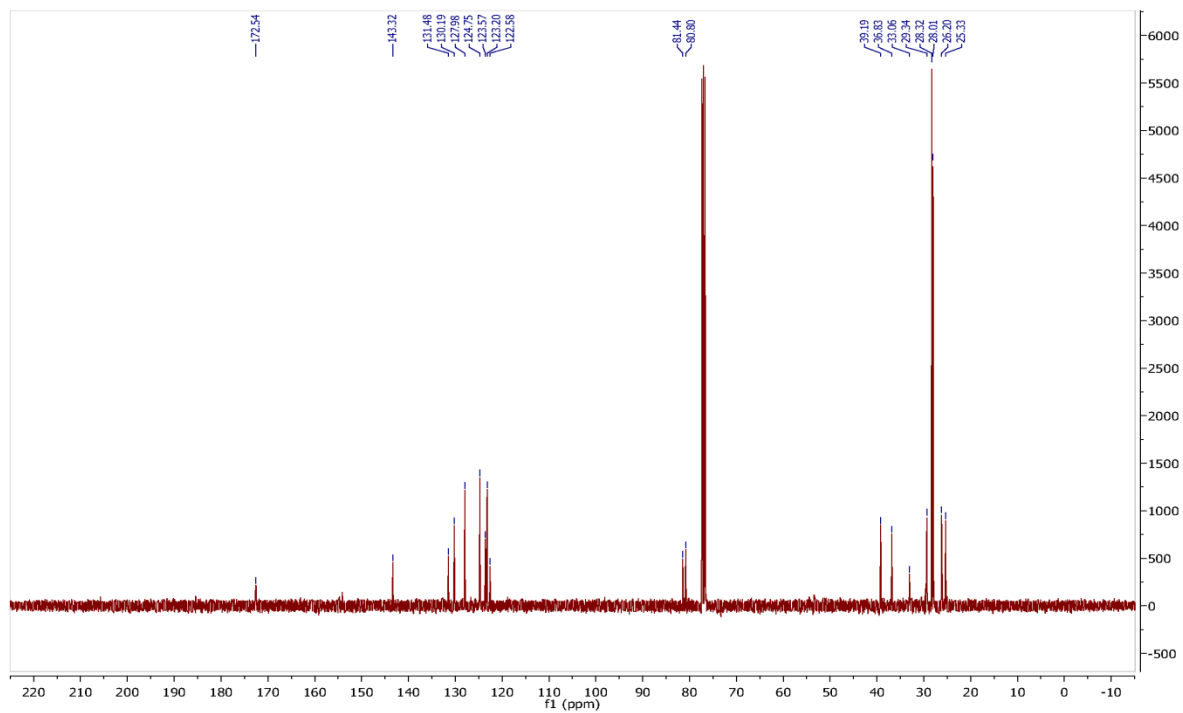
^{13}C NMR of **22a**:



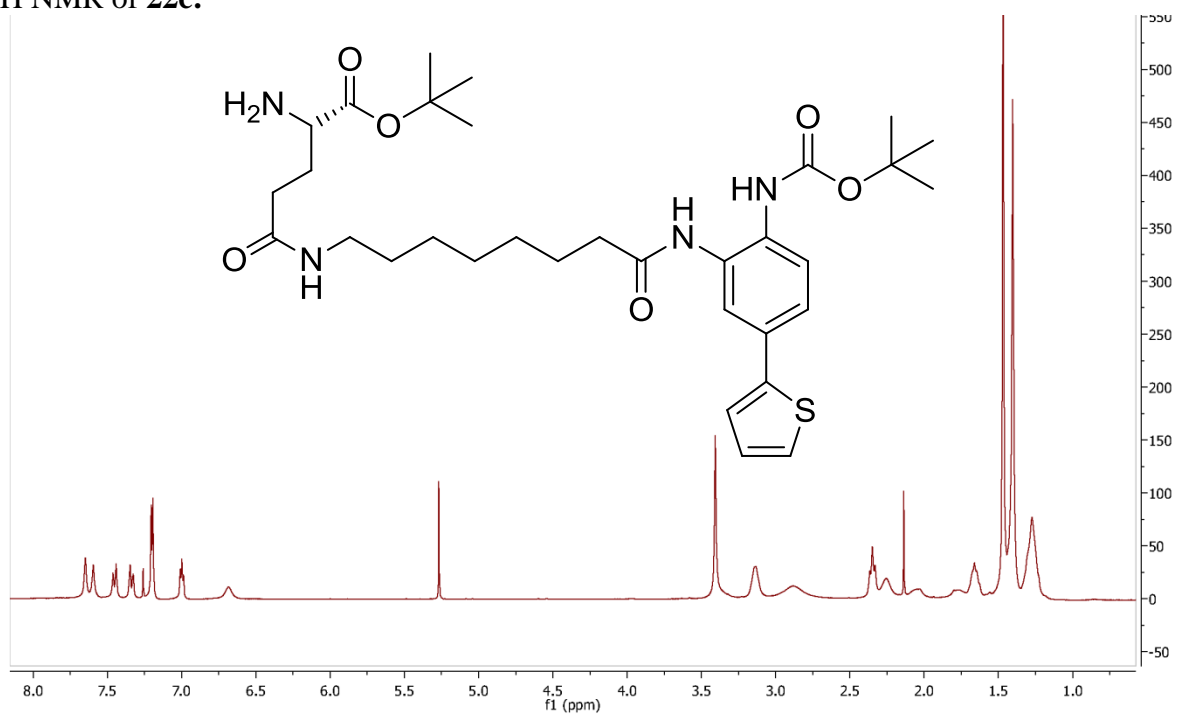
¹H NMR of **22b**:



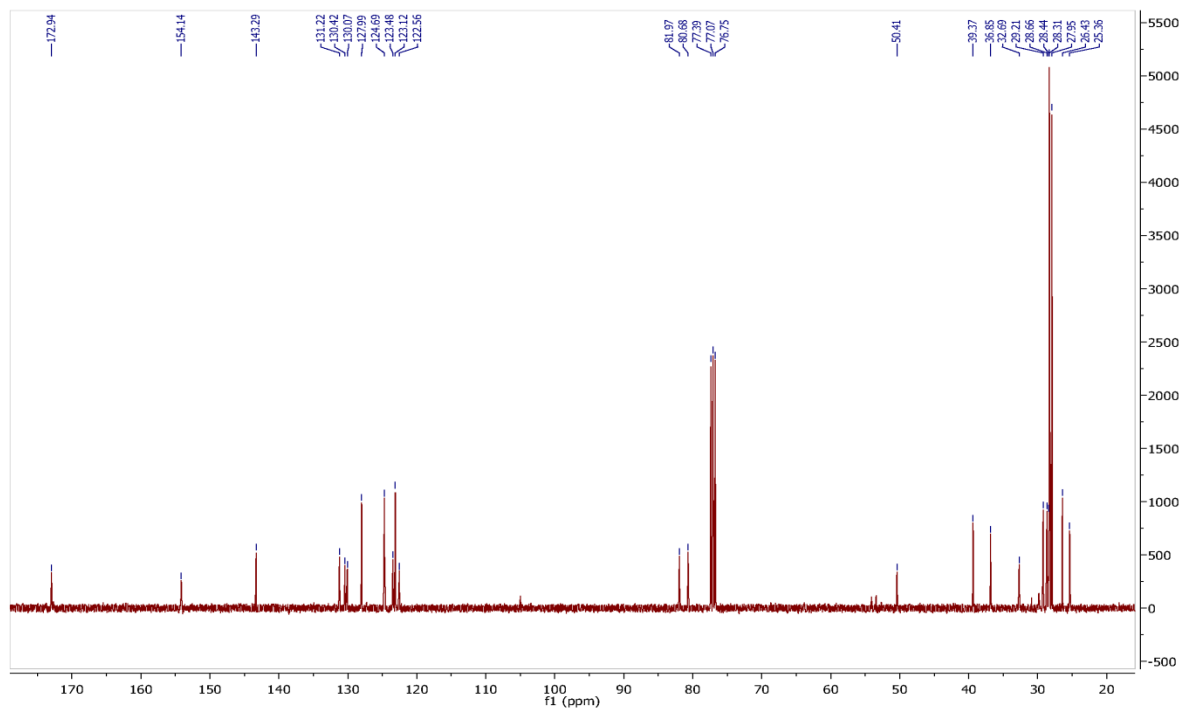
¹³C NMR of **22b**:



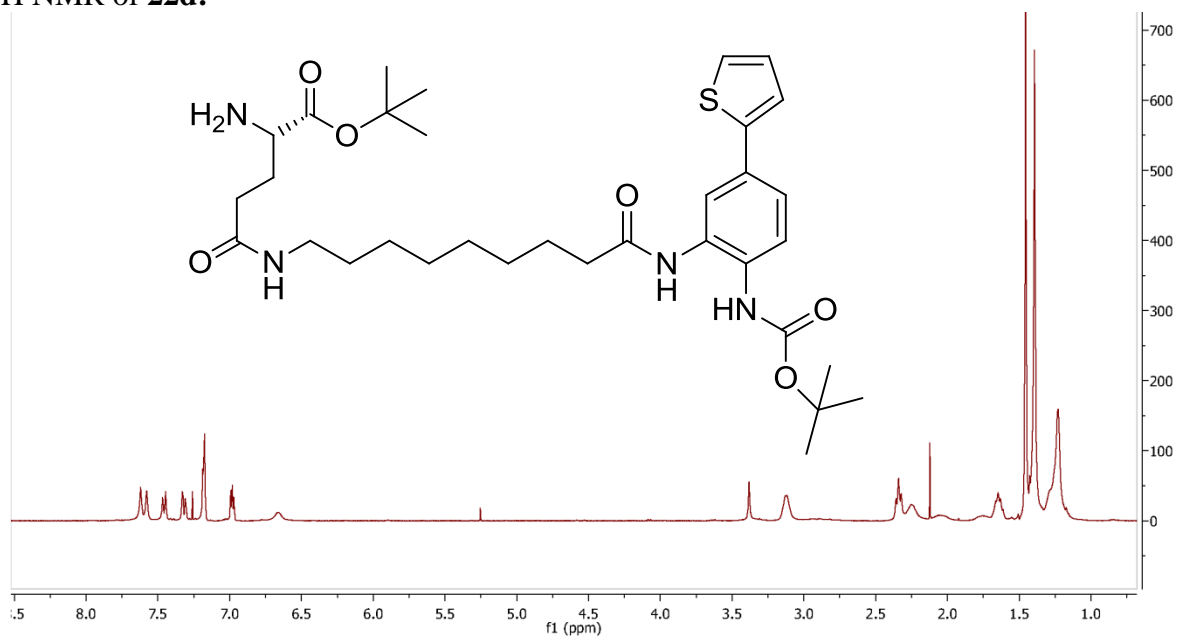
¹H NMR of **22c**:



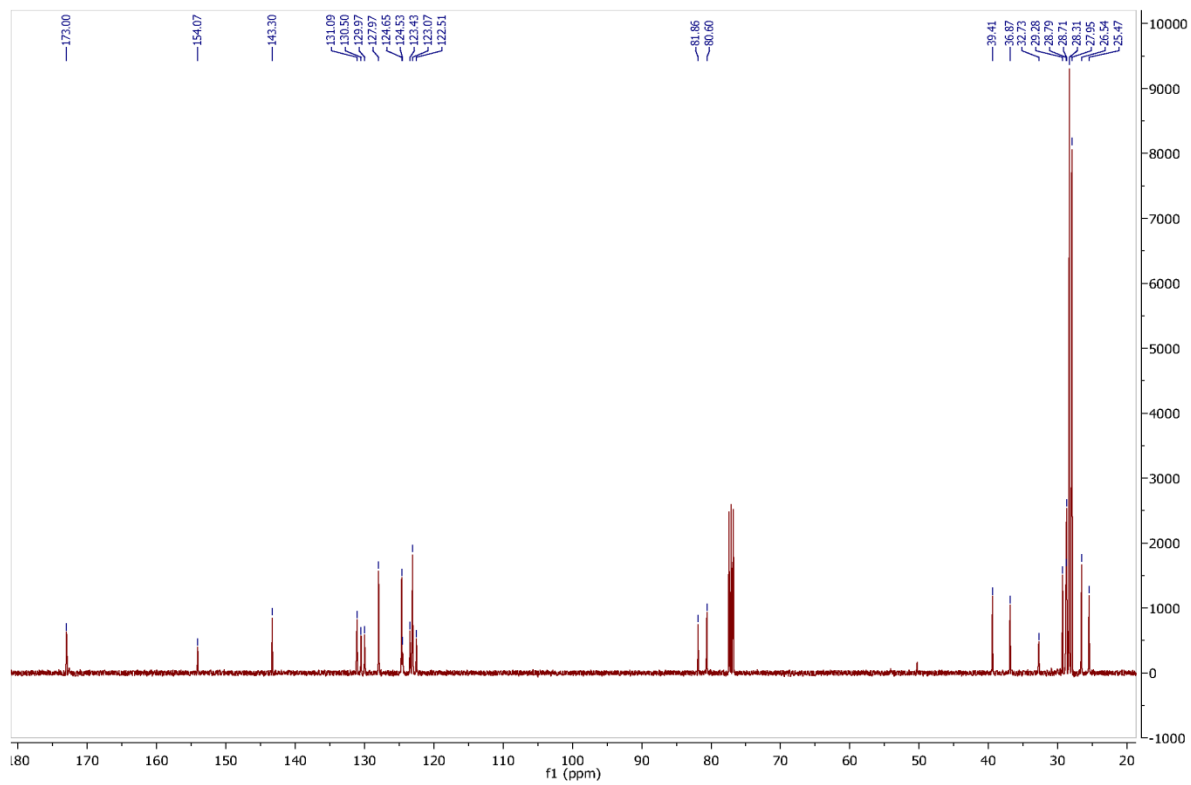
¹³C NMR of **22c**:



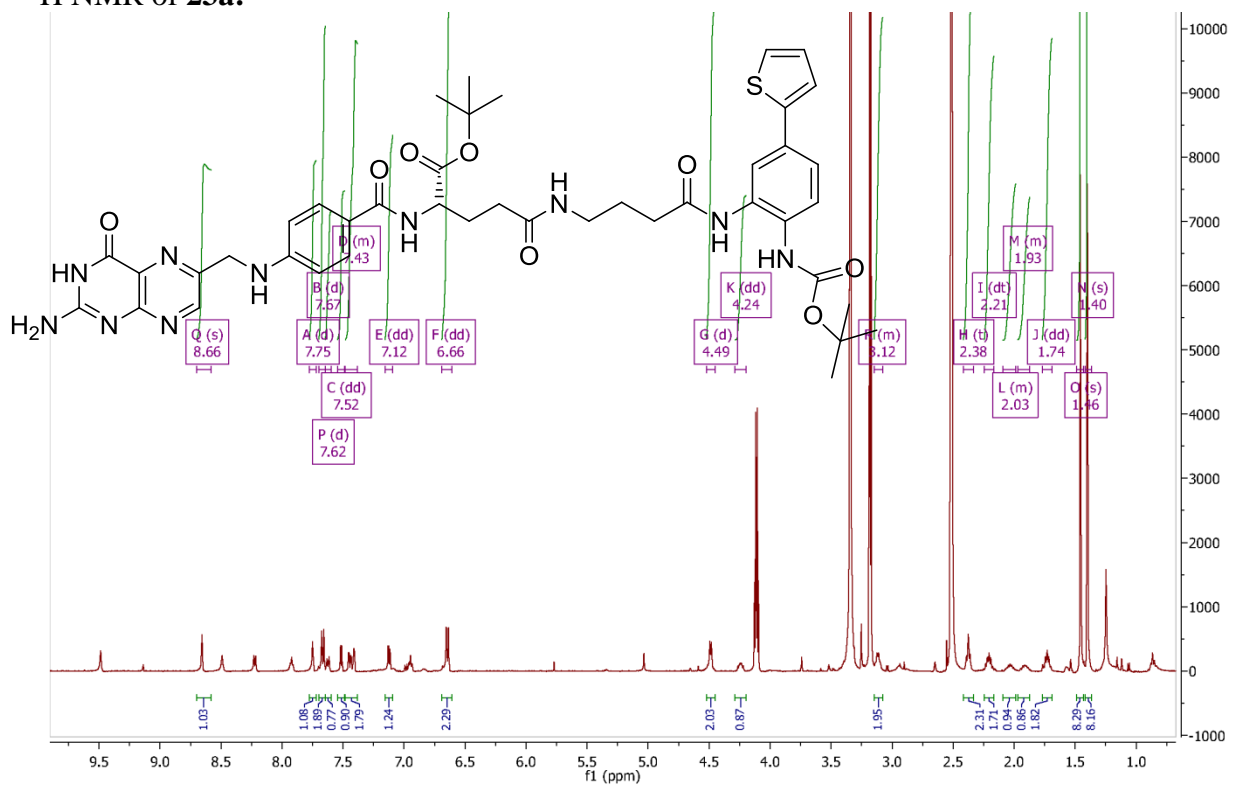
¹H NMR of **22d**:



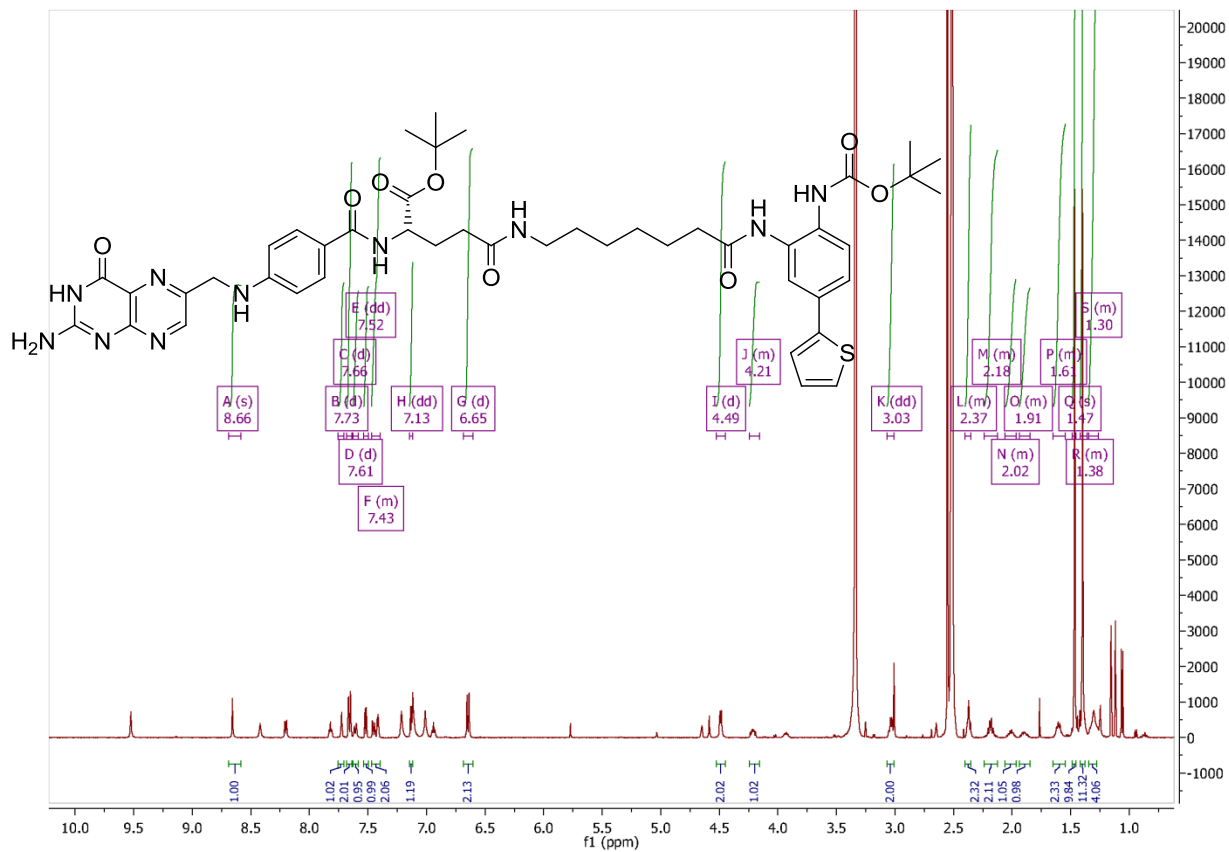
¹³C NMR of **22d**:



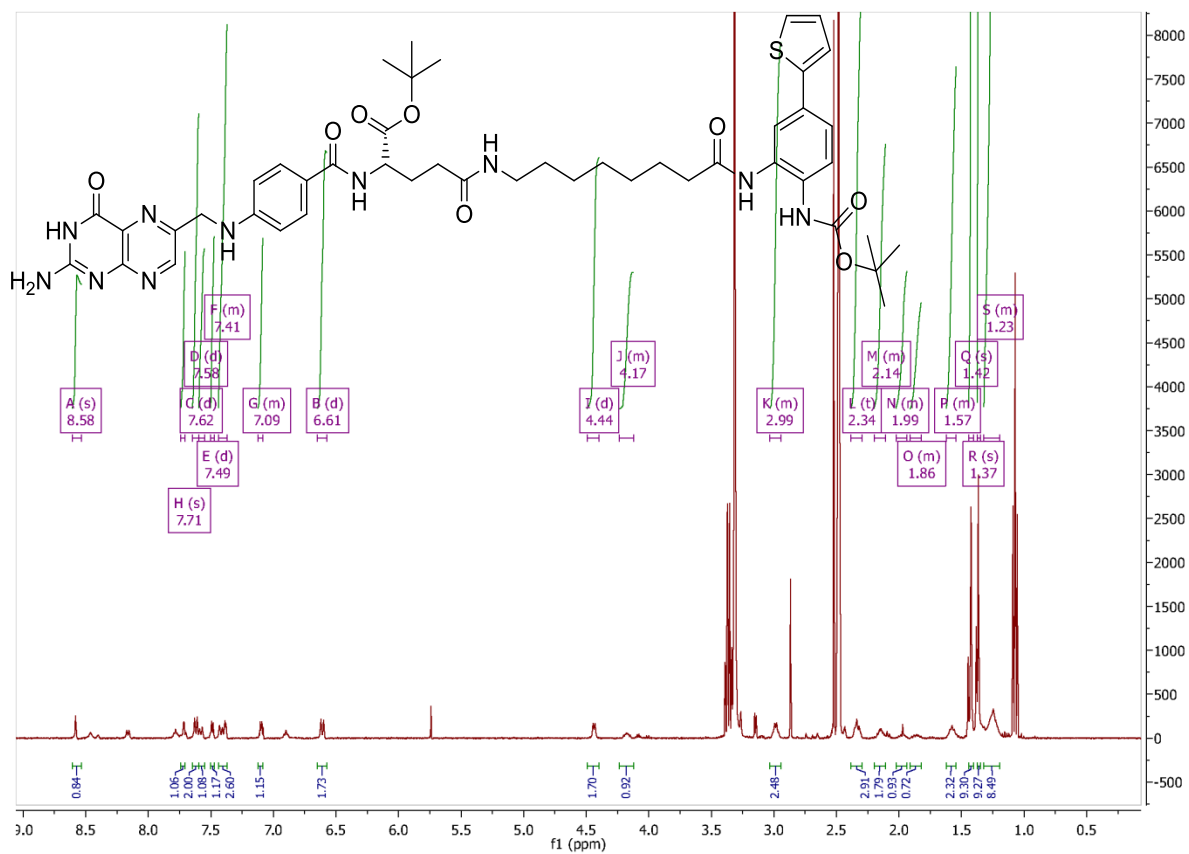
¹H NMR of **23a**:



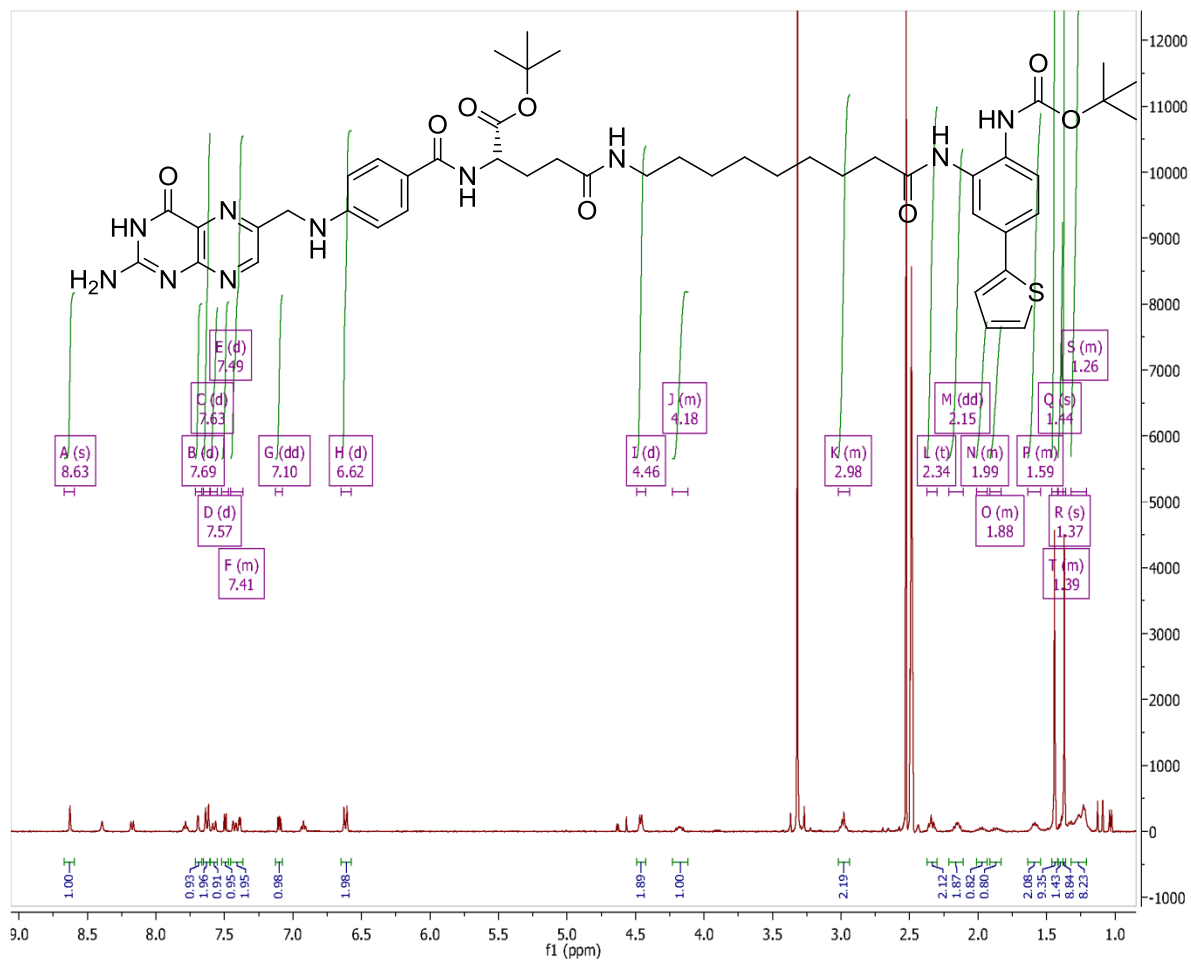
¹H NMR of **23b**:



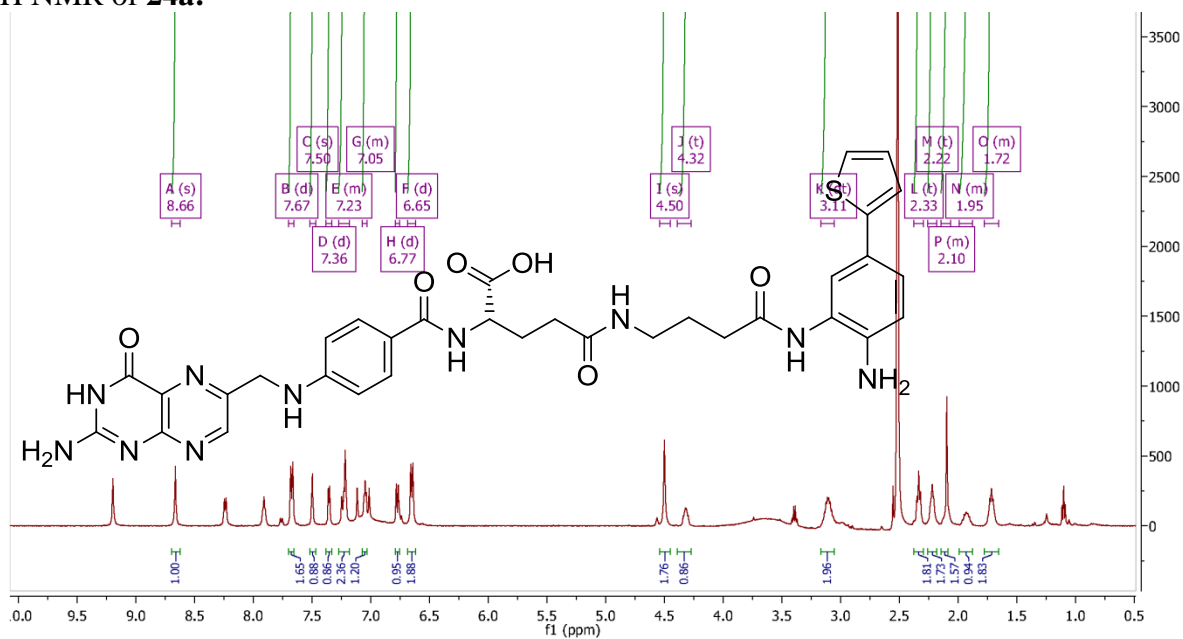
¹H NMR of **23c**:



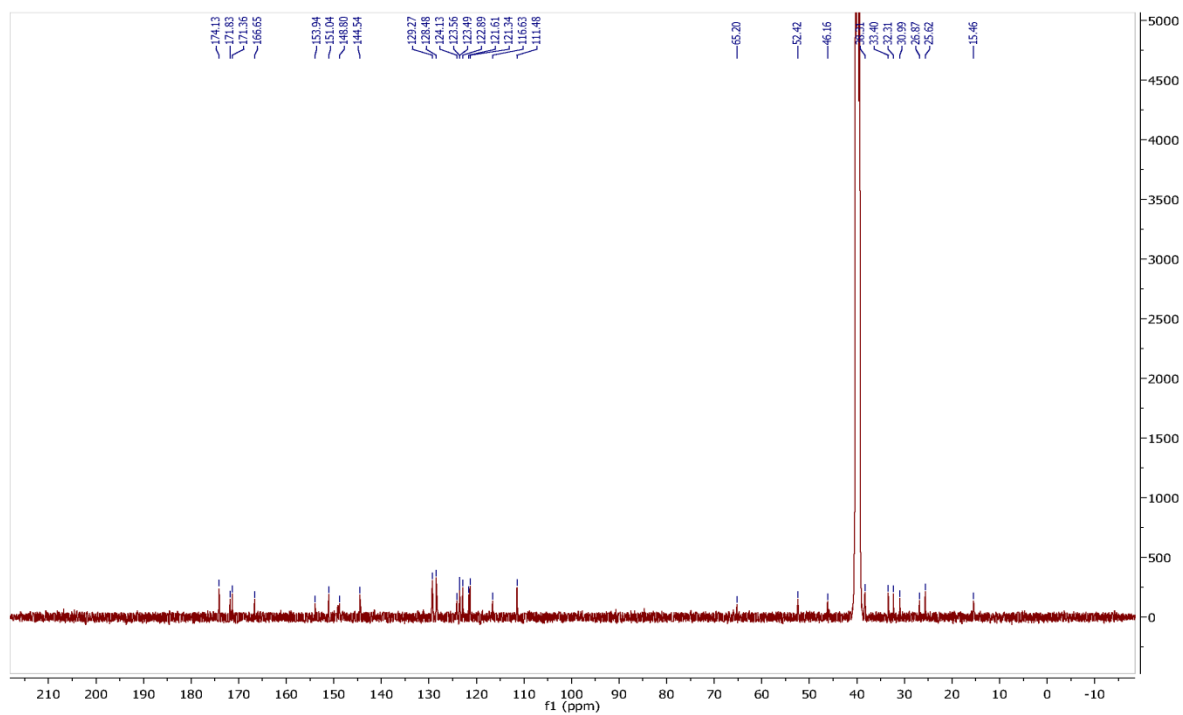
¹H NMR of **23d**:



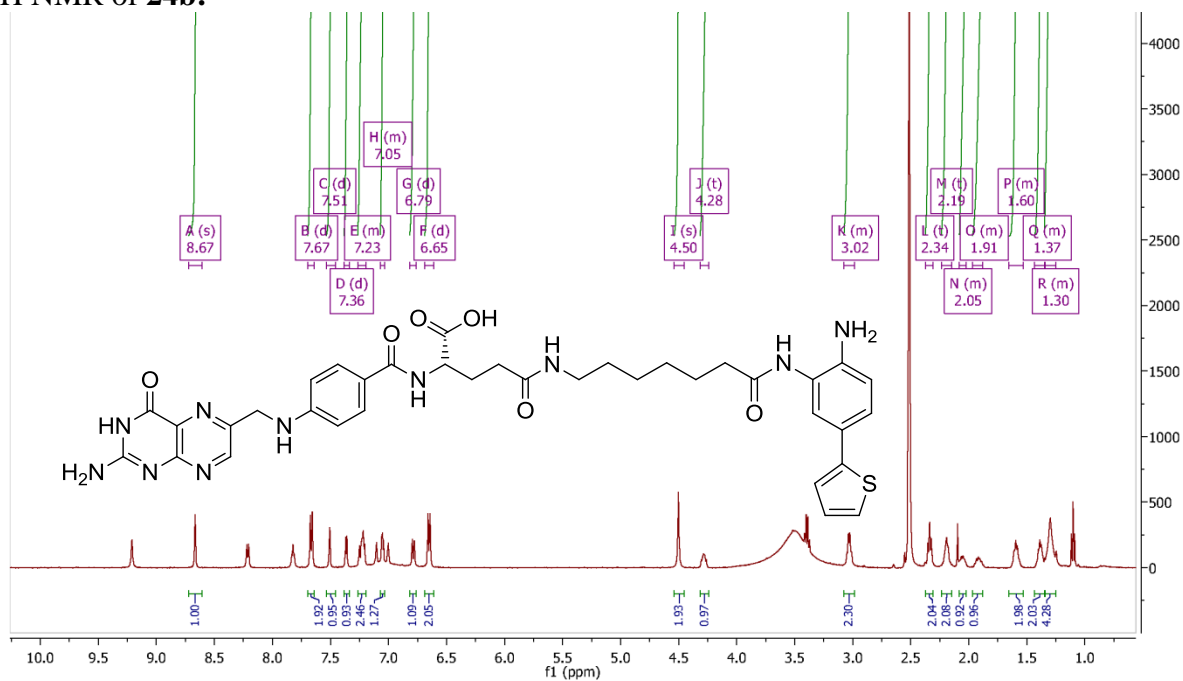
¹H NMR of **24a**:



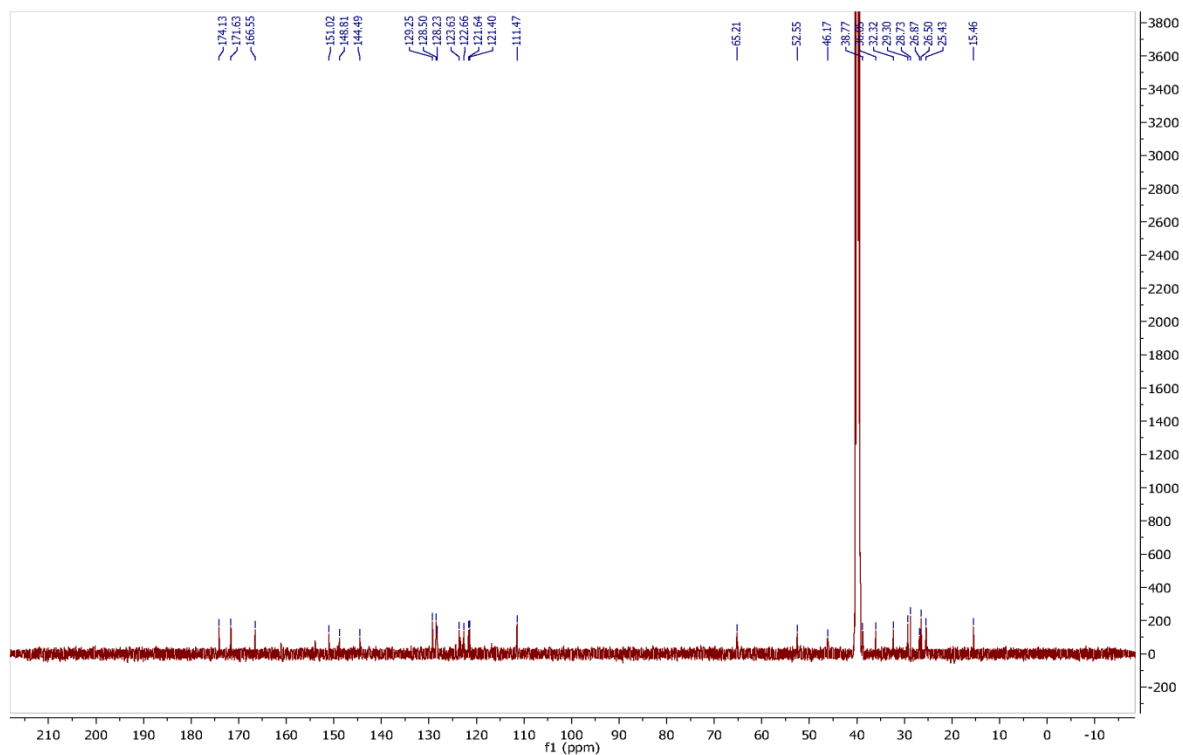
¹³C NMR of **24a**:



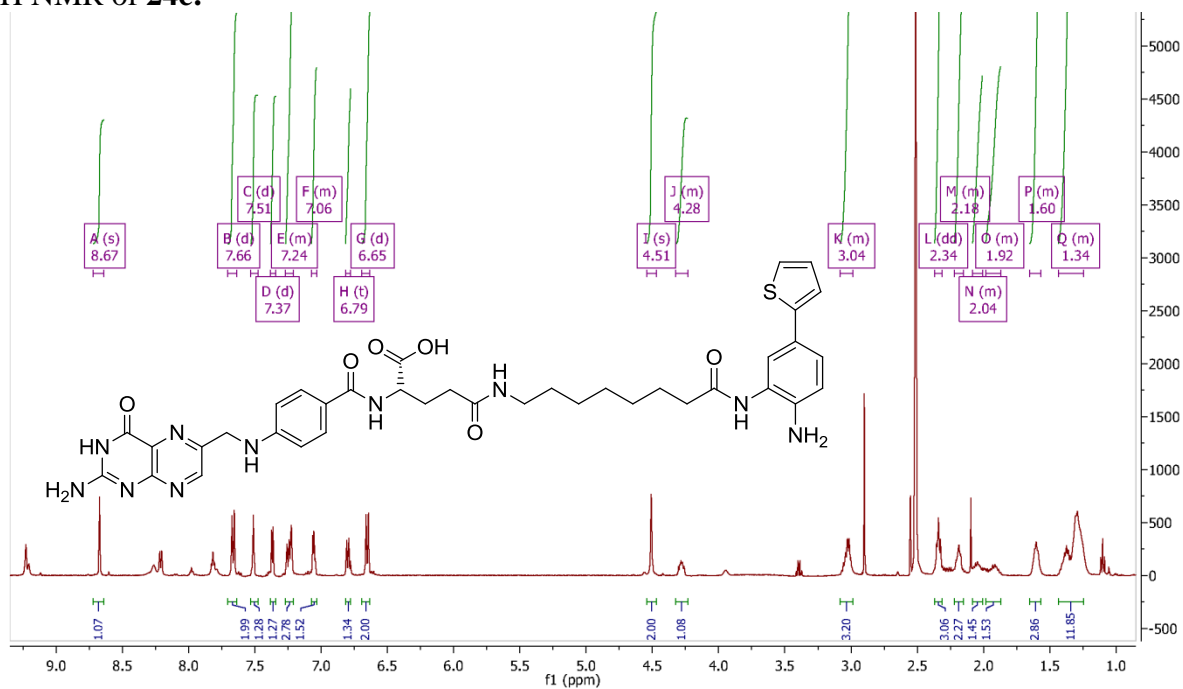
¹H NMR of **24b**:



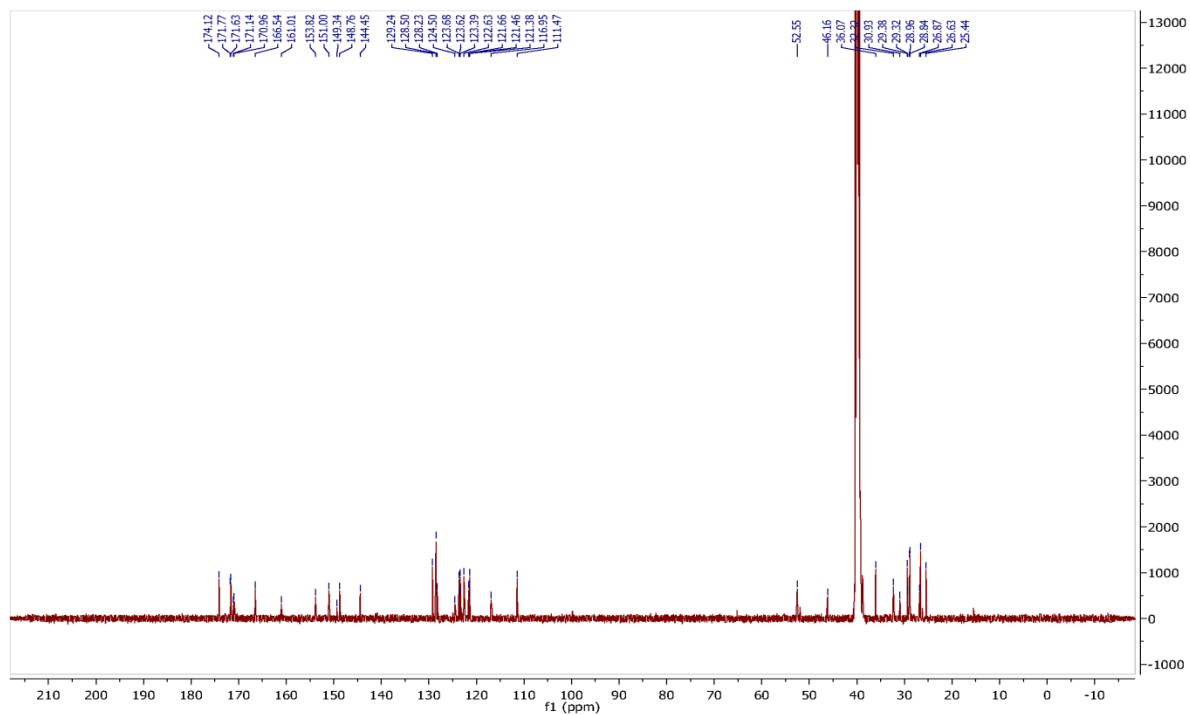
¹³C NMR of **24b**:



¹H NMR of 24c:



¹³C NMR of 24c:



VITA

QUAOVI SODJI

Quaovi Sodji was born in Aneho, TOGO but grew up in Lome where he graduated from high school in 2002. After moving to the US, he attended Georgia Perimeter College in Atlanta, Georgia before transferring to Georgia Tech where he received in B.S in Biochemistry in 2008 before enrolling in the University System of Georgia MD/PhD program. In 2010 he enrolled in the PhD program in the Chemistry/Biochemistry department at Georgia Tech. When he is not working in the lab, Mr. Sodji enjoys listening to music and watching sports.